Final Report

STABILITY OF HIGHWAY BRIDGES SUBJECT TO SCOUR

PHASE I

Submitted to

Alabama Department of Transportation
Research Project 930-585

Prepared by

G. Ed Ramey
Dan A. Brown

SEPTEMBER 2004

Final Report

on

Alabama Department of Transportation
Research Project 930-585

STABIITY OF HIGHWAY BRIDGES SUBJECT TO SCOUR

Prepared by

G. Ed Ramey
Dan A. Brown

Department of Civil Engineering
Auburn University

September 2004

ABSTRACT

Alabama has hundreds of highway bridges that were designed and constructed prior to 1990 and therefore not designed for scour. In addition, there are hundreds of county bridges constructed using standardized designs for which scour analysis is not part of the foundation design. ALDOT is currently performing an assessment of scour susceptibility of its bridges, and a part of this assessment requires an evaluation of the structural stability of these bridges for an estimated scour event. Because of the large number of bridges in the state, and because stability analyses of each bridge represents a considerable effort in time and money, there is a compelling need to develop a simple "screening tool" which can be used, along with the scour analyses, to efficiently assess the susceptibility of these bridges to scour. Also, because of the tendency to use standardized designs with pile bent foundations for many of the smaller bridges in Alabama, it is feasible to pursue the development of such a screening tool.

The objectives of the Phase I work were limited to identifying the primary parameters of importance in assessing the adequacy of pile bents for extreme scour events, and in identifying the best approach to follow in developing a screen tool.

These objectives were address via,

- identification of possible pile/bent failure modes during an extreme scour event.
- theoretical analysis of pile/bent failure modes to identify the critical parameters for each mode.
- sensitivity analyses if pile/bent failure modes for ranges of values of the critical parameters via theoretical analysis and FB-Pier modeling and analysis to assess the sensitivity of the pile/bent failure loads to the critical parameters.

Based on the Phase I work, it appears that the development of a simple screen tool is indeed feasible and the primary parameters of importance and the direction to proceed in the development have been identified. Thus, proceeding to Phase II to develop the "screening tool" is now in order.

ACKNOWLEDGEMENTS

This report was prepared under cooperative agreement between the Alabama Department of Transportation (ALDOT) and the Highway Research Center (HRC) at Auburn University. The PIs are grateful to the ALDOT and HRC for their sponsorship and support of the work.

The PIs are also grateful for the assistance and guidance of several ALDOT engineers during the execution of the research work. Specifically, thanks are due to George Conner, Eric Christie, and Randall Mullins of the ALDOT.

CONTENTS

1. INTRODUCTION

1.1 Statement of Problem

Alabama has hundreds of highway bridges that were designed and constructed prior to 1990 and therefore not designed for scour. In addition, there are hundreds of county bridges constructed using standardized designs for which scour analysis is not part of the foundation design. ALDOT is currently performing an assessment of scour susceptibility of the bridges, and a part of this assessment requires an evaluation of the structural stability of these bridges for an estimated scour event.

The vast majority of these bridges are relatively small, two-lane bridges constructed using a standardized design with pile bents. Analyses of stability may be performed using available computer software such as FBPIER for site specific geotechnical and foundation conditions and for the broad range of AASHTO load cases. An example of such analyses is represented by the recent report of the eight I-20 I-59 Warrior River Relief Bridges performed by Earth Tech, Inc. of Raleigh, NC. However, because of the large number of such bridges in the state, stability analyses of each bridge at each site represents an enormous effort in time and money.

There is a compelling need to develop a simple "screening tool" which can be used, along with the scour analyses, to efficiently and effectively assess the susceptibility of these large numbers of bridges to scour. Such a tool could be used to identify those bridges which are most likely to be deficient and should be prioritized for more detailed study. Because of the tendency to use standardized designs for pile bent foundations and bridge superstructures for many of the smaller bridges in Alabama, it is feasible to pursue the development of such a screening tool.

1.2 Research Objectives

The objective of the proposed research is to develop a plan for creating a screening tool for use in evaluating the stability of simple pile bent supported bridges if an estimated 50-year scour event occurs. This screening tool should address the broad range of typical bridge layouts, substructure designs, pile bent foundations, AASHTO design loads, geotechnical conditions, and scour events encountered in Alabama. It is anticipated that a large amount of analytical work will be required to develop a useful screening tool, and this work is expected to require a coordinated effort from many of Alabama's major research universities. The objective for this initial research (Phase I) is to establish a plan for development of this screening tool, including the framework of the tool and the necessary guidelines and specifications for the analytical and numerical work to be performed in Phase II. Because of the great need for experience and judgment in the analysis of stability of existing structures, there is a compelling need for careful planning in developing the outline of such a screening tool. A well thought-out description of the work that needs to be done is the primary objective of this Phase I research effort.

1.3 Work Plan

The work plan to accomplish the project objective has been broken into the execution of four work tasks. These tasks are identified and briefly described below.

1. Task 1: Information Gathering. This task is to gather information on the range of typical bridges in the state, including details about factors which may be important to the stability of the structure after scour. Standard designs of substructures will be reviewed and assembled into representative categories for further evaluation. Details such as span length, bracing, encasements, batter piles, numbers of piles and spacing, driving criteria used for pile installation,

connections of bent caps to girders, and perhaps many other factors must be considered in establishing the range of bridge and bent types and categorizing these structure classes. This task will involve meeting with ALDOT engineers and considerable interaction to ensure that all of the major factors have been considered.

2. <u>Task 2: Trial Analyses and Sensitivity Studies</u>. This task will further develop the plan for establishing base cases and categories of bridges, bents and geotechnical conditions. Several typical scenarios for analysis of stability after scour will be established; the test cases to be studied in detail are to represent some broad ranges of the spectrum of cases to be analyzed in Phase II. These test cases will be evaluated in a manner similar to that planned for the analyses used to develop the screening tool, and for a range of possible geotechnical/foundation conditions. In evaluating a few select test cases, the research team will be afforded the opportunity to perform trial runs and become familiar with the process which will be needed to accomplish the Phase II research and also to perform sensitivity studies of various parameters which are likely to affect stability. The process of going through the full evaluation of several differing typical structures is essential to develop guidelines for implementation of Phase II. These sensitivity studies will assist in the establishment of appropriate classes of bridge substructure/foundation/geotechnical conditions for development of the screening tool.

3. <u>Task 3: Outline the Screening Tool</u>. As a result of the efforts of Tasks 1 and 2, an outline of the format for the screening tool must be developed. The format must be one which is simple to use and complete for the purpose of identifying the categories of bridge/foundation/ geotechnical conditions. For Task 3, this screening tool outline will be finalized and illustrated in an interim report for presentation to ALDOT engineers for review and comment. It is anticipated that a meeting should be held to explain the proposed screening tool and the general

plans for its use. ALDOT approval of the general plan is required before proceeding to Task 4.

4. Task 4: Development of Specifications and Guidelines for Development of the Screening Tool in Phase II. The final task is to develop the specifications and guidelines necessary for the multiple participants to do the large amount of analytical work involved in developing the full screening tool (which is to be accomplished in Phase II and is beyond the scope of this proposal). A plan for coordinating the work of Phase II will also be proposed in Task 4, including provisions for reviewing and error checking the work as well as implementing the collaborative efforts into a cohesive final document.

1.4 Scope of Work

This Phase I work is limited to identifying the primary parameters of importance in assessing the adequacy of pile bents for an extreme scour event, and in generating a plan for the development of an effective and efficient "screening tool" which uses these parameters to screen ALDOT pile bent foundations to identify those that are adequate and those requiring more detailed analyses to assess their adequacy during an extreme event. The actual "screening tool" will be developed in a follow-up Phase II work effort.

2. THEORETICAL CONSIDERATIONS

2.1 General

Slender bridge bent piles are slender columns and subject to a possible stability or buckling failure. In investigating this failure mode, the first question to address is if the pile or bent can buckle in a sidesway mode. For existing bridges, this mode is not possible (this will be discussed more fully in Chapter 3). Thus the largest value of effective length for a bent pile will be the pile length from the bent cap to the ground line. Smaller values of effective length will probably be in order, depending on the pile end boundary conditions and bracing conditions. Perfect column/pile P-$\Delta_{\mathbb{C}}$ and $P_{failure}$ curves are shown in Figs. 2.1 and 2.2 respectively. As indicated in Fig. 2.1, the perfect pile would exhibit no lateral deflection prior to reaching the buckling (P_{CR}) load. Figure 2.2 illustrates that a perfect pile may fail due to insufficient yield strength (P_y) or due to buckling (P_{CR}) depending on the pile effective length (kL).

Piles (columns) in pile bents are never perfectly straight or subject to perfect concentric loading, and the effects of these imperfect conditions, as well as the effects of pile inelastic behavior, are reviewed below. Also, piles in bents are sometimes encased in concrete which greatly stiffens them, and this is discussed below, as is the bracing a pile may receive from adjacent less heavily loaded piles in the bent. Theoretical considerations of the lateral support and fixity provided by the soil at the ground line, which in turn greatly influences pile buckling loads, are also discussed in this chapter.

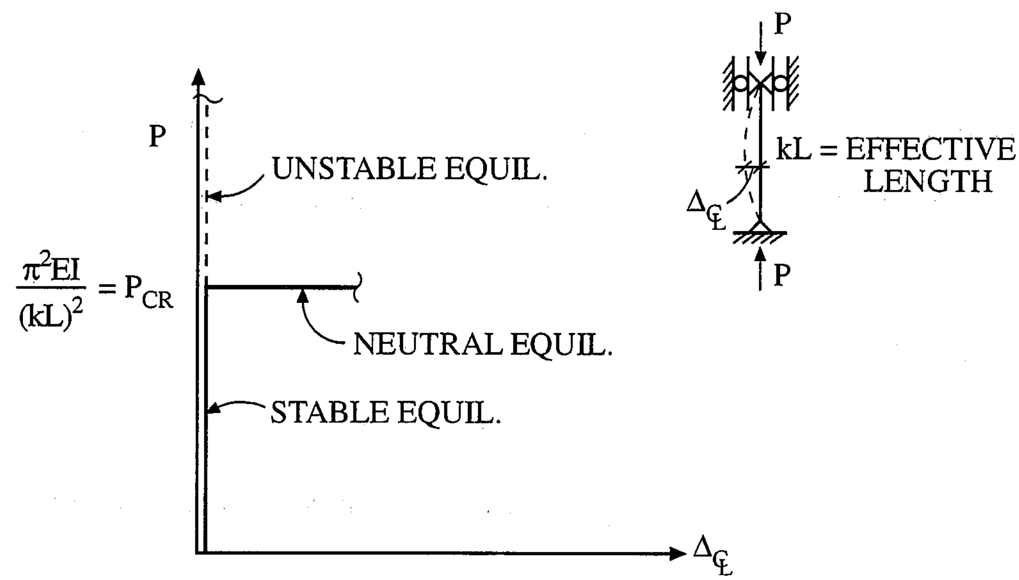

Fig. 2.1. Perfect Pile P-$\Delta_{℄}$ Curve

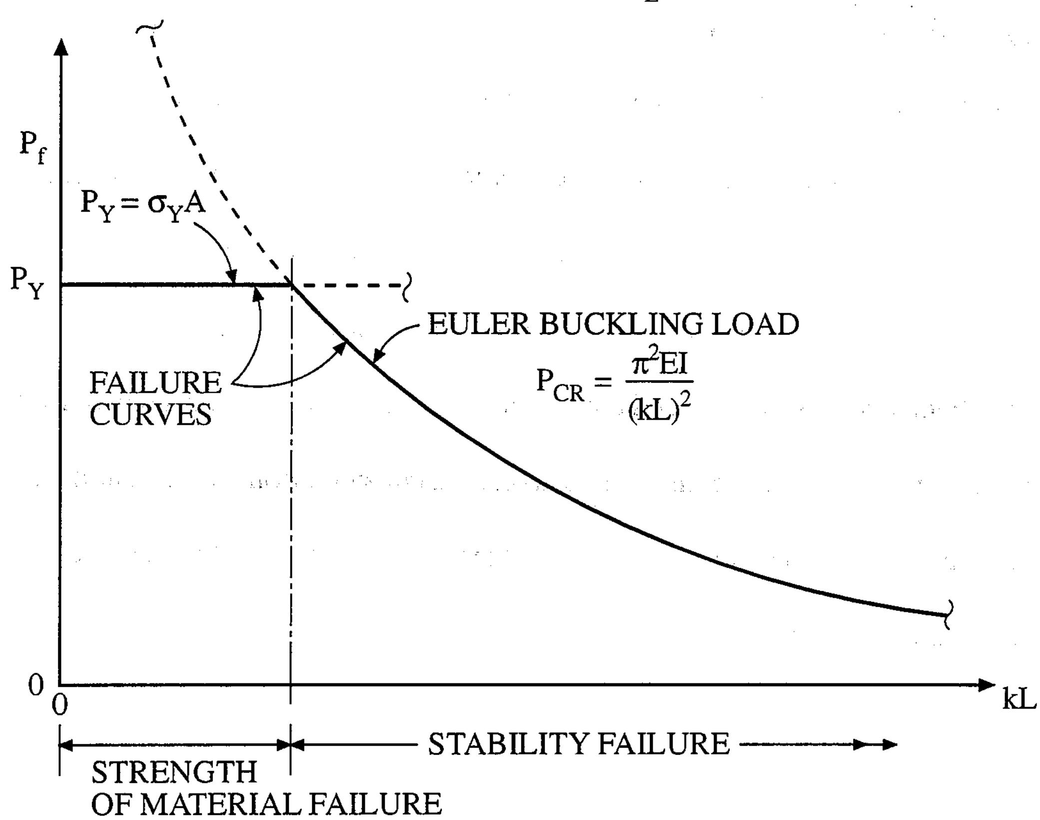

Fig. 2.2. Perfect Pile P_f vs. kL Failure Curves

2.2 Behavior of Imperfect Columns

Imperfect columns are generally considered to be those which are not initially straight or those in which the load is applied with some eccentricity. Let's first consider the case of an initially bent hinged-end column as shown in Fig. 2.3. Let the initial deformations of the column be given by y_o and the additional deformations due to bending by y as shown in Fig. 2.3. The solution of this problem can be simplified, without losing the generality of the results, if the assumed initial deformation is assumed to be of the form

$$y_o = a \sin \frac{\pi x}{\ell} \tag{2.1}$$

The bending strains in the column are caused by the change in curvature, y'', and not by the total curvature, $y_o'' + y''$. Thus, the internal resisting moment at any section is

$$M_x = -EIy'' \tag{2.2}$$

and equating this moment to the externally applied bending moment, $P(y + y_o)$, gives

$$EIy'' + P(y_o + y) = 0 \tag{2.3}$$

where y = additional y displacement or the change in displacement. Substituting Eq. (2.1) for y_o in Eq. (2.3) and using the notation $k^2 = P/EI$ yields,

$$y'' + k^2 y = -k^2 a \sin \frac{\pi x}{\ell} \tag{2.4}$$

as the governing DE of equilibrium for the problem. The solution of Eq. (2.4) and satisfying the problem boundary conditions yields,

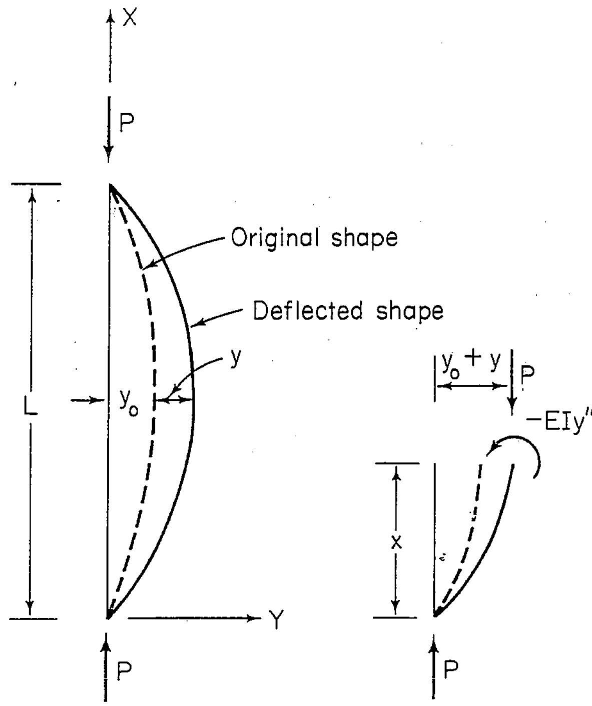

Fig. 2.3. Initially bent column (from Chajes).

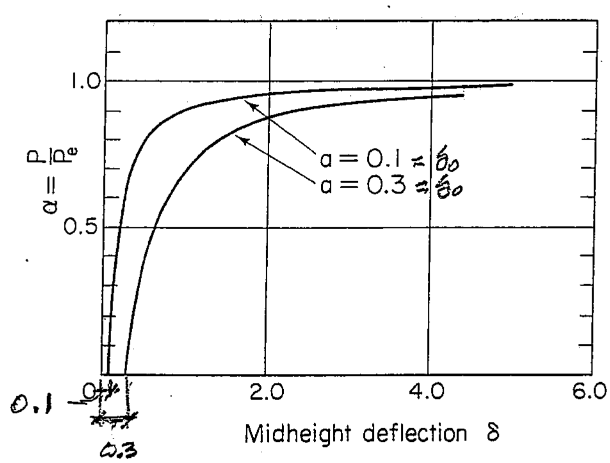

$$y = \frac{P/P_e}{1-P/P_e}\delta_0 \sin\frac{\pi x}{L}$$

At Mid Ht., $x = L/2$

$$\Leftarrow \delta = y_{mh} = \frac{P/P_e}{1-P/P_e}\delta_0$$

Fig. 2.4. Load-deflection curves of initially bent columns (from Chajes).

$$y = \frac{\alpha}{1-\alpha} a \sin\frac{\pi x}{\ell} \tag{2.5}$$

where $\alpha = P/P_e$ where $P_e = \pi^2 \; EI/\ell^2$

Thus the total deflection from the vertical y_t is

$$y_t = y_o + y = \left(1 + \frac{\alpha}{1-\alpha}\right) a \sin\frac{\pi x}{\ell}$$

$$y_t = \frac{a}{1-\alpha} \sin\frac{\pi x}{\ell} \tag{2.6}$$

The total deflection at midheight of the column is

$$\delta = \frac{a}{1-\alpha} = \frac{a}{1-\left(\dfrac{P}{P_e}\right)} \tag{2.7}$$

Fig. 2.4 shows a plot of Eqn. (2.7) for two different values of initial imperfection.

The effects of an imperfect axial loading on column behavior can be determined by considering the initially straight but eccentrically loaded column shown in Fig. 2.5. For this column, equating the internal resisting moment, -EIy", at any section, to the corresponding applied moment, P(e+y), gives

$$EIy'' + P\,(e + y) = 0$$

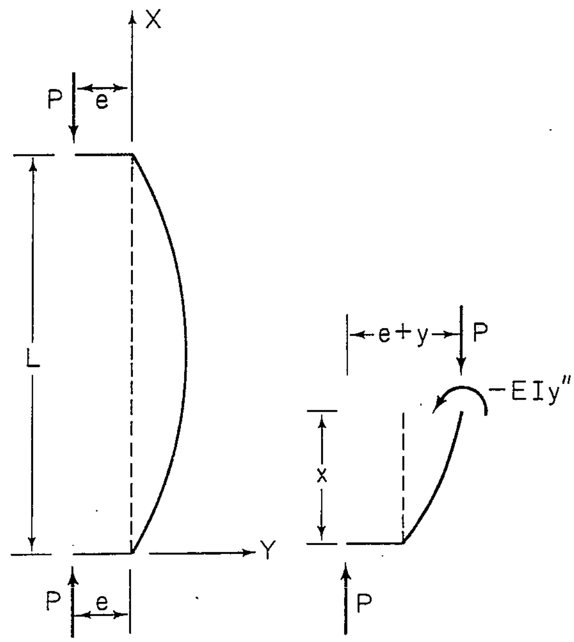

Fig. 2.5. Eccentrically loaded column (from Chajes).

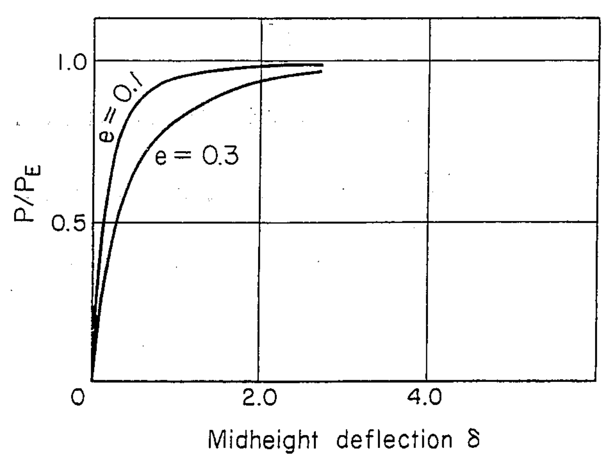

Fig. 2.6. Load-deflection curves of eccentrically loaded columns (from Chajes).

or,

$$y'' + k^2 y = -k^2 e \tag{2.8}$$

where $k^2 = \dfrac{P}{EI}$

The solution of Eqn. (2.8) along with satisfying the problem boundary conditions gives

$$y = e\left(\cos kx + \frac{1-\cos k\ell}{\sin k\ell}\sin kx - 1\right) \tag{2.9}$$

The equation for the midheight deflection, $y = \delta$, is obtained by substituting $x = \ell/2$ into Eqn. (2.9). This yields

$$\delta = e\left(\sec\frac{k\ell}{2} - 1\right) \tag{2.10a}$$

or,

$$\delta = e\left[\sec\left(\frac{\pi}{2}\sqrt{\frac{P}{P_e}}\right) - 1\right] \tag{2.10b}$$

where $P_e = \pi^2 EI/\ell^2$

Fig. 2.6 shows a plot of Eqn. (2.10b) for two different values of load eccentricity or load imperfection.

Summarizing, Figs. 2.4 and 2.6 reflect several important points about the behavior of imperfect columns. Namely,

1. Imperfect columns begin to bend and deflect as soon as the load is applied.
2. The Euler load is a good approximation of the maximum load that a real imperfect column can support.
3. The behavior of imperfect columns provides an alternate method of stability analysis, i.e., "The critical load is the load at which the deformations of a slightly imperfect system increase without bound. To apply this criterion, one gives the structural member or system to be investigated a small initial deformation and then determines the load at which this deformation becomes unbounded."
4. The behavior of an imperfect system can be assessed by giving the system some initial crookedness or by applying the load eccentrically.

2.3 Modification for Inelastic Buckling

Due to residual and bending stresses, points within a pile cross-section will reach their yield stress long before the nominal P/A stress reaches the yield point. Thus, the σ vs. ℓ failure curve should be modified to account for this. The modification commonly taken is to assume a parabolic curve from stress levels of σ_y to $\sigma_y/2$ or from P_y to $P_y/2$ as indicated in Fig. 2.7.

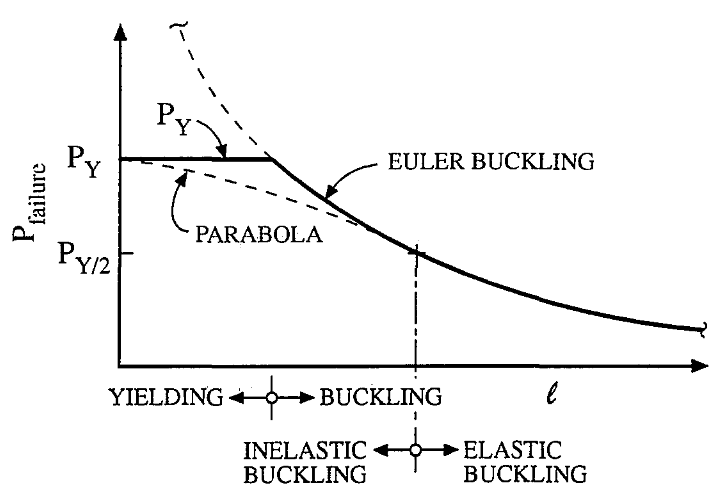

Fig. 2.7. Column $P_{failure}$ vs. ℓ Curve

The equation of the parabola is as follows:

$$P_{CR} = a + b\ell + c\ell^2 \tag{2.11}$$

At $\ell = 0$, $P_{CR} = P_y$, and thus $a = P_y$

$$\frac{dP_{CR}}{d\ell} = 0 = b + 2c\ell$$
$$\therefore b = 0$$
$$\therefore P_{CR} = P_y + c\ell^2 \tag{2.12}$$

Now determine ℓ where $P_{CR} = P_{buckling} = \dfrac{P_y}{2}$

Thus,

$$\frac{2\pi^2 EI_y}{\ell^2} = \frac{P_y}{2}$$

or,

$$\ell^2 = \frac{2\ell^2 EI_y}{P_y/2}$$
$$\ell = \sqrt{\frac{2\pi^2 EI_y}{P_y/2}}$$

or,

ℓ =35.74' (for HP 10 x 42 pile)

ℓ = 42.54' (for HP 12 x 53 pile)

Substituting these values of ℓ into Eqn. (2.12) yields,

$$P_y/2 = P_y + C(35.74)^2$$

$$C = -\frac{P_y}{2(35.74)^2} = -0.175^k/ft.^2 \text{ (for HP 10 x 42 pile)}$$

$$C = -\frac{P_y}{2(42.54)^2} = -0.154^k/ft.^2 \text{ (for HP 12 x 53 pile)}$$

Therefore, for an HP 10 x 42 pile of A36 steel,

$$P_{CR} = P_y - 0.175\ \ell^2$$

$$P_{CR} = 446 - 0.175\ \ell^2 \tag{2.13}$$

where ℓ is in feet and P_{CR} is in kips.

For an HP 12 x 53 pile of A36 steel, the corresponding equation is

$$P_{CR} = P_y - 0.154\ \ell^2$$

$$P_{CR} = 558 - 0.154\ \ell^2 \tag{2.14}$$

Using Eqns. (2.13) and 2.14) yields the inelastic buckling loads in the range $P_y \leq P_{inelastic\ buckling} \leq P_y/2$ and these are shown in Table 2.1 and Fig. 2.7. Table 2.1 and Fig 2.7 also show some $P_{elastic}$ buckling loads for longer piles.

Table 2.1. Inelastic and Elastic Buckling Loads vs. ℓ for HP x 42 and HP 12 x 53 Piles of A36 Steel

ℓ = "H" + S (ft.)	P_{CR} (kips)	
	HP 10 x 42	HP 12 x 53
0	446	558
5	442	554
10	429	543
15	407	523
20	376	496
25	337	462
30	289	419
35	232	369
35.74	223	-
40	178	312
42.54	-	312
45	141	249
50	114	202

* Shaded Values are $P_{elastic}$ Buckling

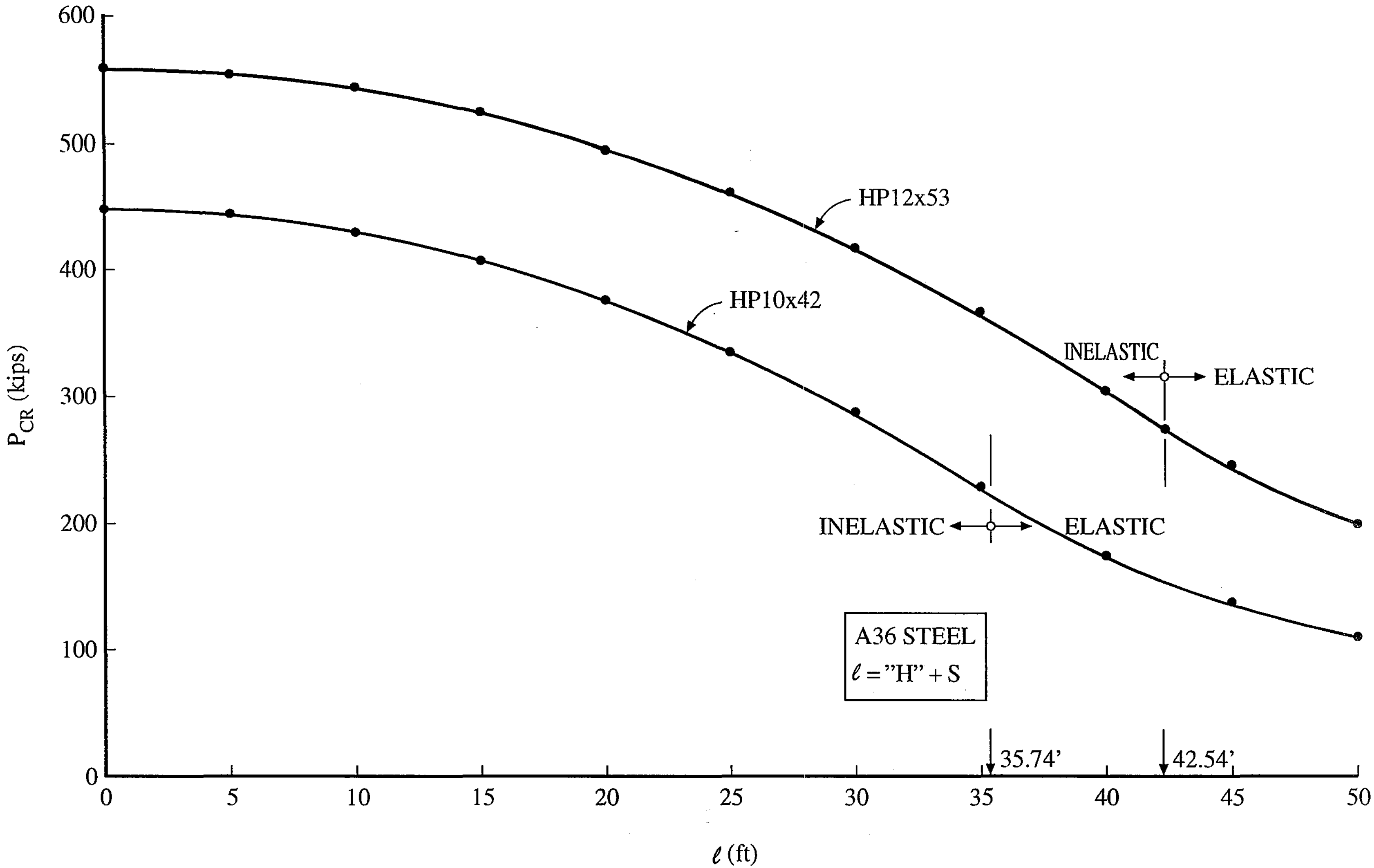

Fig. 2.7. Inelastic and Elastic P_{CR} vs. ℓ for HP10x42 and HP12x53 Piles

Alternatively, in stability problems the effect of member inelasticity on the buckling solution can be reasonably approximated by using the tangent modulus stiffness E_T instead of the elastic modulus, E. This is reflected in Fig. 2.8. The inelastic stiffness is $E_T = \tau E$ where τ is the inelastic stiffness reduction factor. In this formulation,

$$P_{CR} = \frac{\pi^2 E_T I}{(kL)^2} \text{ or } P_{CR} = \frac{\pi^2 \tau E I}{(kL)^2}$$

and, the elastic range is defined by the axial stress in the member, not the slenderness ratio. A member with low slenderness ratio (L/r) will respond elastically if the axial stress is low. In the AISC Specification an axial stress less than 0.3 F_y in ASD or 0.33 F_y in LRFD places the column in the elastic range. The AISC-ASD and LRFD Manuals of Steel Construction tabulate the stiffness reduction factor for P/A stress levels (see Table 2.2).

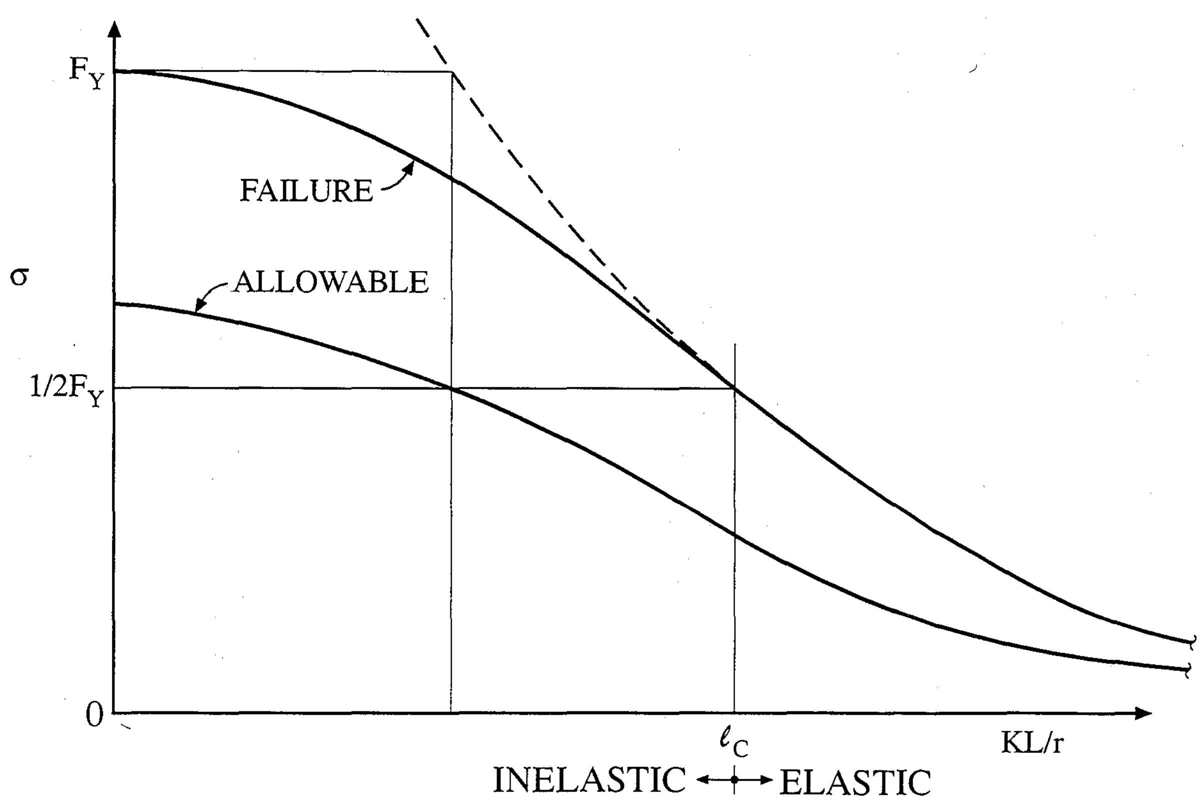

Fig. 2.8. Elastic and Inelastic Buckling Regions

Table 2.2. τ-Values 9th Edition of AISC (from AISC Manual)

F_y = 36 ksi
F_y = 50 ksi

Table A

Stiffness Reduction Factors f_a/F_e'

f_a	F_y 36 ksi	F_y 50 ksi
28.0	—	0.097
27.9	—	0.104
27.8	—	0.112
27.7	—	0.120
27.6	—	0.127
27.5	—	0.136
27.4	—	0.144
27.3	—	0.152
27.2	—	0.160
27.1	—	0.168
27.0	—	0.177
26.9	—	0.184
26.8	—	0.193
26.7	—	0.202
26.6	—	0.210
26.5	—	0.218
26.4	—	0.227
26.3	—	0.236
26.2	—	0.245
26.1	—	0.253
26.0	—	0.262
25.9	—	0.271
25.8	—	0.280
25.7	—	0.288
25.6	—	0.297
25.5	—	0.306
25.4	—	0.315
25.3	—	0.324
25.2	—	0.333
25.1	—	0.342
25.0	—	0.350
24.9	—	0.359
24.8	—	0.368
24.7	—	0.377
24.6	—	0.386
24.5	—	0.394
24.4	—	0.403
24.3	—	0.412
24.2	—	0.421
24.1	—	0.430
24.0	—	0.439
23.9	—	0.447
23.8	—	0.456
23.7	—	0.465
23.6	—	0.473
23.5	—	0.482
23.4	—	0.490
23.3	—	0.499
23.2	—	0.507
23.1	—	0.516
23.0	—	0.524
22.9	—	0.533
22.8	—	0.541
22.7	—	0.549
22.6	—	0.557
22.5	—	0.565
22.4	—	0.574
22.3	—	0.582
22.2	—	0.590
22.1	—	0.598
22.0	—	0.606

f_a	F_y 36 ksi	F_y 50 ksi
21.9	—	0.614
21.8	—	0.622
21.7	—	0.630
21.6	—	0.637
21.5	—	0.645
21.4	—	0.653
21.3	—	0.660
21.2	—	0.668
21.1	—	0.675
21.0	—	0.683
20.9	—	0.689
20.8	—	0.697
20.7	—	0.704
20.6	—	0.712
20.5	0.064	0.718
20.4	0.074	0.725
20.3	0.083	0.732
20.2	0.093	0.739
20.1	0.102	0.746
20.0	0.114	0.753
19.9	0.125	0.760
19.8	0.136	0.766
19.7	0.147	0.772
19.6	0.158	0.778
19.5	0.169	0.785
19.4	0.181	0.792
19.3	0.193	0.798
19.2	0.204	0.804
19.1	0.216	0.810
19.0	0.228	0.816
18.9	0.241	0.822
18.8	0.252	0.827
18.7	0.264	0.833
18.6	0.277	0.839
18.5	0.288	0.844
18.4	0.301	0.849
18.3	0.314	0.855
18.2	0.326	0.860
18.1	0.338	0.865
18.0	0.350	0.871
17.9	0.363	0.875
17.8	0.375	0.880
17.7	0.387	0.885
17.6	0.400	0.890
17.5	0.411	0.894
17.4	0.424	0.899
17.3	0.436	0.903
17.2	0.448	0.908
17.1	0.460	0.912
17.0	0.472	0.917
16.9	0.484	0.920
16.8	0.496	0.924
16.7	0.508	0.928
16.6	0.519	0.932
16.5	0.531	0.935
16.4	0.543	0.939
16.3	0.554	0.942
16.2	0.565	0.946
16.1	0.577	0.950
16.0	0.588	0.952

f_a	F_y 36 ksi	F_y 50 ksi
15.9	0.599	0.956
15.8	0.610	0.959
15.7	0.621	0.962
15.6	0.632	0.964
15.5	0.643	0.967
15.4	0.653	0.970
15.3	0.664	0.972
15.2	0.675	0.974
15.1	0.684	0.977
15.0	0.695	0.979
14.9	0.704	0.981
14.8	0.715	0.983
14.7	0.724	0.985
14.6	0.734	0.987
14.5	0.743	0.988
14.4	0.753	0.990
14.3	0.762	0.991
14.2	0.770	0.993
14.1	0.780	0.994
14.0	0.789	0.995
13.9	0.797	0.996
13.8	0.805	0.997
13.7	0.814	0.998
13.6	0.822	0.998
13.5	0.830	0.999
13.4	0.838	0.999
13.3	0.845	1.000
13.2	0.853	—
13.1	0.860	—
13.0	0.868	—
12.9	0.874	—
12.8	0.881	—
12.7	0.888	—
12.6	0.895	—
12.5	0.901	—
12.4	0.907	—
12.3	0.913	—
12.2	0.918	—
12.1	0.924	—
12.0	0.929	—
11.9	0.934	—
11.8	0.939	—
11.7	0.944	—
11.6	0.949	—
11.5	0.953	—
11.4	0.958	—
11.3	0.962	—
11.2	0.966	—
11.1	0.970	—
11.0	0.973	—
10.9	0.976	—
10.8	0.979	—
10.7	0.982	—
10.6	0.984	—
10.5	0.987	—
10.4	0.989	—
10.3	0.991	—
10.2	0.993	—
10.1	0.995	—
10.0	0.996	—
9.9	0.997	—
9.8	0.998	—
9.7	0.999	—
9.6	1.000	—

2.4 Pile Bracing

Bracing is used to reduce the effective length of a column/pile and thus enhance its stability. In general, braces must have both stiffness and strength, and the requirements and guideline rules for these are:

- Stiffness
  - Use brace system stiffness at least twice the ideal value
  - Connection details can be detrimental
- Strength
  - Brace forces are directly related to the magnitude of initial out-of-straightness
  - Design the brace and its connections for 0.4%-1% of the compressive force

A system's ideal bracing stiffness can best be illustrated with a rigid bar stability problem as shown in Fig. 2.9. As evident in Fig. 2.9, the stability of the rigid bar is directly related to bracing conditions at the top of the bar, i.e., the stiffness and strength of the top spring. Note from this that if a column is perfectly straight and concentrically loaded, the bracing only needs stiffness, i.e., there is no force developed in the brace. However, if the column conditions are not ideal, e.g., if the load is applied with an eccentricity Δ_o, then the brace needs both stiffness and strength.

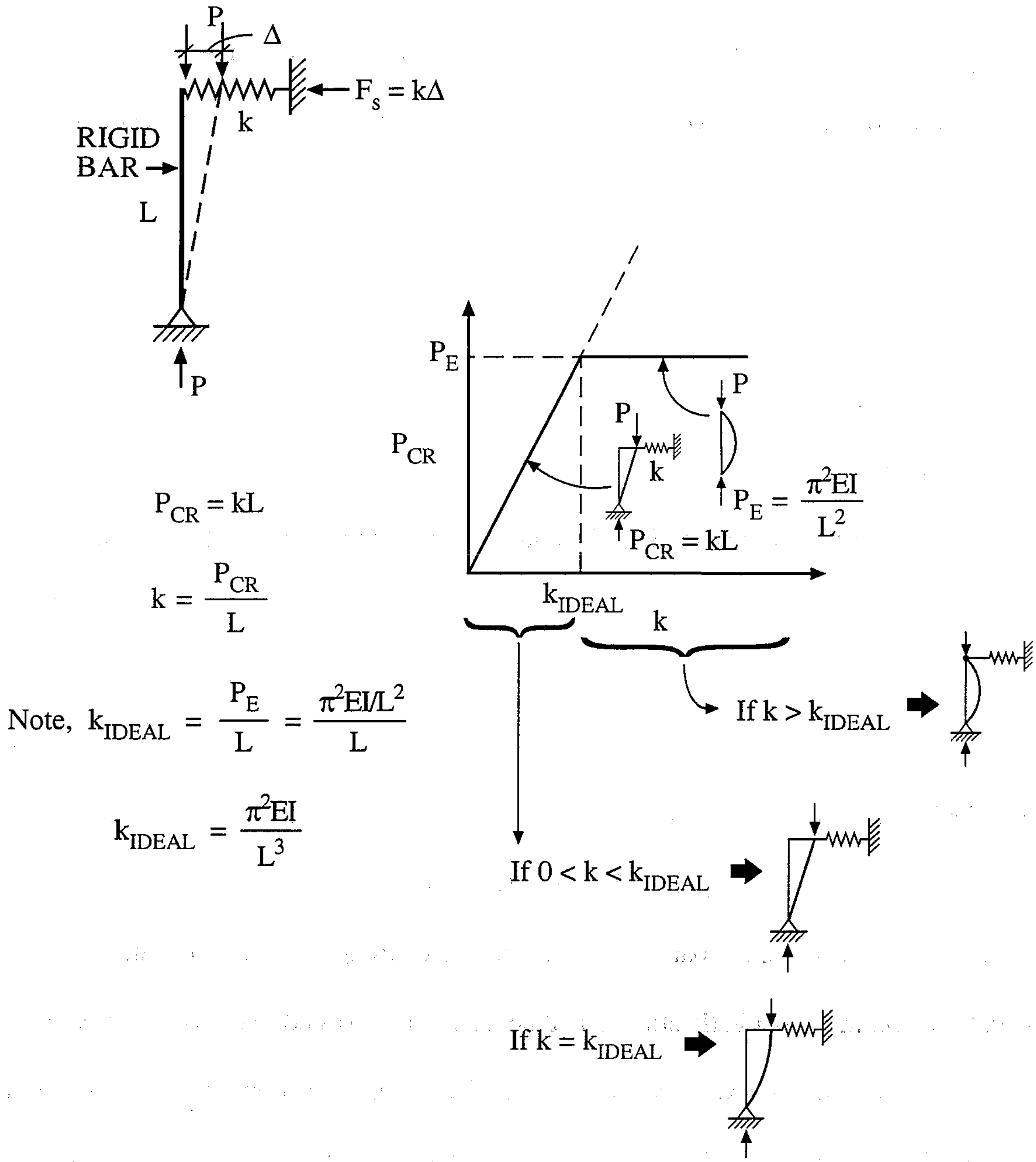

Fig. 2.9. Ideal Bracing for a Rigid Bar Stability Case

Lateral bracing of structural components and systems can be divided into four categories, i.e.,

- relative bracing system
- discrete bracing system
- continuous bracing system
- lean-on bracing system.

These are illustrated in Fig. 2.10.

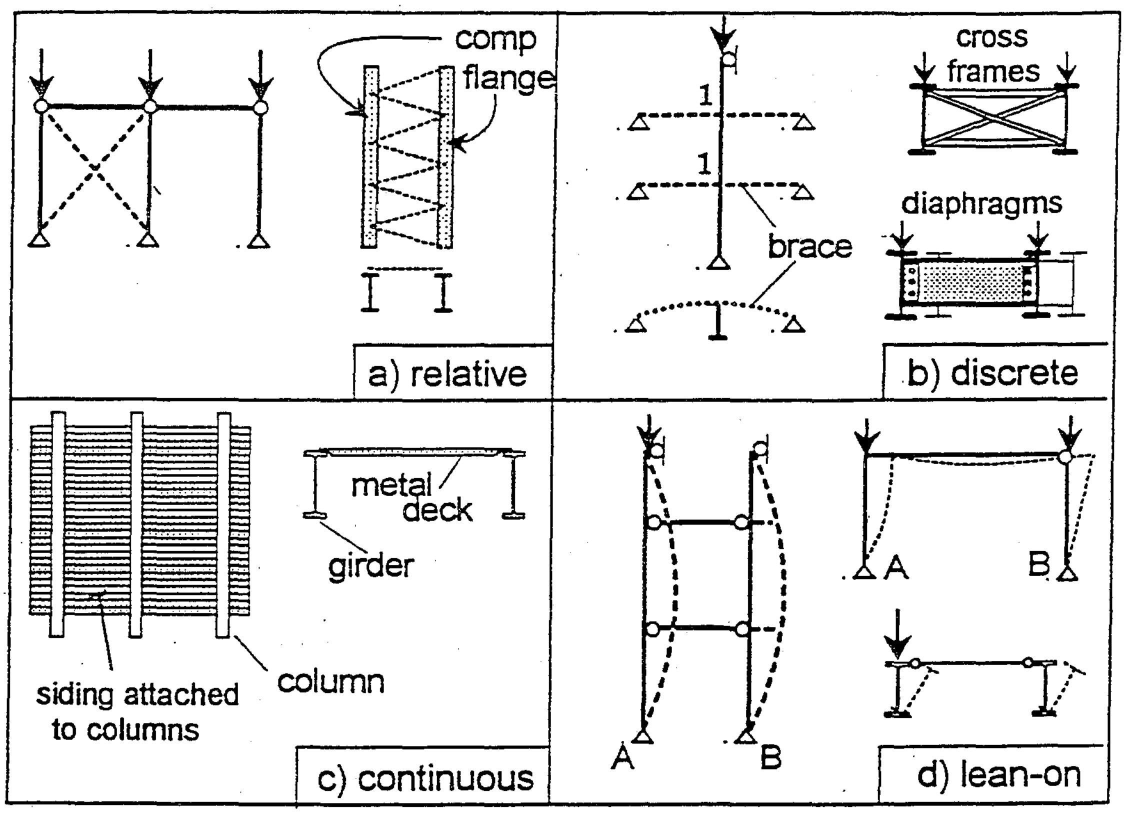

Fig. 2.10. Types of Bracing Systems (from Yura)

A typical pile bridge bent used by the ALDOT is shown in Fig. 2.11. Note that the piling in the bent have continuous bracing below the ground line for buckling about either principal axis. For buckling in the plane of the figure, i.e., in the transverse direction (about the pile's weak axis) the steel angle swaybracing provides relative bracing for piling. Also, adjacent piling in the bent provide lean-on bracing (in the transverse direction) to the most heavily loaded pile in the bent. Lastly, adjacent bents provide lean-on bracing for buckling in the longitudinal direction (about the pile's strong axis).

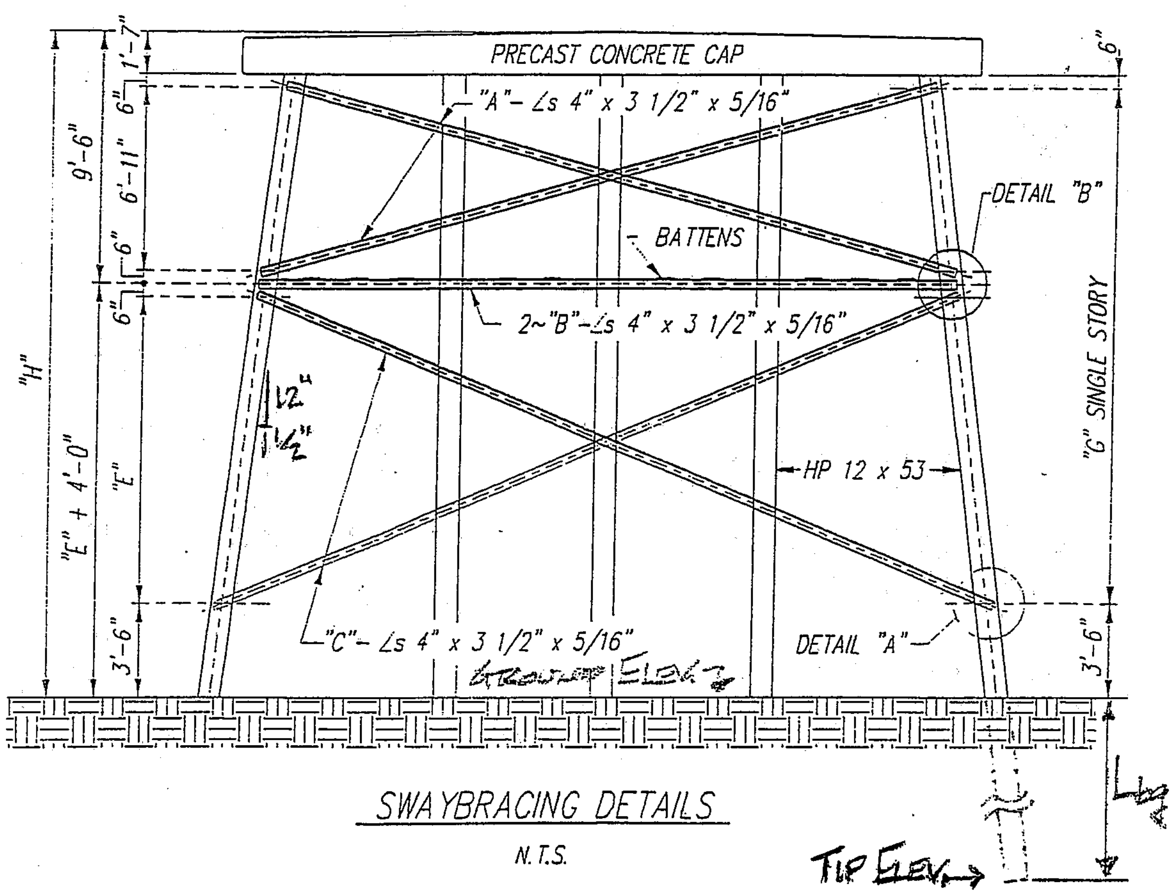

Fig. 2.11. Typical ALDOT Bridge Pile Bent

Most engineers are familiar with the first three bracing categories (a-c) in Fig. 2.10. However, the fourth category, i.e., lean-on bracing, is not as familiar. Because of this and the fact that individual piles and whole pile bents have greater load capacity because of lean-on bracing, we will discuss this bracing system further.

Lean-On Bracing Systems

When compression members lean-on adjacent members for stability support (bracing), the ΣP concept (Yura, 1971) can be used to design the members. The ΣP concept will be explained using the problem shown in Fig. 2.12, in which column A has a load P with three connecting beams attached between columns A and B. There are two principal buckling modes for this structure, the no sway and the sway modes. If column B is sufficiently slender, the system will buckle in the sway mode, shown by the dot-dash line in Figure 2.12a. In the sway mode the buckling strength involves the sum (ΣP_{cr}) of the buckling capacity of each column that

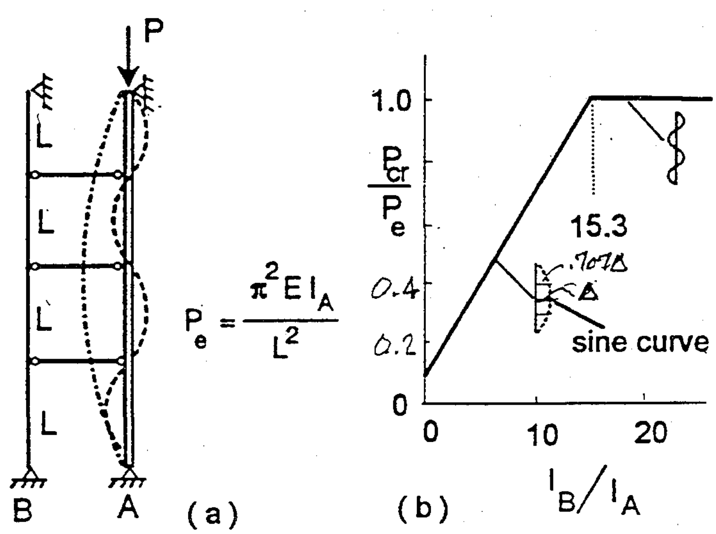

Fig. 2.12. Lean-On Bracing (from Yura)

sways. The system is stable in the sway mode if the sum of the applied loads (ΣP) is less than the ΣP_{cr}. This assumes all the columns have the same height. If column B is sufficiently stiff, the buckling capacity may be controlled by the no sway mode shown dashed. This buckling mode does not involve the lean-on bracing concept. Both modes must be checked.

An exact elastic solution shows that as I_B increases, the Pcr increases linearly in the sway mode. At $I_B/I_A \geq 15.3$, column A buckles in the no sway mode. The I_B required to develop full bracing can be approximated using the ΣP concept. In the sway mode, the elastic capacities of columns A and B are $\pi^2 EI_A/(4L)^2$ and $\pi^2 EI_B/(4L)^2$, respectively. The desired P_{cr} corresponding to the no sway mode is $\pi^2 EI_A/L^2$. Equating the sum of the sway capacities to the P_{cr} in the no sway mode yields,

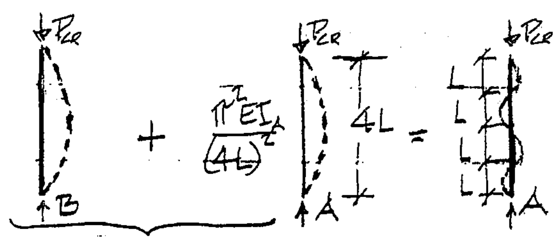

$$\frac{\pi^2 EI_B}{(4L)^2} \qquad + \frac{\pi^2 EI_A}{(4L)^2} \qquad \qquad \frac{\pi^2 EI_A}{L^2}$$

$$\Sigma P_{cr} \qquad = \quad P_{cr} \quad \rightarrow \frac{\pi^2 EI_B}{16L^2} + \frac{\pi^2 EI_A}{16L^2} = \frac{\pi^2 EI_A}{L^2}$$

$$\pi^2 E(I_A + I_B)/(4L)^2 = \pi^2 EI_A / L^2$$

Solution of this equation gives $I_B = 15I_A$ which is close to the exact solution of $I_B = 15.3\ I_A$. In the inelastic range, τ_i is used where τ_i is based on the axial load in each column, P_i. It should be noted that there can be axial load on all of the columns.

Note in Fig. 2.12b, as I_B is increased, the buckling load increases linearly until the ideal brace situation is reached when buckling occurs between the supports. The response shown in Fig. 2.12b indicates that the buckled shape is always a half sine curve until the full bracing is achieved when $I_B = 15.3I_A$. There is no switching from one shape to the next higher mode as occurs for single point bracing, i.e., lean-on bracing is not the same as single point bracing. A lean-on system is one in which the "bracing" member must have the same shape as the "buckling" member. Such systems can be solved using the ΣP concept. An example application of the ΣP concept is given below.

EXAMPLE - Lean-On Bracing Problem:

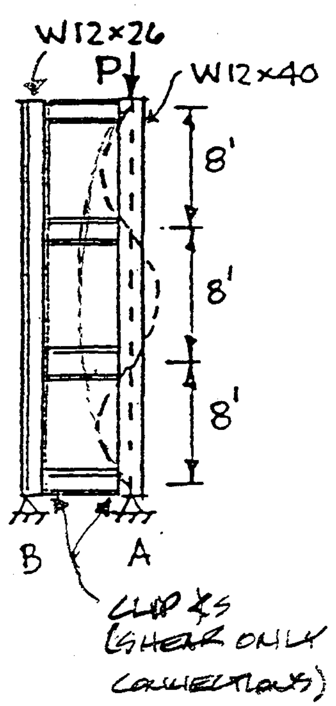

Crane column - Problem

ASD - A36 steel

Is the W12x26 sufficient to fully brace the W12x40?

From AISC Manual $P_{allow} = 217^k$ for L = 8'

ΣP concept: W12x40, A= 11.8 in^2, $I_y = 44.1$ in^4, $r_y = 1.93$

W12x26, A = 7.65, $I_x = 204$ in^4, $r_x = 5.17$

A :

$$\frac{P}{A} = \frac{217}{11.8} = 18.4\text{ksi}, \tau = .301$$

$$P_A = \frac{12}{23}\frac{\pi^2(29000)(44.1)}{(288)^2}(.301) = 24^K$$

B :

$$\tau = 1.0, P_B = \frac{12}{23}\frac{\pi^2(29000)(204)}{(288)^2} = 367^k$$

$$\Sigma P_{cr} = 367 + 24 = 391\text{k} > 217\text{k}$$

$\therefore$Yes, the column is O.K.

A lean-on system relies on the lateral buckling strength of lightly loaded adjacent piles (or pile bents) to laterally support a more heavily loaded pile (or pile bent) when all of the piles (or pile bents) are horizontally tied together. In a lean-on system all piles must buckle simultaneously in sidesway mode of buckling. This is referred to as the ΣP concept and this concept is summarized in Fig. 2.13 and the example problem given in Fig. 2.14.

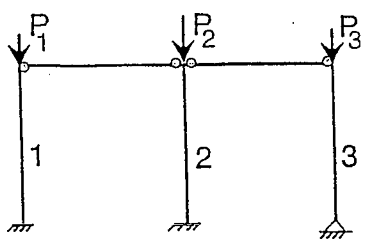

STABILITY CRITERION (FOR SWAY BUCKLING)

$\Sigma P_{cr} > \Sigma P$

service loads in ASD
factored loads in LRFD

Sway Buckling Capacity

$$P_{cr_1} = A \frac{\pi^2 E I_1 \tau_1}{(k_1 L)^2} \quad \text{based on } P_1$$

$$P_{cr_2} = A \frac{\pi^2 E I_2 \tau_2}{(k_2 L)^2} \quad \text{based on } P_2$$

12 / 23 in ASD
0.877 ϕ in LRFD

$$P_{cr_3} = 0$$

Fig. 2.13. Concept for Lean-On Bracing for Sway Buckling Mode (from Yura)

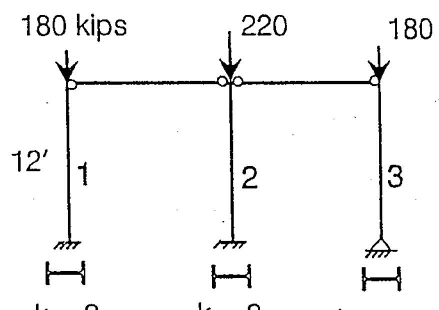

k = 2   k = 2   k = ∞

$\frac{180}{13.3} = 13.5\text{ksi}$ 16.5

$\tau = .830$ .531

all columns W10×45

$F_y = 36$ ksi ASD

$A = 13.3\ \text{in}^2,\ I_x = 248\ \text{in}^4$

$r_x / r_y = 2.15$

$$\frac{12}{23}\frac{\pi^2 (29000)(248)(.83)}{(2 \times 144)^2} = 370 + 237 + 0 = 607 > 580 \text{ kips } OK$$

Fig. 2.14. ASD Example Problem - Is Frame Stable (from Yura)

2.5 Pile Encasement

A typical bridge pile bent with pile encasement requirements and details is shown in Fig. 2.15. Note in the figure that each HP pile is encased for a minimum length of 6 ft. at the original ground or mudline. This encasement length will be longer for piles located in water, and may (where "H" < 13 ft) extend up to the bottom of the bent cap. Also note the light #2 spiral with a 12" pitch used in the encasement. Assuming that the encasement remains in place, i.e., that it doesn't spall off or slip down the pile, it will obviously stiffen the pile and increase its buckling capacity about both axes. However, how much of an increase is not obvious. To establish some bounds and ranges on the increased buckling capacities, limiting cases of I_x and I_y for the two dominant piles used by ALDOT, i.e., for HP 10 x 42 and HP 12 x 53, are determined in Appendix A. Thus limiting case pile cross-section properties are summarized in Table 2.3. It should be noted that the I-values summarized in Table 2.3 do not provide all of the I-values that may be required in an analysis, e.g., no cracking of the concrete was considered. However, they do provide lower bound I-values (uncased values) and upper bound I values (full encased values), and they do provide the reasonable I-values needed to estimate the effects of pile encasements on bent stiffness and stability. It should be noted that pile encasement is one of the primary means employed by ALDOT to stiffen and strengthen existing bridge pile bents.

Because of the light confining spiral reinforcement used in encasing piles (#2 spiral @ 12" pitch), use of the full concrete encasement in an analysis appears to be unconservative. However, the light spiral plus the HP pile may provide confinement for the core concrete, i.e., the concrete within the spiral, and thus we will check partial encased sections for probable composite behavior and enhancement of the pile buckling capacity. A partially encased HP bent pile buckling about its weak and strong axis is shown in Fig. 2.16.

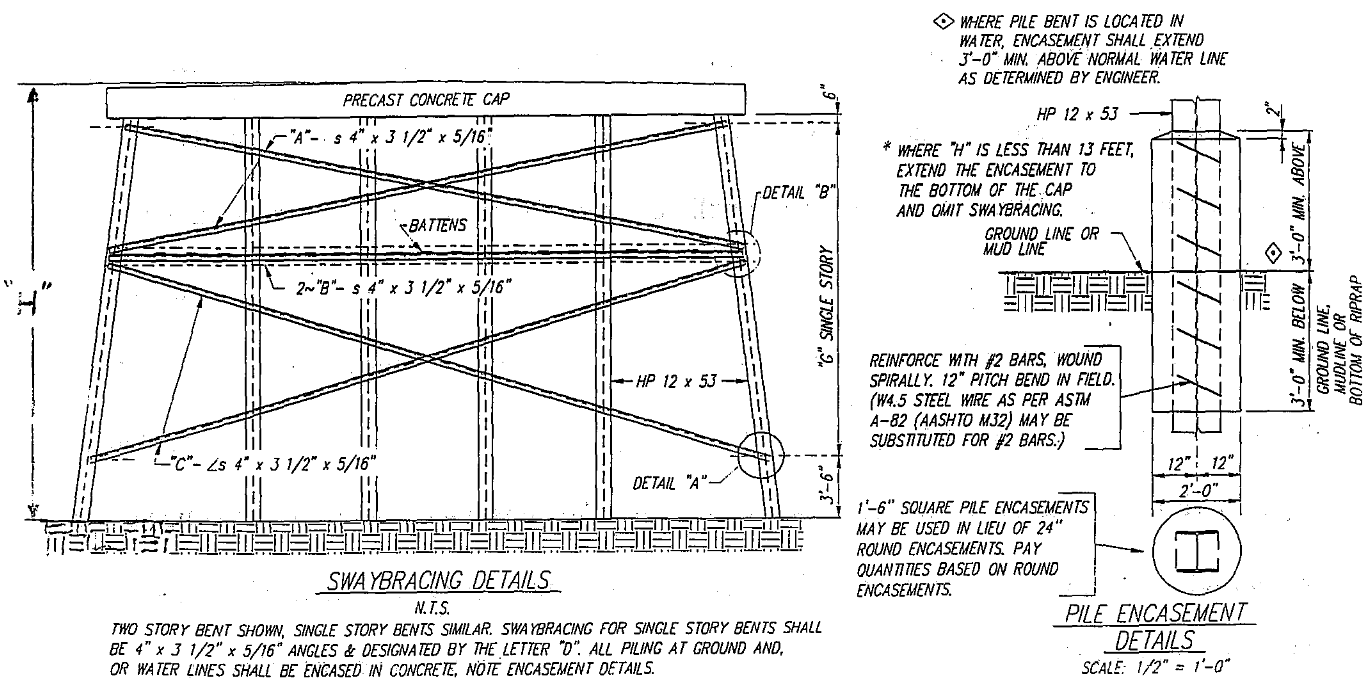

Fig. 2.15. Typical ALDOT Bridge Pile Bent with Pile Encasement Details

Table 2.3. Bent Pile Limiting Case Equivalent All Steel Section Properties

Section	I_x(in^4)	I_y(in^4)	A(in^2)
Uncased			
HP 12 x 53	393	127	15.5
HP 10 x 42	210	71.7	12.4
Full Encased			
HP 12x53 (18"x18")	1351	1095	51.4
HP 10x42 (16"x16")	811	673	40.7
Partial Encased			
HP 12x53	539	311	30.2
HP 10x42	275	159	22.3

Note in Fig. 2.16a that for buckling about the weak axis, the lowest buckling mode and load would be approximately a symmetric mode and thus the member end shears (and shears at every section) would be zero. Thus composite behavior of the HP pile and its encasement is not a problem. For buckling about the strong axis (see Fig. 2.16b), end shears will be developed. To get an estimate of these shears, we will assume a maximum end moment at the bottom of approximately $M_y^{\text{HP section}}$ and a relatively short bent height, $\ell = 16\,\text{ft}$.

Thus, for an HP 10 x 42 pile,

$$M_y = \sigma_y \cdot A_f \cdot d = 36\text{ksi}\left(10.075" \text{ x } 0.42"\right)\left(9.70" - 0.21"\right) = 1446^{"k}$$

$$V_b = V_t = \frac{M_y}{\ell} = \frac{1446^{"k}}{16 \text{ x} 12} = 7.53^k$$

$$\tau_{\text{interface}} \approx \frac{VA'\bar{y}}{I_x b} = \frac{7.53^k \text{ x } \left(10.075" \text{ x } 0.42"\right) \text{x} \left(4.64"\right)}{275^{"4} \text{ x } 9.66"} = 0.055 \text{ ksi}$$

For an HP 12 x 53 pile,

$$M_y = \sigma_y \cdot A_f \cdot d = 36\left(12.045 \text{ x } 0.435\right)\left(11.78 - 0.217\right) = 2182^{"k}$$

$$V_b = V_t = \frac{M_y}{\ell} = \frac{2182^{"k}}{16 \text{ x } 12} = 11.36^k$$

$$\tau_{\text{interface}} \approx \frac{VA'\bar{y}}{I_x b} = \frac{11.36^k \left(12.045" \text{ x } 0.435\right)\left(5.673"\right)}{539^{"4} \text{ x } 11.61"} = 0.054 \text{ ksi}$$

The steel HP pile-concrete encasement interface should be able to sustain the above $\tau_{\text{interface}}$ stresses and thus the partial encased section should act compositely.

Let us now compare the buckling loads for a partially encased and an uncased HP pile. As can be seen in Fig. 2.16, if $I_{xx} = I_{yy}$ of the pile, then buckling about the x-x axes would

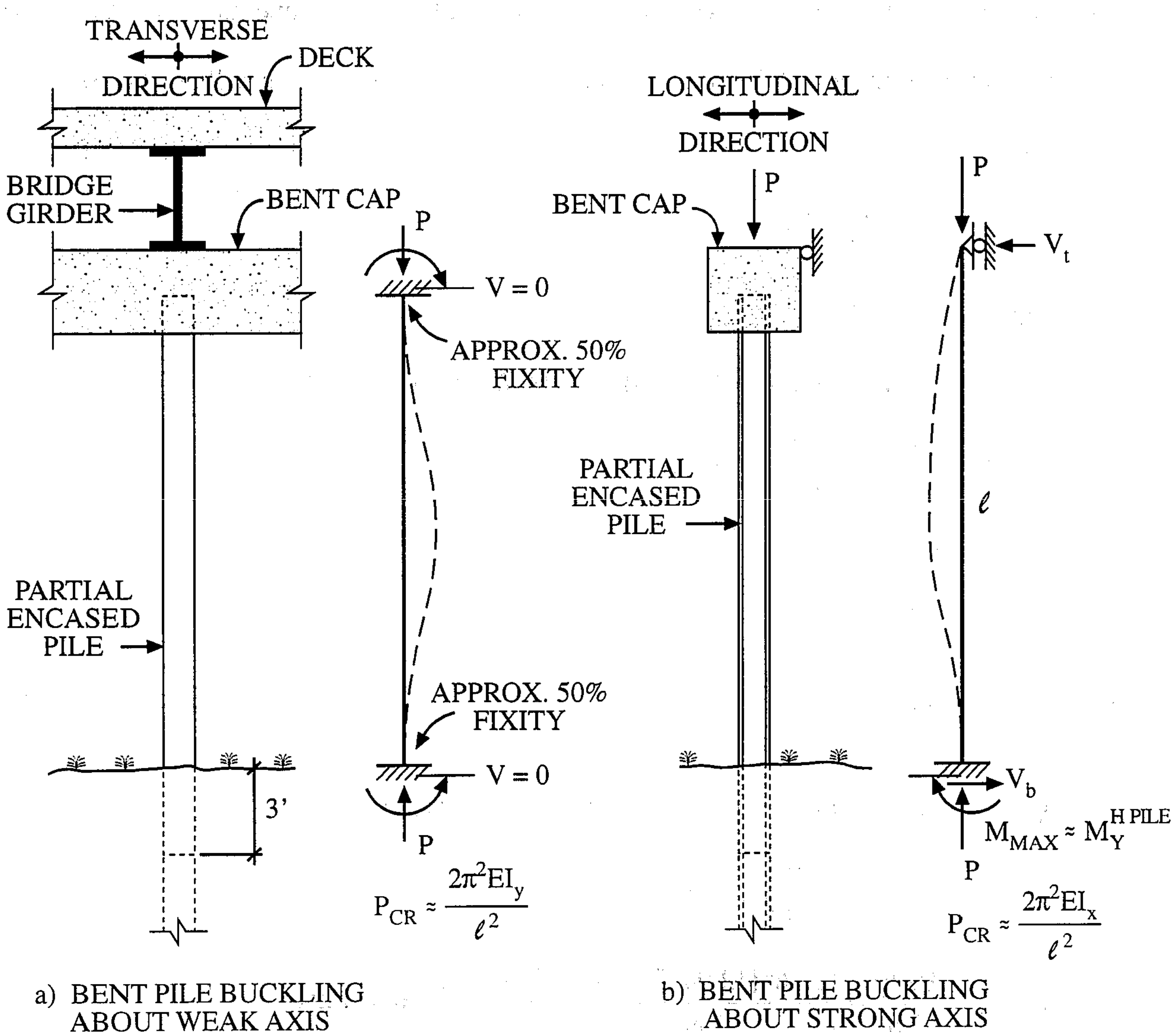

Fig. 2.16. Partial Encased Bent Pile Buckling About Its Weak and Strong Axis

probably control and yield a slightly smaller buckling load than for buckling about the y-y axis. However, as can be seen in Table 2.3, the I_x of the partial encased section is approximately 1.73 times that of I_y. Thus buckling about the weak axis will control.

For the case where the encasement is over the entire bent height and 3 ft. below the ground line as indicated in Fig. 2.16, then using the I_y values from Table 2.3, since P_{CR} varies directly with I.

$$P_{CR}^{\text{partial encased}} = \frac{159}{71.7} P_{CR}^{\text{uncased}} = 2.22\, P_{CR}^{\text{uncased}}\ (\text{for HP10x42 pile})$$

$$P_{CR}^{\text{partial encased}} = \frac{311}{127} P_{CR}^{\text{uncased}} = 2.45\, P_{CR}^{\text{uncased}}\ (\text{for HP12x53 pile})$$

For the case where we start with a partial cased pile over the entire bent height and 3 ft. below ground and then scour begins to occur, P_{CR} values for the resulting changes in ℓ and step change in I of the pile were calculated using Table34 from Roark's Formulas for Stress and Strain (7) and are shown in Table 2.4. The applicable case from Roark's Table 34 is Case 1e (except it is upside-down) and this is shown in Table 2.5. Note that Table 2.5 if for stepped straight bars with both ends fixed. As indicated in Fig. 2.16a, for a bent pile buckling about its weak axis, the end is assumed to have 50% fixity. Thus the values of $P_{CR\text{-encased}}$ and $P_{CR\text{-unencased}}$ in Table 2.4 should be reduced by one-half. However, the ratios of $P_{encased}$ to $P_{unencased}$ shown on the bottom line of Table 2.4 are correct, and these ratios indicate a significant buckling strengthening of the piles via the encasement.

Table 2.4. P_{CR} for Uncased and Partially Cased HP 10 x 42 Piles as Scour Occurs

Scour Case	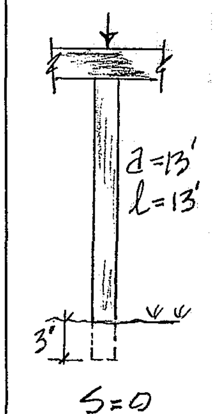	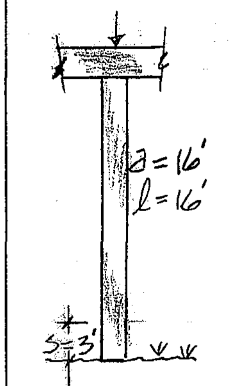	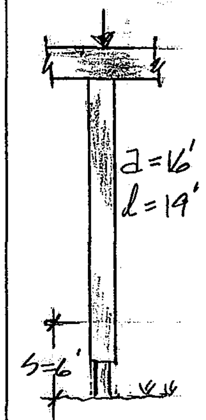	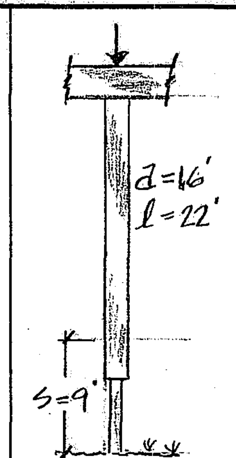	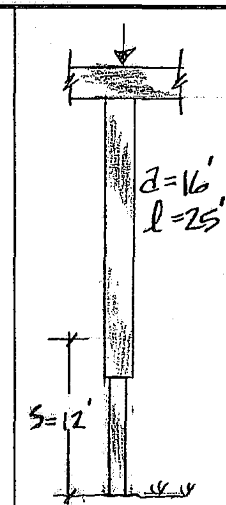	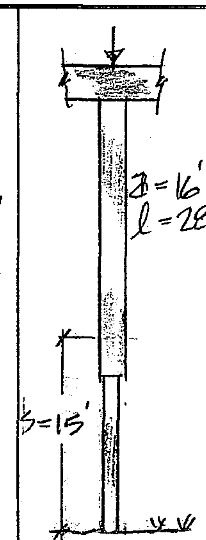	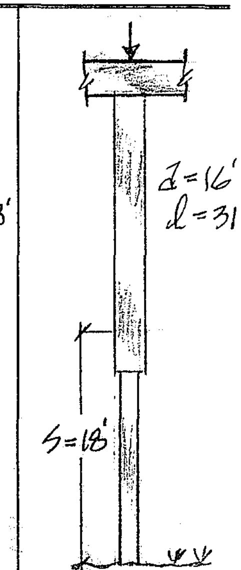
a/ℓ	-	1.0	0.84	0.73	0.64	0.57	0.52
E_2I_2/E_1I_1	-	2.0	2.0	2.0	2.0	2.0	2.0
P_2/P_1	-	0	0	0	0	0	0
$K^{(a)}$	-	7.20	6.84	6.60	6.46	5.73	5.38
$P^{(b)}_{CR\text{-}Encased}$	7480^k	4008^k	2700^k	1943^k	1473	1042^k	798^k
$P^{(c)}_{CR\text{-}unencased}$	3373	2227	1579	1178	912	727	593
$P^{Encased}_{CR} / P^{Unencased}_{CR}$	2.22	1.80	1.71	1.65	1.62	1.43	1.35

Table 2.5. Case le from Roark's Table 34 (7)

1e. Stepped straight bar under end load P_1 and intermediate load P_2; both ends fixed

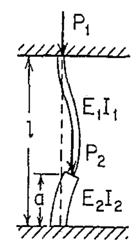

$$P_1' = K_1 \frac{\pi^2 E_1 I_1}{l^2}$$ where K_1 is tabulated below

P_1' = CRITICAL LOAD
E = MODULUS OF ELASTICITY
I = MOMENT OF INERTIA ABOUT CENTROIDAL AXIS PERPENDICULAR TO PLANE OF BUCKLING

E_2I_2/E_1I_1	1.000					1.500					2.000				
a/l / P_2/P_1	$\frac{1}{6}$	$\frac{1}{3}$	$\frac{1}{2}$	$\frac{2}{3}$	$\frac{5}{6}$	$\frac{1}{6}$	$\frac{1}{3}$	$\frac{1}{2}$	$\frac{2}{3}$	$\frac{5}{6}$	$\frac{1}{6}$	$\frac{1}{3}$	$\frac{1}{2}$	$\frac{2}{3}$	$\frac{5}{6}$
0.0	4.000	4.000	4.000	4.000	4.000	4.389	4.456	4.757	5.359	5.462	4.657	4.836	5.230	6.477	6.838
0.5	3.795	3.298	3.193	3.052	2.749	4.235	3.756	3.873	4.194	3.795	4.545	4.133	4.301	5.208	4.787
1.0	3.572	2.779	2.647	2.443	2.094	4.065	3.211	3.254	3.411	2.900	4.418	3.568	3.648	4.297	3.671
2.0	3.119	2.091	1.971	1.734	1.414	3.679	2.459	2.459	2.452	1.968	4.109	2.766	2.782	3.136	2.496
4.0	2.365	1.388	1.297	1.088	0.857	2.921	1.659	1.649	1.555	1.195	3.411	1.882	1.885	2.008	1.523
8.0	1.528	0.826	0.769	0.623	0.479	1.943	1.000	0.992	0.893	0.671	2.334	1.138	1.141	1.158	0.854

2.6 Effect of Soil Subgrade Modulus on Pile Buckling Load

H. Granholm (1) developed an analytical solution for a pile partially embedded in a soil supporting medium as indicated in Fig. 2.17. The analytical solution below is an abridged version of Granholm's work.

The differential equation for the lower part of the pile elastic curve in Fig. 2.17. is

$$EI\frac{d^4y}{dx^4}+P\frac{d^2y}{dx^2}+cy=0 \qquad (2.15a)$$

This equation indicates that the load intensity perpendicular to the axis of the pile is equal to the sum of the soil reaction pressure cy and an additional amount $P\frac{d^2y}{dx^2}$ due to the axial load and curvature of the pile. If we divide through by EI, Eq (2.15a) takes the form.

$$\frac{d^4y}{dx^4}+k^2\frac{d^2y}{dx^2}+a^4y=0 \qquad (2.15b)$$

where $k^2=\frac{P}{EI}$ and $a^4=\frac{c}{EI}$ and c = soil stiffness modulus (lb/ft^2). The differential equation for the upper part of the pile elastic curve is obtained from this equation by taking c = 0 and thus a^4 = 0, and,

$$\frac{d^4y}{dx^4}+k^2\frac{d^2y}{dx^2}=0 \qquad (2.16)$$

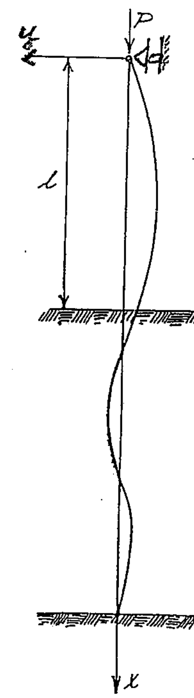

Fig. 2.17 Partially Embedded Pile (1).

By integrating these two equations and observing that the terminal conditions are satisfied, we obtain the condition for the failure by buckling.

The characteristic equation of Eq. (2.15b) has the roots

$$r=\pm\sqrt{-\frac{k^2}{2}\pm\sqrt{-a^4+\frac{k^4}{4}}} \qquad (2.17)$$

The expression $\sqrt{-a^4+\frac{k^4}{4}}$ must be imaginary and thus the roots complex, so that r may be conveniently be written

$$r = \pm h \pm ig, \text{ where}$$

$$2h^2 = -\frac{k^2}{2} + a^2$$

$$2g^2 = \frac{k^2}{2} + a^2$$

The general expression for the complete integral is

$$y = e^{hx}(A \cos gx + B \sin gx) + e^{-hx}(C \cos gx + D \sin gx) \tag{2.18}$$

The undamped terms in Eqn. (2.18) will disappear rapidly when the length of the pile under the surface of the medium is increased. In most cases, therefore, we may assume that the integral can be written under the form

$$y = e^{-hx}(C \cos gx + D \sin gx) \tag{2.19}$$

This implies that the pile is supposed to be of infinite length. The terminal conditions at the tip then vanish and the constants of integration C and C are determined by the conditions at the surface for the lower elastic curve. The elastic curve of the pile below ground will thus form a damped curve of sines.

The equation for the free upper part of the pile leads to a characteristic equation

$$r^4 + k^2r^2 = 0$$

with the roots $r = \pm i k$ and $r = 0$. The last is a double root, so that the integral is

$$y = A_1 + B_1x + C_1 \cos kx + D_1 \sin kx \tag{2.20}$$

If we assume the top of the pile to be hinged, i.e., hinged at $x = 0$ as shown in Fig. 2.17, the two terminal conditions that deflection and bending moment shall vanish for $x = 0$ lead to

$$A_1 = C_1$$

and thus

$$y = B_I x + D_I \sin kx \tag{2.21}$$

To establish the condition of buckling of the whole pile, the relation between the arbitrary constants of integration C, D, and B_I and C_I in Eqns. (2.19) and (2.21) must be fixed. It is obvious that the values of y as given in Eqns. (2.19) and (2.21), as well as the values of their first, second and third derivatives, must coincide at the surface of the medium. To these conditions we shall refer in the following under the name of conditions of continuity. Omitting all intermediate calculations and differentiations we thus obtain, if we put $x = \ell$ in Eqn. (2.21) and its derivatives and x = 0 in Eqn. (2.19) and its derivatives, the following equations:

$$\begin{aligned}
&B_I\, l + D_I \sin kl - C &&= 0\\
&B_I + D_I\, k \cos kl + C\, h - Dg &&= 0\\
&-D_I\, k^2 \sin kl - C(h^2 - g^2) + D2hg &&= 0\\
&-D_I\, k^3 \cos kl - C\, h\,(3g^2 - h^2) - Dg(3h^2 - g^2) &&= 0
\end{aligned} \tag{2.22}$$

The determinantal equation formed from this system of equations

$$\begin{vmatrix} 1 & \sin kl & -I & 0 \\ I & k \cos kl & h & -g \\ 0 & -k^2 \sin kl & -(h^2 - g^2) & 2\,hg \\ 0 & -k^3 \cos kl & -h(3g^2 - h^2) & -g\,(3h^2 - g^2) \end{vmatrix} = 0 \tag{2.23}$$

expresses the condition of buckling. Developing the determinant, we obtain for the computation of the critical load

$$\tan\, kl = kl \cdot \frac{I - \left(\frac{kl}{al}\right)^2 - \frac{I}{al}\left(\frac{kl}{al}\right)^2 \sqrt{2 - \left(\frac{kl}{al}\right)^2}}{I + \left(\frac{kl}{al}\right)^2 - \left(\frac{kl}{al}\right)^4 + al\left(\frac{kl}{al}\right)^2 \sqrt{2 - \left(\frac{kl}{al}\right)}} \tag{2.24}$$

Eqn. (2.24) is similar to the equation obtained when treating Euler's fixed-pinned column, i.e.,

$$\tan\, kl = kl$$

If we assume al to be infinitely great, i.e., if the medium is supposed to be absolutely rigid, Eqn. (2.24) is changed into Euler's equation for a fixed-pinned column which is thus obtained as a special case.

A well-known graphical construction is applied for the solution of Euler's equation consisting in the determination of the points of intersection between the curve y = tan kl and the straight line $y = k\ell$. This graphical construction suggests a similar procedure for solving Eqn. (2.24). The simplest way to find its roots for various values of al is to determine the point of intersection between y = tan kl and the curve that is represented by the right hand member of the equation as indicated in Fig. 2.18.

After thus determining the roots of the equation for a series of values of al we can graphically represent kl as a function of al. For kl we introduce the denomination <u>factor of buckling</u>. In Fig. 2.19 the relation between the <u>factor of buckling</u> and al is shown graphically. With knowledge of the <u>factor of buckling</u>, we can determine the critical load P from the relation

$$P_{CR} = \overline{k\ell}^{\,2}\, \frac{EI}{l^2} \tag{2.25}$$

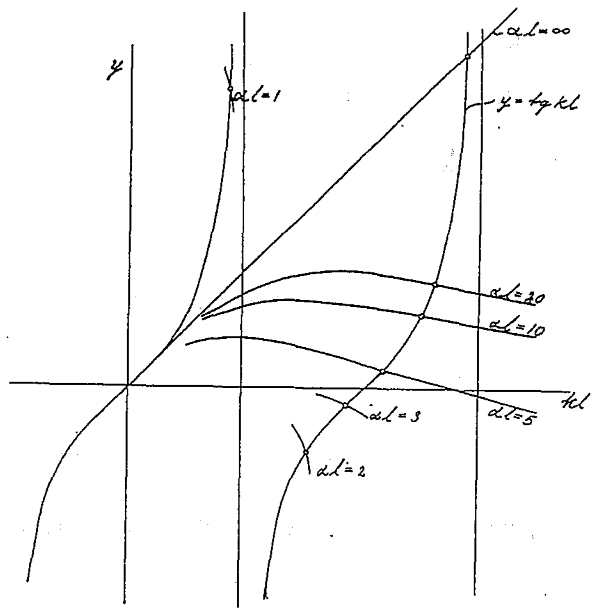

Fig. 2.18. Graphical Solution of Eqn. (2.24) (1).

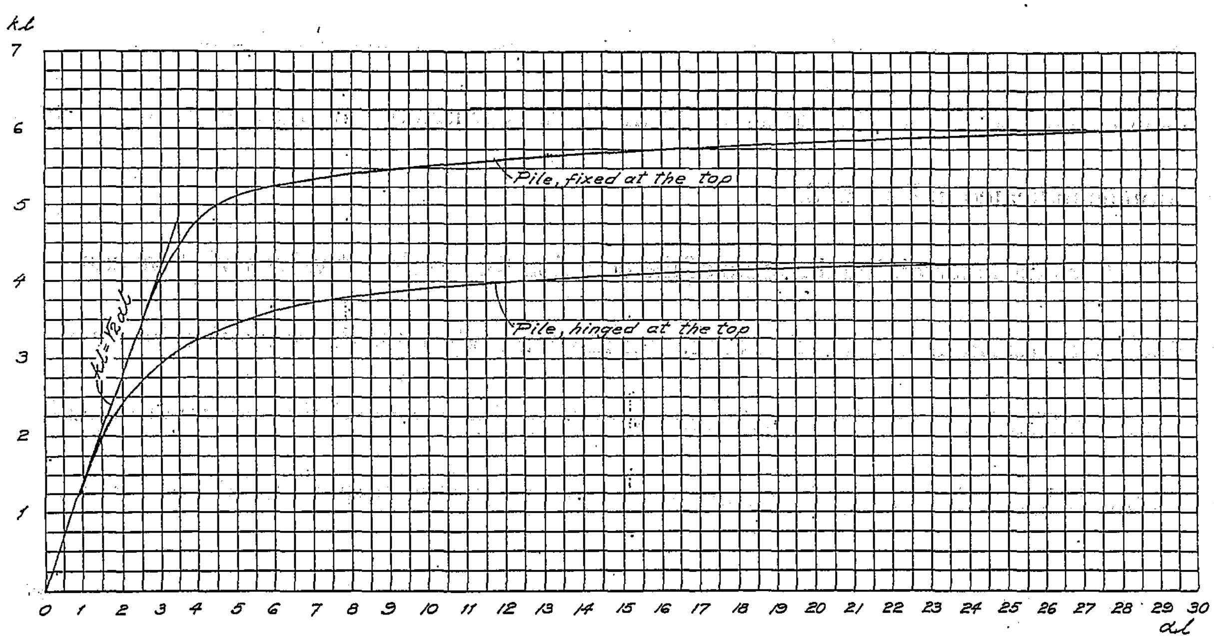

Fig. 2.19. Relation Between al and kl for Pile Hinged and Fixed at Top (1)

Note, by definition

$$(kl)^2 = \frac{P}{EI} l^2$$

or,

$$P_{CR} = (kl)^2 \frac{EI}{l^2} = \overline{k\ell}^2 \frac{EI}{\ell^2}$$

For increasing values of al, the <u>factor of buckling</u>, kl, approaches asymptotically the value 4.49 (approximately = $\pi\sqrt{2}$), which means that the critical load for increasing length of the pile or for increasing rigidity of the medium asymptotically approaches the critical load for Euler's fixed-pinned case. At the origin the function has the tangent $kl = al \cdot \sqrt{2}$. The value al = 0 thus corresponds to the load $P = 2a^2 EI$, or, if we introduce the coefficient of lateral displacement c, instead of $P = 2a^2 EI$, we obtain

$$P = 2\sqrt{cE}$$

This value of P corresponds to the minimum buckling load when a pile is fully embedded (l = 0) in the soil, i.e.,

$$P_{min}^{\text{fully embedded}} = 2\sqrt{CEI_{min}} \tag{2.26}$$

This equation was also derived from the differential equation of bending by Granholm.

Granholm also determined the characteristic equation for the case where the top of the pile in Fig. 2.17 is fixed (rather than pinned), and his results for that condition are also shown in Fig. 2.19.

It will be shown in Chapter 3 that the support conditions for a bent pile buckling in the longitudinal direction, i.e., about its strong axis, are those of a pile hinged at the top in Fig. 2.19. For the same pile buckling in the transverse direction, i.e., about its weak axis, its top is between a pinned and a fixed condition. For this case, values of kl for both the pinned and fixed top could be extracted and the average of these used to estimate P_{CR}.

To gain a feeling of the sensitivity of pile and bent buckling capacity to soil subgrade modulus (k_o) and coefficient of lateral displacement (C) values, let us use Granholm's Fig. 2.19 to determine the buckling load about each axis for two of ALDOT's most widely used bent piles, i.e.,

HP 10x42 ($I_x = 210$ in^4, $I_y = 71.7$ in^4, $A = 12.4$ in^2)

HP 12x53 ($I_x = 393$ in^4, $I_y = 127$ in^4, $A = 15.5$ in^2)

For this sensitivity analysis, we will assume the conditions shown in Fig. 2.20. It should be noted that Earth Tech, Inc. used soil subgrade modulus values of

$k_0 = 28.94, 43.4, 57.9, 86.8, 115.7, 289.4$ lb/in^3

in their analysis with FB Pier. Thus, we have expanded their range of k_0 values at both the low and high ends to provide a range where the high value of k_0 is more than 100 larger than the lower value used.

Recall in Granholm's Eqn. (2.24) for the pile top being pinned that

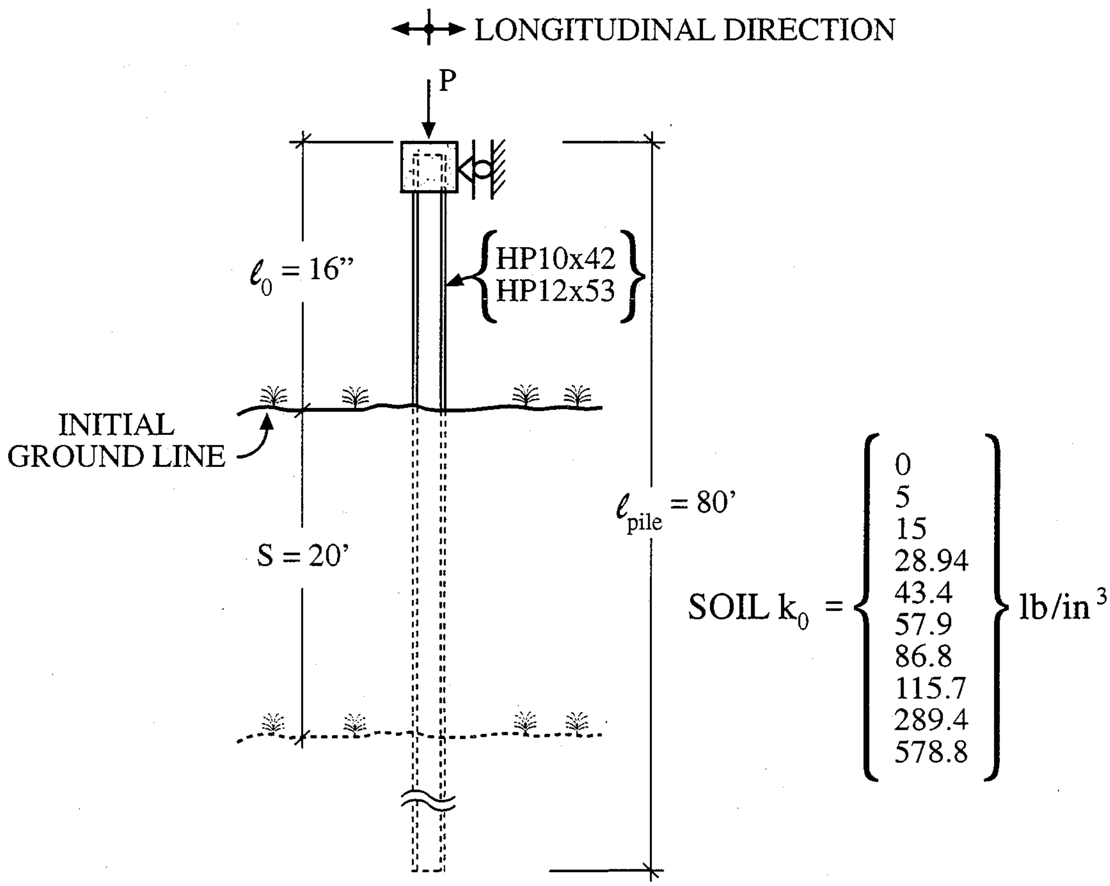

Fig. 2.20. Pile Conditions for Sensitivity Analysis Using Granholm's Equations

$$k = \sqrt{\frac{P}{EI}}$$

$$a = \sqrt[4]{\frac{C}{EI}}$$

$$C = \text{soil coefficient of lateral displacement } (\text{lb}/\text{in}^2)$$

$$C = k_0 b$$

$$k_0 = \text{soil subgrade modulus } (\text{lb}/\text{in}^3)$$

$$b = \text{pile width (in)}$$

For the k_0 values shown in Fig. 2.20 and the pile sizes and lengths above ground (l) shown, al values can be calculated. These were used with Fig. 2.19 to determine the kl values corresponding to buckling and from this the buckling load, P_{CR}. The P_{CR} values for each of the two pile sizes and two directions of buckling are shown in Tables 2.6-2.9 and in Figs. 2.21-2.24.

Note in Tables 2.6 and 2.7 for buckling in the longitudinal direction (about the piles' strong axis) that for $k_0 = 0$, the pile would be a pin-pin column with l = 80 ft. and $P_{CR} = 65^k$ and 122^k respectively. Upper bound values of the buckling load (P_{CR}^{UB}) for l = 16 ft. and l = 36 ft. are given in the footnotes of Tables 2.6 and 2.7 as those for a fixed-pin column. In Tables 2.8 and 2.9 for buckling in the transverse direction (about the pile's weak axis) that for $k_0 = 0$, the pile would be partially fixed at the top by the bent cap (50% fixity was assumed) and pinned at the bottom with l = 80 ft. and $P_{CR} = 33.4^k$ and 59^k respectively. P_{CR} values for assumed conditions of 50% fixity at each end for l = 16 ft. and l = 80 ft. are given in the footnotes of Tables 2.8 and 2.9.

Note in Figs. 2.21-2.24 the rather insensitivity of the pile buckling load, P_{CR}, to the soil subgrade modulus value, k_0. This insensitivity becomes quite extreme as the scour value increases from S = 0 to S = 20 ft. as evident from the figures.

Table 2.6. P_{CR} vs. k_0 for HP 10 x 42. Pile Buckling in Longitudinal Direction or About Strong Axis

k_0 (lb/in³)	$C=k_0b$ (lb/in²)	$C^{1/4}$	$(EI)^{1/4}$	$a = \sqrt[4]{C/EI_s}$ (per in.)	al, l = 16'	al, l = 36'	kl (pin at top), l = 16'	kl (pin at top), l = 36'	$P_{CR} = (kl)^2 EI_s/l^2$ (kips), l = 16'	$P_{CR} = (kl)^2 EI_s/l^2$ (kips), l = 36'
0	0	0	279.4	0	0	0			65*	65*
5	50	2.659	279.4	0.00952	1.83	4.11	2.30	3.25	874	345
15	150	3.500	279.4	0.01253	2.41	5.41	2.65	3.52	1160	405
28.94	289	4.123	279.4	0.01476	2.83	6.38	2.87	3.67	1361	440
43.4	434	4.564	279.4	0.01634	3.14	7.06	2.97	3.73	1457	455
57.9	579	4.905	279.4	0.01756	3.37	7.59	3.05	3.77	1536	46[illegible]
86.8	868	5.428	279.4	0.01943	3.73	8.39	3.18	3.82	1671	477
115.7	1157	5.832	279.4	0.02087	4.01	9.02	3.25	3.87	1745	489
289.4	2894	7.335	279.4	0.02625	5.04	11.34	3.45	3.96	1967	512
578.8	5788	8.722	279.4	0.03122	5.99	13.49	3.62	4.05	2164	536

$(EI)^{1/4} = (29{,}000{,}000 \times 210)^{1/4} = 279.4$

$$^{*}\text{For } k_0 = 0 \rightarrow \ell = 80', P_{CR} = \frac{\pi^2 EI_s}{80^2 \times 12^2} = \frac{\pi^2 \times 29{,}000 \times 210}{6400 \times 144} = 65^k$$

$$P_{CR}^{U.B.} = \frac{20.2 EI_s}{\ell^2} = \frac{20.2 \times 29{,}000 \times 210}{192^2} = 3337^k \rightarrow P_{CR}^{UB} = \frac{20.2 \times 29{,}000 \times 210}{432^2} = 659^k$$

$$P_y = A\sigma_y = 12.4 \times 36 = 446^k$$

Table 2.7. P_{CR} vs. k_0 for HP 12 x 53. Pile Buckling in Longitudinal Direction or About Strong Axis

k_0	$C=k_0b$	$C^{1/4}$	$(EI)^{1/4}$	$a = \sqrt[4]{C/EI_s}$	al		kl (pin at top)		$P_{CR} = (kl)^2 EI_s/l^2$ (kips)	
(lb/in^3)	(lb/in^2)			(per in.)	l = 16'	l = 36'	l = 16'	l = 36'	l = 16'	l = 36'
0	0	0	326.7	0	0	0			122*	122*
5	60	2.783	326.7	0.00852	1.64	3.68	2.15	3.15	1429	606
15	180	3.663	326.7	0.01121	2.15	4.84	2.50	3.43	1933	719
28.94	347	4.316	326.7	0.01321	2.54	5.71	2.73	3.60	2305	792
43.4	521	4.777	326.7	0.01462	2.81	6.32	2.87	3.65	2548	814
57.9	695	5.134	326.7	0.01571	3.02	6.79	2.95	3.71	2692	841
86.8	1042	5.682	326.7	0.01739	3.34	7.51	3.05	3.76	2877	864
115.7	1388	6.104	326.7	0.01868	3.59	8.07	3.13	3.80	3031	882
289.4	3473	7.677	326.7	0.02350	4.51	10.15	3.37	3.90	3513	929
578.8	6946	9.129	326.7	0.02794	5.36	12.07	3.50	4.00	3789	977

$(EI)^{1/4} = (29{,}000{,}000 \text{ x } 393)^{1/4} = 326.7$

$$^{*}\text{For } k_0 = 0 \rightarrow \ell = 80', P_{CR} = \frac{\pi^2 EI_s}{80^2 \text{ x } 12^2} = \frac{\pi^2 \text{ x } 29{,}000 \text{ x } 393}{6400 \text{ x } 144} = 122^k$$

$$P_{CR}^{UB} = \frac{20.2\, EI_s}{\ell^2} = \frac{20.2 \text{ x } 29{,}000 \text{ x } 393}{192^2} = 6245^k \rightarrow P_{CR}^{UB} = \frac{20.2 \text{ x } 29{,}000 \text{ x } 393}{432^2} = 123$$

$$P_y = A\sigma_y = 15.5 \text{ x } 36 = 558^k$$

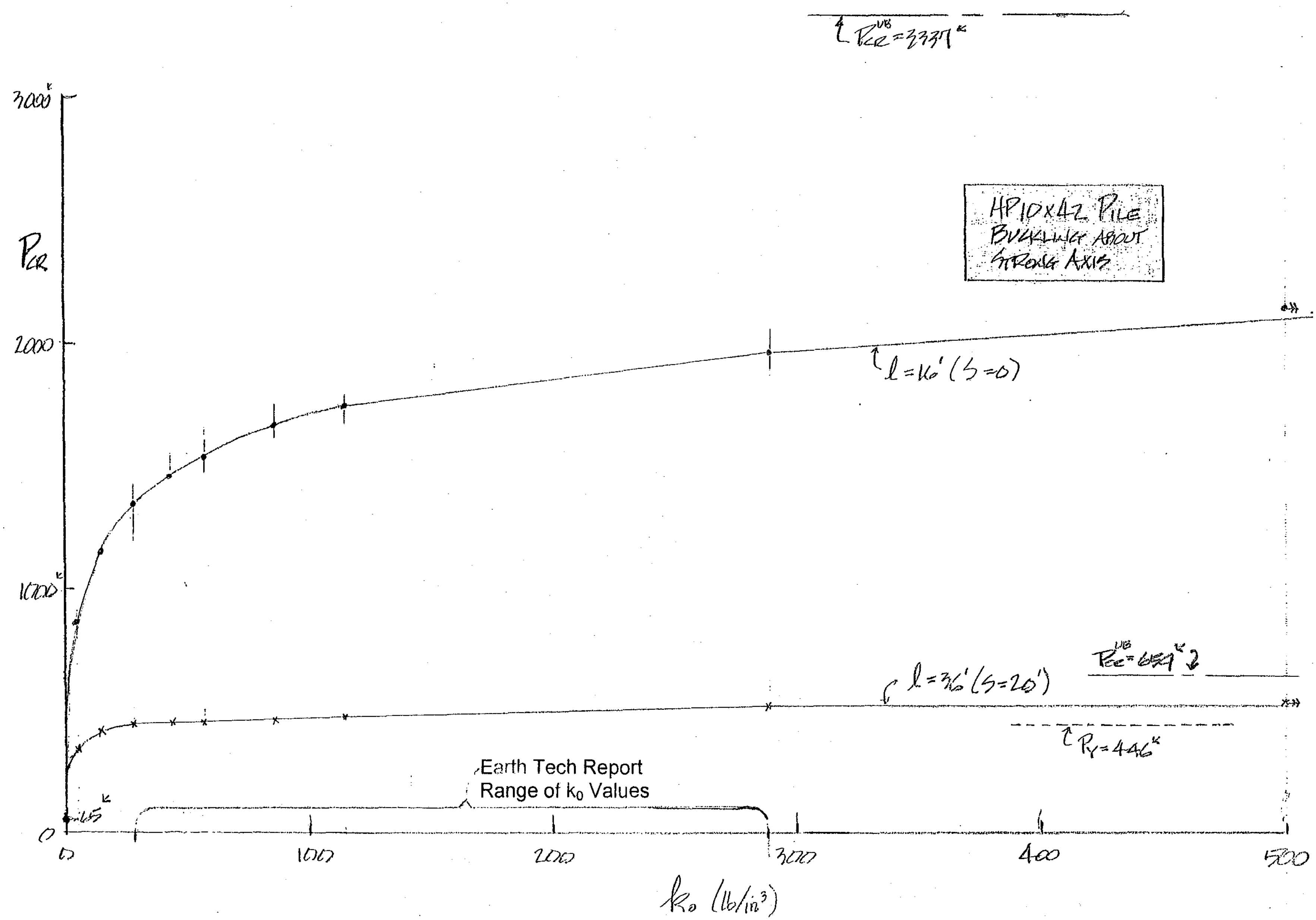

Fig. 2.21. P_{CR} vs. k_0 for HP 10 x 42 Bent Pile Buckling About Strong Axis

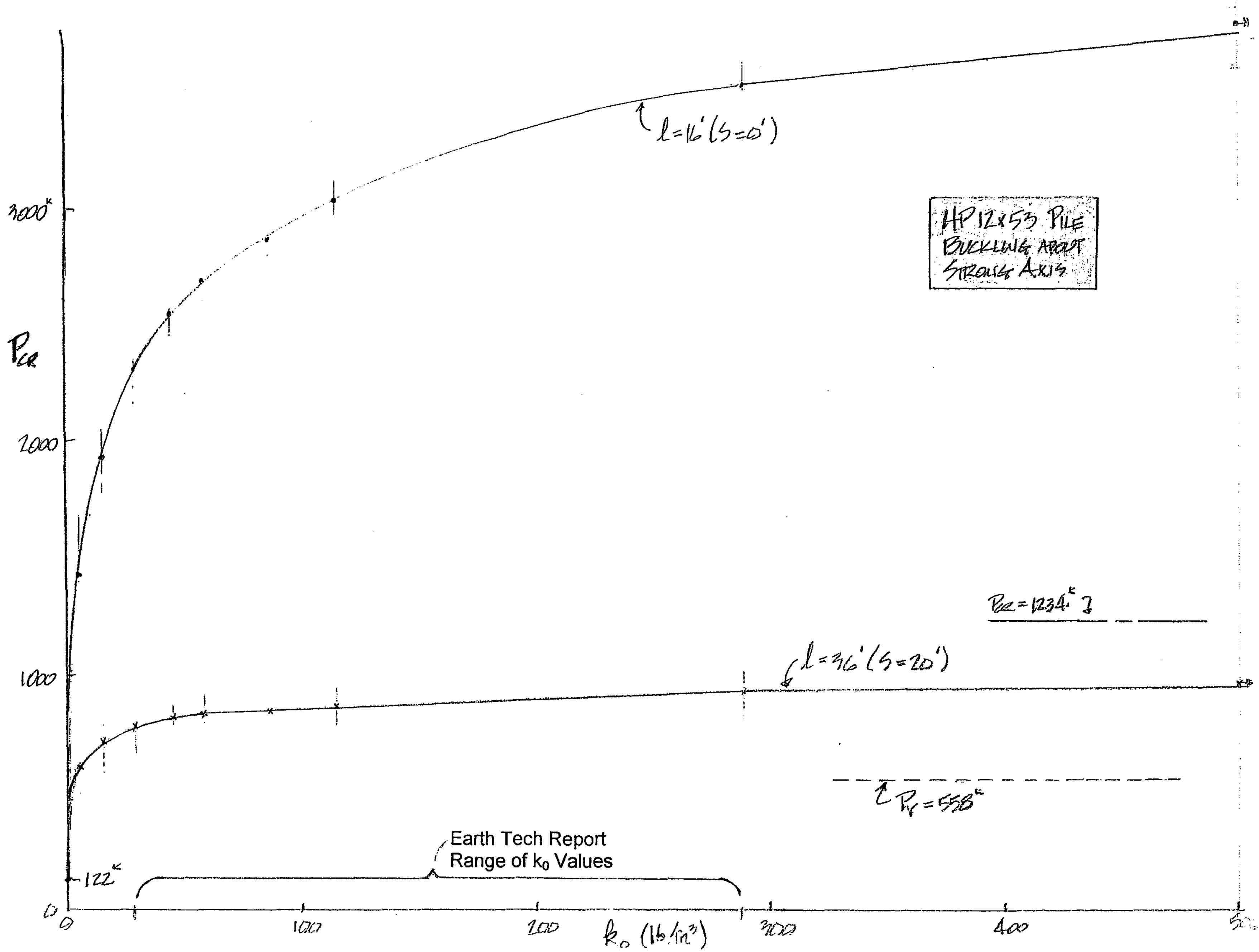

Fig. 2.22. P_{CR} vs. k_0 for HP 12 x 53 Bent Pile Buckling About Strong Axis

Table 2.8. P_{CR} vs. k_0 for HP 10 x 42 Pile Buckling in Transverse Direction or About Weak Axis

k_0 (lb/in³)	$C = k_0 b$ (lb/in²)	$C^{1/4}$	$(EI)^{1/4}$	$a = \sqrt[4]{C/EI_w}$ (per in.)	al		kl (top pinned)		kl (top fixed)		$P_{CR} = (kl)_{ag}^2 EIw/l^2$ (kips)	
					l = 16'	l = 36'	l = 16'	l = 36'	l = 16'	l = 36'	l = 16'	l = 36'
0	0	0	213.54	0	0	0					33*	33*
5	50	2.659	213.54	0.01245	2.39	5.38	2.52	3.52	3.30	5.19	478	211
15	150	3.500	213.54	0.01639	3.15	7.08	2.97	3.74	4.12	5.37	709	231
28.94	289	4.123	213.54	0.01931	3.71	8.34	3.15	3.82	4.65	5.45	858	239
43.4	434	4.564	213.54	0.02137	4.10	9.23	3.25	3.87	4.85	5.50	925	245
57.9	579	4.905	213.54	0.02297	4.41	9.92	3.32	3.92	4.97	5.53	969	249
86.8	868	5.428	213.54	0.02542	4.88	10.98	3.45	3.96	5.12	5.58	1036	254
115.7	1157	5.832	213.54	0.02731	5.24	11.80	3.50	4.00	5.17	5.62	1060	258
289.4	2894	7.335	213.54	0.03435	6.60	14.84	3.70	4.08	5.31	5.72	1145	268
578.8	5788	8.722	213.54	0.04084	7.84	17.64	3.80	4.16	5.40	5.78	1194	275

$(EI)^{1/4} = (29{,}000{,}000 \times 71.7)^{1/4} = 213.54$

$$* \text{ For } k_0 = 0 \rightarrow l = 80', P_{CR} = \frac{1.5\pi^2 EI_w}{80^2 x 12^2} = \frac{1.5 x \pi^2 x 29{,}000 x 71.7}{6400 x 144} = 33.4^k$$

$$P_{CR}^{50\%\text{ fixity each end}} \approx \frac{2\pi^2 EI_w}{\ell^2} = \frac{2\pi^2 x 29{,}000 x 71.7}{192^2} = 1114^k \rightarrow P_{CR}^{50\%\text{ fix each end}} = \frac{2\pi^2 x 29{,}000 x 71.7}{432^2} = 220^k$$

$$P_y = \sigma_y A = 446^k$$

Table 2.9. P_{CR} vs. k_0 for HP 12 x 53 Pile Buckling in Transverse Direction or About Weak Axis

k_0 (lb/in³)	$C = k_0 b$ (lb/in²)	$C^{1/4}$	$(EI)^{1/4}$	$a = \sqrt[4]{C/EI_w}$ (per in.)	al		kl (top pinned)		kl (top fixed)		$P_{CR}=(kl)^2_{avg}EIw/l^2$ (kips)	
					l = 16'	l = 36'	l = 16'	l = 36'	l = 16'	l = 36'	l = 16'	l = 36'
0	0	0	246.35	0	0	0					59*	59*
5	60	2.783	246.35	0.01130	2.17	4.88	2.53	3.45	3.00	5.12	764	362
15	180	3.663	246.35	0.01487	2.86	6.42	2.87	3.67	3.90	5.31	1145	398
28.94	347	4.316	246.35	0.01752	3.36	7.57	3.07	3.76	4.37	5.42	1383	416
43.4	521	4.777	246.35	0.01939	3.72	8.38	3.17	3.84	4.64	5.46	1523	427
57.9	695	5.134	246.35	0.02084	4.00	9.00	3.24	3.87	4.80	5.50	1615	433
86.8	1042	5.682	246.35	0.02306	4.43	9.96	3.34	3.91	4.98	5.53	1729	440
115.7	1388	6.104	246.35	0.02478	4.76	10.70	3.40	3.94	5.15	5.56	1826	445
289.4	3473	7.677	246.35	0.03116	5.98	13.46	3.62	4.04	5.26	5.68	1970	466
578.8	6946	9.129	246.35	0.03706	7.12	16.01	3.74	4.12	5.37	5.75	2073	481

$(EI)^{1/4} = (29{,}000{,}000 \times 127)^{1/4} = 246.35$

$$\text{*For } k_0 = 0 \rightarrow \ell = 80', P_{CR} = \frac{1.5\pi^2 EI_w}{80^2 x 12^2} = \frac{1.5\pi^2 x 29{,}000 x 127}{6400 \times 144} = 59^k$$

$$P_{CR}^{50\%\text{ Fixity Each End}} \approx \frac{2\pi^2 EI_w}{\ell^2} = \frac{2\pi^2 \times 29{,}000 \times 127}{192^2} = 1972^k \Rightarrow P_{CR}^{50\%\text{ Fix Each End}} = \frac{2\pi^2 \times 29{,}000 \times 127}{432^2} = 390^k$$

$P_Y = 558^k$

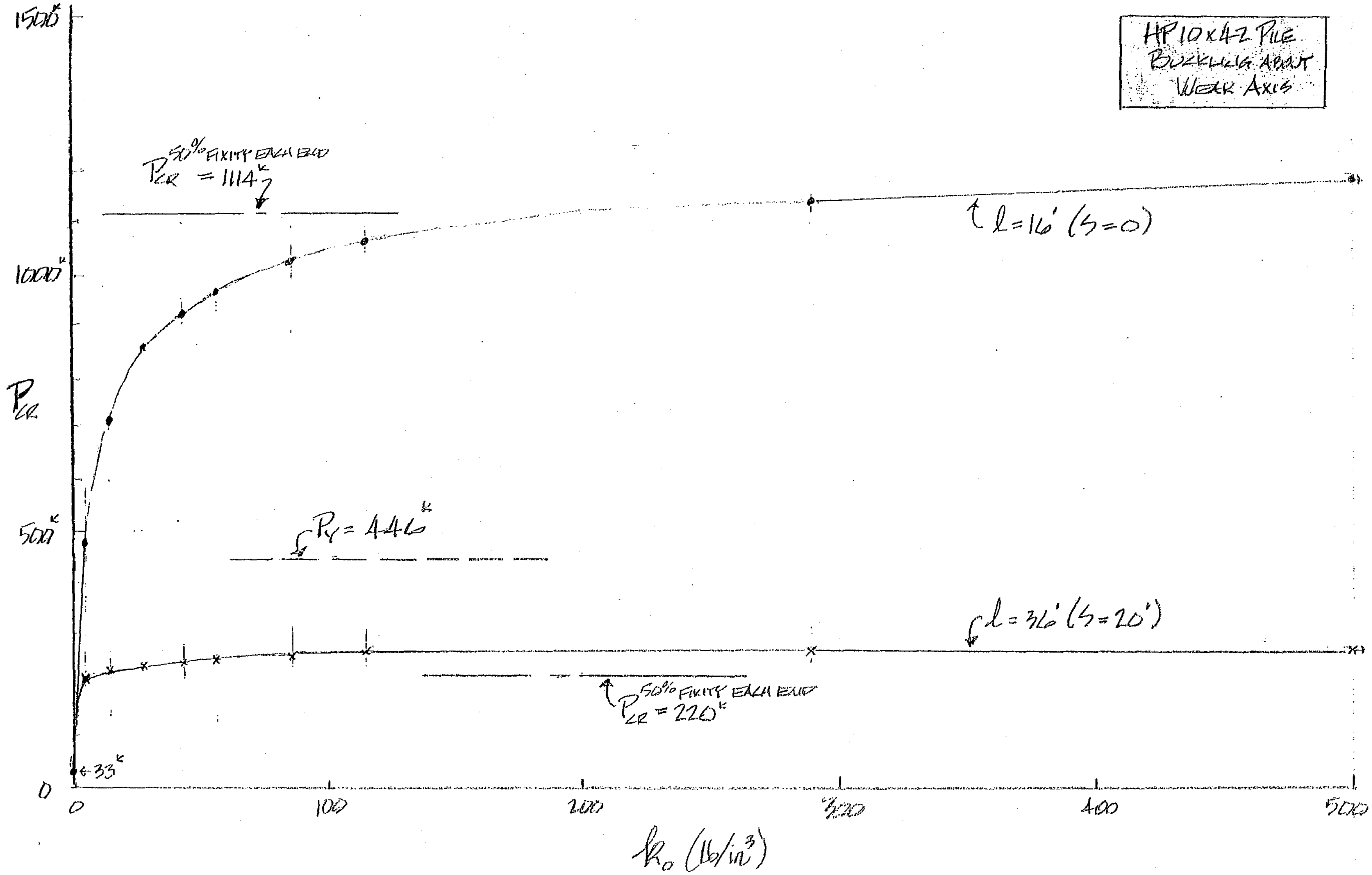

Fig. 2.23. P_{CR} vs. k_o for HP 10 x 42 Bent Pile Buckling About Weak Axis

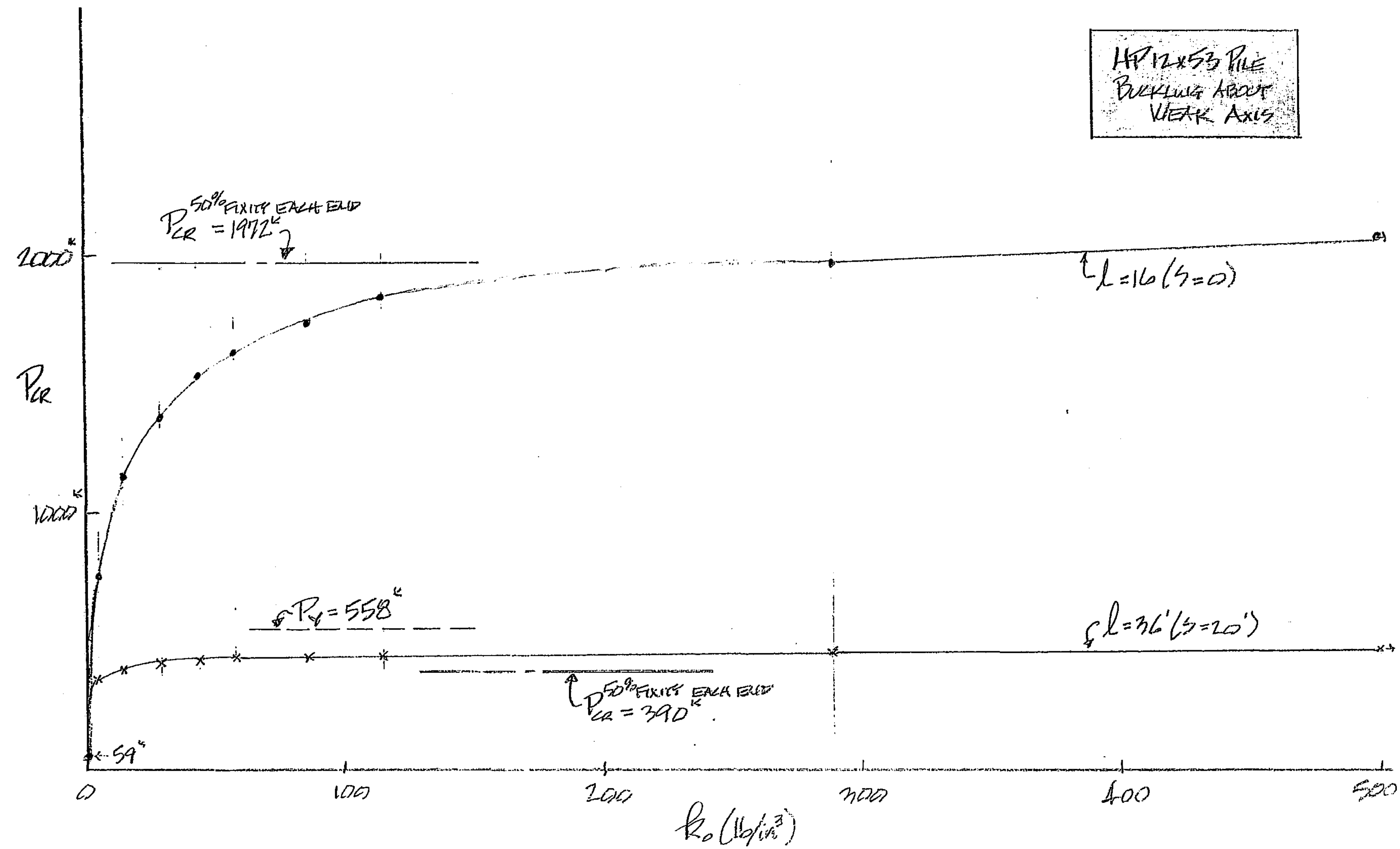

Fig. 2.24. P_{CR} vs. k_o for HP 12 x 53 Bent Pile Buckling About Weak Axis

3. FAILURE MODES OF BRIDGE PILE BENTS DURING EXTREME SCOUR EVENTS

3.1 General

A typical bridge pile bent used by the ALDOT is shown in Fig. 3.1. Possible failure modes for such bents in a major flood/scour event are listed below and shown graphically in Fig. 3.2.

1. Buckling of Bent Piles in Longitudinal Direction (P_{CR}^{X-Axis})
2. Buckling of Bent Piles in Transverse Direction (P_{CR}^{Y-Axis})
3. Crushing/Yielding of Piles
4. Plunging Failure of Piles
5. Failure of Bent Cap
6. Local Yielding of Bent Piles (Due to $\sigma_Z = -\frac{P}{A} \pm \frac{M_x Y}{I_X} \pm \frac{M_y X}{I_Y}$)

Bridge superstructure and bent cap maximum possible sidesway displacements vary from bridge to bridge, and are different in the transverse and longitudinal directions. Limiting cases for each of these two principle directions of interest are discussed in the ensuing sections.

It should be noted that all piles in the bent must fail in modes 1-4 above to have a bent failure as each pile will get lean-on support from the adjacent piles if it reaches its failure load first, i.e.,

$$P_{failure}^{Bent} = \sum_{1}^{No.Piles} P_{failure}^{Pile} \tag{3.1}$$

Note further that the first two failure modes (piles buckling about their strong or weak axis) are quite possible during a major scour event since the buckling capacities vary as the inverse of the

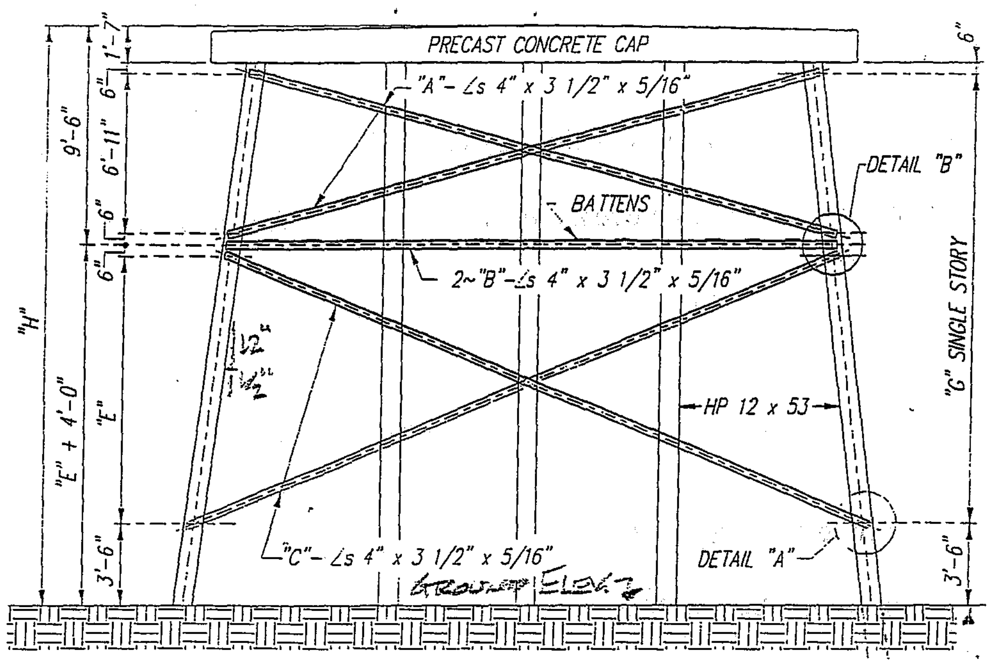

Fig. 3.1. Typical ALDOT Bridge Pile Bent

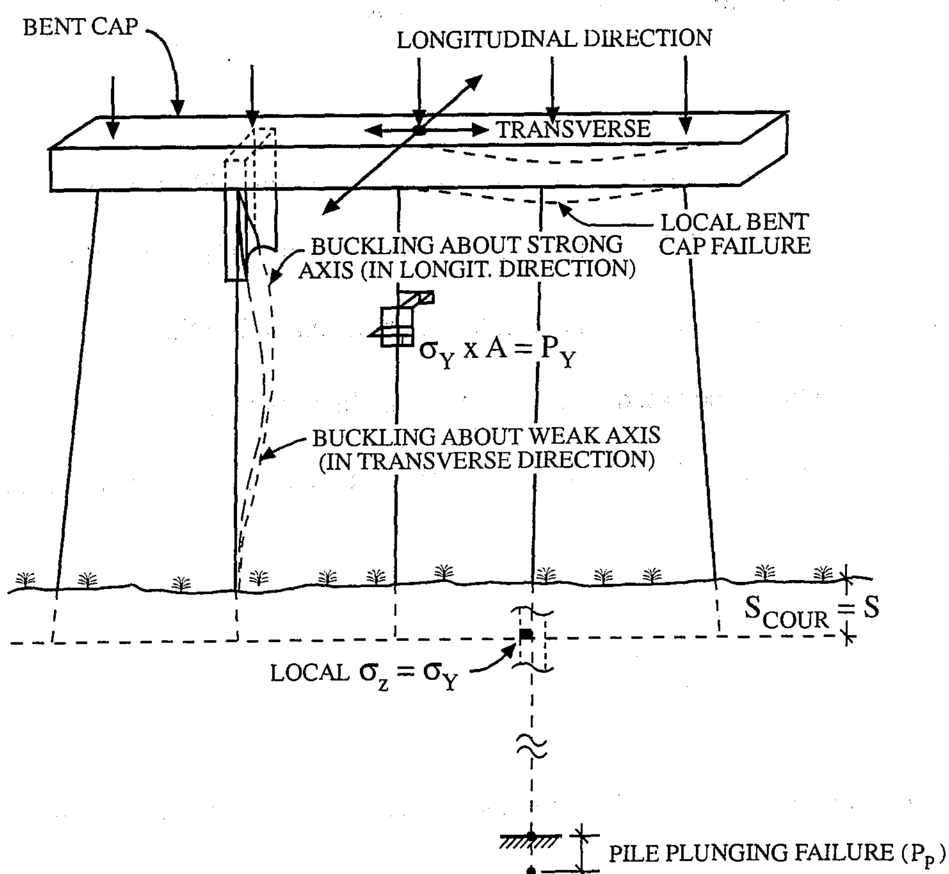

Fig. 3.2. Possible Failure Modes for Bridge Pile Bents

square of the pile length above ground. This length will dramatically increase due to scour. Crushing/yielding of the pile will not be possible since the scour event does not change $P_{applied}$ or P_Y of the pile. Plunging of the pile due to inadequate soil support of the pile is possible but quite unlikely since all that is being lost during the scour event is the soil frictional resistance of the soil scoured away. This should be a rather small percent of the pile resistance capacity. Failure of the bent cap is unlikely due to the superstructure girders sitting directly above the piles. An individual pile would need to plunge or buckle to significantly stress and possibly fail the bent cap. Even in this case, the cap is unlikely to fail as will be shown in Section 3.6. Local yielding of the HP piling near the new ground line (after the scour event) due to $\sigma_Z = -\frac{P}{A} \pm \frac{M_X Y}{I_X} \pm \frac{M_Y X}{I_Y}$ stresses is quite possible. However, such local point yielding can be tolerated and will not have serious consequences. Each of the failure modes above is examined and discussed in greater detail in the ensuing sections.

3.2 Bent Pile Buckling in Longitudinal Direction

Maximum possible longitudinal displacements of bridge superstructures and bent caps depends on the thermal expansion joint spacing included in the bridge superstructure. For example, for the 272' long (made continuous for LL) span shown in Fig. 3.3, the 1 ½" expansion joint space between continuous spans appears to be quite realistic and good. If a 816' span bridge is made up of three such continuous spans, as indicated in Fig. 3.4, then the first bent (see Fig. 3.4) will have the largest longitudinal movement or sidesway possible and will be 4 ½" for the bridge of Fig. 3.4.

For simple span bridges, the maximum possible longitudinal sidesway will also be the first bent (see Fig. 3.5) and will be 1 ½" for the seven span example bridge illustrated in Fig. 3.5.

Figure 3.6 makes use of an approximate equation to estimate the buckling load for buckling in the longitudinal direction for three cases,

Case I - Sidesway

Case II - No Sidesway

Case III - Limited Sidesway

It should be noted that the sidesway mode of buckling is possible during the construction of the bridge before all spans are in place and connected to the abutments. Because of the sizeable construction loads, i.e., cranes, concrete trucks, etc. that may get on the partially constructed bridge during this phase, the structural design of the pile bents for stability is probably controlled

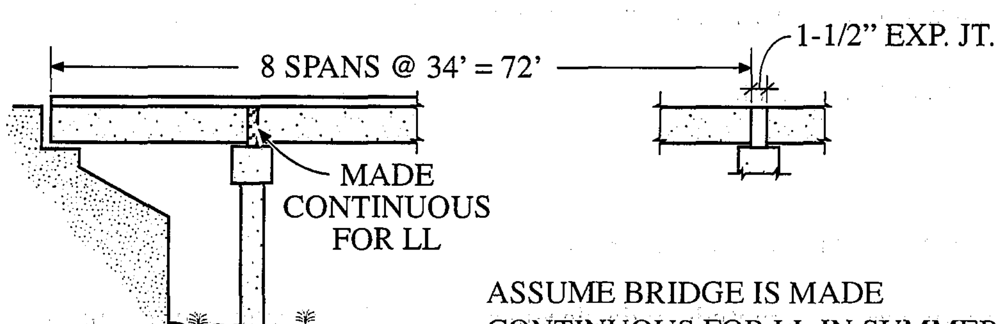

ASSUME BRIDGE IS MADE CONTINUOUS FOR LL IN SUMMER WITH TEMP CONC. = 85°F

$\Delta_{temp} = \alpha \Delta T L$

ASSUME IN WINTER AFTER A MAJOR FLOOD/SCOUR EVENT, THE TEMP DROPS TO 30°F

$\therefore \Delta T = 55°F$

$= 6 \times 10^{-6k/1C/°F} \times 55°F \times 272' \times 12"$

$= 1.08'$ ➡ S_{AY} 1.10" ($\therefore$ 1-1/2" EXP. JT IS GOOD)

Fig. 3.3. Thermal Expansion/Contraction for 272' Span

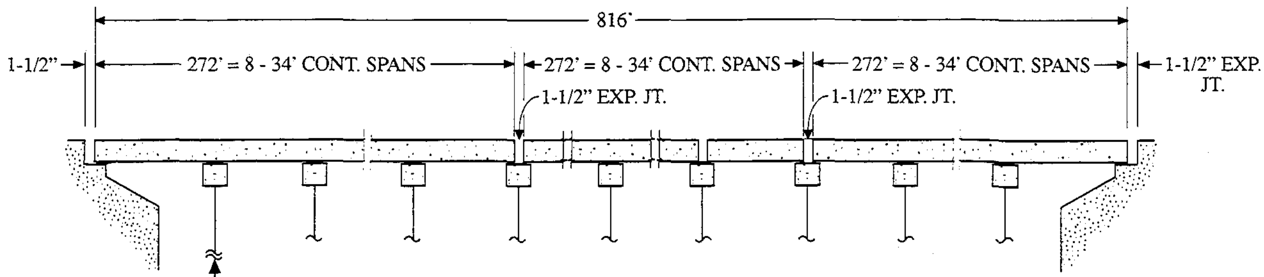

THIS 1ST BENT WILL HAVE LARGEST LONGITUDINAL MOVEMENT WHICH WILL BE,

$$\Delta_L^{MAX} = \sum_{i=1}^{\text{NO. EXP. JTS.}} \text{EXP. JT. CL. SPACE} + \text{CL. SPACE AT ONE ABUT.}$$

FOR BRIDGE ABOVE,

$$\Delta_L^{MAX} = \sum_{1}^{2} 1\text{-}1/2'' + 1\text{-}1/2'' = 4\text{-}1/2''$$

Fig. 3.4. Maximum Longitudinal Sidesway for 816' Continuous Span Bridge

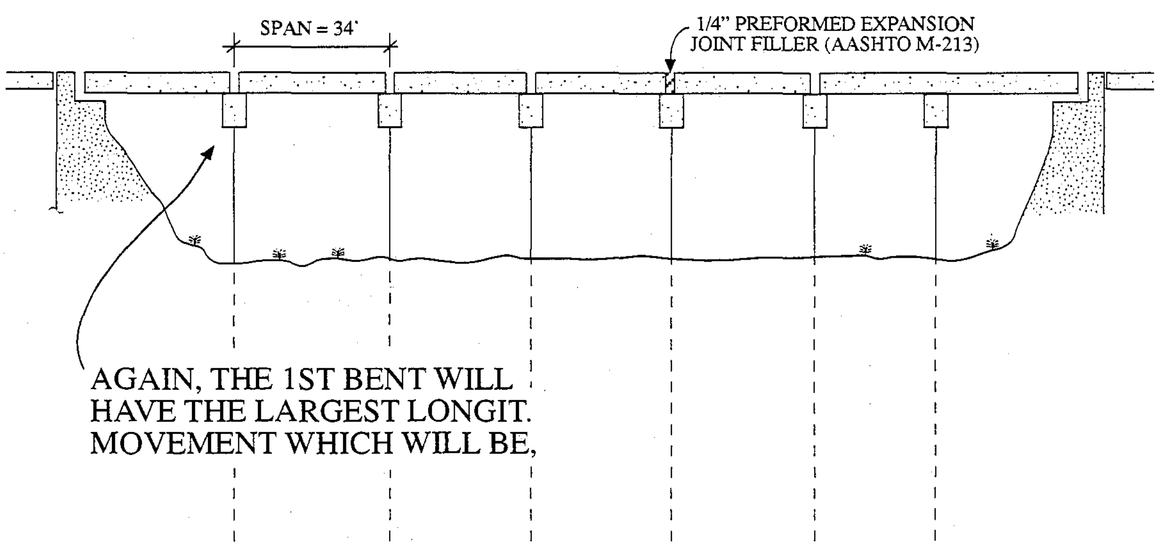

$$\Delta_L^{MAX} \approx \text{(NO. SPACES - 1) (CL SPACE BETWEEN SPANS)}$$

FOR BRIDGE ABOVE,

$$\Delta_L^{MAX} \approx (7 - 1)\,(1/4'') = 1\text{-}1/2''$$

Fig. 3.5. Maximum Longitudinal Sidesway for 238' Simple Span Bridge

APPROXIMATE EQ.

$$P_{CR} = \frac{N^2\pi^2 EI}{4L^2}$$

WHERE N = NO. QUARTER WAVES IN LENGTH L

CASE I - SIDESWAY

$$P_{CR} \approx \frac{(1)^2\pi^2 EI}{4L^2} \approx \frac{2.47EI}{L^2}$$

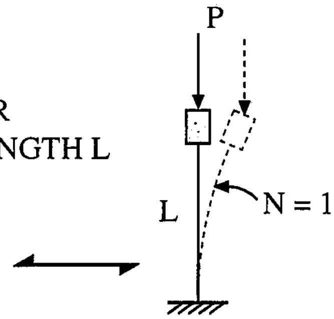

FOR CASE I WE CAN GET LEAN-ON BRACING SUPPORT FROM THE CAP IF ALL PILES IN THE BENT ARE NOT AT P_{CR} ALSO, WE CAN GET LEAN-ON SUPPORT FROM OTHER BENTS IF ALL BENTS IN THE BRIDGE ARE NOT LOADED TO P_{CR}^{BENT}

CASE II - NO SIDESWAY

$$P_{CR} \approx \frac{(3)^2\pi^2 EI}{4L^2} \approx \frac{9\pi^2 EI}{4L^2} \approx \frac{22.2EI}{L^2}$$

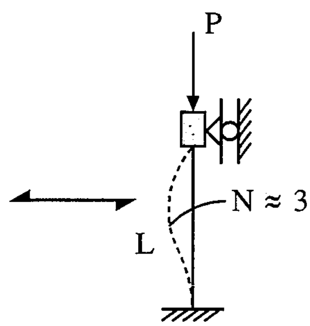

FOR CASE II WE CAN NOT GET LEAN-ON SUPPORT FROM ADJACENT BENTS, BUT CAN GET LEAN-ON SUPPORT FROM ADJACENT PILES IN A BENT.

CASE III - LIMITED SIDESWAY

$$P_{CR} \approx \frac{22.2EI}{L^2}$$

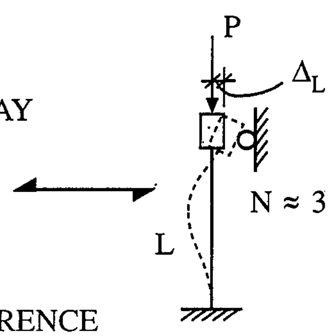

Δ_L = LIMITED LONGIT. DISPL. = LIMITED SIDESWAY

NOTE FOR CASE II ABOVE ALSO APPLIES TO CASE III.

FACTOR OF 8-9 DIFFERENCE IN P_{CR} FOR CASES II & III RELATIVE TO CASE I. USE LOWER VALUE OF 8.

LONGITUDINAL BUCKLING MODES:

CASE I

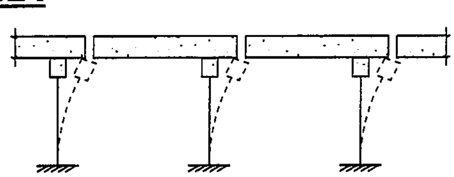

CASES II & III

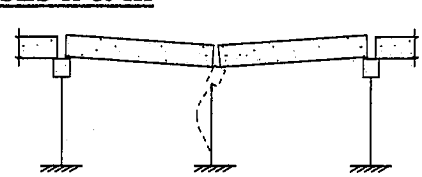

Fig. 3.6. Longitudinal Buckling Loads and Modes for Cases I, II, III.

by sidesway buckling in the longitudinal direction, i.e., Case I. However, after bridge construction is completed, it can only undergo limited sidesway in the longitudinal direction, i.e., Case III, and its longitudinal buckling capacity increases 8 fold as indicated in Fig. 3.6.

Because of limited sidesway possible in the longitudinal direction, existing bridge piles and bents will have two values of P_{cr} for longitudinal buckling, i.e.,

$P_{cr}^{(1)}$ = sidesway buckling at a load somewhat less than $\dfrac{\pi^2 EI_x}{4\ell^2}$

$P_{cr}^{(2)}$ = nonsidesway buckling after the occurrence of the limited sidesway of Δ_L^{max}

at a load of approximately $\dfrac{2\pi^2 EI_x}{\ell^2}$

The nonsidesway buckling mode at $P_{cr}^{(2)}$ will be required to actually fail the pile bent and bridge at a load of approximately $P_{cr}^{(2)} \approx 8\, P_{cr}^{(1)}$. This sequence of events and failure loads are summarized in Figs. 3.7 and 3.8 for a perfect pile/column and an imperfect pile/column respectively. As indicated by these figures for reasonable imperfections, which are small,

$$P_{cr}^{\text{imperfect}} \approx P_{cr}^{\text{perfect}} \tag{3.2}$$

and P_{cr} is independent of $\Delta_{\text{long.}}^{max}$, and

$$P_{\text{collapse of bent/bridge}} = P_{cr}^{(2)} \approx 8\, P_{cr}^{\text{flagpole pile/bent}} \tag{3.3}$$

Alternatively, in terms of pile length for failure for a given P load,

$$L_{\text{failure}}^{\text{sidesway}} = L_f^s = \sqrt{\frac{\pi^2 EI_x}{4P}} \tag{3.4a}$$

$$L_{\text{failure}}^{\text{Limited sidesway}} = L_f^{LS} = \sqrt{\frac{2\pi^2 EI_x}{P}} \tag{3.4b}$$

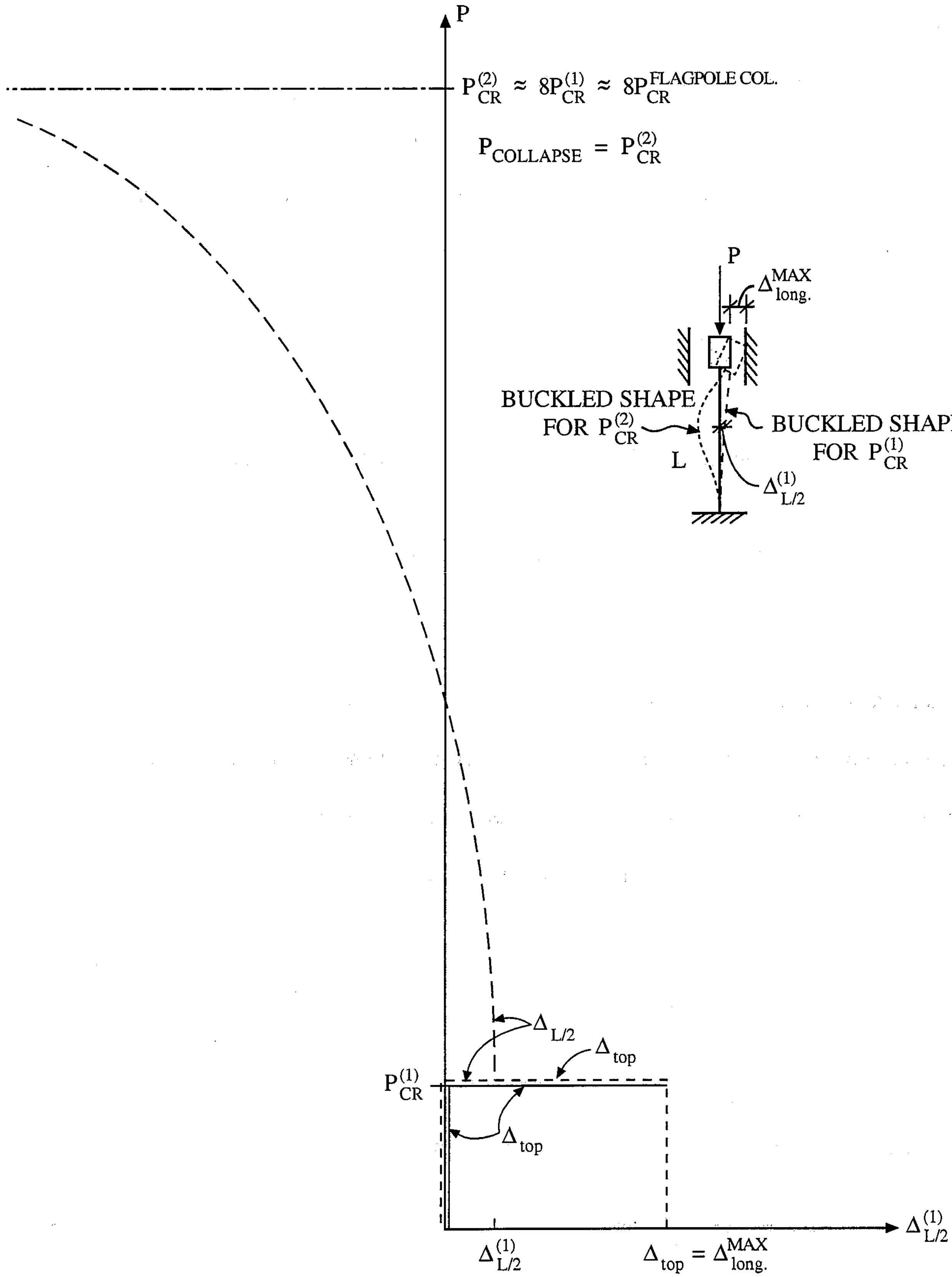

Fig. 3.7. P-Δ Curve for Perfect Bent Pile with Limited Sidesway Possible

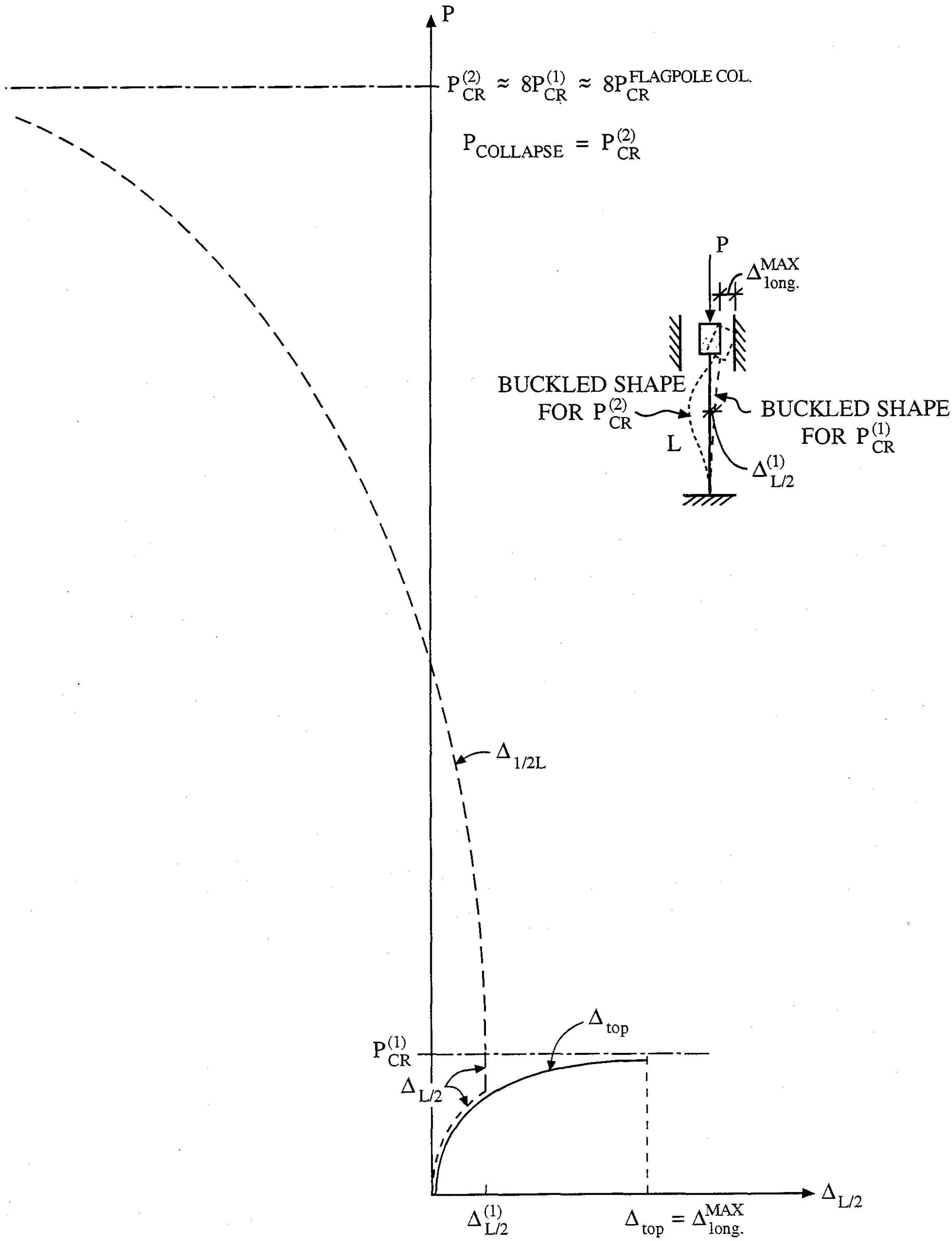

Fig. 3.8. P-Δ Curve for Imperfect Bent Pile with Limited Sidesway Possible

Therefore,

$$\frac{L_f^{LS}}{L_f^S} = \frac{\sqrt{\dfrac{2\pi^2 EI_x}{P}}}{\sqrt{\dfrac{\pi^2 EI_x}{4P}}} = \sqrt{8} = 2.828 \tag{3.5a}$$

or,

$$L_f^{LS} = 2.828\, L_f^S \tag{3.5b}$$

Thus, for a pile bent modeled to buckle in a sidesway mode as in Fig. 3.9a, or with limited sidesway as in Fig. 3.9b, we would have,

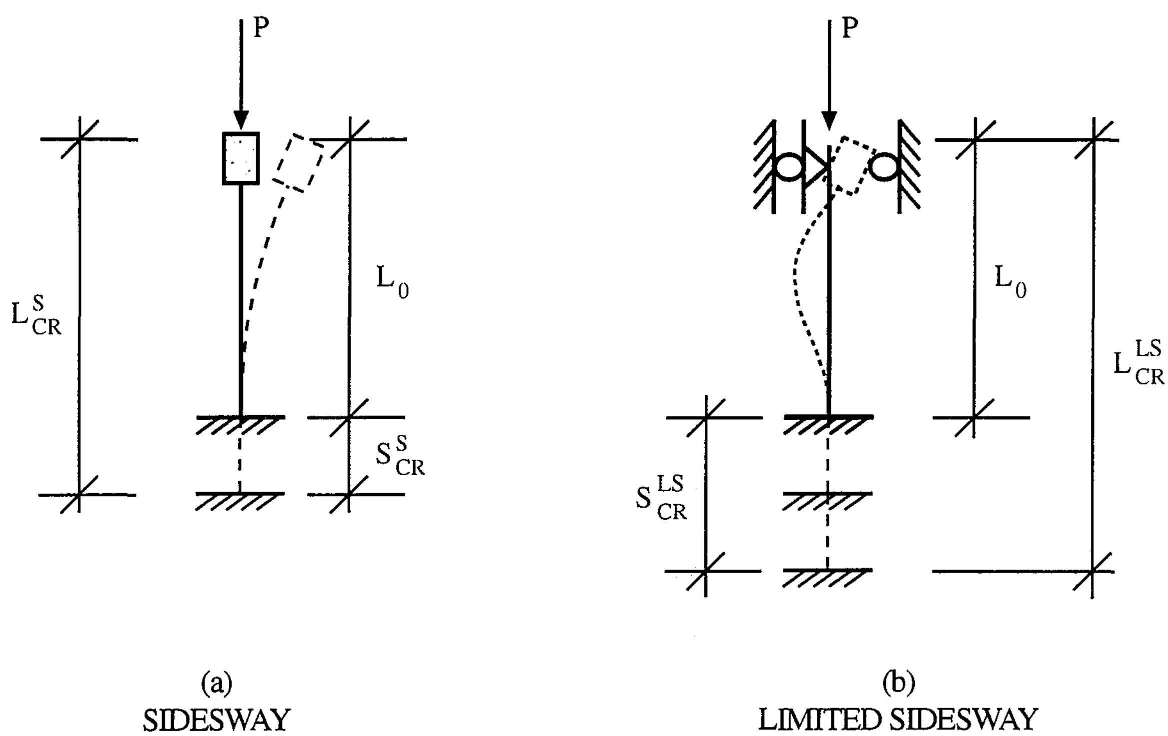

Fig. 3.9. Bent Longitudinal Buckling Modeling

$$L^{S}_{CR} = L_0 + S^{S}_{CR} \tag{3.6}$$

and,

$$\begin{aligned} L^{LS}_{CR} &= 2.828\, L^{S}_{CR} = 2.828\,(L_0 + S^{S}_{CR}) \\ &= 2.828\, L_0 + 2.828\, S^{S}_{CR} \\ &= L_0 + \underbrace{1.828\, L_0 + 2.828\, S^{S}_{CR}}_{S^{LS}_{CR} \quad \text{(see Fig 3.9b)}} \end{aligned} \tag{3.7}$$

Or,

$$S^{LS}_{CR} = 1.828\, L_0 + 2.828\, S^{S}_{CR} \tag{3.8}$$

Thus, for a given L_0 and P load, one can determine L^{S}_{CR} from $L^{S}_{cr} = \sqrt{\dfrac{\pi^2 EI_x}{4P}}$ and then

$$S^{S}_{CR} \text{ from } S^{S}_{CR} = L^{S}_{CR} - L_0.$$

S^{LS}_{CR} can then be calculated from

$$S^{LS}_{CR} = 1.828\, L_0 + 2.828\, S^{S}_{CR}$$

and the values for S^{S}_{CR} and S^{LS}_{CR} can be compared.

This was done for an HP10x42 pile under a 120^{k} load and the results are shown in Fig.

3.10. Note in this figure that for a given pile under a given P-load, the critical scour value decreases linearly with the initial length of the pile above ground, L_0. Also, note the dramatic increase in the critical scour value when the limited sidesway in the longitudinal direction is considered.

Also since L^S_{CR} varies inversely with the square root of P, i.e., $L^S_{CR} = \sqrt{\frac{\pi^2 EI_x}{4P}}$, L_{CR} and thus

S_{cr} is not real sensitive to the pile loading. This is illustrated for a HP10x42 pile with the cap being 15' above the ground line in Fig. 3.11.

3.3 Bent Pile Buckling in Transverse Direction

Due to

- angle iron swaybracing
- batter piles on each end of the bent
- lateral support from continuous superstructure

as indicated in Fig. 3.12, and if the bridge is continuous, or made continuous for live loads, due to the lateral support provided to the pile bent at the top from the bridge superstructure, pile bents of the type used by the ALDOT cannot sidesway in the transverse direction. Therefore, buckling of the bent piles in the transverse direction (about pile's weak axis) will be a nonsidesway mode with partial fixity at the top due to the bent cap (assume 50% fixity) and partial fixity at the bottom due to the ground stiffness modulus (assume 50% fixity).

As explained in the previous section, after very limited sidesway in the longitudinal direction, the top of a bent cap will be restrained from further longitudinal movement and the piles will then act as pinned-ended columns at their top. This will render the pile as

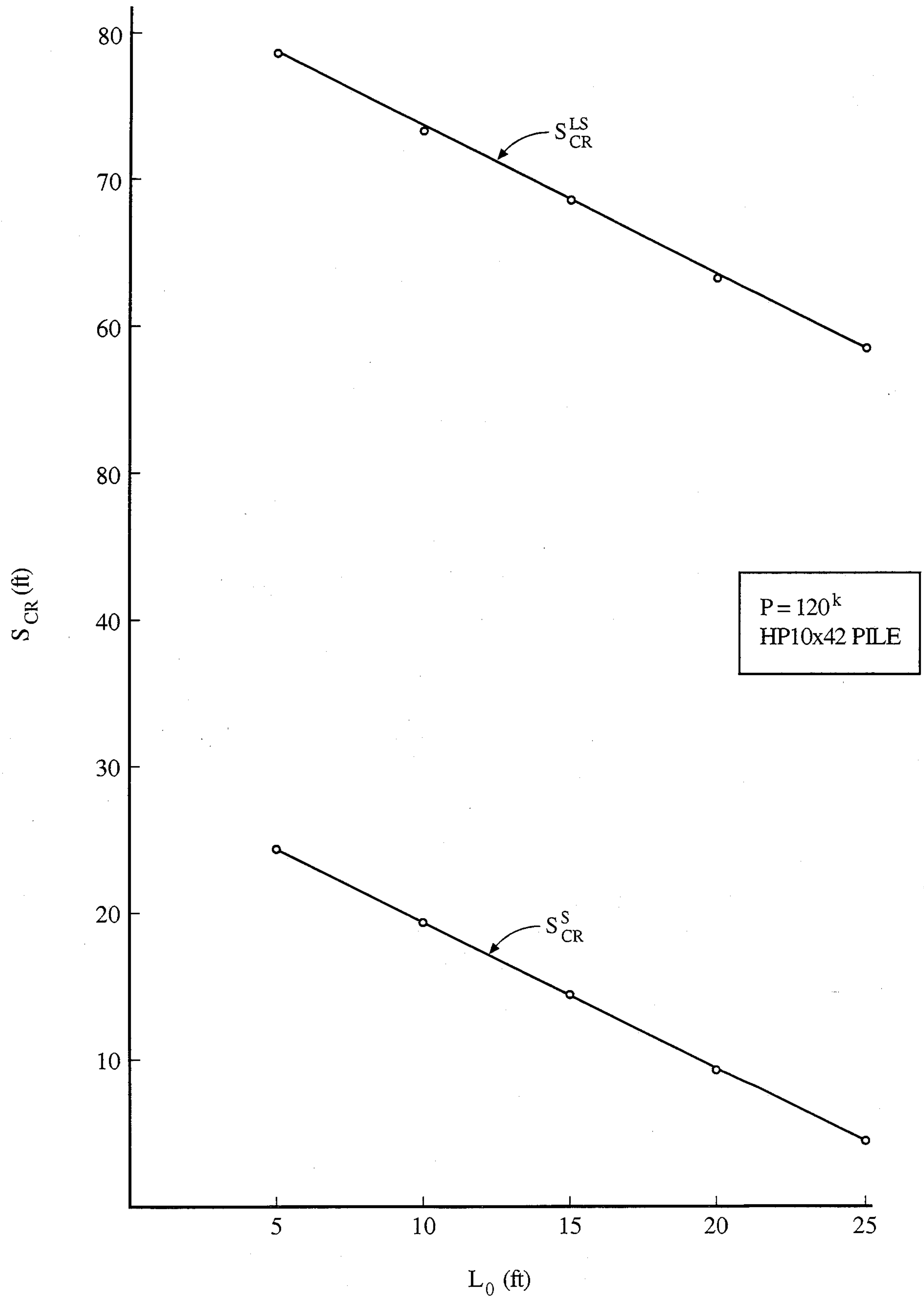

Fig. 3.10. S_{CR} vs. L_0 for Pile Buckling in Longitudinal Direction

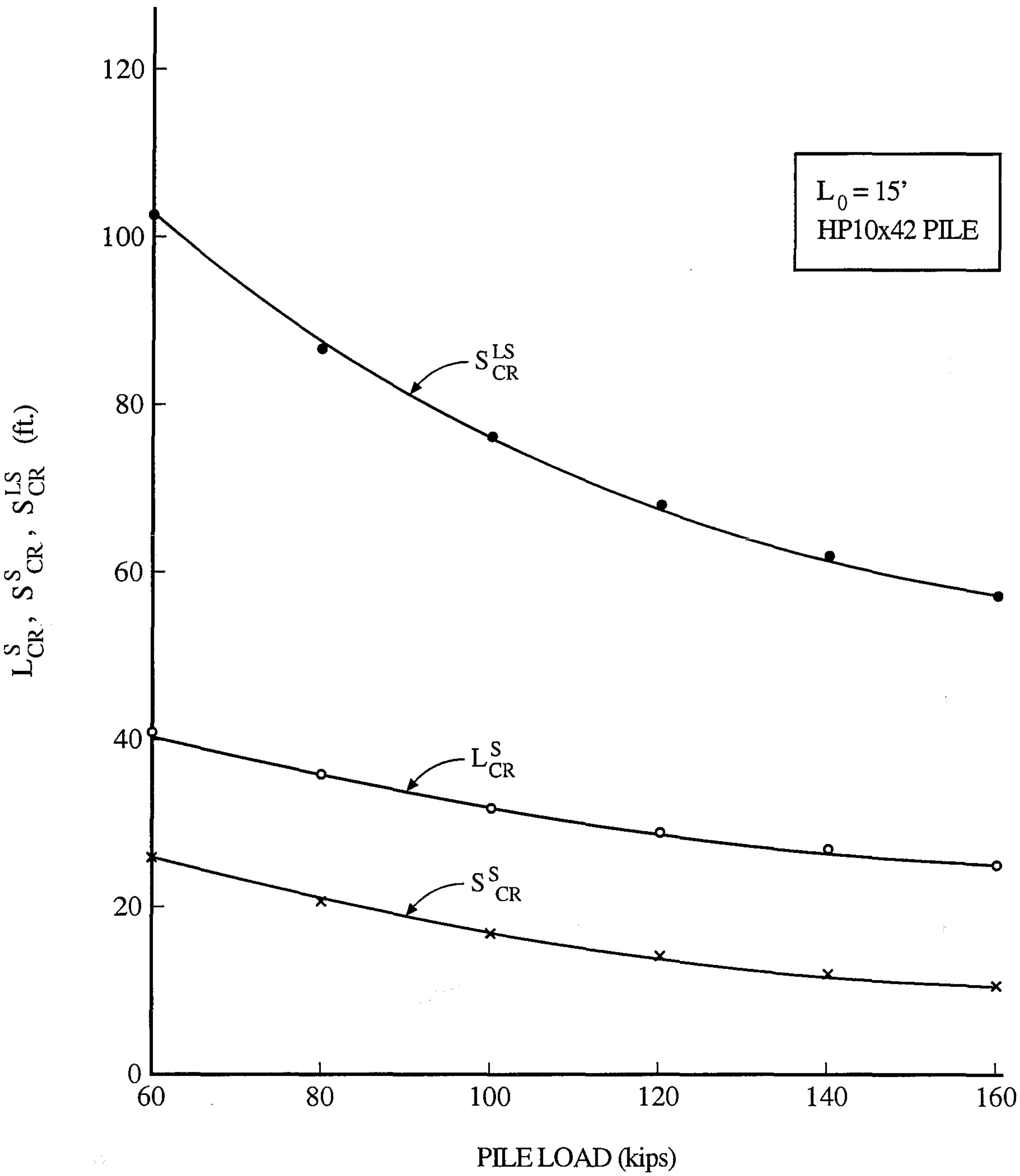

Fig. 3.11. L_{CR} vs. S_{CR} vs. P for Pile Buckling in Longitudinal Direction

approximately a fixed-pin ended column for buckling about its strong axis and will make buckling of the pile about its weak axis the controlling mode of buckling failure. If one assumes that the swaybracing does not buckle, then for the case of "H" = 25' (the largest value) and S = 20' (the largest probable value), as indicated in Fig. 3.12,

$$\ell_{mp} = \frac{"E" or "G"}{2} + 3.5' + S = \frac{11.5}{2} + 3.5 + 20 = 29.25'$$

$$P_{CR}^{mp} \approx \frac{1.5\pi^2 EI_y}{\ell_{mp}^2} = \frac{1.5\pi^2(29,000)(71.1)}{29.25^2 \text{x} 144} = 250^k$$

assume 50%
fixity at bottom

$$\ell_{ep} = 3.5' + S = 3.5' + 20 = 23.5'$$

$$P_{CR}^{ep} \approx \frac{1.5\pi^2 EI_y}{\ell_{ep}^2} = \frac{1.5\pi^2(29,000)(71.7)}{23.5^2 \text{x} 144} = 387^k$$

$$\ell_{ip} = \frac{"E" or "G"}{4} + 3.5' + S = \frac{11.5}{4} + 3.5' + 20' = 26.4'$$

$$P_{ip} \approx \frac{1.5\pi^2(29,000)(71.7)}{26.4^2 \text{x} 144} = 307^k$$

TWO STORY BENT					
SWAYBRACING TABLES					
"H"	"E"	"A"	"B"	"C"	WT. LBS.
20'-0"	6'-6"	25'-6"	25'-6"	27'-3"	1205
21'-0"	7'-6"	25'-6"	25'-6"	27'-7"	1209
22'-0"	8'-6"	25'-6"	25'-6"	28'-0"	1216
23'-0"	9'-6"	25'-6"	25'-6"	28'-5"	1223
24'-0"	10'-6"	25'-6"	25'-6"	28'-11"	1230
25'-0"	11'-6"	25'-6"	25'-6"	29'-5"	1238

Largest "H" Value →

BATTEN WEIGHT TO BE ADDED TO ABOVE TABLES. 10-BATTENS REQ'D, 5/16" X 7 1/2" X 1'-6 1/4" @ 12.1# EACH.

NOTE: WEIGHT GIVEN IS TOTAL FOR TWO PIECES OF EACH LENGTH OF SWAYBRACING SHOWN IN BOTH TABLES.

SINGLE STORY BENT			
SWAYBRACING TABLES			
"H"	"G"	"D"	WT. LBS.
13'-0"	7'-5"	25'-8"	395
14'-0"	8'-5"	26'-1"	401
15'-0"	9'-5"	26'-7"	409
16'-0"	10'-5"	27'-1"	417
17'-0"	11'-5"	27'-7"	425
18'-0"	12'-5"	28'-1"	432
19'-0"	13'-5"	28'-8"	441

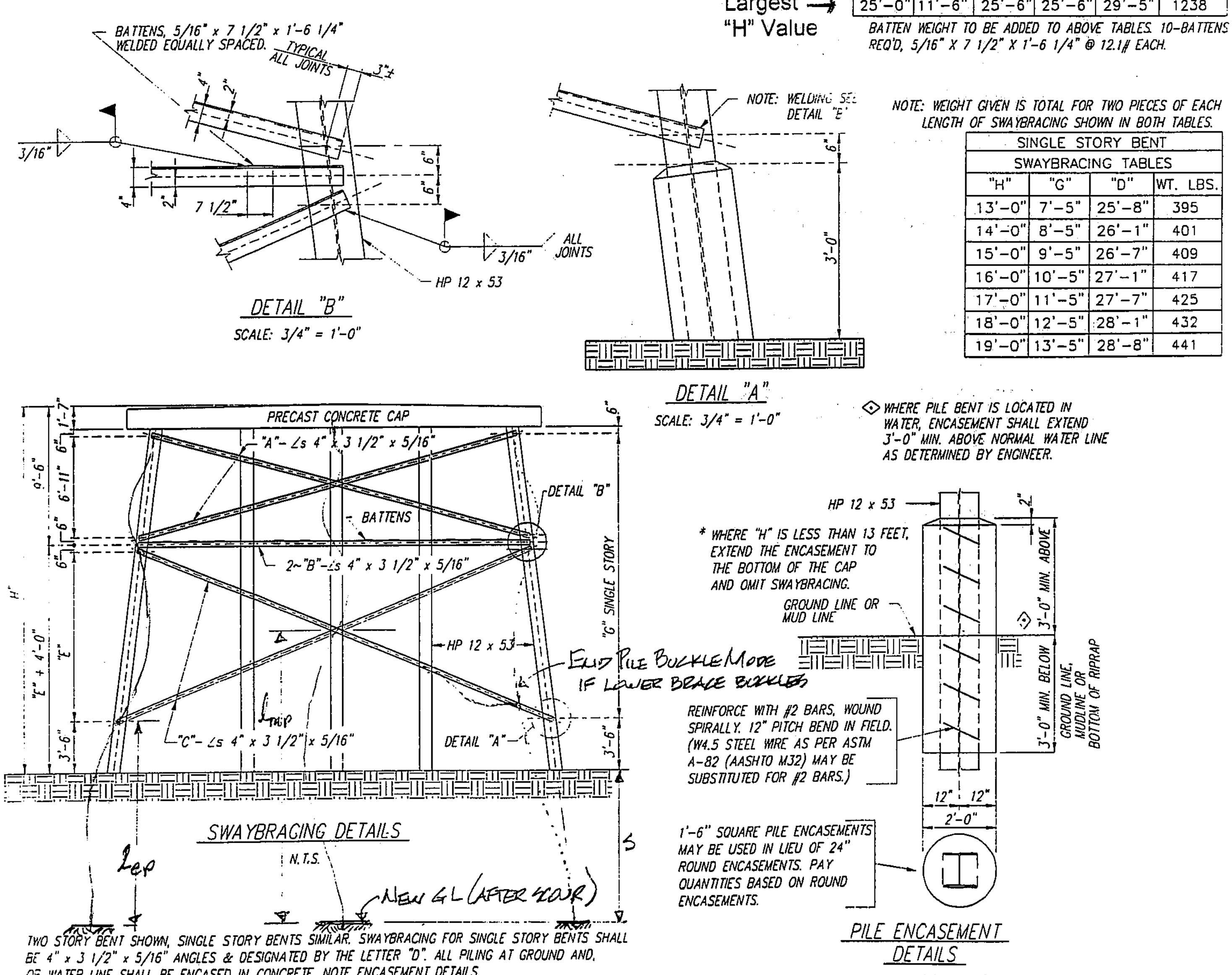

Fig. 3.12. Bent Transverse Buckling

Due to "lean-on" bracing provided by adjacent piles,

$$P_{CR}^{bent} = \Sigma P_{CR}^{piles} = 250^k + 2(307) + 2(387) = 1638^k$$

$$P_Y^{bent} = 5P_Y^{pile} = 5(446^k) = 2230^k$$

Note, however, that the swaybracing members are relatively small angle iron and whereas they should prevent swaying of the bent, they will probably buckle themself rather than prevent buckling of the individual piling (see right end pile in Fig. 3.12). Therefore, it will be assumed that the swaybracing and batter piles will prevent transverse sidesway buckling of the bents, but that the bent piling will buckle in the transverse direction from the bent cap (assume 50% fixity) to the new ground line after scour (assume 50% fixity) at a load per pile of,

$$P_{CR} \approx \frac{2\pi^2 EI_w}{\ell^2} \tag{3.9}$$

where

$$I_w = I_{weak\,axis} = I_y$$

ℓ = "H" (on pile bent standards) + S = height from new ground level to top of bent cap.

And, due to "lean-on" bracing from adjacent piles,

$$P_{CR}^{bent} = \Sigma P_{CR}^{piles} \tag{3.10}$$

Using Eqn. (3.9) yields the elastic values of P_{CR} shown in Table 3.1 for ℓ values from 15'-40' for HP 10 x 42 HP and 12 x 53 piles. These elastic failure loads are presented graphically in the form of P_{CR} vs. ℓ curves in Fig. 3.13a. As indicated in Chapter 2, for $P_{CR} > P_y/2$, inelastic buckling loads should be used as shown in Fig. 3.13b.

Table 3.1. Elastic P_{CR} vs. ℓ for HP 10x42 and HP 12x53 Piles*

ℓ (ft)	$P_{CR}^{HP10x42}$ (kips)	$P_{CR}^{HP12x53}$ (kips)
15	**1267**	**2244**
20	**713**	**1263**
25	**456**	**808**
30	**317**	**561**
35	**233**	**413**
40	**178**	**316**

*P_{CR} Based on Buckling in Transverse Direction as given by Eqn. (3.9).

$P_Y^{10x42} = 12.4 \text{ x } 36 = 446^K$

$P_Y^{12x53} = 15.5 \text{ x } 36 = 558$

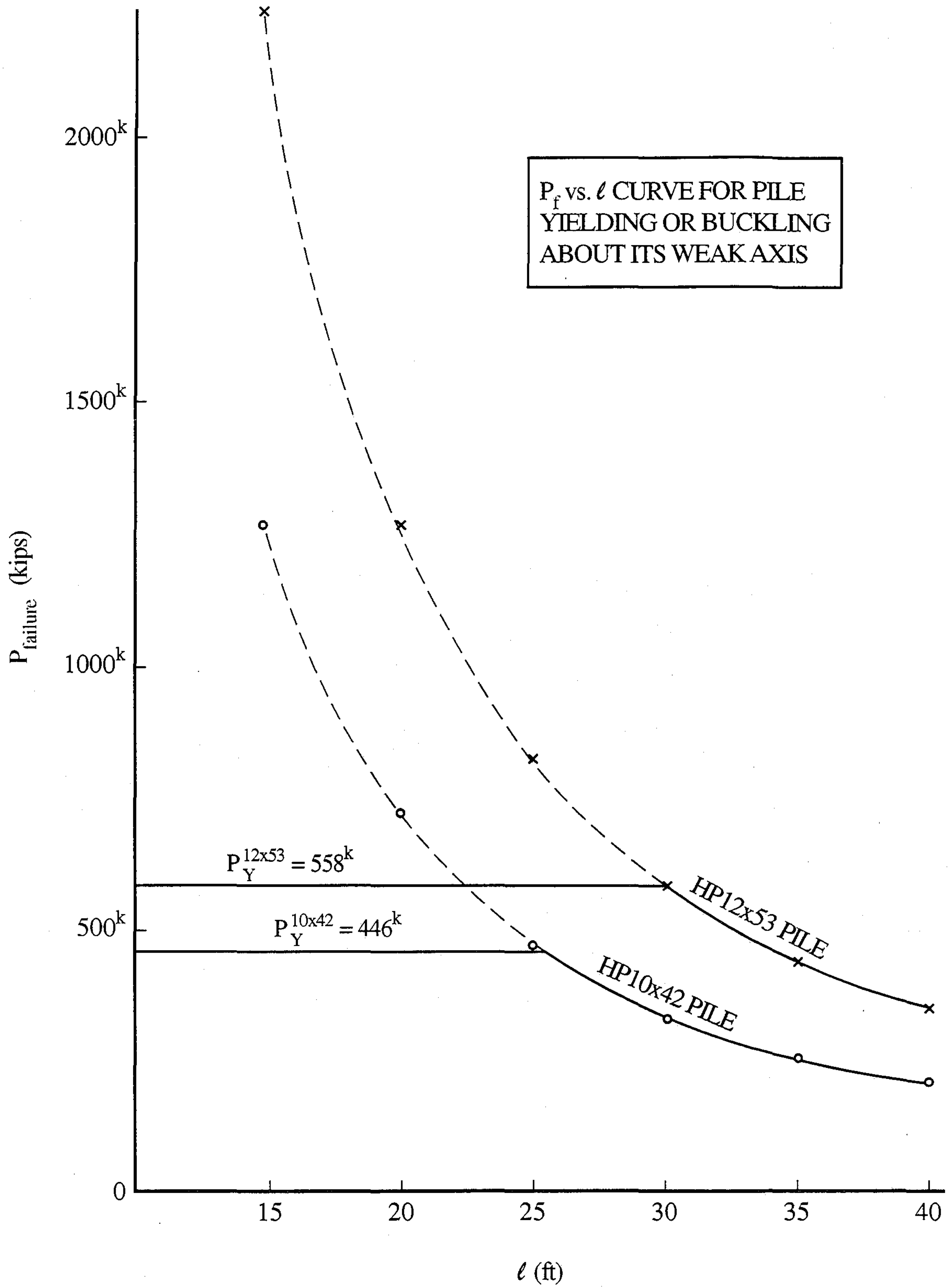

Fig. 3.13a. ElasticTransverse/Weak Axis Buckling of a Single Bent Pile for a Given Length (ℓ) Above Ground Line After Scour

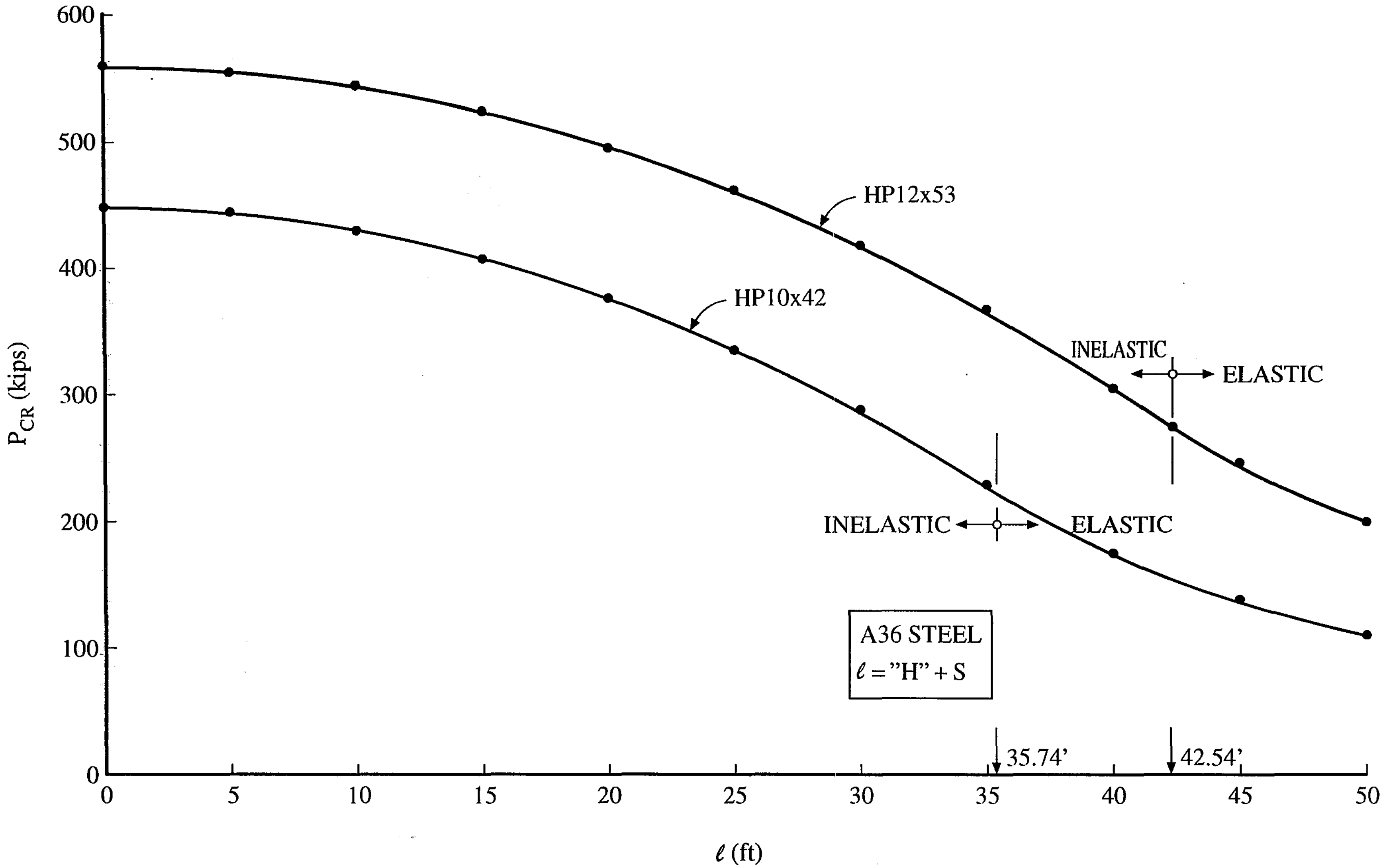

Fig. 3.13b. Transverse/Weak Axis Buckling of a Single Bent Pile for a Given Length (ℓ) Above Ground Line After Scour

The assumption of 50% fixity at the pile top, i.e., at the bent cap, seems quite reasonable since the piles are typically embedded 1 ft. into the cap as indicated in Fig. 3.15 or connected by weldment to anchor plates in the cap as indicated in Fig. 3.16.

It appears that bridge pile bents are sometimes used without x-bracing but with pile encasement extending from 3 feet below ground line to the underside of the cap. However, because of the light steel spiral employed in the encasement, and the vibratory nature of bridge and bent loads due to truck traffic, the pile concrete encasement could be lost with time (though ALDOT engineers report no such losses). Thus, let us examine the case of a bent without x-bracing and without pile encasement, but with batter piles at each end of the bent to see if the batter piles will provide sufficient lateral bracing to prevent sidesway buckling in the lateral or transverse direction. To simplify the analysis, we will work with the simplified bent model shown in Fig. 3.14.

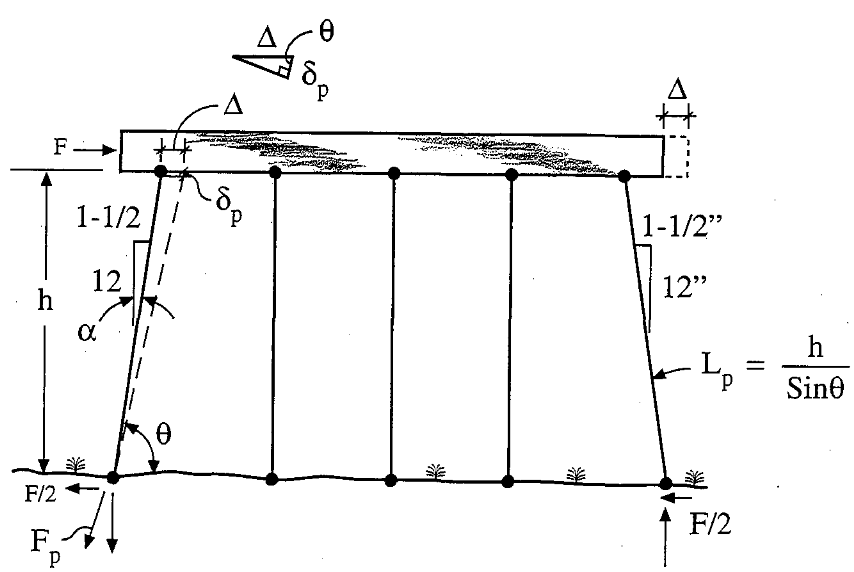

Fig. 3.14. Simplified Bent Model

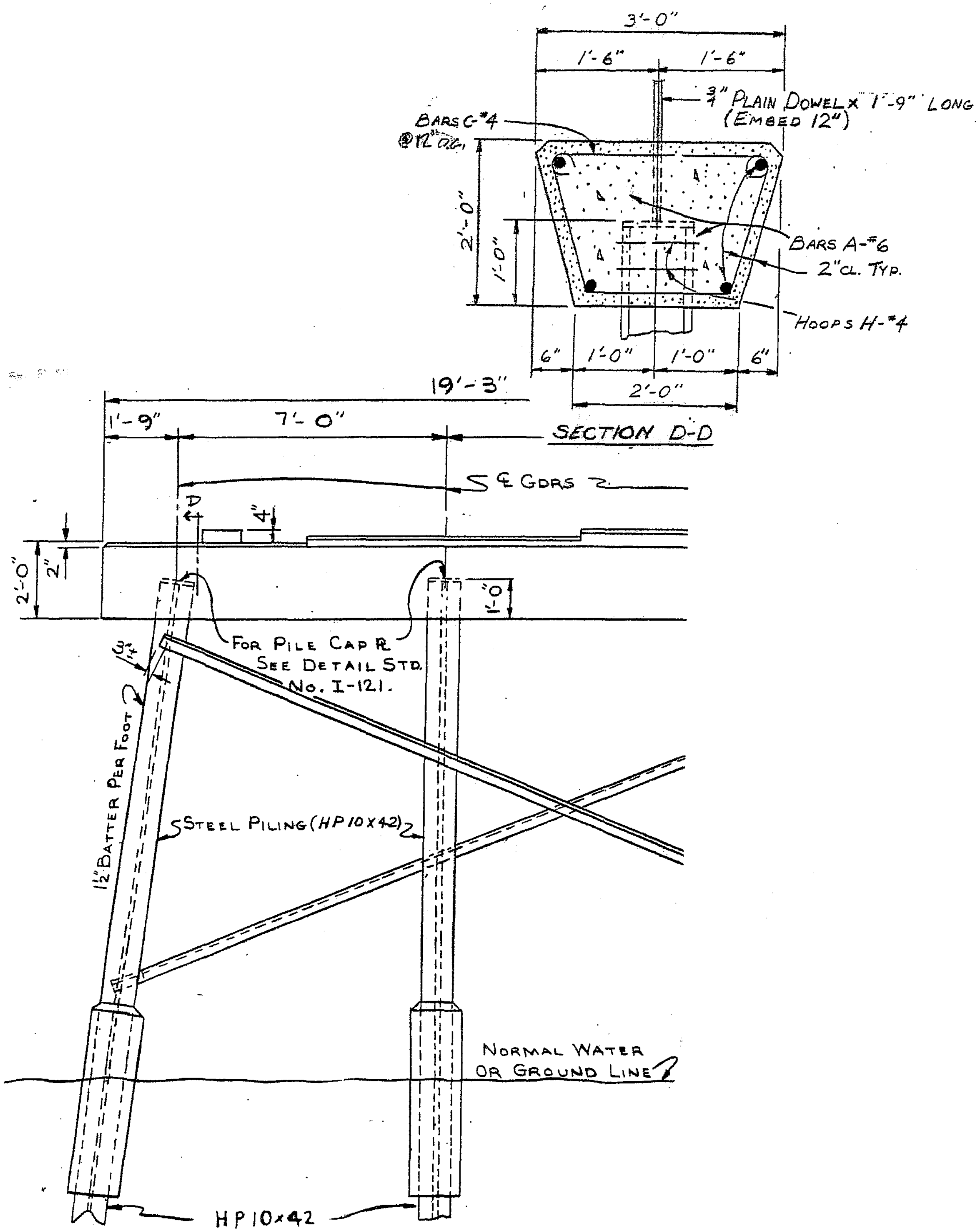

Fig. 3.15. Pile Connections/Embedment to Bent Cap

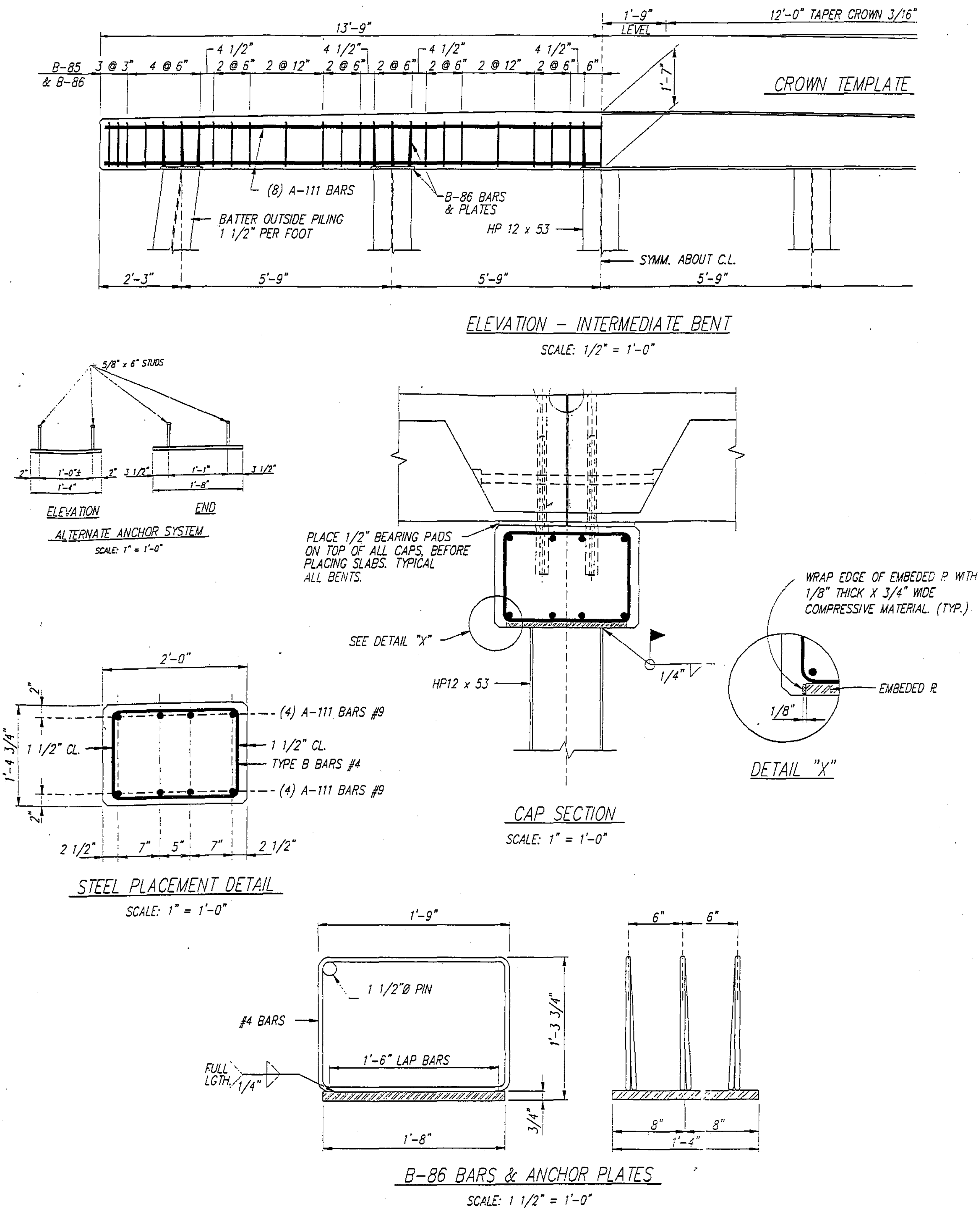

Fig. 3.16. Pile Connections by Anchor Plates to Bent Cap

For this simplified model,

$$\tan\alpha = \frac{1.5}{12} = 0.125$$

$$\alpha = 7.125°$$

$$\therefore \theta = 90° - \alpha = 82.875°$$

$$\text{Cos }\theta = \frac{F/2}{F_p}$$

$$F_p = \frac{F/2}{\text{Cos }\theta}$$

$$\delta_p = \frac{F_p L_p}{A_p E_p} = \frac{\dfrac{F}{2\text{Cos }\theta} \text{ x } \dfrac{h}{\text{Sin }\theta}}{A_p E_p} = \frac{Fh}{2A_p E_p \text{Cos }\theta \text{Sin }\theta}$$

$$\text{Cos }\theta = \frac{\delta_p}{\Delta}$$

$$\Delta = \frac{\delta_p}{\text{Cos }\theta} = \frac{Fh}{2A_p E_p \text{Cos}^2\,\theta \text{ Sin }\theta}$$

$$F = \underbrace{\frac{2A_p E_p \text{Cos}^2\theta \text{ Sin }\theta}{h}}_{k_{Equiv}} \; \Delta$$

Therefore for a HP 10 x 42 bent,

$$k_{Equiv} = \frac{2 \text{ x } 12.4\text{in}^2 \text{ x } 29{,}000 \text{ ksi x Cos}^2\ 82.815 \text{ x Sin } 82.895}{h} = \frac{10{,}980^k}{h}$$

For a HP 12 x 53 bent (A = 15.5 in^2),

$$k_{Equiv} = \frac{13{,}725^k}{h}$$

Thus, k_{Equiv} for various values of h are as shown in Table 3.2 and in Fig.3.17.

Table 3.2 Bent k_{EQ} for 15' ≤ h ≤ 40'

h	k_{EQ}^{10x42}	k_{EQ}^{12x53}
15' (180")	61.0 k/in	76.3 k/in
20' (240")	45.8	57.2
25' (300")	36.6	45.8
30' (360")	30.5	38.1
35' (420")	26.1	32.7
40' (480")	22.9	28.6

In general, columns bracing requirements are

- Stiffness – to hold the braced point in place
- Strength – Brace force and strength are directly related to the initial out-of-straightness and load eccentricities.

For an ideal column pinned at its base the ideal bracing requirements would be as indicated in Fig. 3.18.

Thus,

$$k_{ideal} = \frac{P_e}{h}$$

For the simplified bent model shown in Fig. 3.14,

$$k_{ideal}^{pile} = \frac{P_e^{pile}}{h}$$

$$k_{ideal}^{bent} = \frac{\Sigma P_e^{pile}}{h} = \frac{5P_e^{pile}}{h}$$

Values of k_{ideal}^{bent} are given in Table 3.3 for steel HP 10 x 42 and HP 12 x 53 for the simplified bent in Fig. 3.14. These values of k_{ideal}^{bent} are also shown plotted on Fig. 3.17 for convenience in comparing the k-values.

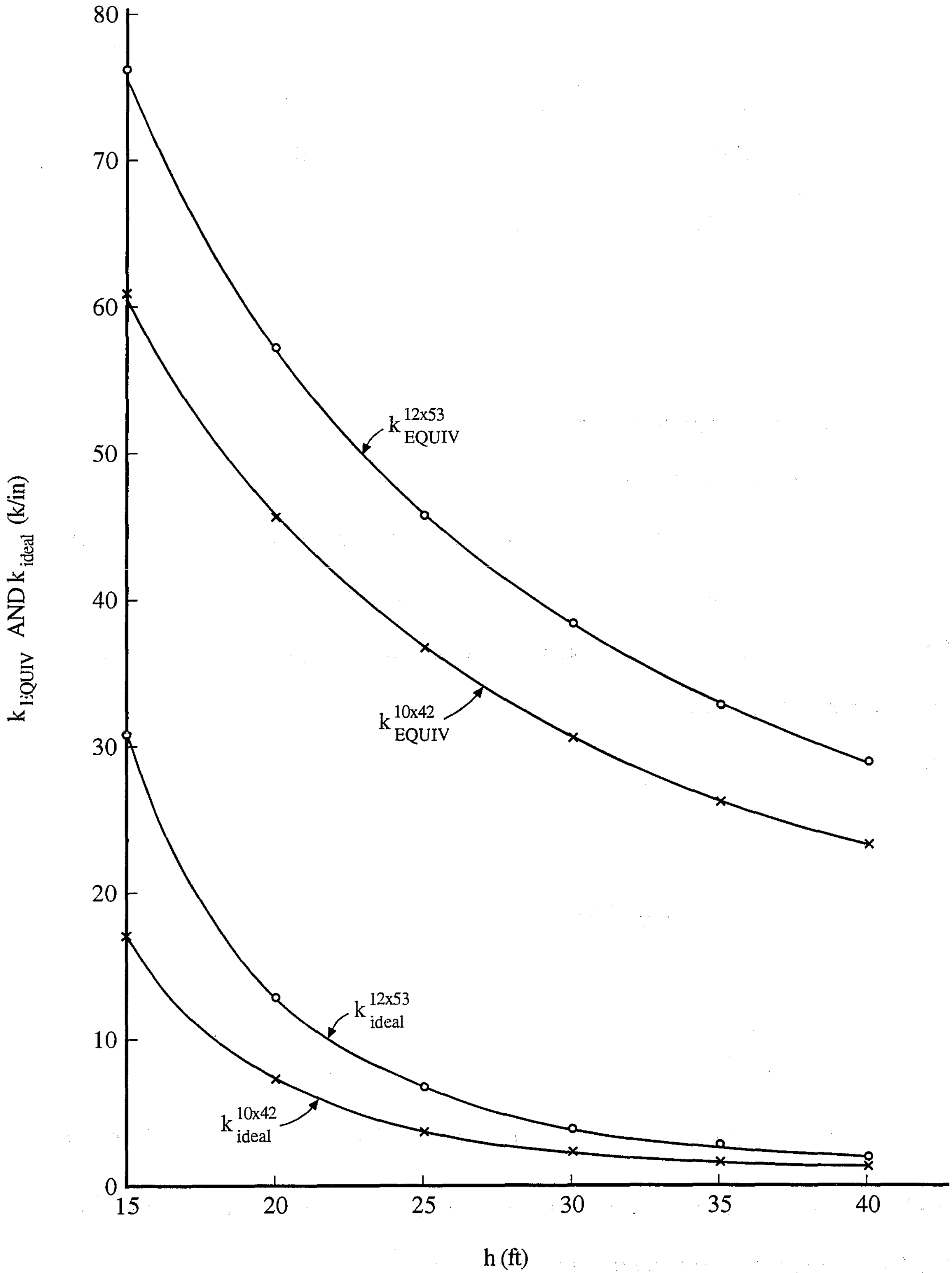

Fig. 3.17. k_{EQ} vs h for Simplified Bent Model for HP 10 x 12 and HP 12 x 53 Piles

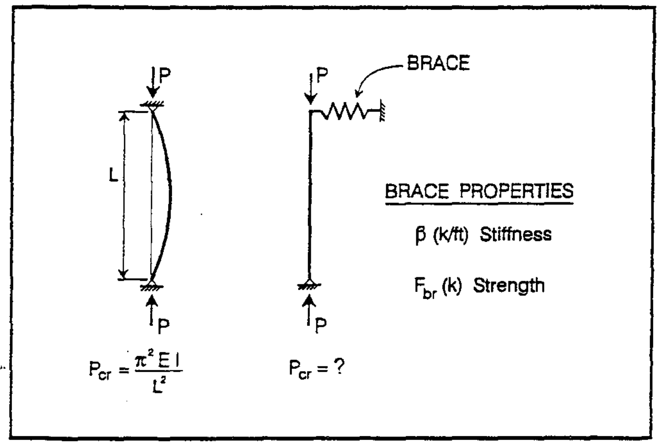

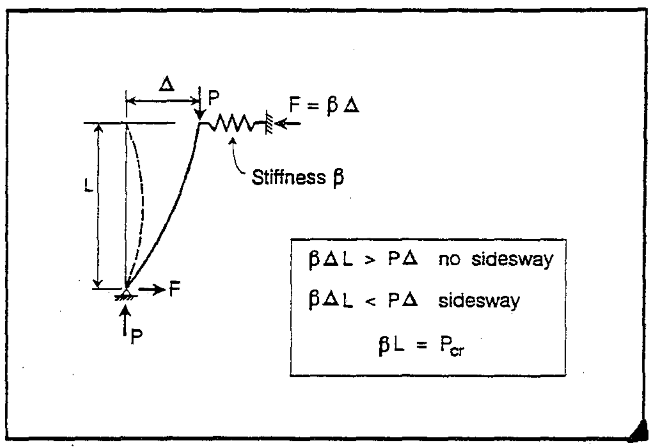

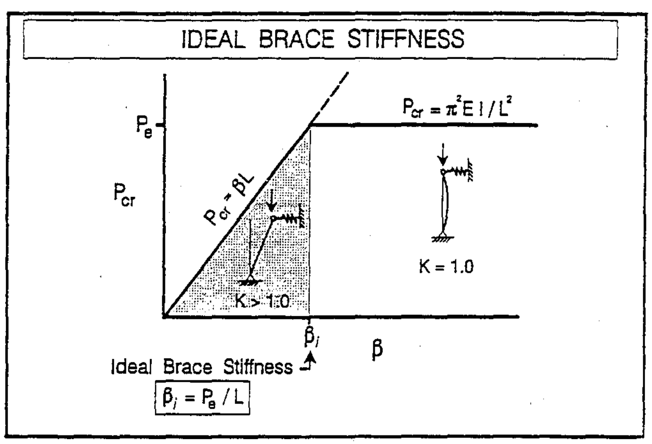

Figure 3.18. Ideal Brace Stiffness (Yura)

Table 3.3. Simplified Bent k_{ideal} vs ℓ Values

ℓ	$P_e = \frac{\pi^2 EI_y}{\ell^2}$		$k_{ideal}^{bent} \approx \frac{5P_e}{\ell}$	
	P_e^{10x42}	P_e^{12x53}	k^{10x42}	k^{12x53}
15' (180")	633^k	1122^k	17.6 k/in	31.2 k/in
20' (200")	356	631	7.42	13.1
25' (300")	228	404	3.80	6.73
30' (360")	158	280	2.19	3.89
35' (420")	116	206	1.38	2.45
40' (480")	89	158^k	0.93	1.65

For columns/piles with a fixed base requires a top brace with a stiffness of five times that of the ideal brace stiffness shown in Fig. 3.18 to achieve 95% of the fully braced P_{CR} (3). This condition is shown in Fig. 3.19.

The K = 0.7 condition shown in Fig. 3.19 is approximately the condition of ALDOTs bents in the transverse direction if they are presented from sideswaying. Thus, for these bents,

$$k_{ideal}^{pile} \approx \frac{5P_e}{\ell}$$

$$k_{ideal}^{bent} \approx \frac{\sum^{\text{no piles}} 5P_e}{\ell}$$

For a 5 pile bent, the k_{ideal}^{bent} values given in Table 3.3 should be multiplied by 5 to determine the k_{ideal}^{bent} for the actual pile end conditions. This would be true if $P_{failure}$ = P_{CR} = elastic buckling load. However, for the smaller length bent columns/piles (where k_{ideal} is fairly large), the pile failure mode will be one of inelastic buckling at loads well below the elastic buckling loads. In this case,

$$k_{ideal}^{bent} \approx \frac{\sum^{\text{no piles}} 5P_{CR}}{\ell}$$

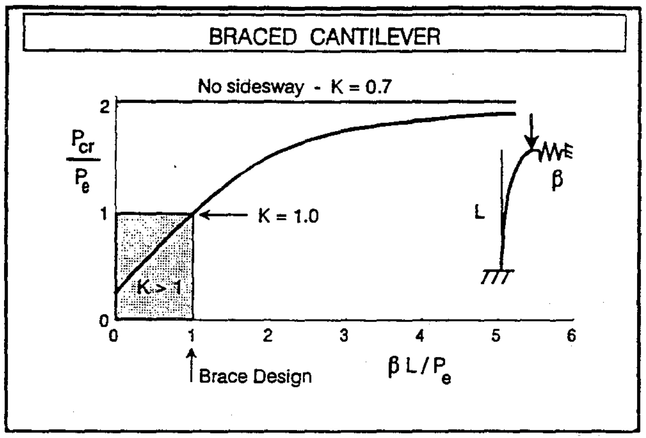

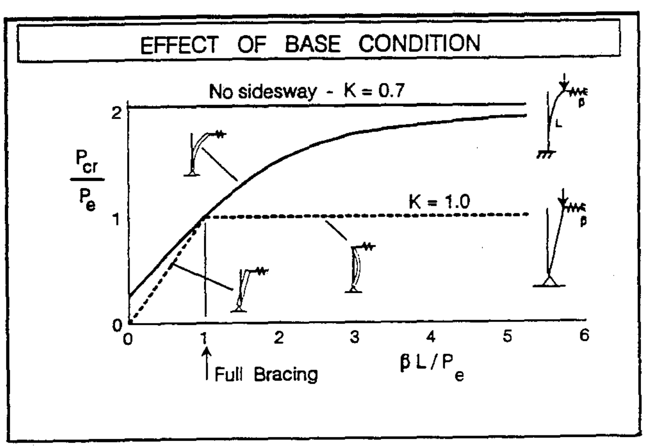

Figure 3.19. Brace Stiffness Required for Fixed Base Condition

Elastic and inelastic buckling loads were determined from Fig. 3.20 and k_{ideal}^{bent} used these values to determine k_{ideal}^{bent} for a 5-pile bent. These are shown in Table 3.4. A plot of these k_{ideal} values are shown superimposed on the approximate $k_{equivalent}$ vs h (or ℓ) curves developed earlier in Fig. 3.2 1. Note that this plot indicates that the batter piles should provide sufficient lateral support to develop the nonsidesway capacity of the pile bent, i.e., k_{eq} of batter piles > k_{ideal}^{bent}. However, for ℓ or h values below 20 feet, the approximate k_{EQ} and the k_{ideal}^{bent} values are quite close and the bents should be x-braced in addition to having the batter piles. Lateral load F vs Δ curves with and without vertical bent cap loadings should be developed for a pile bent without x-bracing via linear and nonlinear stiffness analysis to verify the $k_{equivalent}$ values shown in Fig. 3.2 1.

Table 3.4. Elastic and Inelastic Buckling Loads and k_{ideal}^{bent} Values for 5-Pile Bents of HP 10 x 42 and HP 12 x 53 Piles

	$P_e \approx \dfrac{\pi^2 E_t I_y}{\ell^2}$		$k_{ideal}^{bent} = \dfrac{\sum^{\text{no piles}} 5\, P_{cr}}{\ell}$ *	
ℓ (or h)	$P_{CR}^{10 \times 42}$	$P_{CR}^{12 \times 53}$	HP 10 x 42	HP 12 x 53
15' (180")	366^k	487^k	50.8 k/in	67.6 k/in
20' (240")	305	433	31.8	45.1
25' (300")	228	366	19.0	30.5
30' (360")	158	280	11.0	19.4
35' (420")	116	206	6.90	12.3
40' (480")	89	158	4.64	8.23

* Values shown are for a 5-pile bent.

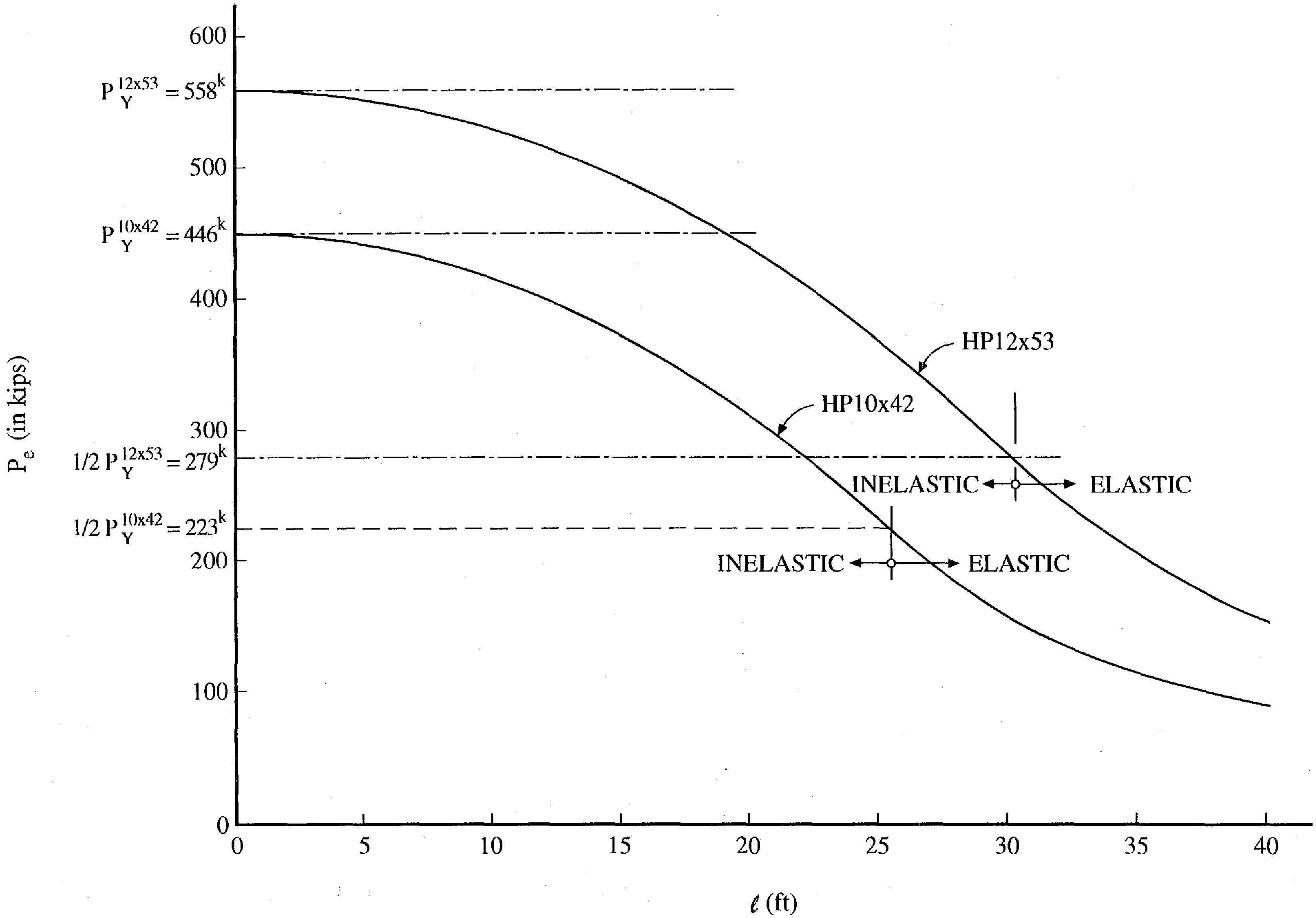

Fig. 3.20. Elastic and Inelastic Values of P_e for HP 10 x 42 and HP 12 x 53 Piles

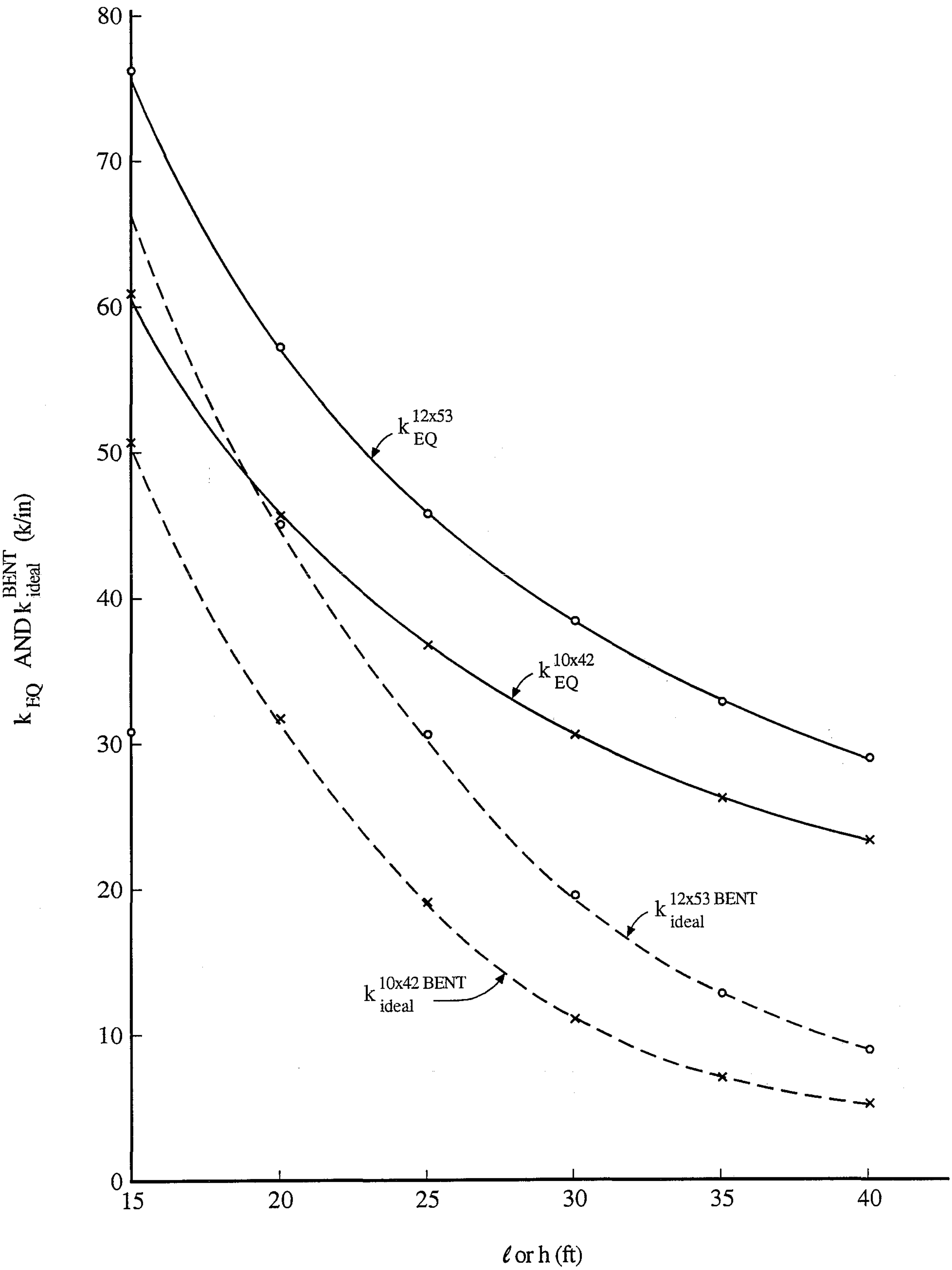

Fig. 3.21. Approximate Values of k_{EQ} and k_{ideal} for 5-Pile Bents of HP 10 x 12 and HP 12 x 53 Piles

3.4 Crushing or Yielding of Piles

As indicated in Section 3.1, crushing or yielding of the bent piles is really not a viable failure mode. An extreme scour event does not change $P_{max\ applied}$ or P_y and hence a bent that will not fail in this mode before scour, will not fail in this mode after scour.

3.5 Plunging Failure of Piles/Bent

All static pile formulas estimate pile capacity by the following basic equation:

$$P_u = P_t + P_f \tag{3.11}$$

where P_u = ultimate pile capacity

P_t = load carried in point bearing

P_f = load carried by friction along perimeter of pile

Differences in Eqn. (3.11) lie in the methods used to evaluate the friction and point-bearing portions of the equation. Appendix D shows results from an earlier study (2) on pile capacity predictions by a static formula vs. $P_{failure}$ for some Alabama pile load test data.

Plunging of the bent piles due to inadequate pile tip bearing and side frictional forces during an extreme scour event is possible, but not very likely. Assuming the scour is local around the piles and not over the entire river bed adjacent to the bent, then the soil confining pressures at greater depths will remain about the same. Thus, the loss of soil support during the scour event will be the frictional resistance provided by the soil over the top 15 feet or so of the embedded pile (over the depth of the soil scoured away). Normally the top 15 feet of soil is soft or loose and does not provide a high percentage of the pile frictional resistance. Losing this soil resistance via scour of the soil would reduce the factor of safety of the pile/bent below the design value, but should still provide a F.S. >1.0. As indicated in Appendix D, a reasonable and probable upper-bound estimate for P_f in the top layer(s) that will be scoured away would be,

$$P_f \approx 1.5^k/\text{ft}.$$

Thus, for an S = 15',

$$\Delta P_f = -1.5^k/\text{ft. x } 15' = -22.5^k$$

Or, each pile in the bent would lose 22.5^k of its support capacity during a 15 foot scour event. This should not result in a pile/bent plunging failure.

An alternative approach in estimating the percent of pile capacity loss during a major scour event is given below. Recall that

$$P_{capacity} = P_t + P_f$$

If the pile tip is founded in good soil, we should be able to assume for a steel H-pile (see Table D.1 in Appendix D),

$$P_t \approx 0.10\, P_{capacity}$$

$$P_f \approx 0.90\, P_{capacity}$$

At a particular bridge site, assume that S = 15', and the soil at the pile tip is good such that

$$P_f \approx 0.90\, P_{capacity}$$

$$P_t \approx 0.10\, P_{capacity}$$

For this case, for piles of different original embedment length below ground, ℓ_{bg}, estimates of reductions in P_f and $P_{capacity}$ would be as shown in Table 3.5 (see Fig. 3.22 for parameter definitions).

As can be seen in Table 3.5, an $\ell_{bg} \geq 2.5$ S would probably be sufficient to not have a pile plunging failure (would retain 64% of original pile capacity). However, to be a bit more conservative, we will say that an $\ell_{bg} \geq 3$ S will be sufficient to prevent a pile plunging failure (would retain 70% of original pile capacity). It should be noted that for steel H-piles with their

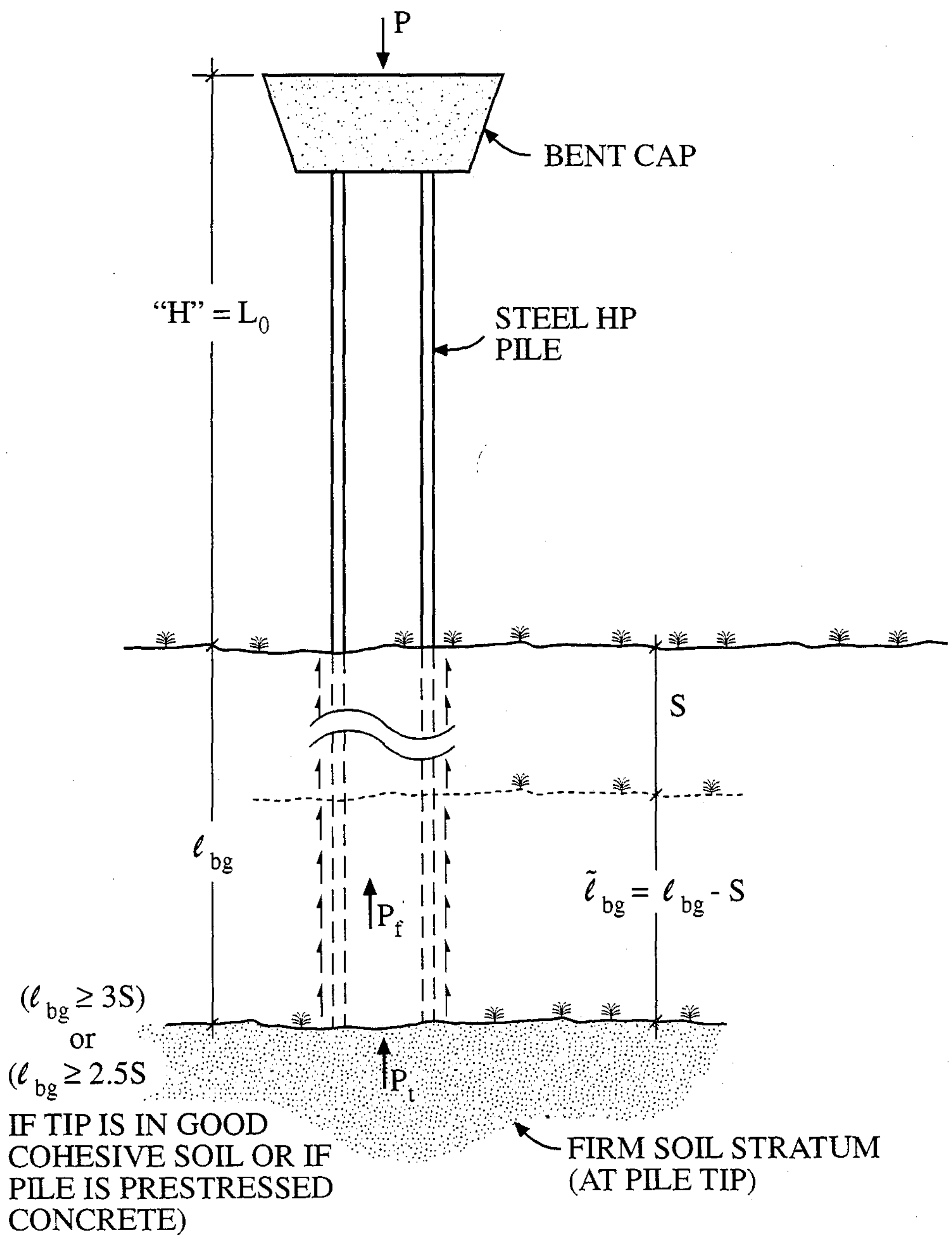

Fig. 3.22. Minimum Pile-Soil Setting Conditions Needed to Prevent a Pile Plunging Failure

tips in a good cohesive soil, P_t is considerably larger than the 10% of $P_{capacity}$ used in the case above. This is also true of prestressed concrete piles with their tips in either cohesionless or cohesive soils. For these cases, the loss of $P_{capacity}$ due to scour will be smaller than for the case described above, and thus a pile plunging failure should not occur in a scour event in these cases for an ℓ_{bg} as low as 2.0 S. Again, to be a bit more conservative, we will say that an $\ell_{bg} \geq 2.5$ S will be sufficient to prevent a pile plunging failure in these cases..

Table 3.5. Estimated Pile Capacity Loss/Retained After Extreme Scour Event

ℓ_{bg} (ft)	S (ft)	ℓ_{bg} (ft)	P_f		$P_{capacity} = P_f + P_t$	
			% Loss[1]	% Retained	% Loss[2]	% Retained
70	15	55	21.5	78.5	19.4	80.6
60	15	45	25	75	22.5	77.5
50	15	35	30	70	27.0	73.0
45[3]	15	30	33.3	66.7	30.0	70.0
40	15	25	37.5	62.5	33.8	66.2
37.5[4]	15	22.5	40	60	36.0	64.0
30	15	15	50	50	45.0	55.0

(1) % Loss of $P_f = S/\ell_{bg} \times 100$
(2) % Loss of $P_{capacity} = 0.90 \times$ % Loss of P_f
(3) ℓ_{bg} corresponding to $\ell_{bg} = 3.0$ S
(4) ℓ_{bg} corresponding to $\ell_{bg} = 2.5$ S

In summary, for a given pile/bent, if the pile tip is embedded in a firm soil with good bearing capacity, and if the length of the pile below the original ground line is greater than 3.0 times the maximum scour, S to occur at the site, then the piles and bent should continue to have a F.S. > 1.0 against a pile plunging failure. Or, if the tip is founded in a good cohesive soil or the pile is a prestressed concrete pile then the pile should not plunge if $\ell_{bg} \geq 2.5$ S. These minimum conditions are graphically illustrated in Fig. 3.22. If neither of the above conditions is met at the site, then a closer examination should be made concerning a possible pile plunging failure

3.6 Failure of Bent Cap

Failure of the pile bent cap is unlikely as indicated earlier due to the superstructure girders sitting directly above the piles. Significant relative vertical displacement between piles could cause failure of the cap in cases where the cap is lightly reinforced (as some are). Let us examine the forces set up in the cap in the event of a pile plunging or buckling failure.

From an examination of numerous pile bent standards, many pile cap geometries and pile spacings appear to be as shown in Fig. 3.23. For the pile cap indicated in this figure, for the pile to plunge or buckle, the P_{load} would have to exceed $137.8^k + P_{plunging}$ or $P_{buckling}$ of the pile as can be seen from FBD(a) in Fig. 3.23. The P_{load} will never be this large and the failure indicated in Fig. 3.23 will not occur.

Lightly reinforced bent cap such as the one shown in Fig. 3.24 are very susceptible to cap flexural failures as indicated. They provide very little reserve strength for resisting an applied P_{load} if the pile capacity P_{pile} is exceeded as indicated in Fig. 3.24. However, even in this case, due to transverse continuity of the bridge superstructure, there would be a redistribution of loads across the width of the bridge (and bent cap) if at a given pile location, $P_{load} > P_{pile}$.

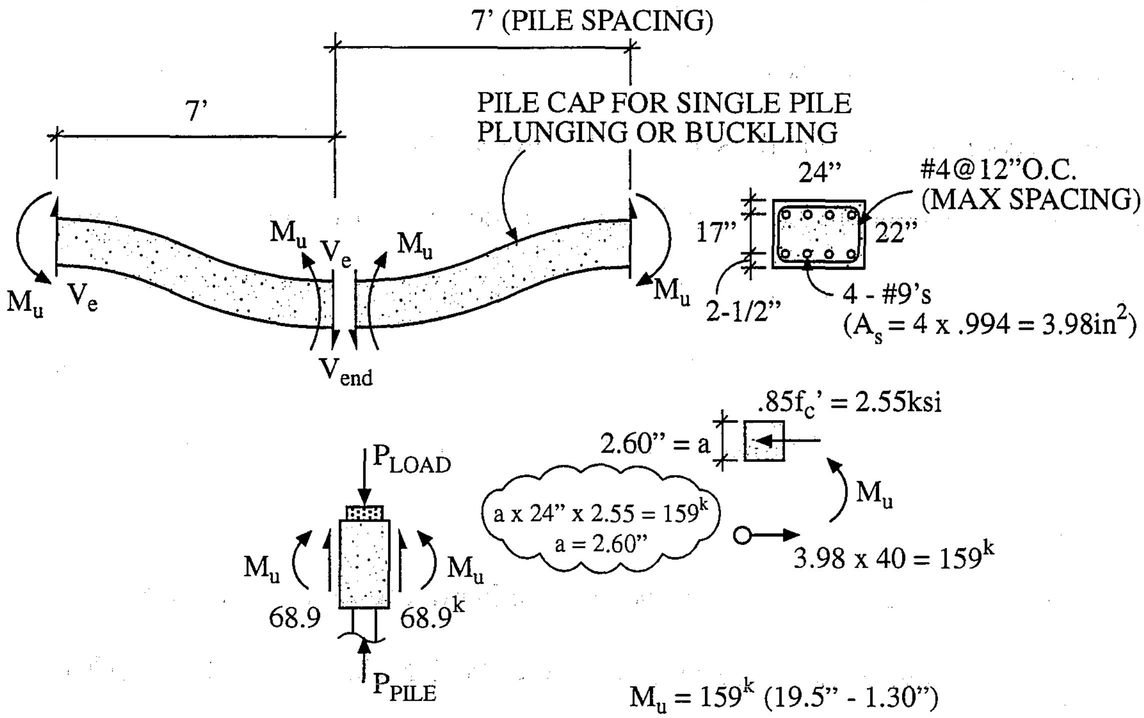

FBD (a)

$$M_u = 159^k\,(19.5" - 1.30")$$
$$= 241^{1k}$$

$$V_{end} = \frac{2M_u}{7'} \quad \frac{2 \times 241^{1k}}{7} = 68.9^k$$

$$2V_{end} = 137.8^k$$

CHECK SHEAR CAPACITY

$$V_u = \phi V_c + \phi V_s$$
$$= \phi(2\sqrt{fc'}\, b_w d) + \phi\left(\frac{A_n f_y d}{S}\right)$$
$$= 0.85(2\sqrt{3000} \times 24 \times 19.5)$$
$$+ 0.85\left(\frac{2 \times 0.20 \times 40 \times 19.5}{12}\right)$$
$$= 43.56^k + 22.10^k$$

$$V_u = 65.7^k \Leftarrow$$

∴ IF $P_{LOAD} \geq 137.8^k + P_{CR\text{ - PILE (BUCKLING OR PLUNGING)}}$
THE PILE CAP WILL FAIL AS INDICATED ABOVE

CLOSE ENOUGH SHEAR CAPACITY TO DEVELOP FULL END M_u'S OF THE CAP.

Fig. 3.23. Examination of Pile Cap Flexural Failure for Case of Well Reinforced Cap.

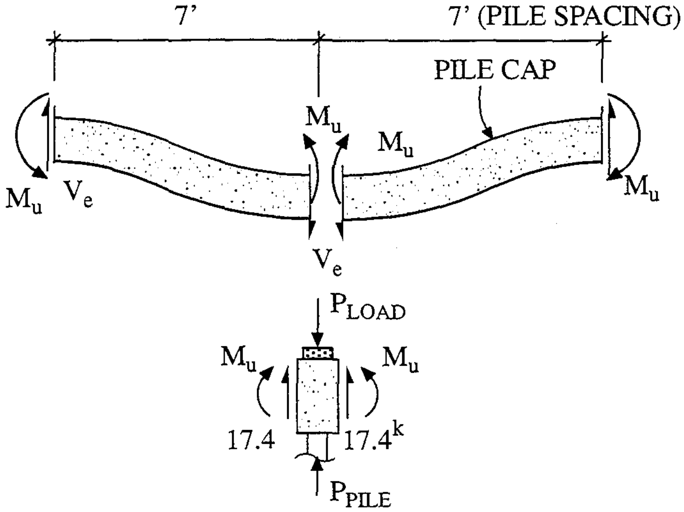

FBD (a)

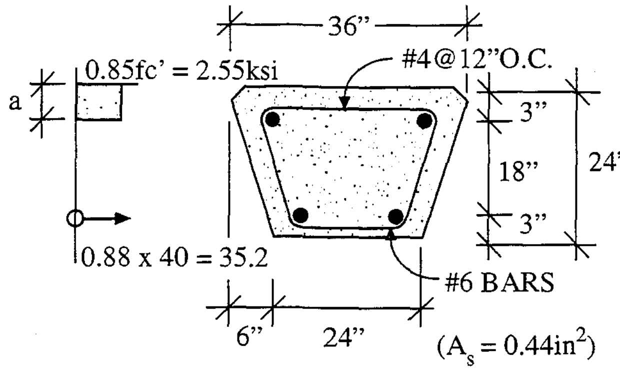

$a \times 2.55 \times 36" = 35.2$

$a = 0.384"$

$M_u = 159^k\,(19.5" - 1.30")$

$= 732^{11k} = 61^{1k}$

$$V_{end} = \frac{2M_u}{7'} \quad \frac{2x61^{1k}}{7} = 17.4^k$$

$2V_{end} = 34.8^k$

$\therefore$ IF $P_{LOAD} \geq 34.8^k + P_{CR\text{-PILE}}$ (BUCKLING OR PLUNGING)

THE PILE CAP WILL TRY TO FAIL AS INDICATED ABOVE. HOWEVER IF THIS CONDITION IS EVER REACHED, THERE WILL BE A REDISTRIBUTION OF LOAD ACROSS THE WIDTH OF THE BRIDGE (AND BENT CAP}.

CHECK SHEAR CAPACITY

$$V_u = \phi V_c + \phi V_s$$
$$= \phi(2\sqrt{fc'}\,b_w d) + \phi\left(\frac{A_n f_y d}{S}\right)$$
$$= 0.85(2\sqrt{3000} \times 30 \times 21)$$
$$+\ 0.85\left(\frac{2 \times 0.20 \times 40 \times 21}{12}\right)$$
$$= 58.7^k + 23.8^k$$
$$= 82.5^k$$

$\Leftarrow$ CAP HAS SUFFICIENT SHEAR CAPACITY TO DEVELOP FULL END M_u'S.

Fig. 3.24. Examination of Pile Cap Flexural Failure for Case of Lightly Reinforced Cap.

3.7 Local Yielding of Pile Due to Combined Normal Stresses

As indicated earlier, local yielding of the bent piles near the new ground line after an extreme scour event due to $-\frac{P}{A} \pm \frac{M_x y}{I_x} \pm \frac{M_y x}{I_y}$ stresses is quite possible.

Strong axis bending stresses at the ground line caused by longitudinal truck braking forces when coupled with axial pile stresses and nominal bending about the pile weak-axis can easily reach the pile yield stress. However, such high local stresses can be tolerated and will not lead to collapse of the bridge bent. In the worse-case scenario, they could lead to plastic hinges forming at the base of the pile bents which would continue to function in a stable and effective manner as indicated in Fig. 3.25. However, due to the large flexibility of the pile bents in the longitudinal direction because of their relatively small I_x value and their long length above ground ("H" + S), most of a truck's longitudinal braking force will be transmitted horizontally along the superstructure into the abutment.

The large longitudinal flexibility (and small stiffness) of a typical pile bent is indicated in Fig. 3.25. Note also in Fig. 3.25 that for 1-girder line of loading, a truck braking force, F_B, of 4.8^k would result in a plastic hinge developing at the groundline for a 30" high HP 10 x 42 pile bent. Actual truck braking forces are larger than this and hence, most of a truck braking force will have to be transmitted longitudinally to an abutment.

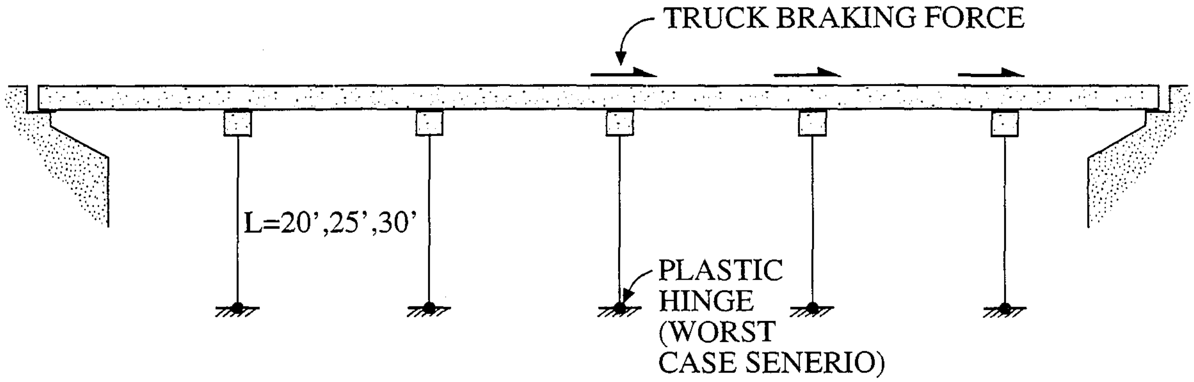

L = "H" + S

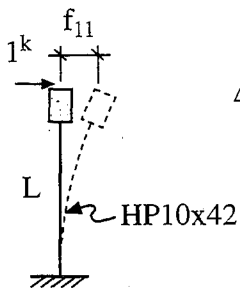

$$\Delta_{TOP} = f_{11} = \frac{1^k L^3}{3EI_x}$$

FOR L = 20' ➡ $f_{11} = \dfrac{F_k x 20^3 x 1728}{3x29{,}000x210} = 0.757^{11/k}$ ➡ $k_{11} = 1.32^{k/11}$

FOR L = 25' $f_{11} = 1.48^{11/k}$ $k_{11} = 0.676^{k/11}$

$$k_{11} = \frac{1}{F_{11}}$$

FOR L = 30' $f_{11} = 2.56^{11/k}$ $k_{11} = 0.391^{k/11}$

NOTE THE LARGE FLEXIBILITIES (f_{11}) AND SMALL STIFFNESS (k_{11}) VALUES FOR THE BENT.

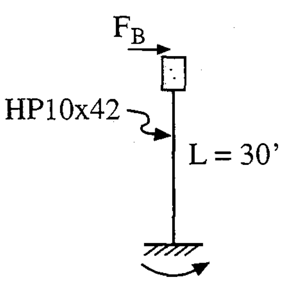

$M_P = \sigma_Y x z_x$

$= \dfrac{36x48.3}{12}$

$= 145^{1k}$

F_B x 30' = $M_P = 145^{1k}$

$F_B = 4.8^k$ ➡ NOTE, THIS WOULD RESULT IN $\Delta_{TOP} = \dfrac{F_B L^3}{3EI}$

$= 12.26" \rightarrow$

∴ MOST OF TRUCK BRAKING FORCE WILL HAVE TO BE TRANSMITTED TO AN ABUTMENT.

Fig. 3.25. Worst-Case Scenario for Plie Bending Stresses and Large Longitudinal Bent Flexibilities.

4. PILE/BENT TRIAL ANALYSES AND PARAMETER SENSITIVITIES USING FB-PIER

4.1 General

FB-Pier is a graphical user interface computer program operating in a windows environment for the analysis of pile group foundations. The program was developed by the University of Florida for the Florida Department of Transportation and Federal Highway Administration. There are eight general types of pile foundation problems that the user may model with FB-Pier. They are:

1) pile and cap only
2) general bridge piers
3) high mast lighting and signs
4) retaining walls on top of pile groups
5) sound walls
6) equivalent stiffness of pile group analysis
7) pile bents
8) column analysis

These eight problem types or categories are illustrated graphically in Fig. 4.1. Each of the eight categories starts the user with an initial default data structure and limits the screens that the user subsequently modifies or asks the user if they wish to change problem type

Early in the investigation, we secured the computer program FB-Pier and began modelling and analyzing the example problems in the Users Guide and Manual to learn how to use the program and its capabilities. Later, we performed parameter sensitivity analyses using

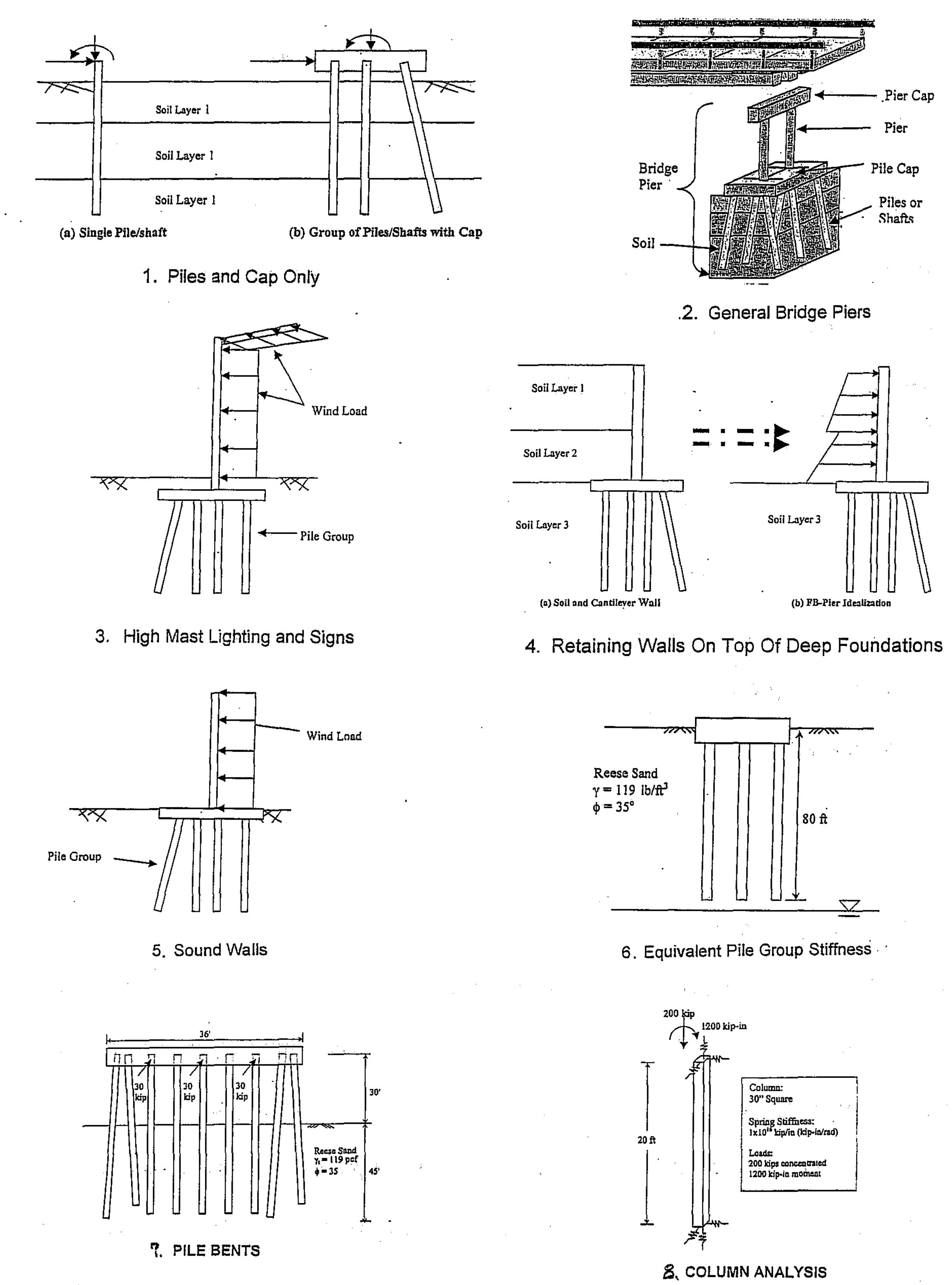

Fig. 4.1. Eight Problem Types That Can Be Modeled with FB-Pier

the program to gain a better understanding of the behavior of pile bents and their sensitivities to various system parameters. These analyses and their results are presented in the following sections.

4.2 Develop P-Δ Curves for a Pile Bent in Longitudinal Direction for Various Levels of Scour

For this problem, rather than work with the complete bent, one pile in the bent was analyzed by itself as indicated in Fig. 4.2. As indicated in the figure, an HP 10 x 42 pile was used with an initial length above ground of $\tilde{L}$ = 20 ft. The top of the pile/bent cap was assumed to be pinned as indicated in Fig. 4.2 and the P load was assumed to be applied with an eccentricity of 3 in. as indicated. The load eccentricity was used because it was though to be realistic and also so that the pile would be a beam-column and thus have a beam-column P-Δ curve. As P was incrementally increased from zero to failure (where FB-Pier would not converge) the pile lateral deflection at $\tilde{L}/2$ was monitored and later plotted. As the amount of scour was increased in increments of 5 ft. to a maximum value of 20 ft. (i.e., S = 0, 5, 10, 15, 20), $\tilde{L}$ was always taken as the length of pile above ground. Soil and other parameter values used in the FB-Pier modeling are shown in Table 4.1. The resulting P-$\Delta_{\tilde{L}/2}$ curves generated in these analyses are shown in Fig. 4.3.

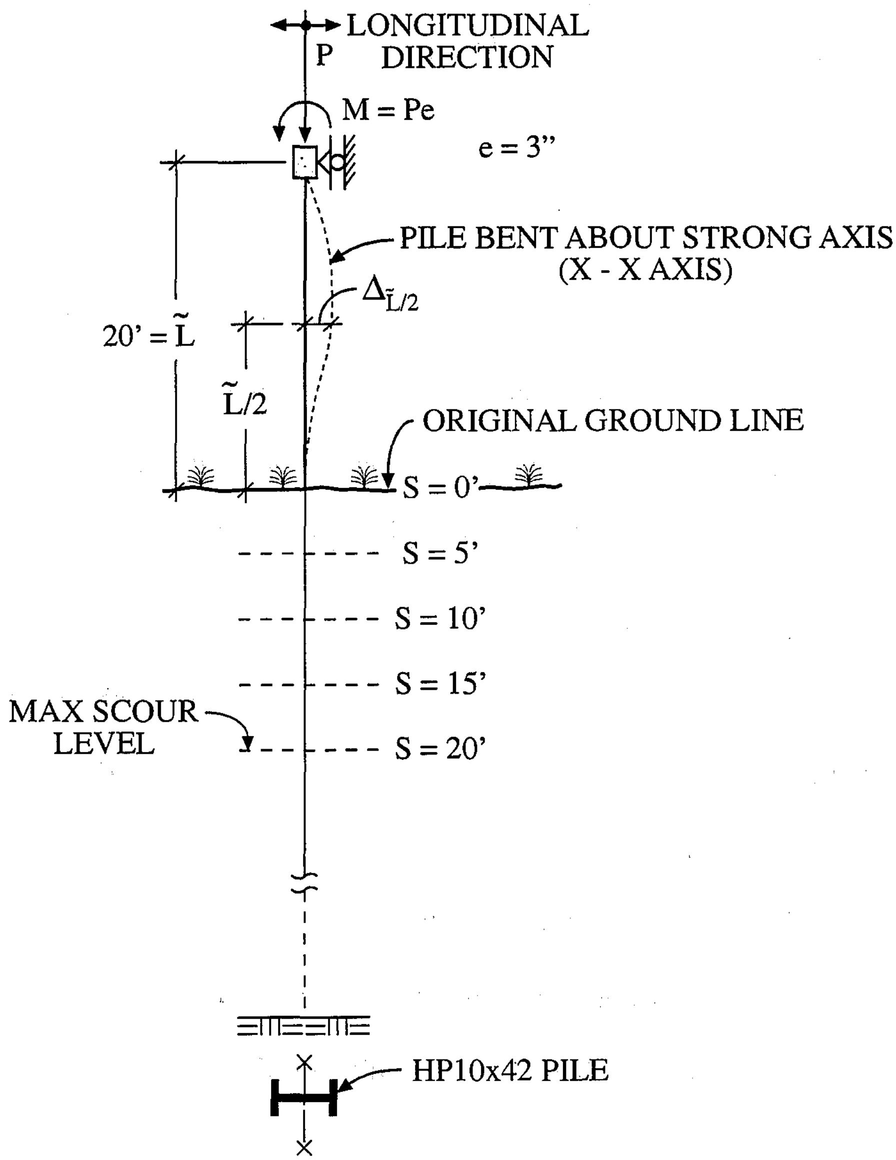

Fig. 4.2. Single Pile Analyzed to Determine P-$\Delta_{\tilde{L}/2}$ Curve in Longitudinal Direction

Table 4.1. Soil and Other Parameter Values Used in FB-Pier Modeling of Problems Shown in Figs. 4.2 and 4.4.

Pile: HP 10 x 42

Pile length: 80 ft.
Initial pile length above ground: 20 ft.
Sand (Reese):

> Unit weight = 120 pcf
> Internal friction angle = 35
> Subgrade modulus = 150 lb./in.^3
> Poisson's ratio = 0.3
> Shear modulus = 3.5 ksi
> Vertical failure shear = 1152 psf
> Torsional shear stress = 1152 psf

Tip:

> Shear modulus = 3.5 ksi
> Poisson's ratio = 0.35
> Axial bearing failure = 640 kips

Scour depth (ft.):

> 0, 5, 10, 15, 20

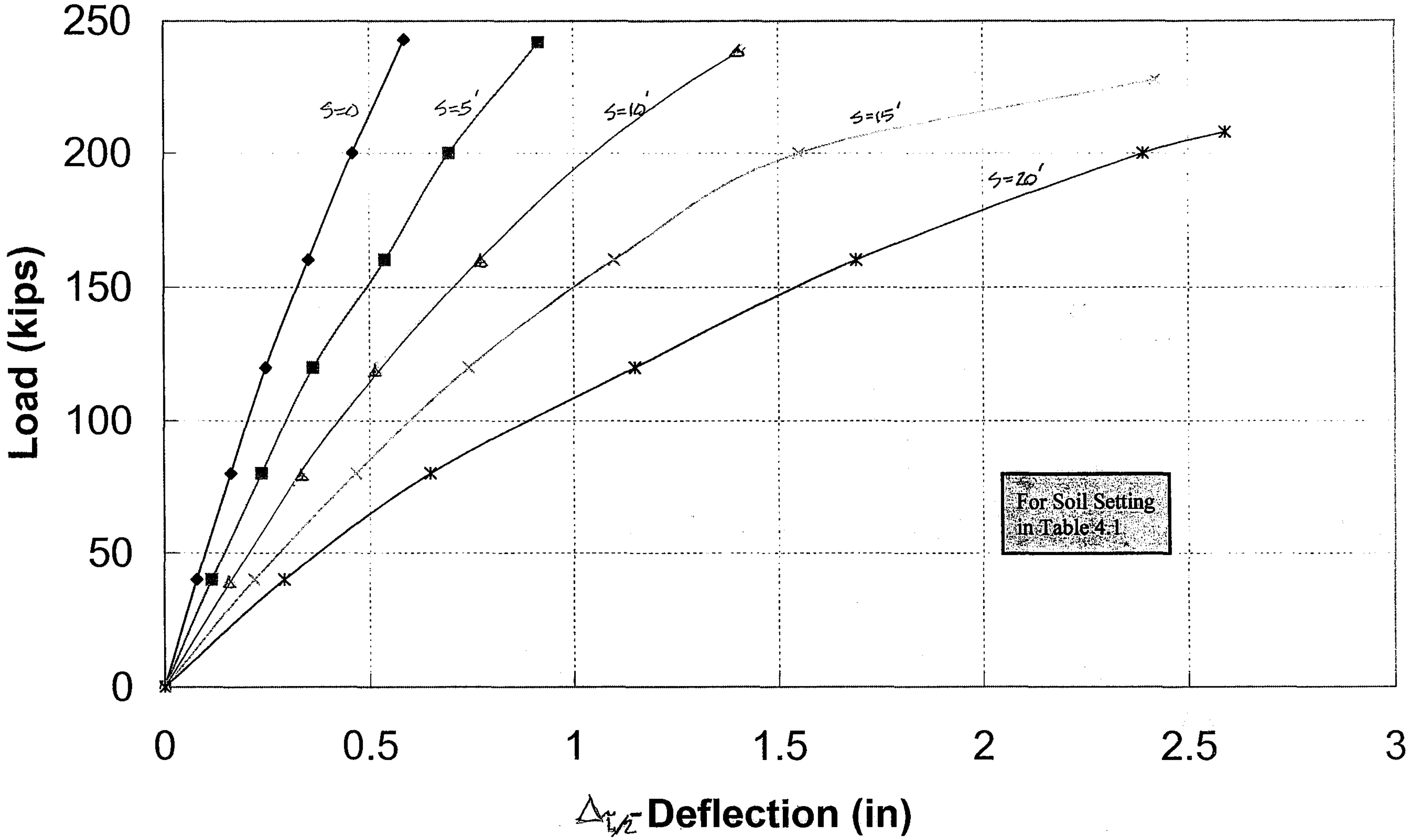

Fig. 4.3. P-$\Delta_{L/2}$ Curves in Longitudinal Direction for Single HP 10 x 42 Pile in Fig. 4.2.

4.3 Develop P-Δ Curves for a Pile Bent in Transverse Direction for Various Levels of Scour

The same pile bent and setting as analyzed for the longitudinal P-$\Delta_{\tau/2}$ curves in the previous section is investigated here to develop transverse P-Δ_{top} curves. However, because of the batter of the end piles, the whole bent must be modeled and analyzed to obtain the curves. Hence, the pile bent modeled and analyzed to determine the P-Δ_{top} curves for scour values of 0, 5', 10', 15', and 20' is as shown in Fig. 4.4. In the analyses, the 1^k horizontal force at the bent cap was held constant and the P_{loads} were incrementally increased until FB-Pier would not converge (this was viewed as the failure load). Note in this case, the piles were bending about their weak axis (Y-Y axis). Soil and other parameter values used in the FB-Pier modeling were the same as those used in the previous analyses and are given in Table 4.1. The resulting P-Δ_{top} curves generated in the analyses are shown in Fig. 4.5.

4.4 Effect of Pile Batter on Bent P-Δ_{top} Curves in Transverse Direction

To determine the sensitivity of pile bent P-Δ_{top} curves in the transverse direction, the pile bent of the previous section (see Fig. 4.4) was re-analyzed using FB-Pier, for end pile batters of 1 in 12 or 0.083, 1 ½ in 12 or 0.125, and 2 in 12 or 0.167. The same soil setting and conditions as identified in Table 4.1 were used in the analyses, and the results are shown in Figs. 4.6-4.8. To make the results more friendly to assessing the effects of end pile batter, the data is re-plotted in Figs. 4.9 - 4.13 to show the curves for all three batters on the same plot for each scour level.

4.5 Effect of Soil Subgrade Modulus on Single Bent Pile P-Δ Curve in Longitudinal Direction

To gain an understanding of the sensitivity of a bent pile P-$\Delta_{\tau/2}$ curve and $P_{failure}$ prediction to the supporting soil subgrade modulus, a single pile was analyzed using FB-Pier and

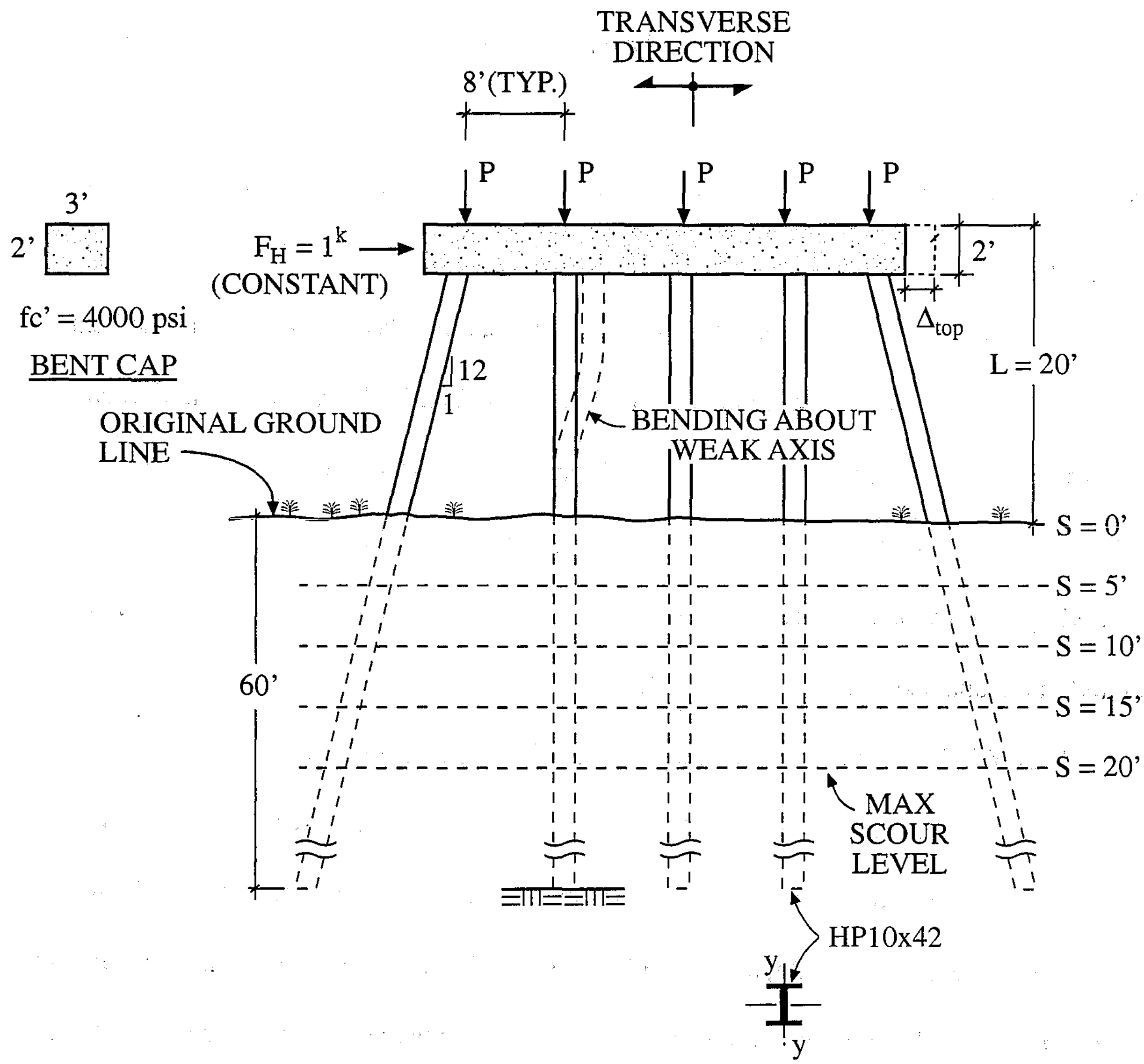

Fig. 4.4. Pile Bent Analyzed to Determine P-Δ_{top} Curve in Transverse Direction

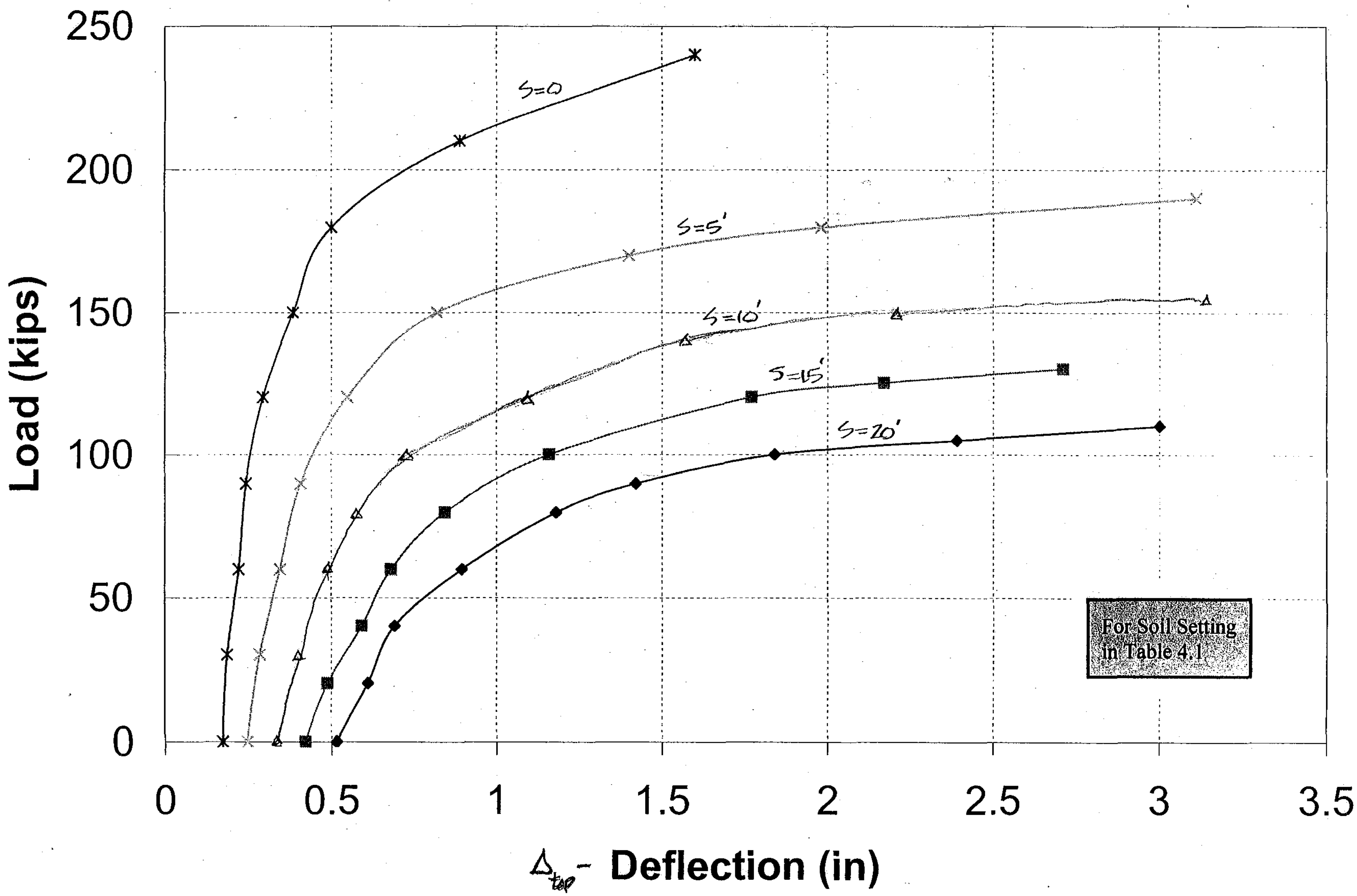

Fig. 4.5. P-Δ_{top} Curves in Transverse Direction for HP 10 x 42 Pile Bent in Fig. 4.4

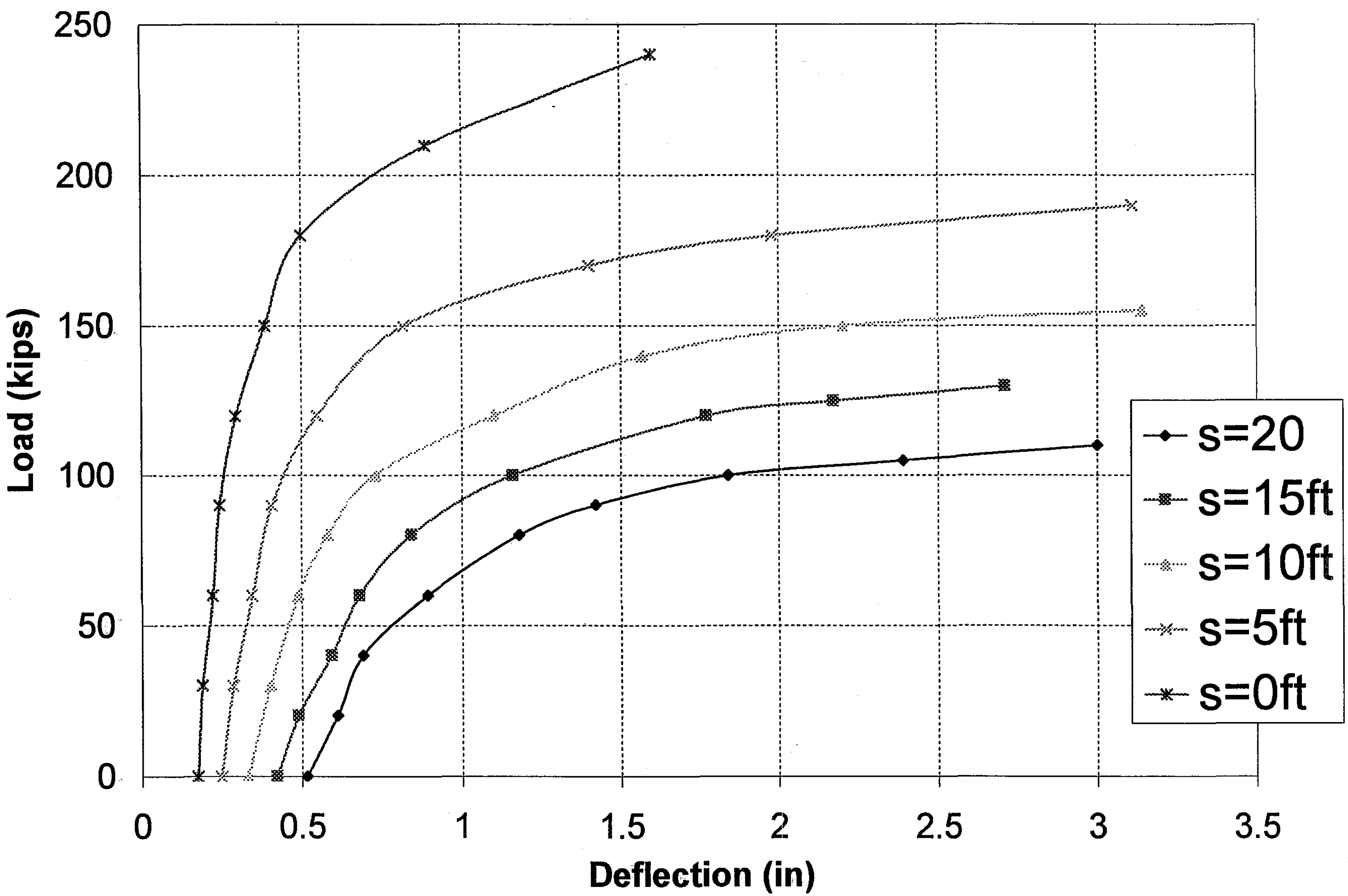

Fig. 4.6. P-Δ_{top} Curves in Transverse Direction for Pile Bent in Fig. 4.4 for Batter = 0.083

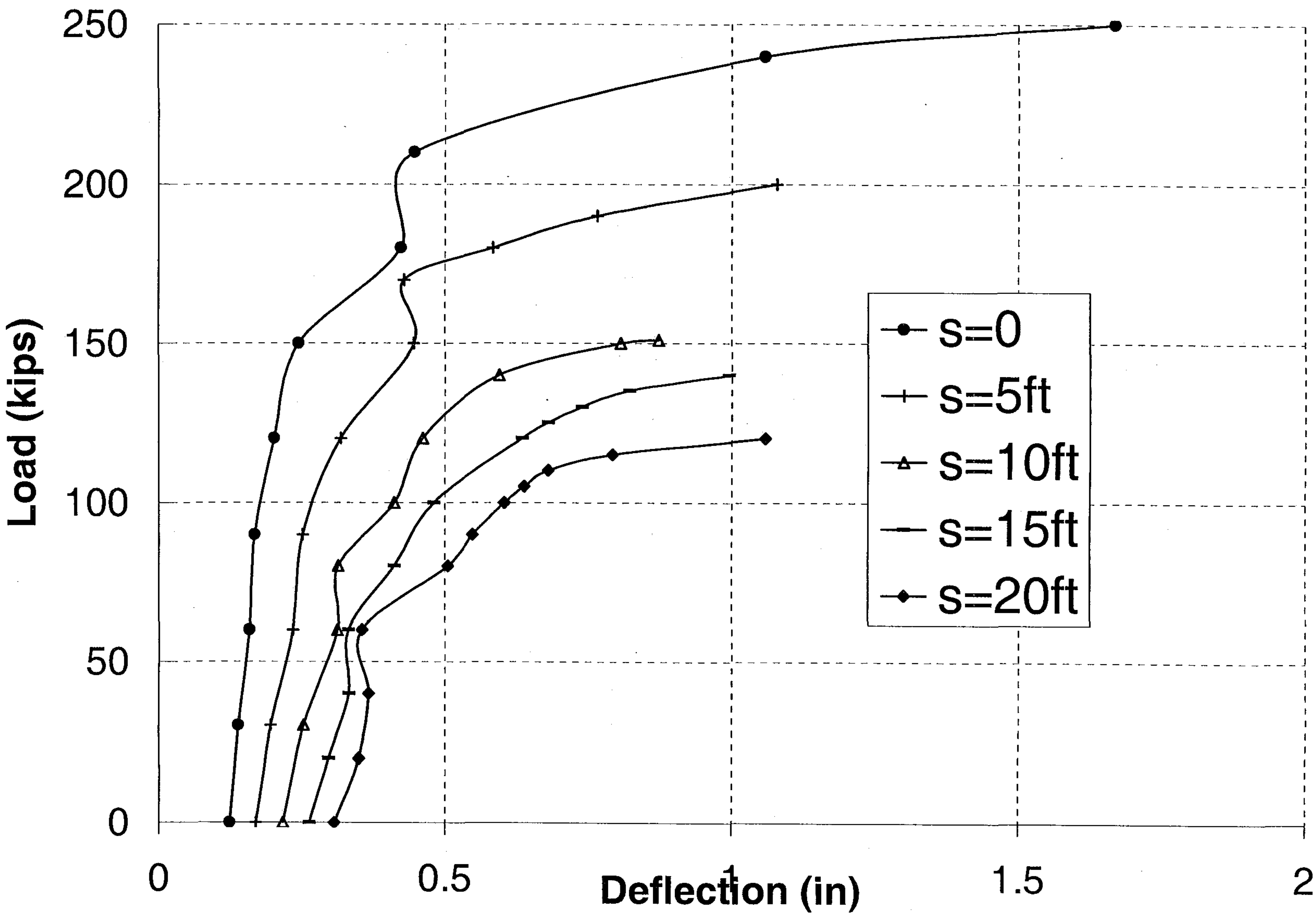

Fig. 4.7. P-Δ_{top} Curves in Transverse Direction for Pile Bent in Fig. 4.4 for Batter = 0.125

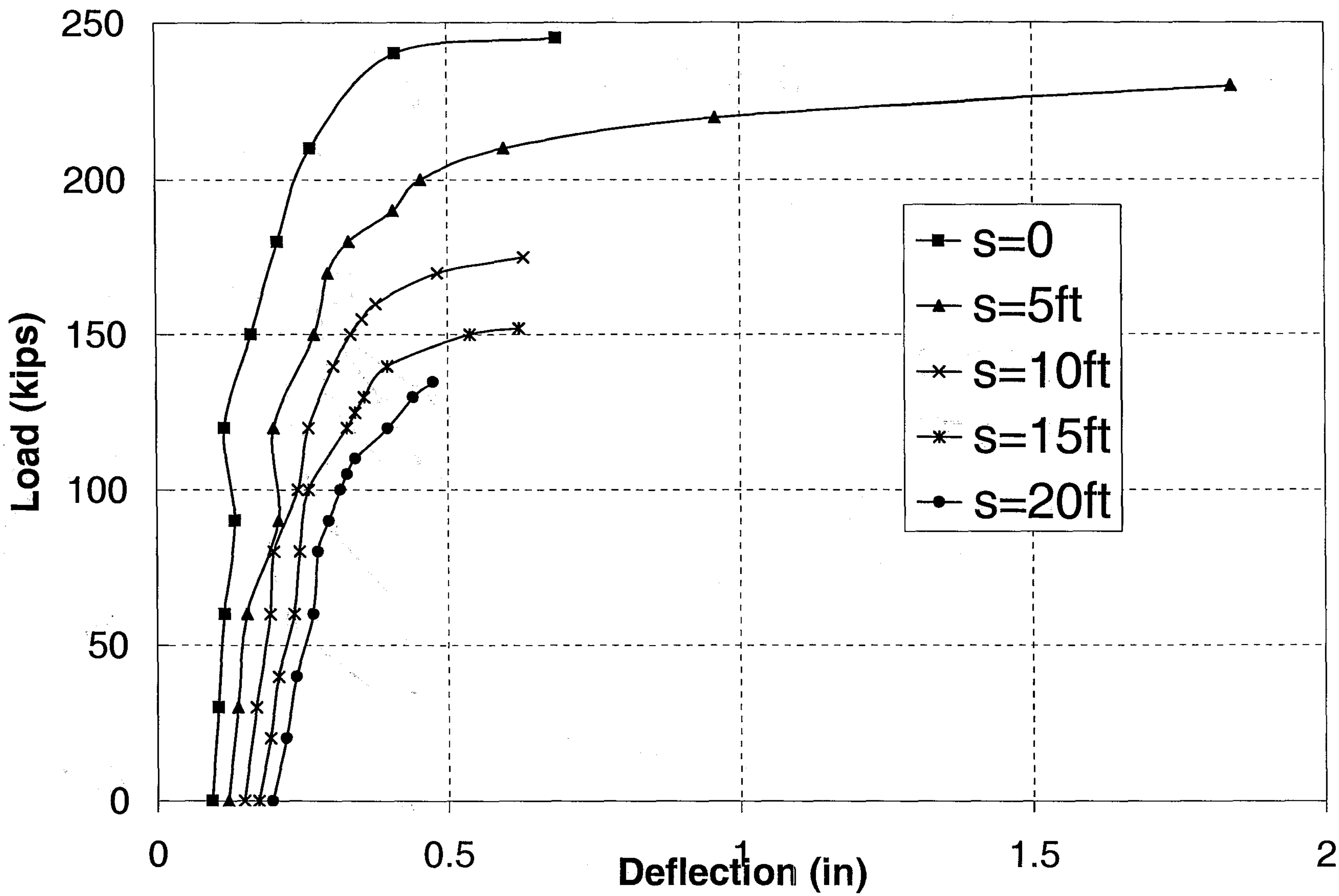

Fig. 4.8. P-Δ_{top} Curves in Transverse Direction for Pile Bent in Fig. 4.4 for Batter = 0.167

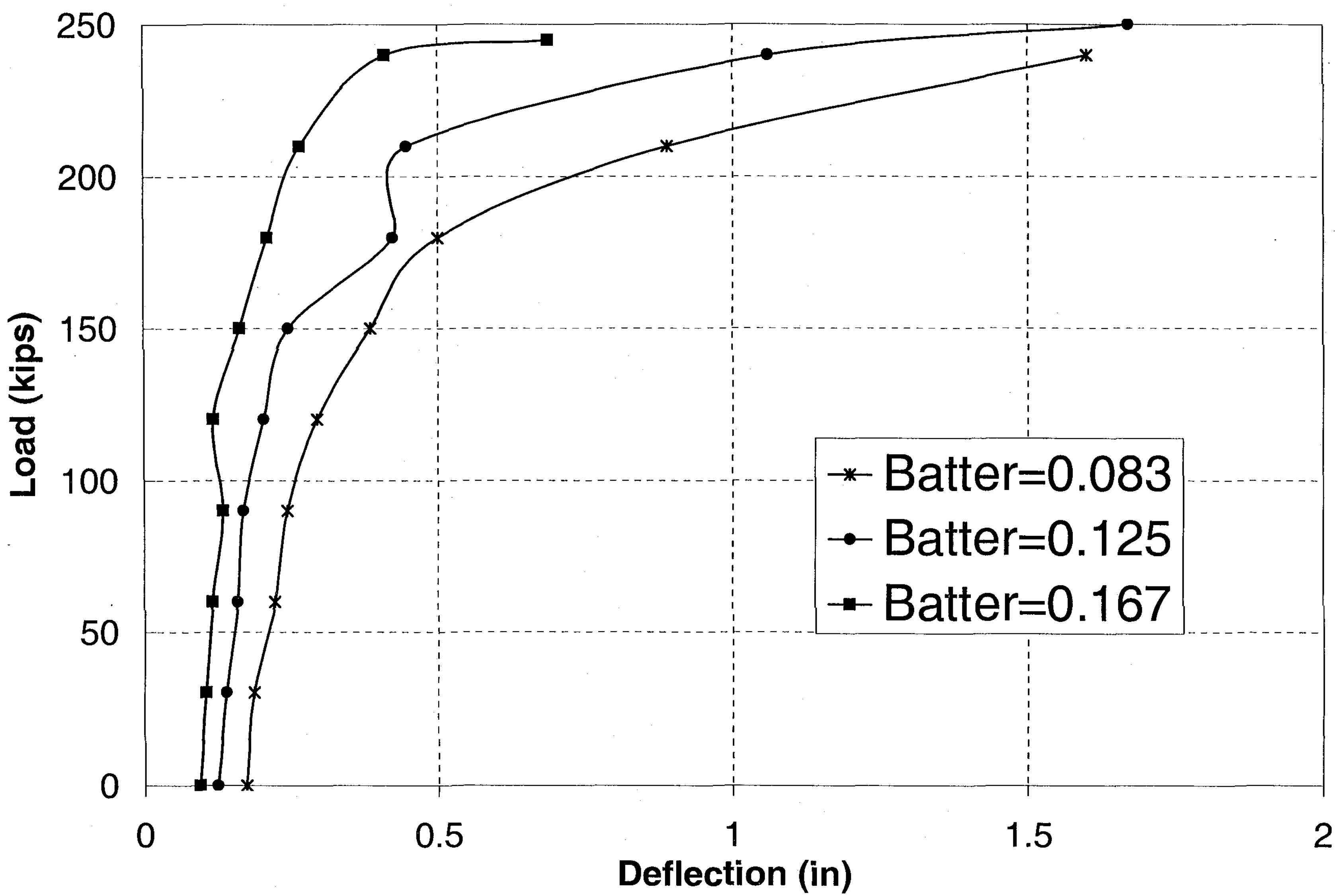

Fig. 4.9. P-Δ_{top} Curves in Transverse Direction for Pile Bent in Fig. 4.4 for All Batters for S = 0.

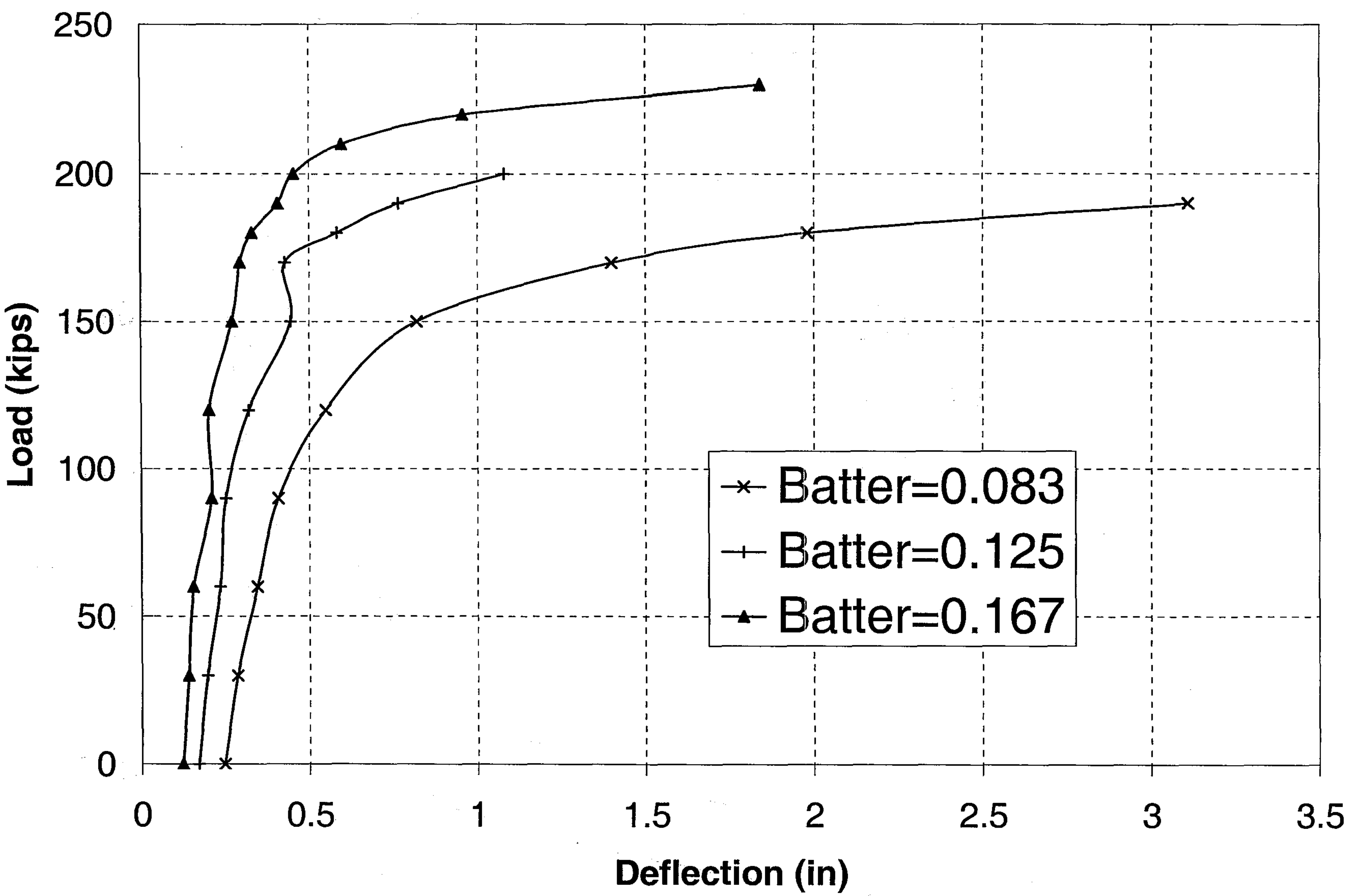

Fig. 4.10. P-Δ_{top} Curves in Transverse Direction for Pile Bent in Fig. 4.4 for All Batters for S = 5 ft.

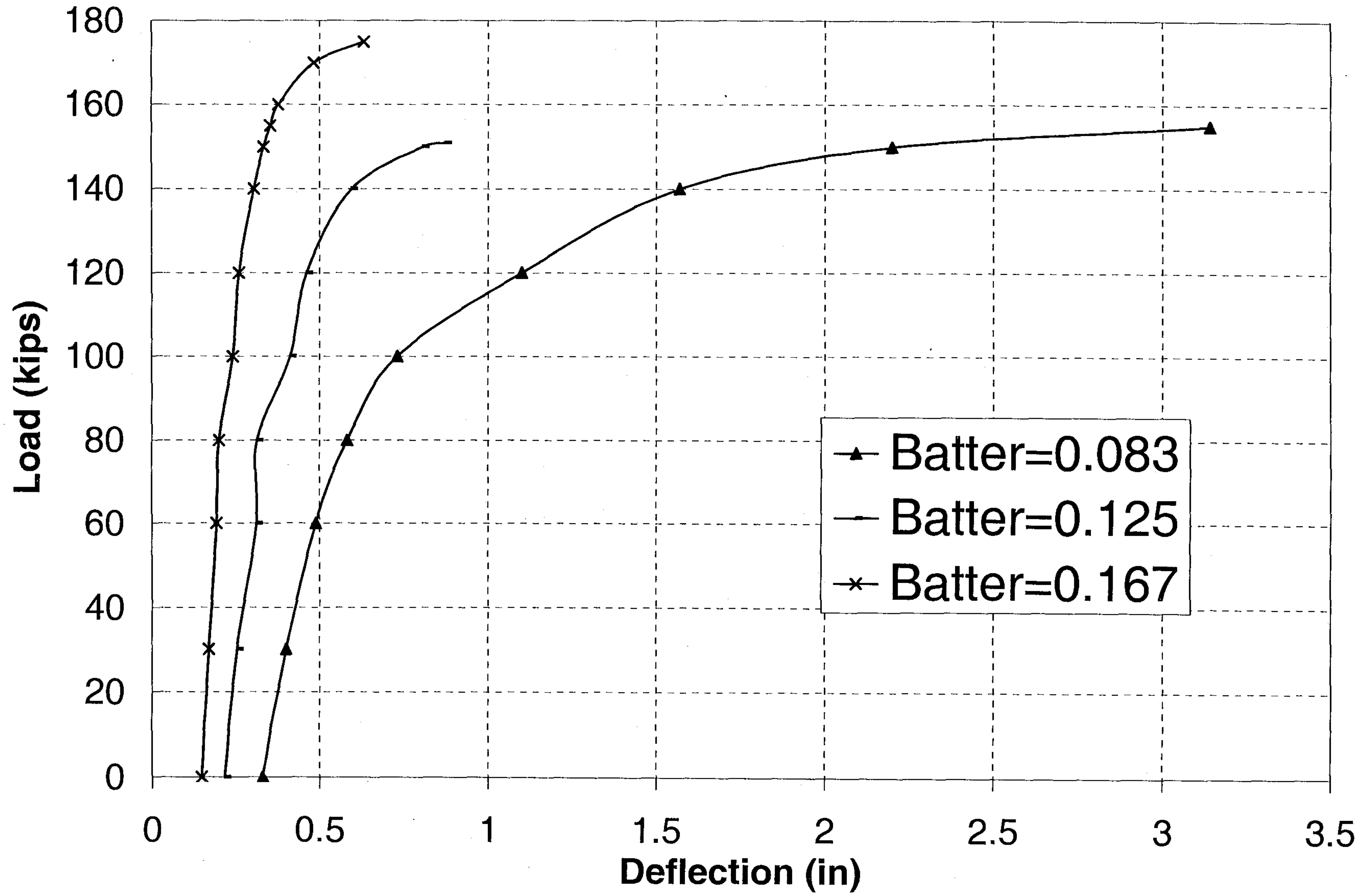

Fig. 4.11. P-Δ_{top} Curves in Transverse Direction for Pile Bent in Fig. 4.4 for All Batters for S = 10 ft.

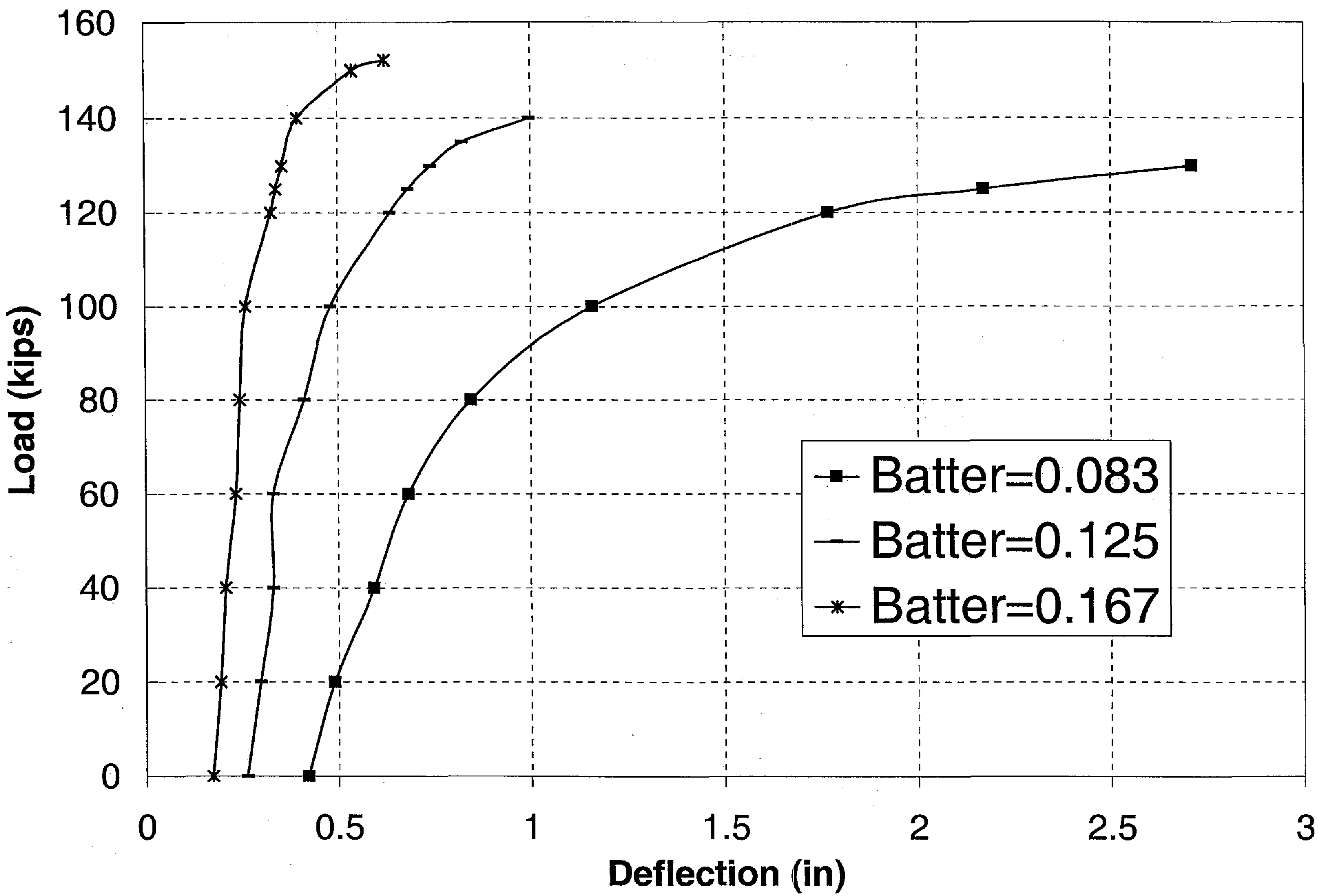

Fig. 4.12. P-Δ_{top} Curves in Transverse Direction for Pile Bent in Fig. 4.4 for All Batters for S = 15 ft.

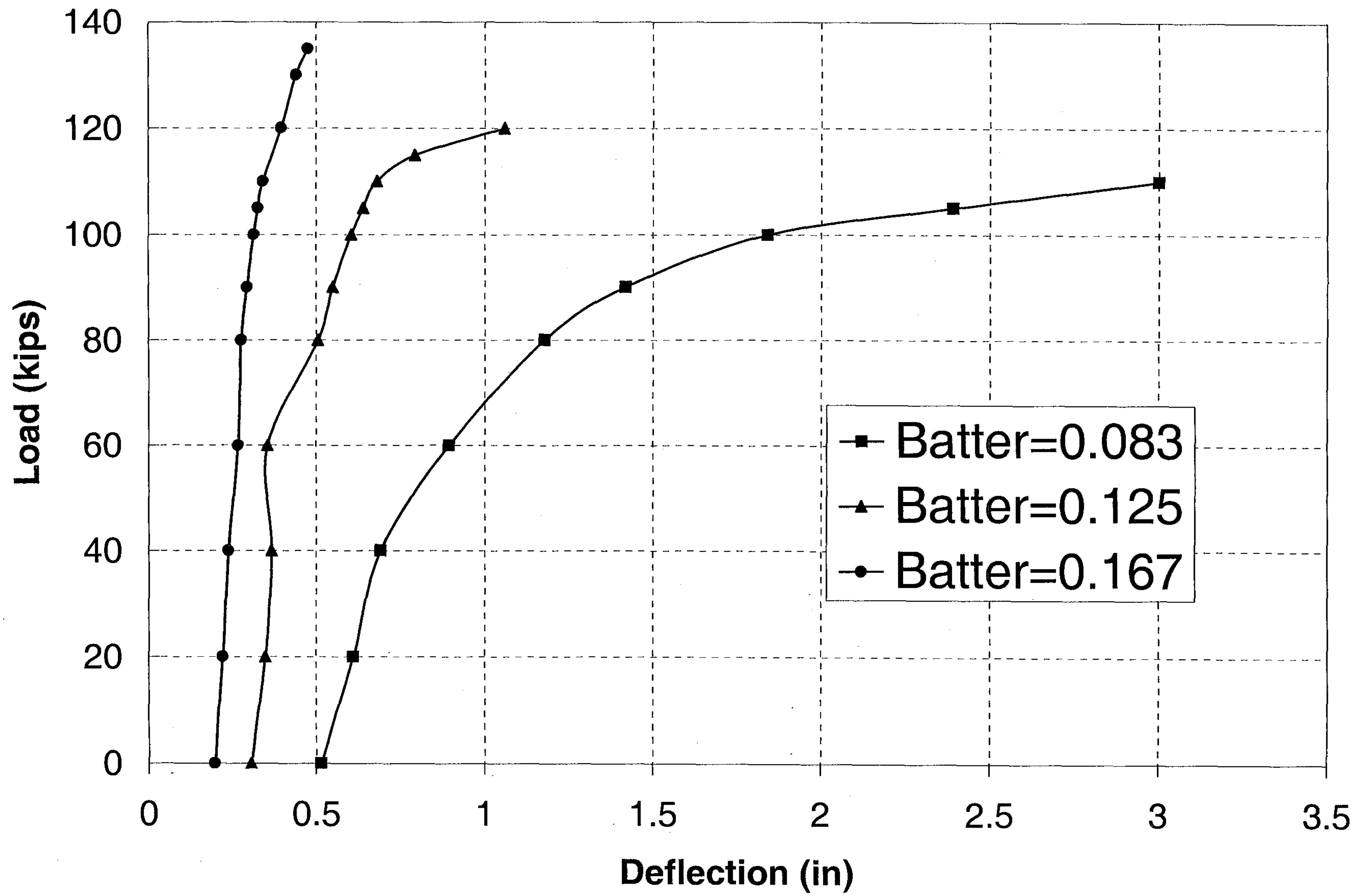

Fig. 4.13. P-Δ_{top} Curves in Transverse Direction for Pile Bent in Fig. 4.4 for all Batters for S = 20 ft.

a broad range of k_0 (lb./in.^{3}) values. The single pile setting/conditions are as shown in Fig. 4.14 and Table 4.2. Again, an eccentricity of loading of 4" was used to produce an applied end moment at the pile top of 4" x P so as to produce a P-$\Delta_{L/2}$ curve as qualitatively indicated in Fig. 4.14. Soil and other parameter values used in the FB-Pier modeling are given in Table 4.2. The resulting P-$\Delta_{\tau/2}$ curves generated in these analyses are shown in Fig. 4.15 for a HP 10 x 42 pile and in Fig. 4.16 for a HP 12 x 53 pile. Note in Figs. 4.15 and 4.16 that the P_{CR} value for k = 0 had to be determined analytically or using the FB-Pier column analysis category as indicated in Fig. 4.17. Also note in Figs. 4.15 and 4.16 that the "failure" loads (program would not continue) implied by FB-Pier for the other k values (the largest P-load for each k value) was the load to cause first yielding of most highly stressed fiber in the pile rather than the load where the pile becomes unstable. To get the stability limit or buckling load for each k value, we should increase the pile yield stress to a large value and rerun the analyses. Also note in Figs. 4.15 and 4.16 that the subgrade modulus has a small effect on the P-Δ curve but almost no effect on the failure load (as determined by FB-Pier). Analytical analyses also indicate that the soil subgrade modulus has little effect on a pile's buckling load.

4.6 Effect of Soil Internal Friction Angle on Single Bent Pile P-Δ Curve in Longitudinal Direction

The same pile conditions as indicated in Fig. 4.14 and Table 4.2 were used to assess the effects of the soil internal friction angle, ϕ, on the P-Δ curve and predicted failure load. For this case, however, the soil subgrade modulus was held constant at a value of k = 85.05 lb./in^3 and ϕ was varied from

$$\phi = 20°, 25°, 30°, 35°, 40°$$

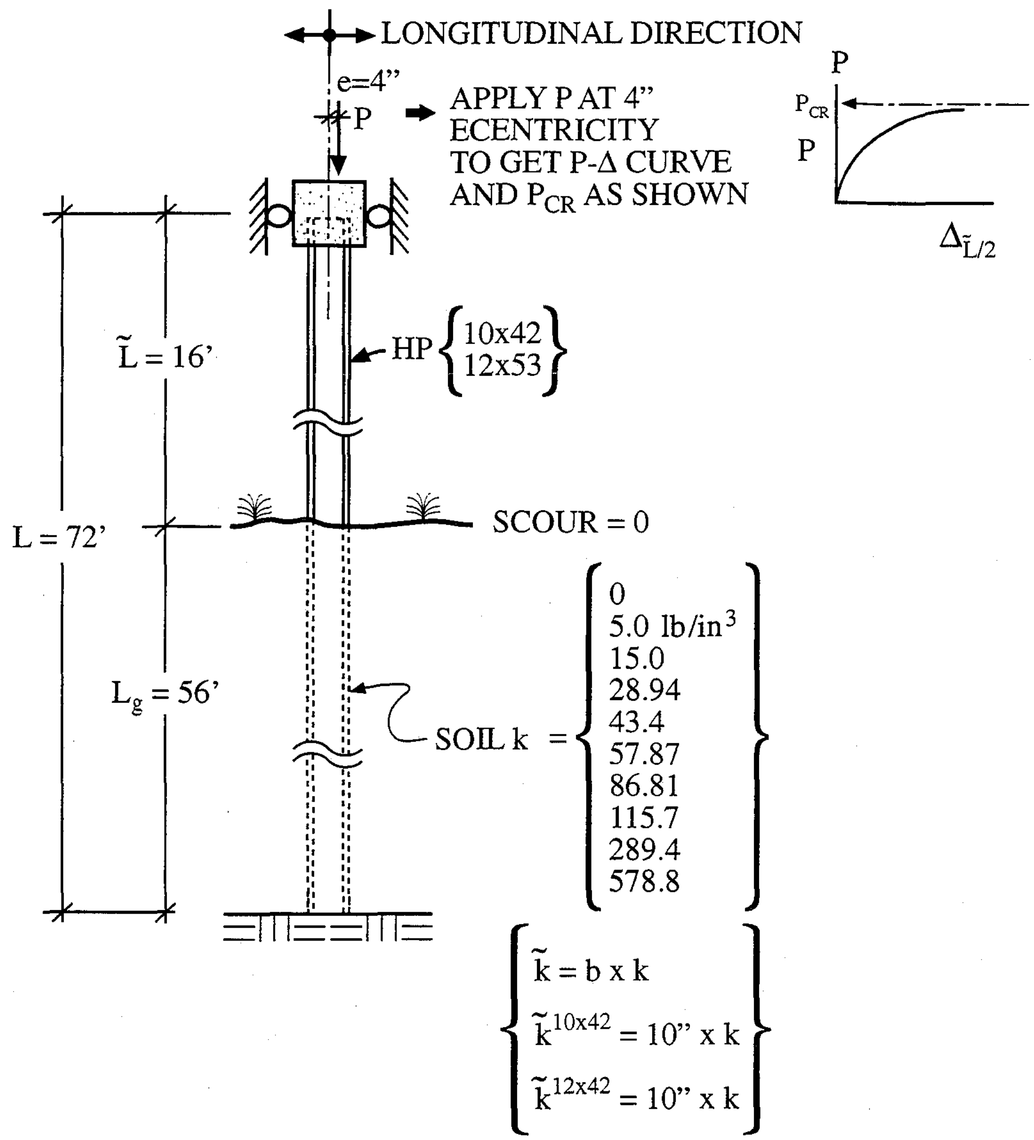

Fig. 4.14. Single Pile Analyzed to Determine Sensitivity of P-$\Delta_{\tilde{L}/2}$ Curve and P_{CR} to Soil Modulus, k

Table 4.2. Soil and Other Parameter Values Used in FB-Pier Modeling of Problem Shown in Fig. 5.14

Pile: HP 10 x 42, HP 12 x 53

Length: 72 ft., with 16 ft. above the mudline

Sand (O'Neill):

Unit weight = 110 pcf
Internal friction angle = 35°
Poisson's Ratio = 0.3
Shear modulus = 1.5 ksi
Vertical failure shear = 600 psf
Torsional shear stress = 600 psf

Tip:

Shear modulus = 3.5 ksi
Poisson's Ratio = 0.35
Axial bearing failure = 640 kips

Subgrade modulus: Ranging from 5.0 to 578.8 (lb./in.^{3})

5.0, 15.0, 28.94, 43.4, 57.87, 86.81, 115.7, 289.4, 578.8

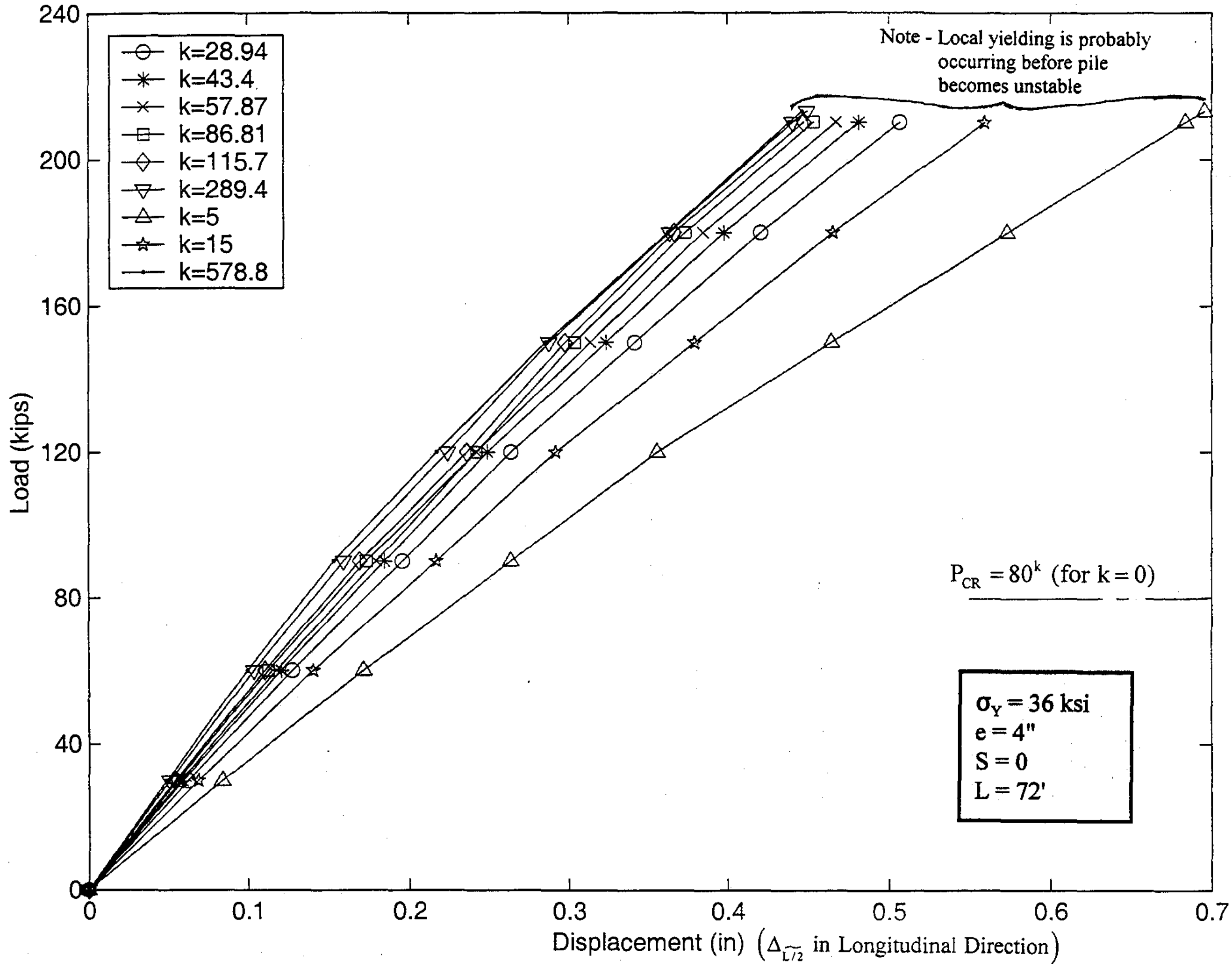

Fig. 4.15. P-$\Delta_{\widetilde{L/2}}$ in Longitudinal Direction for HP 10 x 42 Pile in Fig. 4.14 for a Range of k Values.

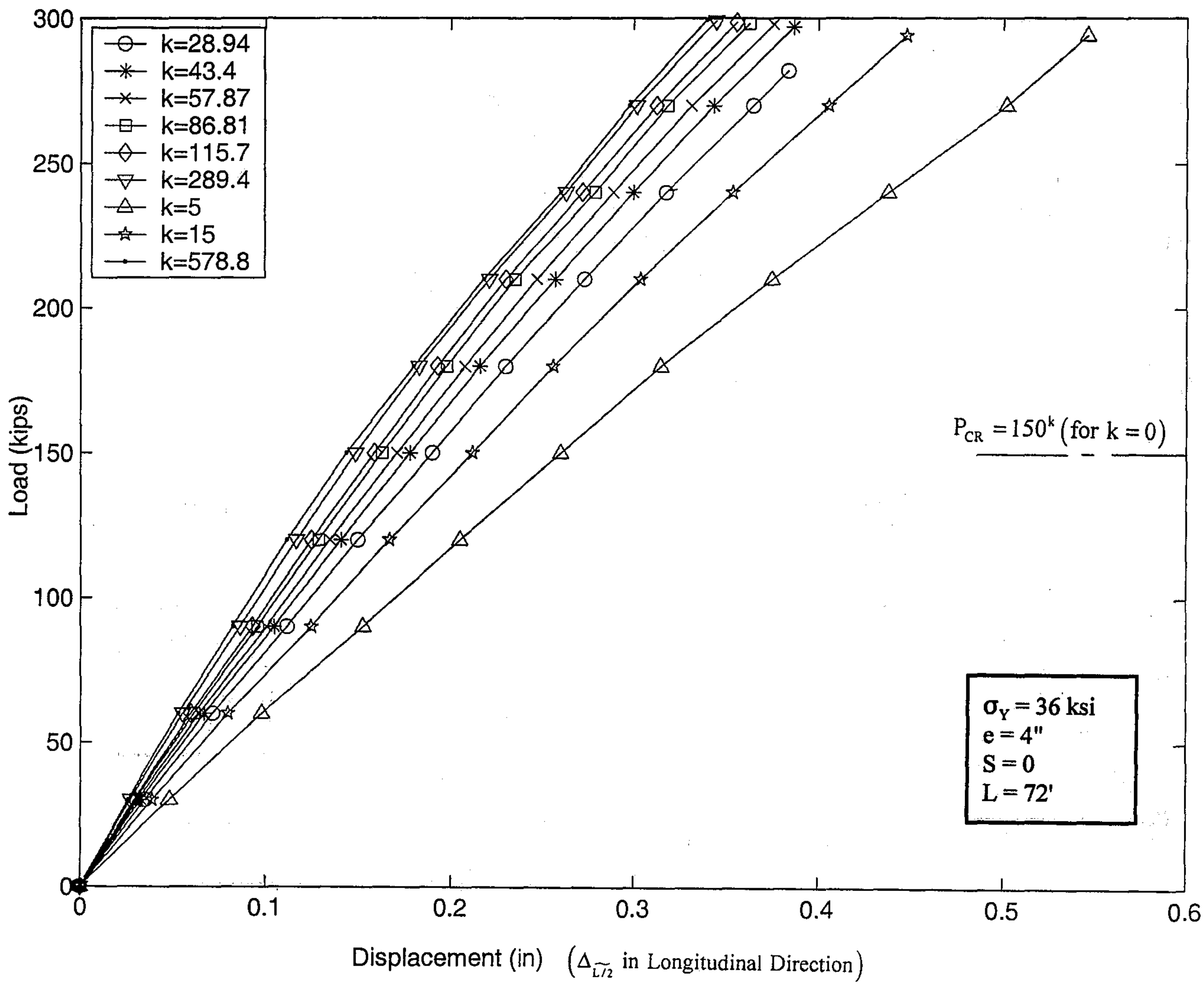

Fig. 4.16. P-$\Delta_{\tilde{L}/2}$ in Longitudinal Direction for HP 12 x 53 Pile in Fig. 4.14 for a Range of k Values.

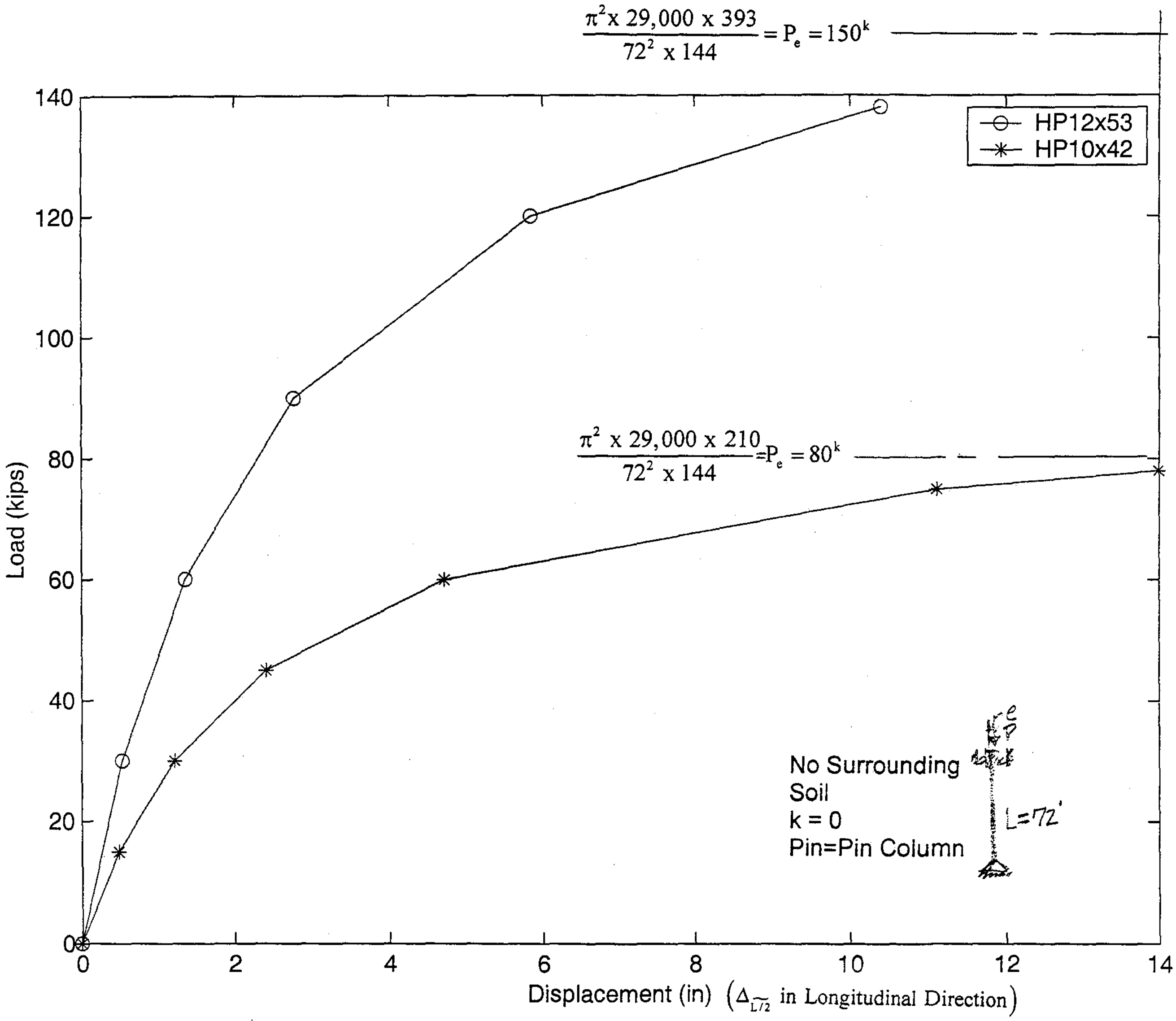

Fig. 4.17. Column Analysis Results for L = 72 ft. Using FB-Pier

Also, only the HP 12 x 53 pile was analyzed. The results of this sensitivity analysis using FB-Pier are shown in Fig. 4.18. Note in that figure that the internal friction angle, ϕ, has no significant influence on the P-Δ curve or the failure load.

4.7 Effect of Clay Soil S_u Value on Single Bent Pile P-Δ Curve in Longitudinal Direction

The same pile conditions as indicated in Fig. 4.14 and Table 4.2 were used to assess the effects of clay soil S_u values on the P-Δ curve and predicted failure load. However, for this case the soil subgrade modulus was held constant and S_u was varied from

S_u = 250 psf, 500 psf, 1000 psf (for HP 10 x 42 pile)

S_u = 250 psf, 500 psf, 1000 psf, 1500 psf (for HP 12 x 53 pile)

The FB-Pier P-Δ results are shown in Fig. 4.19 for the HP 10 x 42 pile and in Fig. 4.20 for the HP 12 x 53 pile. Note in these figures that the clay S_u value had a dampened effect on the P-Δ curve (deflections reduced by a factor of about 0.57 for an S_u increase by a factor of 6.0) and no significant influence on the failure load. Again, it appears that FB-Pier is detecting a local yielding of the pile as the failure load rather than an instability.

4.8 Comparison of FB-Pier and Granholm Eq Results of Pile Buckling for Various k_o Soils

The pile conditions used in Chapter 2 to determine the buckling loads using Granholm's Eqns. were also modeled and analyzed using FB-Pier. In these analyses, a large value of σ_y was used (σ_y = 360 ksi) so that FB-Pier would continue to increment the load and iterate to get the buckling load, and a large value of pile tip axial bearing load was used to assure a non-plunging failure of the piles. The pile conditions and soil k_o values used along with the other parameter values used in the FB-Pier analysis are shown in Fig. 4.21 and

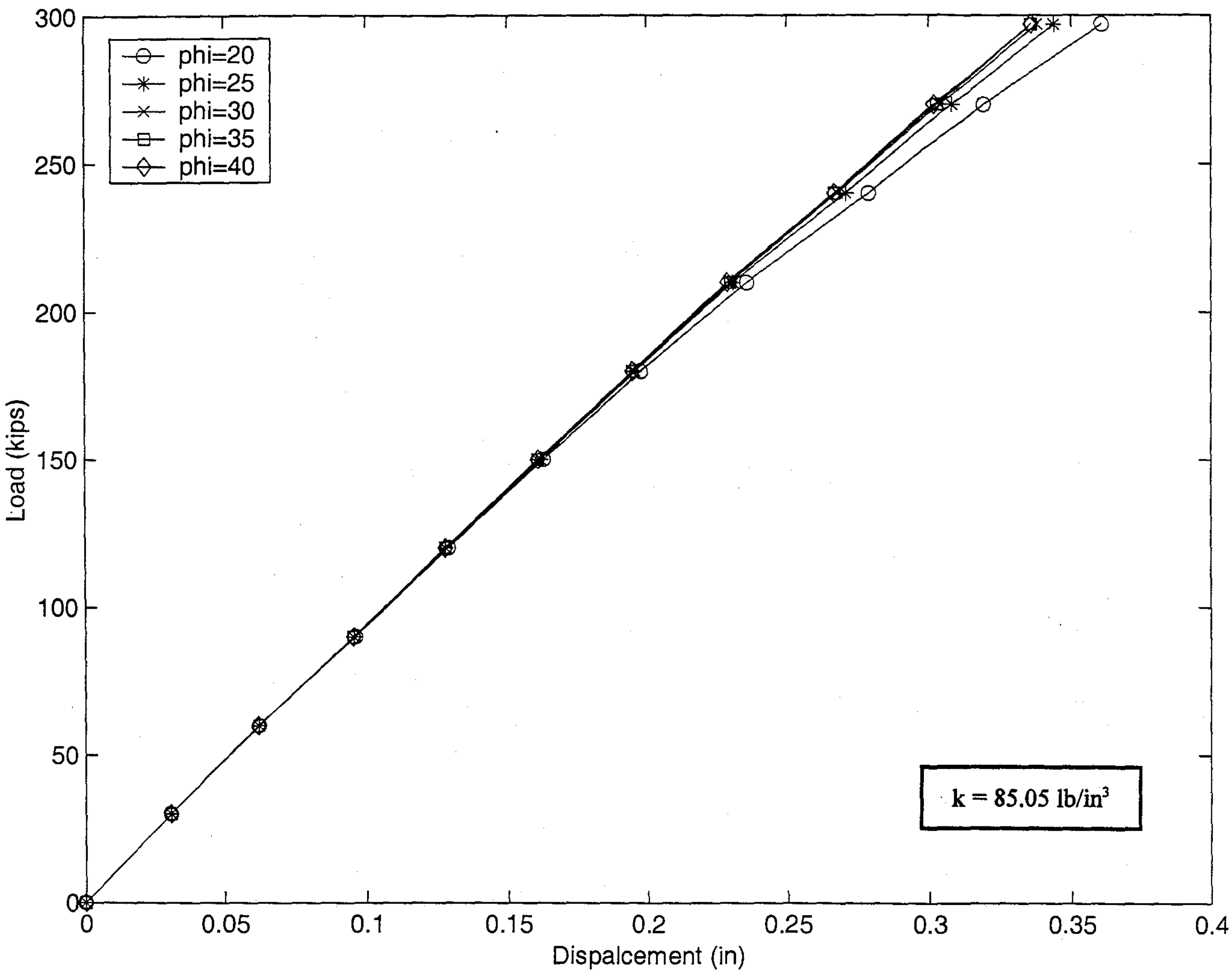

Fig. 4.18. P-$\Delta_{\tau/2}$ in Longitudinal Direction for HP 12 x 53 Pile in Fig. 4.14 in Sandy Soil for a Range of ϕ Values

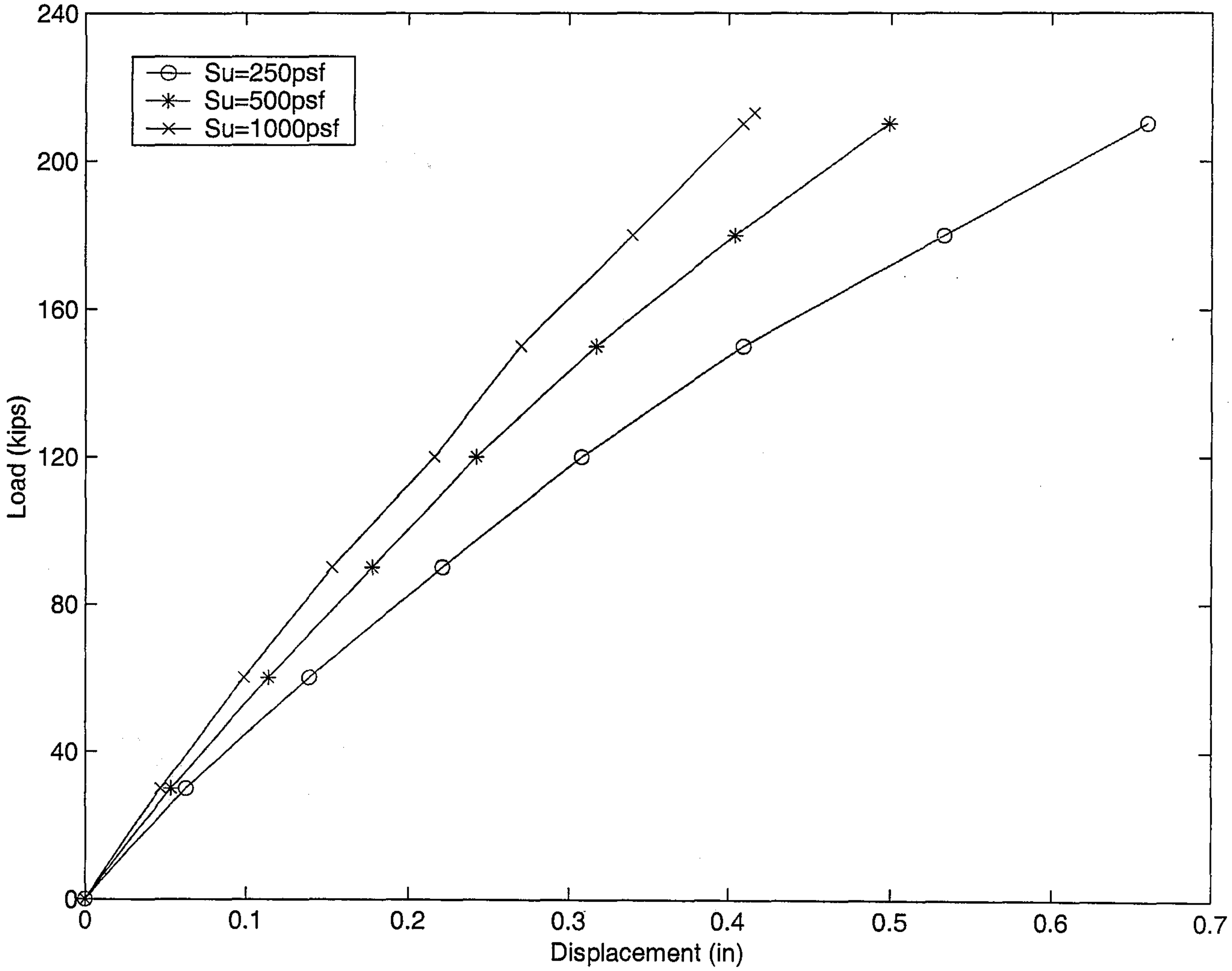

Fig. 4.19. P-$\Delta_{\tau/2}$ in Longitudinal Direction for HP 10 x 42 Pile in Fig. 4.14 in Clay Soil for a Range of S_u Values

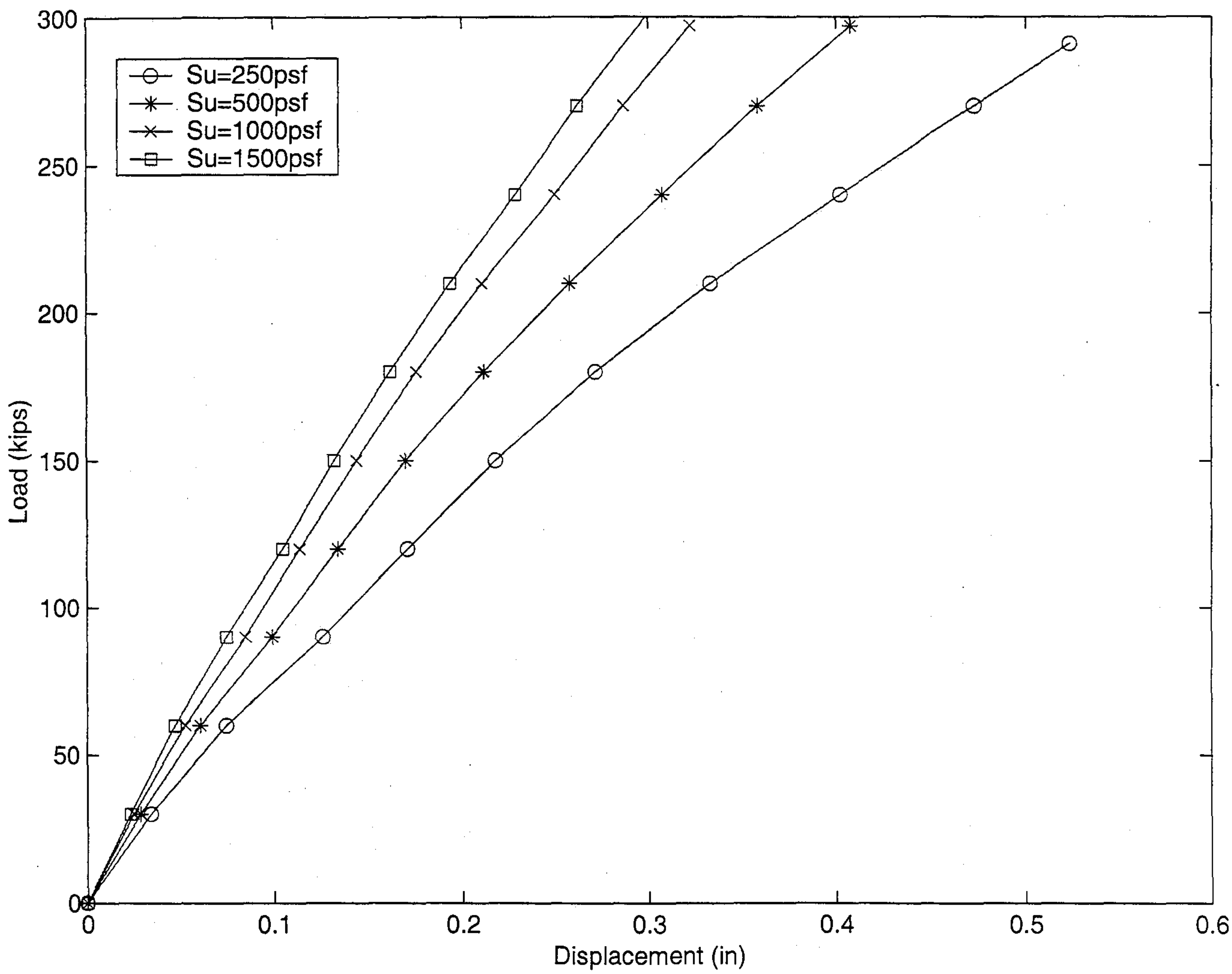

Fig. 4.20. P-$\Delta_{\tau/2}$ in Longitudinal Direction for HP 12 x 53 Pile in Fig. 4.14 in Clay Soil for a Range of S_u Values

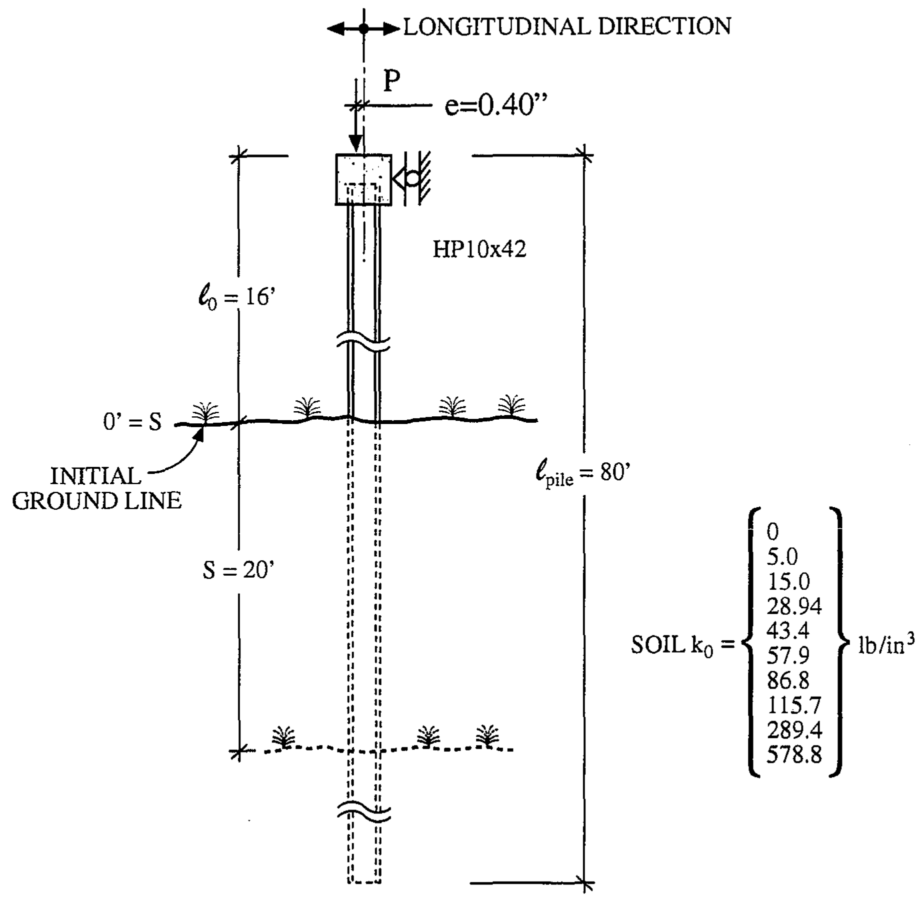

Fig. 4.21. Pile Conditions for Comparison of FB-Pier and Granholm's Equations Results

Table 4.3. In the FB-Pier analysis, only buckling of a single HP 10 x 42 pile about its strong axis was considered.

Results of the FB-Pier analyses are shown in Fig. 4.22 for S = 0 and in Fig. 4.23 for S = 20'. Both of these figures indicate a great insensitivity of the P-Δ curve and the failure/buckling load to the soil subgrade modulus, k. This same behavior was evident in the analytical analysis conducted in Chapter 2. Plots showing P_{CR} vs. k_o as determined by Granholm Eqn. and by FB-Pier for both S = 0 and S = 20' are presented in Fig. 4.24 for convenience in comparing the two analysis results. Note in this figure that the results for both analyses for S = 20' are in good agreement. However, for S = 0' the Granholm Eqn. gave much larger failure loads. This is probably due to Granholm Eqn. assuming elastic behavior of the pile and not including geometric nonlinear effects.

Table 4.3. Soil and Other Parameter Values in FB-Pier Modeling of Problem Shown in Fig. 4.21.

Pile: HP 10 x 42, S = 0 and 20 ft., eccentricity = 0.4 in., yielding stress = 360 ksi

Length: 80 ft., with 16 ft. above the mudline

Sand (O'Neill):

Unit Weight = 110 pcf
Internal friction angle = 20
Poisson's Ratio = 0.3
Shear Modulus = 1.5 ksi
Vertical Failure Shear = 5000 psf
Torsional Shear Stress = 5000 psf

Tip:

Shear Modulus = 3.5 ksi
Poisson's Ratio = 0.35
Axial bearing failure = 1000 kips

Subgrade Modulus: Ranging from 5 to 578.8 (lb./in.^{3})

5, 15, 28.94, 43.4, 57.87, 86.81, 115.7, 289.4, 578.8

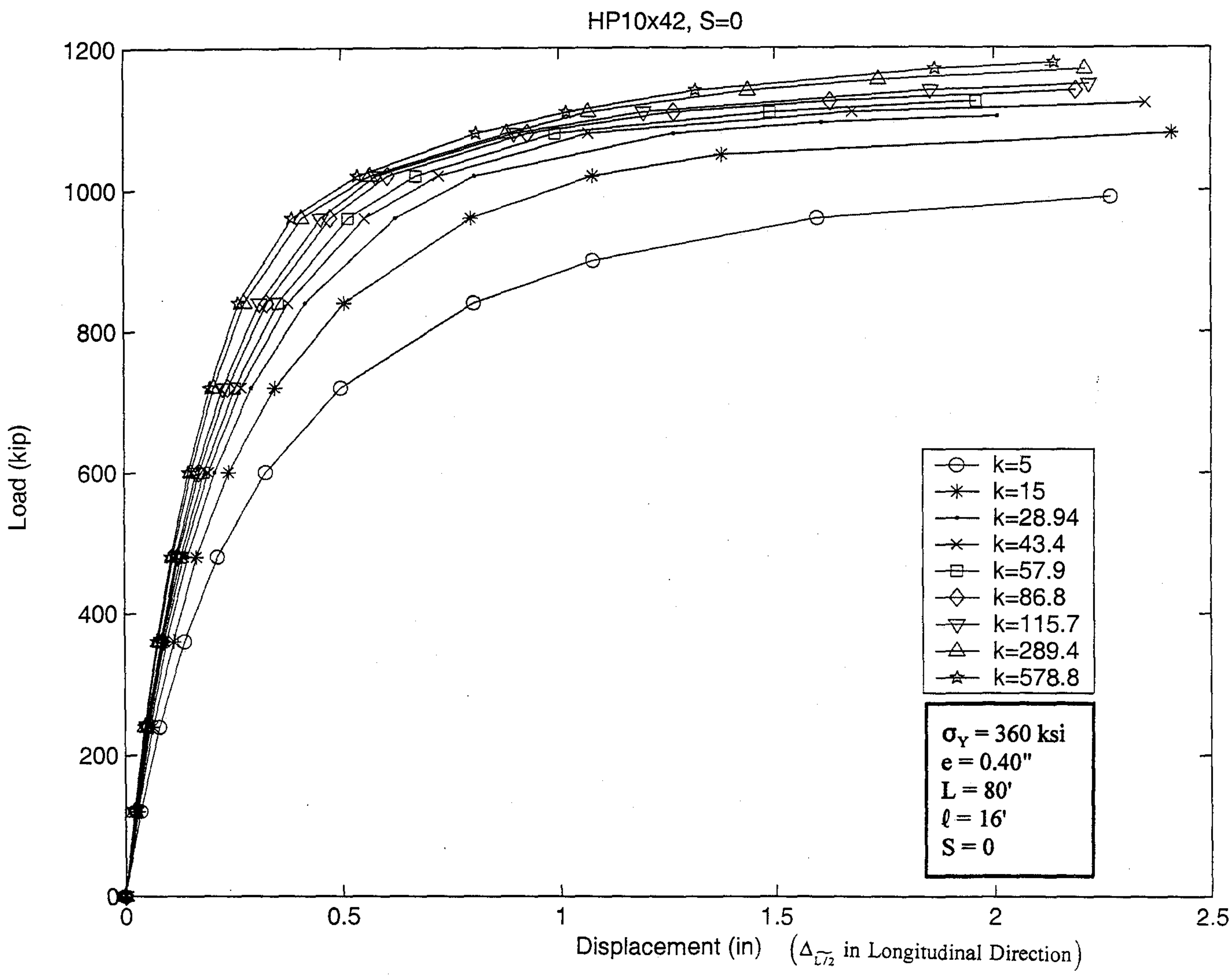

Fig. 4.22. P-$\Delta_{\tau/2}$ in Longitudinal Direction for Pile in Fig. 4.21 and Table 4.3 for a Range of k Values and S = 0.

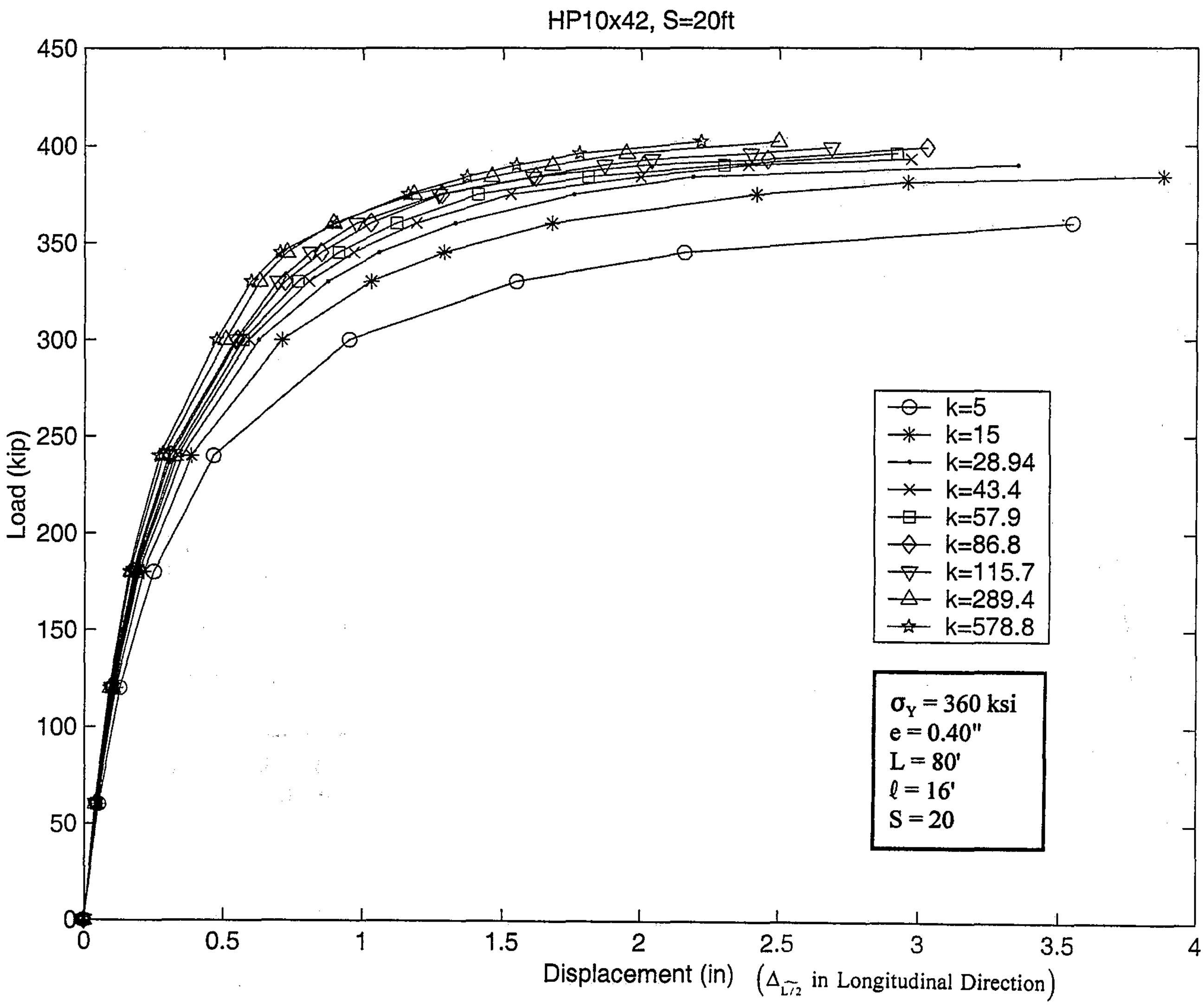

Fig. 4.23. P-$\Delta_{\tau/2}$ in Longitudinal Direction for Pile in Fig. 4.21 and Table 4.3 for a Range of k Values and S = 20 ft.

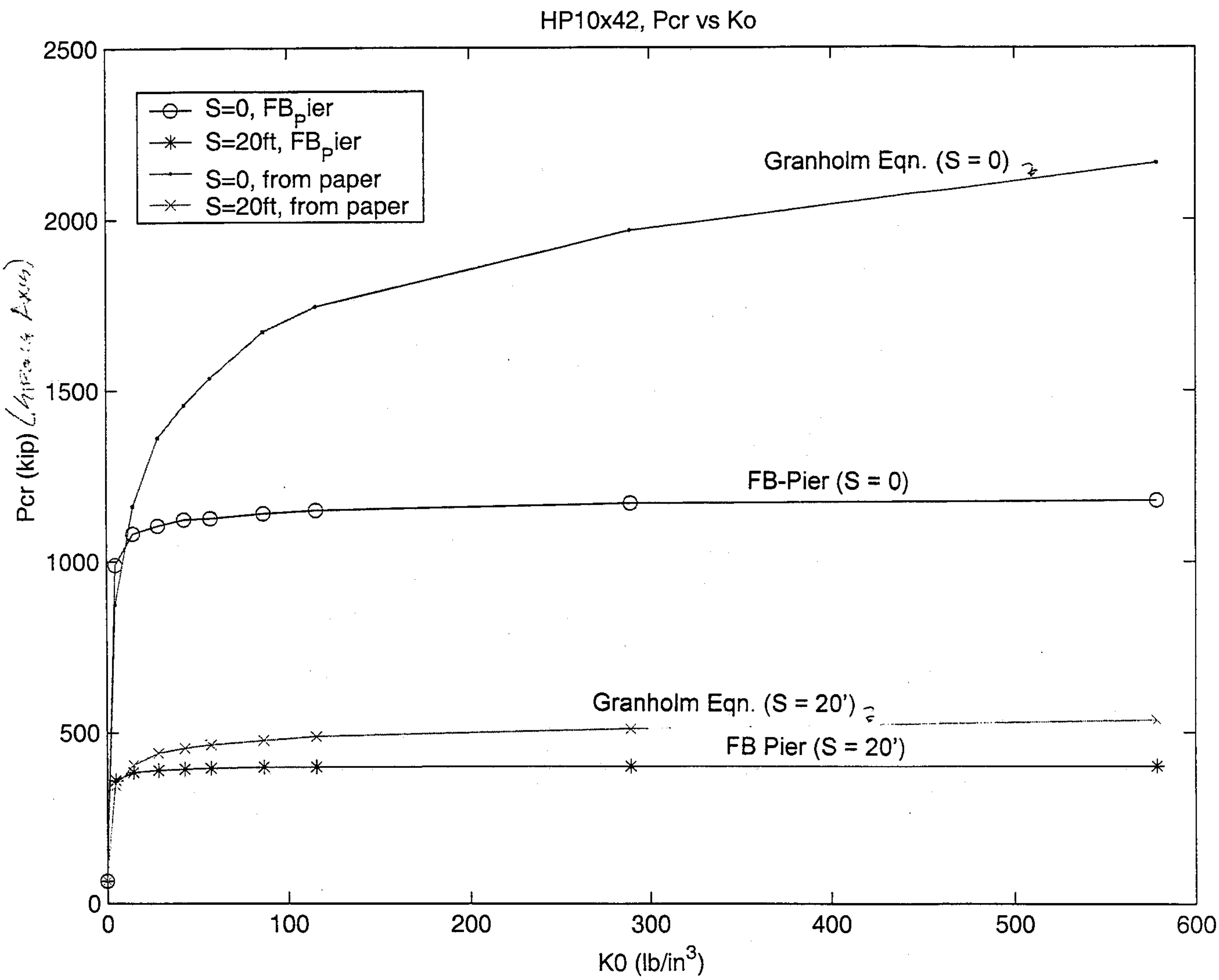

Fig. 4.24. Comparison of FB-Pier and Granholm Eqn. P_{CR} vs. k_o Results for Single HP 10 x 42 Pile Buckling About Its Strong Axis.

5. BRIDGE PILE/BENT MAXIMUM VERTICAL LOADS

5.1 General

Most of the bridge superstructure and pile bents of interest in this investigation were designed for H20 or HS20 truck and lane loads. These standard AASHTO loadings are shown in Figs. 5.1 and 5.2. In placing truck and lane loads in traffic lanes, the AASHTO design truck and lane loadings are meant to cover a 10-ft. width. These loads are then placed in 12 ft. traffic lanes spaced across the bridge from curb-to-curb. If the curb-to-curb width is between 20 ft. and 24 ft., two design lanes are used, each of which is half the curb-to-curb distance. The number and spacing of design traffic lanes is based on the layout which creates the maximum stress. Table 5.1 shows the number of design lanes based on a bridge's curb-to-curb width. Most of the bridges of interest in this study appear to have widths in the range of 24-40 ft., and thus would have 2 to 3 design traffic lanes of load applied to them.

Table 5.1. Design Traffic Lanes (8)

Curb-to-Curb Width	No. of Lanes
20 to 30 ft.	2
30 to 42 ft.	3
42 to 54 ft.	4
54 to 66 ft.	5
66 to 78 ft.	6
78 to 90 ft.	7
90 to 102 ft.	8
102 to 114 ft.	9
114 to 126 ft.	10

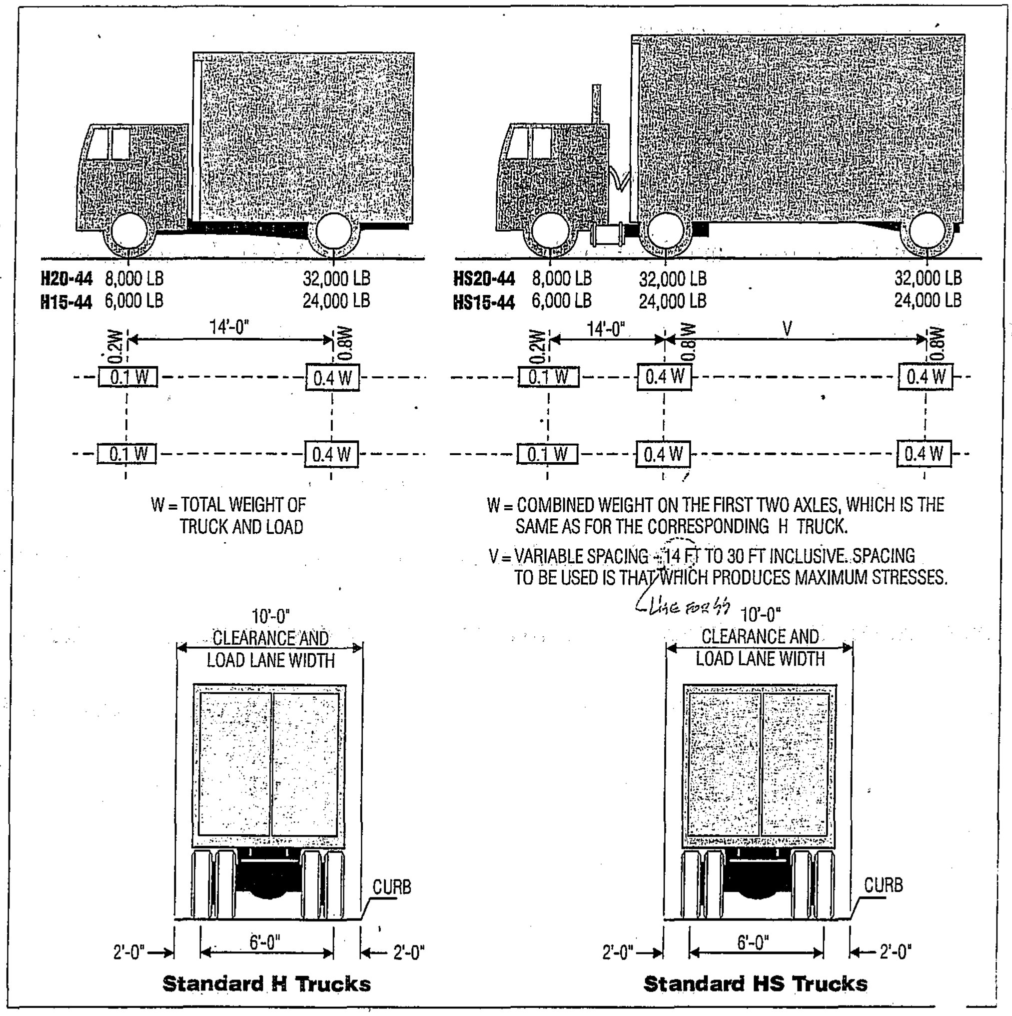

Fig. 5.1. AASHTO Standard H & HS Design Trucks.

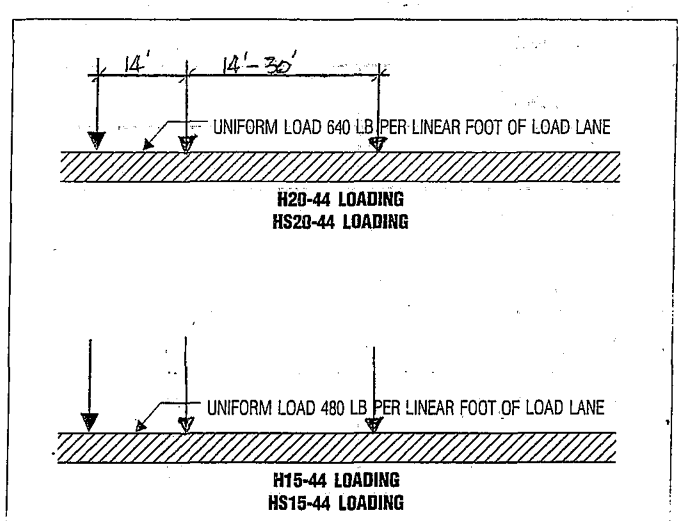

Fig. 5.2. AASHTO H and HS Lane Loading

5.2 Pile/Bent Dead Load

Procedure for estimating the dead load (DL) force acting on top of a bent pile and on the bent are shown below. These procedures are then applied to the typical ALDOT deck-girder superstructure shown in Fig. 5.3. Two procedures are shown,

Method I - for cases where estimated superstructure quantities are readily available on an ALDOT Standard.

Method II - for cases where estimated quantities are not readily available.

For Method II, a girder-line approach is taken to first determine the DL acting on a bent pile.

<u>Method I</u>:

Superstructure weight per span = W_{SST}

W_{SST} = Concrete quantity x 27 ft.^{3}/yd.^{3} x 0.145^k/ft.^{3} + Rebar Wt. + No. girders x L x w_{gir}

Bent Cap Weight = W_{cap}

$W_{cap} = b_{cap} \times d_{cap}$ x girder spacing x No. girders x 0.150^k/ft.^{3}

For the S-4034P superstructure standard in Fig. 5.3, the estimated DLs would be as follows.

$$W_{SST} = 37.6 \text{ yd.}^3 \times 27 \text{ ft.}^3/\text{yd.}^3 \times 0.145^k/\text{ft.}^3 + 12.6^k + 6 \times 34 \times 0.287^{k/'}$$

$$= 147.2^k + 12.6^k + 58.5^k \qquad = 218.3^k$$

$$W_{cap} = 2' \times 3' \times 7' \times 6 \times 0.150^k/\text{ft.}^3 = \underline{37.8}^k$$

$$F^{DL}_{BENT} = 256.1^k$$

$$F^{DL}_{PILE} = 256.1/6 = 42.7^{k/pile}$$

<u>Method II</u>:

Superstructure DL per pile is,

Deck: 7'/12 x Girder Spac. x L x 0.150^k/ft.^{3}

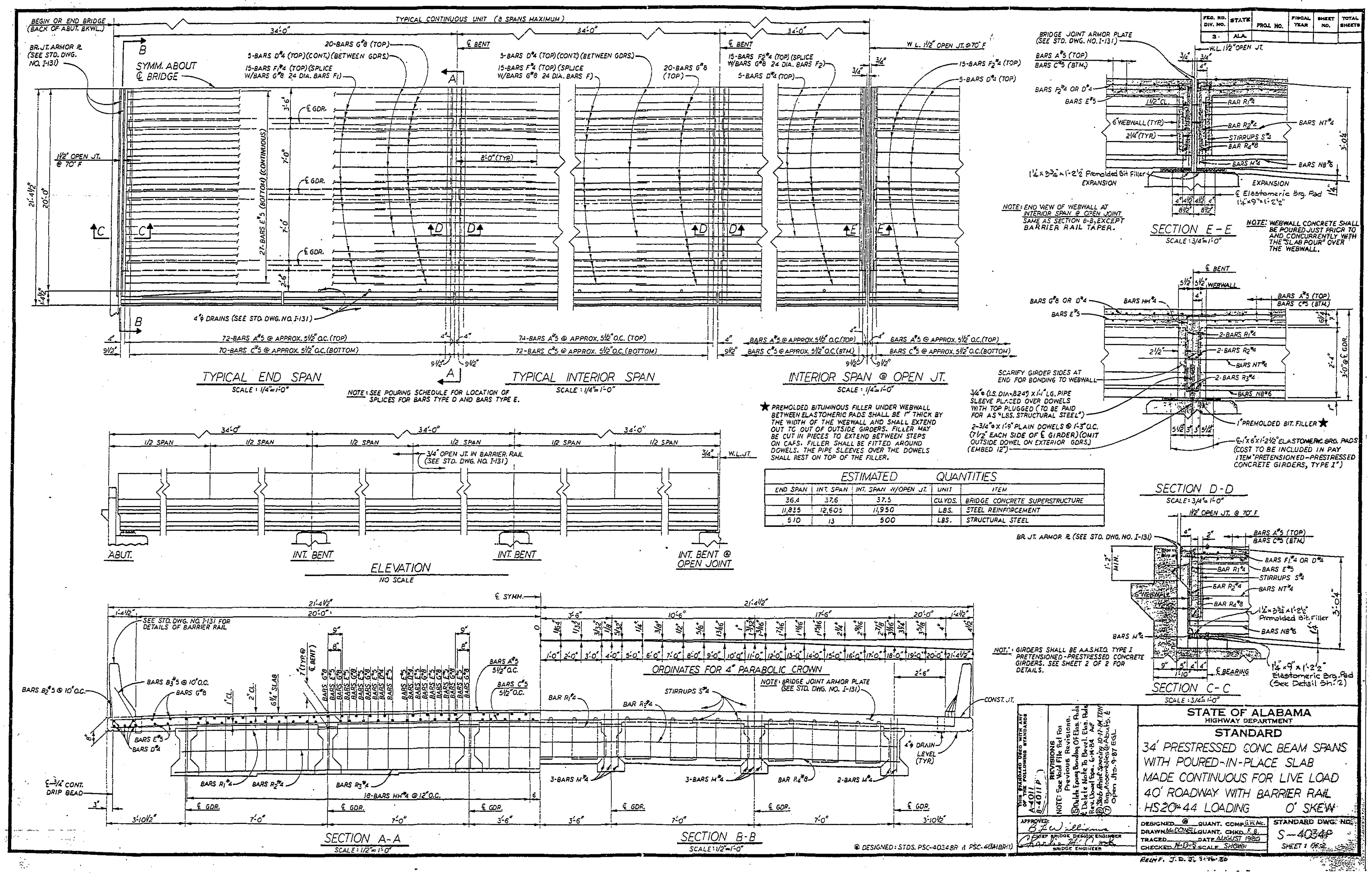

Fig. 5.3. A Typical ALDOT Deck-Girder Superstructure

Bent Diaph: 11'/12 x Girder Depth x Girder Spac. x $0.150^{k}/ft.^{3}$

Barrier Rails: 2 x w_{br} x L/No. piles per bent

Girder: w_{girder} x L

Bent Cap: 3' x 2' x girder spac. x $0.150^{k/'}$

Therefore, for the S-4034 P standard,

Deck: 7'/12 x 7' x 34' x 0.150 = 20.8^{k}

Bent Diaph: 11/12 x 2.33' x 7' x 0.150 = 2.24^{k}

Barrier Rails: (2 x 0.390 x 34')/6 = 4.42

Girder: $0.287^{k/1}$ x 34 = 9.76^{k}

Bent Cap: 3' x 2' x 7' x $0.150^{k/1}$ = $\underline{6.3^{k}}$

$F^{DL}{}_{Pile} = 43.5^{k/pile}$

$F^{DL}{}_{Bent} = 43.5 \times 6 = 261^{k}$

5.3 Maximum Pile/Bent Truck and Lane Load

A girder-line approach is taken to estimate the maximum vehicular LL (plus impact) on a bent pile, and the approach is illustrated with its application to the superstructure shown in Fig. 5.3. A somewhat similar approach is taken to obtain the maximum vertical load on the pile bent.

$P^{LL}{}_{pile\ max}$ for Fig. 5.3 is as follows:

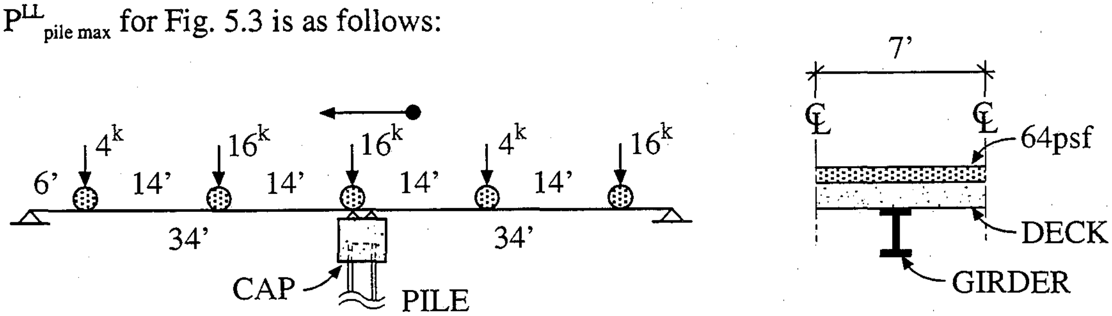

$$P^{LL}{}_{pile\ max} = 16^{k} + \frac{20}{34} \times 16^{k} + \frac{6}{34} \times 4^{k} + \frac{20}{34} \times 4^{k} + \frac{6}{34} \times 16^{k} + 0.064 \times 7' \times 34'$$

$$= 16^{k} + 9.41 + 0.71 + 2.35 + 2.82 + 15.23 = 46.52^{k}$$

$$P^{LL}{}_{pile\ max} = 46.52 \times \underbrace{1.3}_{\text{I.F.}} = 60.5^{k}$$

$P^{LL}_{\text{bent max}}$ for Fig. 5.3 is determined using 3 design lane loads and 2 design truck lanes of loading as indicated below.

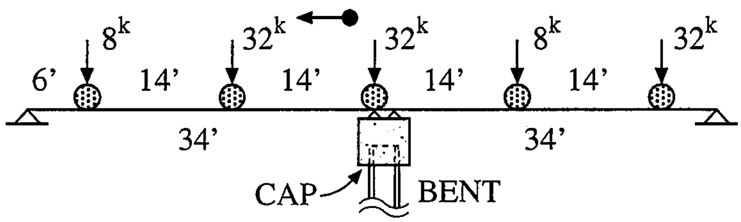

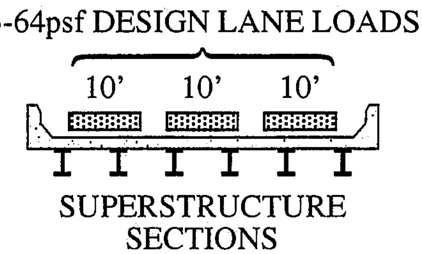

REVERSE LOADS GOING IN OTHER DIRECTION, I.E., DOUBLE TRUCKLOAD ON BENT TO ACCOUNT FOR OTHER LANE.

$$
\begin{aligned}
P^{LL}_{\text{bent max}} &= \left[32^k + \frac{20}{34} \text{ x } 32^k + \frac{6}{34} \text{ x } 8^k + \frac{20}{34} \text{ x } 8^k + \frac{6}{34} \text{ x } 32^k\right]2 + [0.064 \text{ x } 10' \text{ x } 34']3 \\
&= [32 + 18.82 + 1.41 + 4.70 + 5.64]2 + [21.76]3 \\
&= 125.1 + 65.3 = 190.4^k \\
P^{LL}_{\text{MAX BENT}} &= 190.4^k \text{ x } \underbrace{1.3}_{\text{I.F.}} = 247.5^k
\end{aligned}
$$

5.4 Maximum Pile/Bent Vertical Loads

Using the results from Sections 5.2 and 5.3 above yields, for the superstructure shown in Fig. 5.3, the following unfactored maximum pile and bent vertical loads.

$$
\begin{aligned}
P_{\text{PILE MAX}} &= P^{\text{PILE}}_{\text{DL}} + P^{\text{PILE}}_{\text{LL-MAX}} = 42.7^k + 60.5^k = 103.2^k \\
P_{\text{BENT MAX}} &= P^{\text{BENT}}_{\text{DL}} + P^{\text{BENT}}_{\text{LL-MAX}} = 256.1^k + 247.5^k = 503.6^k
\end{aligned}
$$

It should be noted that Earth Tech, Inc. in their analysis of a bridge quite similar in size to the S-4034P superstructure considered here worked with 33 load conditions and determined $P_{pile\ max} = 124.2^k$. However, it was not clear in their work if this was a factored load or not. Also, recall in Section 3.2 where it was shown that for a given bent pile, ℓ_{CR} is given by

$$\ell_{CR} = \sqrt{\frac{\text{constant } \pi^2 EI}{P}}$$

Thus, ℓ_{CR} varies inversely with square root of P, and is not real sensitive to the pile loading. That is, a small error in P will not greatly affect the predicted ℓ_{CR}.

6. ASSESSING ADEQUACY OF PILE BENTS FOR AN EXTREME SCOUR EVENT

6.1 General

As indicated in Chapter 3, possible failure modes of bridge pile bents during extreme scour events are as follows:

(1) Buckling of Bent Piles in Longitudinal Direction

(2) Buckling of Bent Piles in Transverse Direction

(3) Crushing or Reaching P_y of Piles

(4) Plunging Failure of Piles (Soil Failure)

(5) Local Yielding of Piles $\left(\sigma_z = -\frac{P}{A} \pm \frac{M_x y}{I_x} \pm \frac{M_y x}{I_y} = \sigma_y\right)$

(6) Flexural Failure of Bent Cap

Also, as indicated in Chapter 3, flexural failure of the bent cap can only occur if $P_{girder\ max} > P_{buckling}$ or $P_{plunging}$. In such a case, flexural failure of the cap must be prevented to gain lean-on support from the adjacent piles in the bent. If $P_{girder\ max}$ is less than $P_{buckling}$ and is less than $P_{plunging}$ then flexural failure of the bent cap will not occur.

Local yielding of a bent pile is not a catastrophic situation and only results in local permanent deformations in the pile. Note that the piles may reach a fully plastic moment state at the section of M_{max}, i.e., the pile ground line, and not have a catastrophic situation. Thus this is not a failure condition of concern.

Crushing of the pile, or the pile reaching the P_y load, is implicitly checked if inelastic buckling is considered. Also $P_{max\ applied}$ and P_y of the piles ~~is~~ are unaffected by a scour event, and therefore crushing of the piles will not occur.

Thus, only buckling of the bent piles (either elastic or inelastic buckling) or plunging of the piles (soil failure) will be a catastrophic failure mode, and thus these are the only two modes of failure of concern and requiring checking.

In checking P_{pile}^{max} for possible plunging failure, if the length of a steel HP pile (with its tip founded in a firm soil stratum) below ground prior to scour is greater than 3.0 S, then plunging should not occur. That is, if

$$\ell_{bg} \geq 3.0 \text{ S}$$

then $P_{pile\ capacity} > P_{pile}^{max}$

For cases where the above condition is not met, but 2.5 S < ℓ_{bg} < 3.0 S, and the pile tip is founded in a firm cohesive soil layer or the pile is a prestressed concrete pile, then the pile should be safe from plunging. If these conditions are not met then a more comprehensive analysis should be made to determine if the pile/pile bent is safe against a plunging failure.

In checking P_{pile}^{max} for possible buckling failure, the first step is to verify that the piles and bent can not sidesway a significant distance in either the longitudinal or transverse directions. To verify this in the longitudinal direction requires that the superstructure be positively connected to the bent caps and that the superstructure is restrained from significant longitudinal movement by the bridge abutments. To verify this in the transverse direction, the pile bents must be x-braced and have a batter pile at each end of the bent. These batter requirements may be waved if the superstructure has continuous spans (or made continuous for live load) and is positively connected to the bent caps. If the pile bent can not sidesway significantly in either direction (which should be the case), then nonsway buckling of steel HP piles in the transverse direction (about their weak axis) will control and P_{CR} (either elastic or inelastic) can be determined from Fig. 6.6. If this value of $P_{CR} > P_{pile}^{max}$ then there will be no pile or bent buckling failure.

For cases where $P_{pile}^{max} > P_{CR}$, then the bent must get "lean-on" support from adjacent piles in the bent. To achieve this, the bent cap must be capable of transmitting the excess load to the adjacent piles and $\Sigma P_{CR}^{Bent} > P_{bent}^{max}$. In this case, the flexural capacity of the bent cap must be checked as indicated in Section 3.6 to be assured that it has adequate strength. If the cap has adequate strength, and after allowing "lean-on" support, the pile bent still appears to not have sufficient buckling capacity to resist the applied load, then a more detailed and comprehensive analysis should be undertaken.

6.2 Information Needed to Assess Pile Bent Adequacy

Information needed to perform an analysis to assess the stability of pile bents during major scour events is given below.

1. Scour Information

   Estimated magnitude of an extreme scour event. From stream crossing hydrologic and soil setting data. This information is available from USGS and ALDOT.

2. Pile Bent Geometry and Design Information

   See Fig. 6.1 on the following page and the information highlighted. This information is available on the ALDOT Bent Standard for the bridge under investigation.

3. Pile Driving and Soil Profile Information

   The following information is needed or is helpful in this category:

- Pile length and tip elevation
- Ground elevation
- Water table elevation
- Driving resistance of last foot
- Soil bearing strength (or descriptive characteristics) at pile tip
- Soil characteristics in region from ground line to 15' below ground line

4. Bridge Superstructure Information

   The following information is needed in this category (to estimate the bent loading and sidesway potential):

   - -SS or continuous spans
   - -Number of bents or spans
   - -Span length(s)
   - -Girder type, size, and number/span
   - -Width and number of lanes
   - -Design LL
   - -Expansion joint number and width (to assess limit of sidesway)
   - -Connection of superstructure to bent cap

   This information is available on the ALDOT Superstructure Standard for the bridge under investigation.

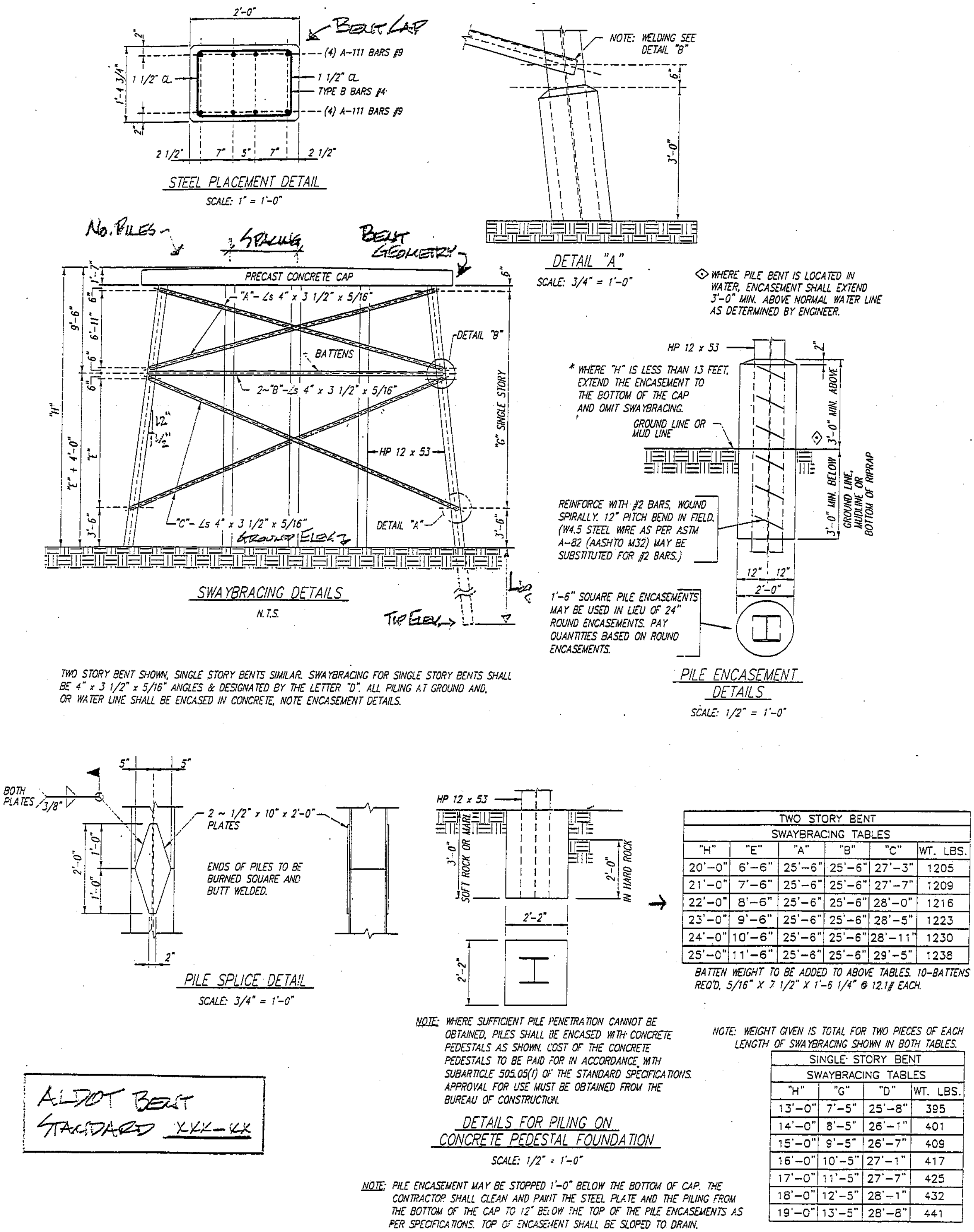

TWO STORY BENT SWAYBRACING TABLES

"H"	"E"	"A"	"B"	"C"	WT. LBS.
20'-0"	6'-6"	25'-6"	25'-6"	27'-3"	1205
21'-0"	7'-6"	25'-6"	25'-6"	27'-7"	1209
22'-0"	8'-6"	25'-6"	25'-6"	28'-0"	1216
23'-0"	9'-6"	25'-6"	25'-6"	28'-5"	1223
24'-0"	10'-6"	25'-6"	25'-6"	28'-11"	1230
25'-0"	11'-6"	25'-6"	25'-6"	29'-5"	1238

BATTEN WEIGHT TO BE ADDED TO ABOVE TABLES. 10-BATTENS REQ'D, 5/16" X 7 1/2" X 1'-6 1/4" @ 12.1# EACH.

NOTE: WEIGHT GIVEN IS TOTAL FOR TWO PIECES OF EACH LENGTH OF SWAYBRACING SHOWN IN BOTH TABLES.

SINGLE STORY BENT SWAYBRACING TABLES

"H"	"G"	"D"	WT. LBS.
13'-0"	7'-5"	25'-8"	395
14'-0"	8'-5"	26'-1"	401
15'-0"	9'-5"	26'-7"	409
16'-0"	10'-5"	27'-1"	417
17'-0"	11'-5"	27'-7"	425
18'-0"	12'-5"	28'-1"	432
19'-0"	13'-5"	28'-8"	441

Fig. 6.1. Typical Pile Bent Geometry and Information (From ALDOT Pile Bent Standard)

6.3 Assessing Bent Pile Buckling

The following are the primary parameters or questions of concern in checking for a possible bent pile buckling failure due to a major scour event (see Fig. 6.2).

1. L_o (or "H")

2. Maximum potential scour at the site, S

3. Pile type/size/orientation

4. Can bent cap sidesway significantly in longitudinal direction? How are girders connected to pile cap and what is maximum possible longitudinal movement of superstructure?

5. Can bent cap sidesway significantly in transverse direction? Does bent have swaybracing and end batter piles?

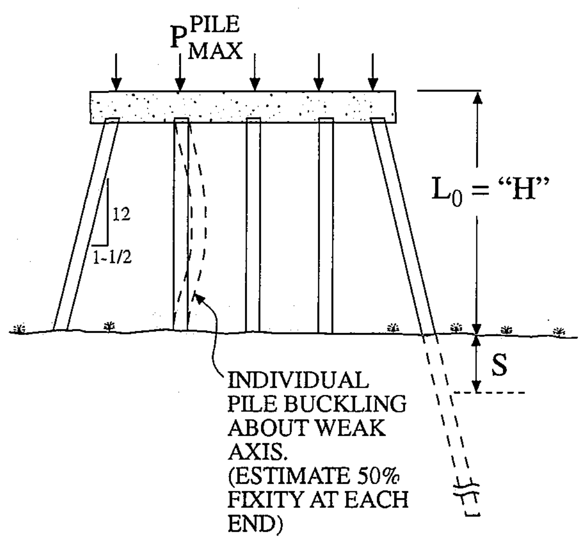

Fig. 6.2. Typical Pile Bent Above Ground

6. Are piles encased in concrete and if so, over what length?

7. Maximum possible load on a pile, P^{pile}_{max}?

8. Maximum possible load on bent, P^{bent}_{max}?

Note that "H" + S = ℓ, bent sidesway condition, pile size and P_{max} load are the most important parameters affecting the pile/bent buckling capacity.

Red flag conditions for checking more closely for possible pile buckling failure are:

1. If bent can sidesway. The most likely cases will be where bent swaybracing is not used.

2. "H" + S is large (i.e., "H" + S $\geq$ 35' for HP 10 x 42
$\geq$ 40' for HP 12 x 53)

3. Small pile section size (HP 10 x 42). Note that

$P_{CR}^{12x53} \approx 40\%$ greater than P_{CR}^{10x42} about either axis.
75%

4. Pile loading is exceptionally large (P >150^k for steel H-piles).

6.4 Assessing Bent Pile Plunging

The following are the primary parameters or questions of concern in checking for a possible bent pile plunging failure due to a major scour event (see Fig. 6.3).

1. Pile type/size
2. Pile maximum load, P_{max}^{pile}
3. Bent maximum load, P_{max}^{bent}
4. Is upper 15' of pile embedment (before scour) probably carrying a significant portion of pile load?
5. Maximum potential scour at the site, S
6. Length of pile embedment in ground, ℓ_{bg}, before scour.
7. Driving resistance of last foot of driving and/or soil bearing strength (or descriptive characteristics) at pile tip.

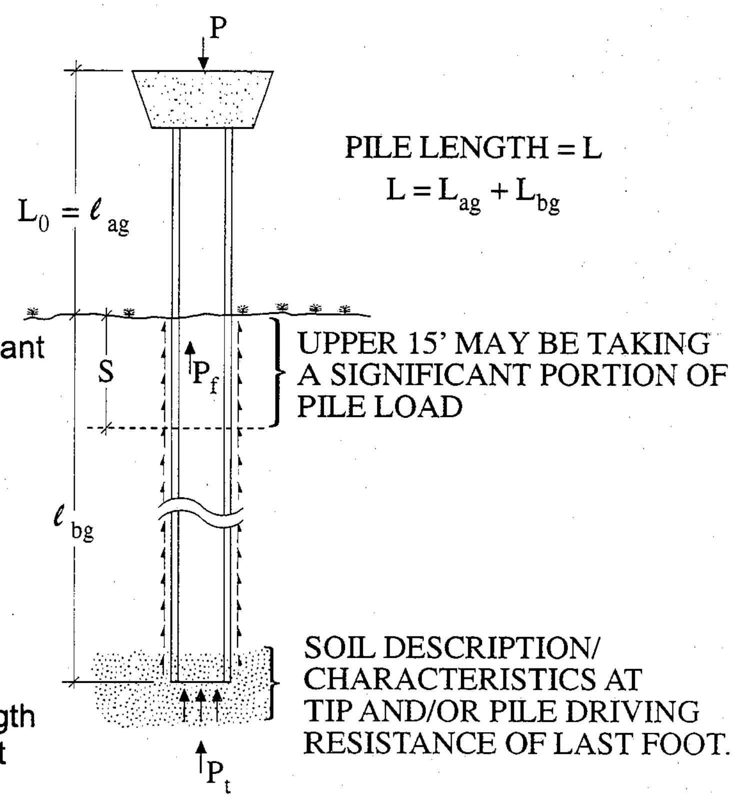

Fig. 6.3. Pile Bent Soil Setting

Red flag conditions for checking more closely for possible pile plunging failure:

1. Pile not driven to firm layer at its tip.

2. $\ell_{bg} < 3.0$ S for piles with small P_t capacity and
$\ell_{bg} < 2.5$ S for piles with good P_t capacity.

3. Upper 15' of pile embedment (before scour) was probably carrying a significant portion (over 25%) of the pile load.

4. Pile loading is exceptionally large ($P > 150^k$ for steel H-piles).

6.5 Information Needed to Assess Bent Cap Failure

The following are the primary parameters or questions of concern in checking for a possible bent cap failure due to a major scour event.

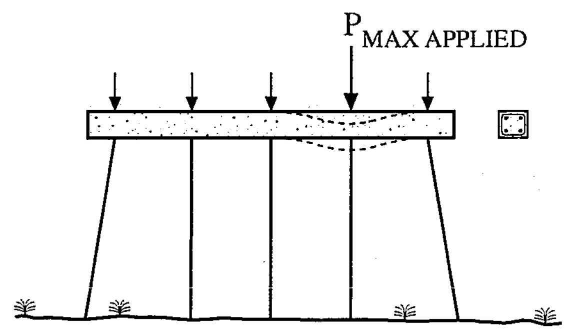

Fig. 6.4. Pile Bent Cap and Loading

1. $P_{max\ applied}$ must exceed $P_{buckling}$ or $P_{plunging}$ for the most heavily loaded pile in the bent, i.e., one of the piles must be failing as indicated in Fig. 6.4 to get a possible flexural/ shear failure in the bent cap. If this is not the case, then failure of the cap is not possible.

2. If $P_{max\ applied} > P_{buckling}$ or $P_{plunging}$, then to gain "lean-on" support from the adjacent piles, the bent cap must not fail.

3. Cap f_c'

4. Cap sectional dimensions, A_s in top and bottom, stirrup steel size and maximum spacing.

5. Pile spacing.

6. $P_{max\ applied}$ (see Fig. 6.4)

7. P_{max}^{bent}

Red flag conditions for checking more closely for possible bent cap failure are:

1. $P_{max\ applied}$ to a single pile in the bent is approximately equal to or greater than $P_{buckling}$ or $P_{plunging}$ for that same pile.

2. The width and depth of the cap are both less than 24".

3. The area of steel reinforcement in the top and bottom face of the cap is less than 1.5 in.^{2} (in each face) and/or the maximum stirrup spacing in the cap is greater than 12".

6.6 Procedure for Assessing the Adequacy of Bridge Pile Bents

The following procedure should be used in assessing the adequacy of a swaybraced bridge pile bent for an extreme scour event. To make this check, we will perform a girder-line analysis for the loading and response of a single pile in the bent. If this pile proves adequate, then we will surmise that the bent is adequate. If it proves inadequate, then a more detailed and comprehensive investigation of the bent should be undertaken. It should be noted that the procedure described below is applicable only for bents where sidesway buckling is presented in the longitudinal direction (by superstructure and abutments) and in the transverse direction (by swaybracing and batter piles).

Procedure:

1. Determine "H" (see Fig. 6.5)

2. Determine S (from ALDOT scour data set)

3. Determine ℓ_{bg} before scour ($\ell_{bg} = L_{pile} - \text{"H"}$)

4. Determine ℓ_{max}
(maximum unsupported pile/ column length above ground after an extreme event)
ℓ_{max} = "H" + S

5. Determine pile type and size (HP 10 x 42 or HP 12 x 53 or other)

6. Determine type (cohesive or cohesionless) and description of soil at pile tip to assess bearing capacity and/or P_{tip}

7. For the given bridge superstructure estimate $P_{max\ load}$ as follows:

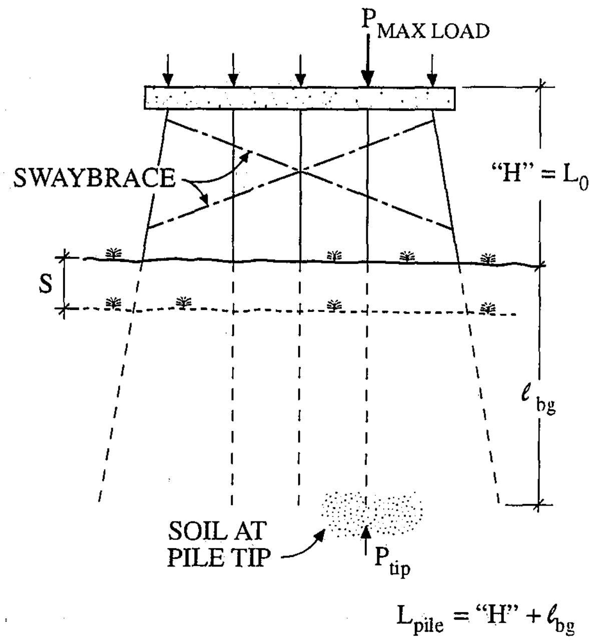

Fig. 6.5. Typical Pile Bent

P_{DL}: Deck: $\frac{7'}{12}$ x Gir. Spac. x Span Length x $0.150^{k}/ft.^{3}$ =

Diaph: $\frac{11'}{12}$ x Gir. Depth x Gir. Spac. x 0.150 =

Girder: Girder Wt./ft. x Span Length =

Cap: Cap Width x Cap Depth X Gir. Spac. x 0.150 =

P_{DL} =

P_{LL}: Uniform
Load: $0.064^{k}/ft.^{2}$ x Gir. Spac. x Span Length =

Truck
Load: $16^{k} + 16^{k}\left(\frac{L-14}{L}\right) + 4^{k}\left(\frac{L-28}{L}\right)$ =

Σ =

$P_{LL} = I.F.(\Sigma) = 1.3\,(\Sigma)$

$P_{max\ load} = P_{DL} + P_{LL}$

8. Check for pile plunging failure:

If pile is prestressed concrete and tip is founded in a firm soil layer, P_{tip} capacity will be substantial and the pile should be safe from plunging if the length of pile embedment before scour, ℓ_{bg}. is greater than 2.5 S, i.e., $\ell_{bg} > 2.5$ S.

If pile is steel H-pile and tip is founded in a firm cohesive soil layer, the effective pile tip area will be large. In turn, P_{tip} capacity will be substantial and the pile should be safe from plunging if $\ell_{bg} > 2.5$ S.

If pile is steel H-pile and tip is founded in a firm cohesionless soil layer, the effective pile tip area will be small. In turn, P_{tip} capacity will be small and the pile should be safe from plunging if $\ell_{bg} > 3.0$ S.

9. Check for pile buckling failure:

In checking the stability of a pile/bent, what really matters is the height of the bent after scour, or, "H" + S = ℓ_{max}. Go to $P_{failure}$ vs. ℓ_{max} curve using the ℓ_{max} and the pile size in (4) and (5) above and determine P_f (see Fig 6.6).

As can be seen from Fig. 6.6, the bent stability status for a range of "H" + S values for HP 10 x 42 and HP 12 x 53 pile bents are as shown in Table 6.1.

Table 6.1. Pile Bent Stability for Range of "H" + S Values

HP 10 x 42 Piles	**Stability Status**	**HP 12 x 53 Piles**
"H" + S $\leq$ 25'	$P_{CR} > \frac{3}{4} P_y$ bent is definitely stable	"H" + S $\leq$ 30'
25' < "H" + S $\leq$ 35'	$\frac{1}{2} P_y < P_{CR} < \frac{3}{4} P_y$ If $P_{max\ applied} < \frac{1}{2} P_y$, bent is definitely stable If $P_{max\ applied} > \frac{1}{2} P_y$, then determine P_{CR} from Fig. 6.6 and compare with $P_{max\ applied}$	30' < "H" + S $\leq$ 40'
35' < "H" + S	$P_{CR} < \frac{1}{2} P_y$ Determine P_{CR} from Fig. 6.6and compare with $P_{max\ applied}$	40' < "H" + S

10. Compare $P_{failure}$ with $P_{max\ load}$ to determine the approximate F.S. against a pile buckling failure. If the F.S. $\geq$ 1.4, the bent is adequate to withstand the extreme scour event. If F.S. < 1.4, perform a more complete and accurate analysis of the pile bent.

11. If the single pile will not plunge or buckle, then the bent cap cannot fail in bending or shear and thus the cap is adequate.

12. If the single pile is adequate, then the pile bent is adequate.

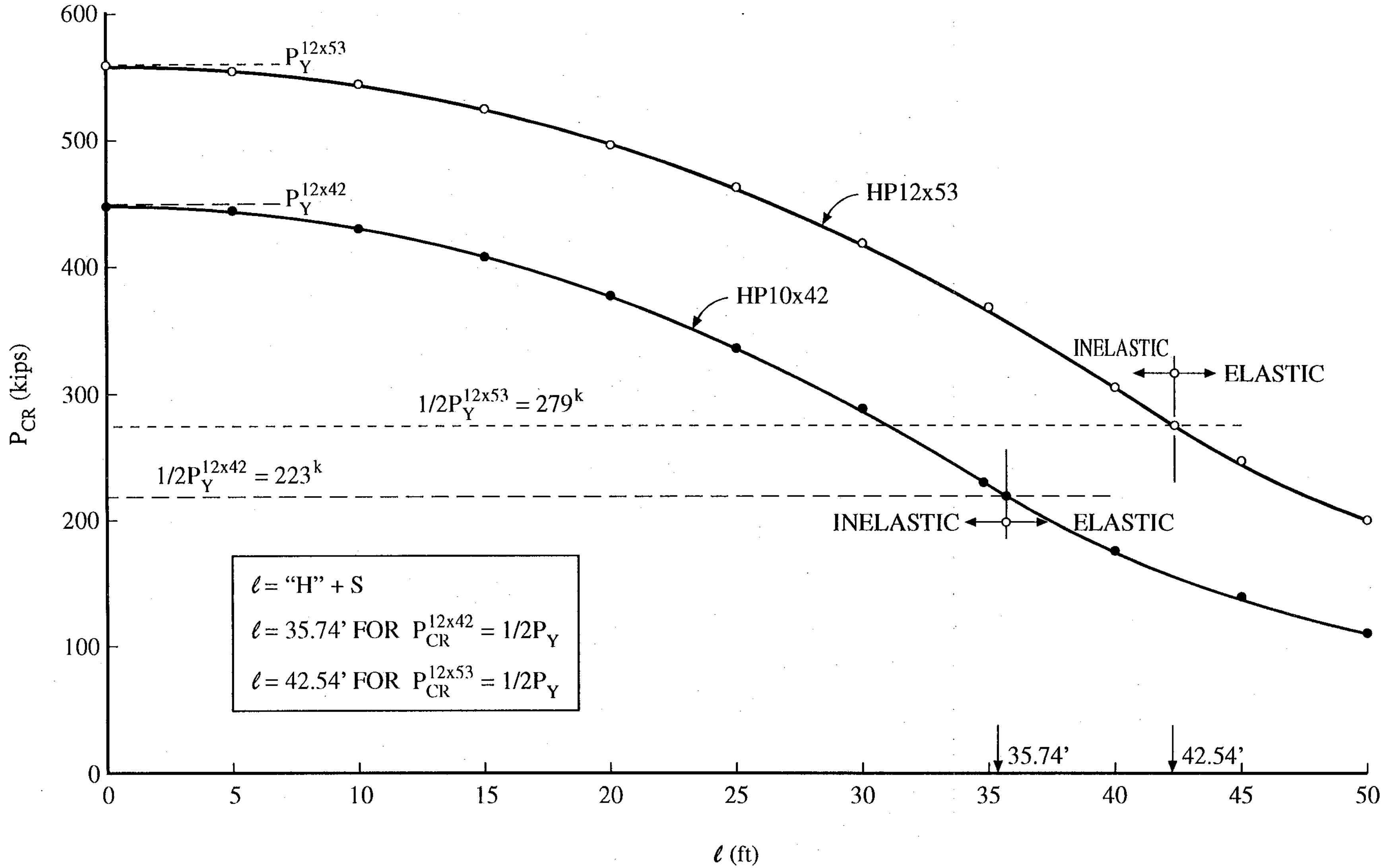

Fig. 6.6. Transverse/Weak Axis Buckling of a Single Bent HP Pile of A36 Steel for a Given Length (ℓ_{max}) Above Ground Line After Scour.

7. CONCLUSIONS AND RECOMMENDATIONS

Based on considerations of possible bridge bent failure modes along with theoretical analyses conducted during Phase I of this investigation, it appears that a screening of bridge pile bents to assess their adequacy during an extreme scour event will be quite feasible and can be performed with minimal effort. Furthermore it appears that this screening will probably indicate that the vast majority of the pile bents are adequate and do not require closer examination. However, prior to finalizing the screening procedure to be employed, some additional evaluations and verifications should be performed. These are listed below:

1. Need to check to see if an improved and simpler means of screening to assure a nonplunging failure of a pile or of a pile bent can be identified. Actual piles probably have a much higher tip capacity then the 0.10 pile failure load used in Chapter 6. Fred Conway recently indicated that ALDOT tries to drive steel HP piles to a stratum where the piles can achieve a 9 ksi tip bearing stress. This would translate to

   $$P^{10 \times 42}_{\text{tip capacity}} = 12.4 \text{ in}^2 \times 9 \text{ ksi} = 112^k$$

   If the HP piles do in fact have large P tip capacities, then an extreme scour event should never cause a pile or pile bent plunging failure.
2. Evaluate cases of piling founded in hard layers with almost zero embedment after a scour event, and decide on the appropriate procedure for handling these cases in the screening tool.

3. Need to further investigate pile encasement details and requirements to be able to confidently assess the integrity and composite behavior of encased piles up to the buckling load.
4. Need to verify by stiffness frame analyses that bent piles with 1 ½" in 12" batter piles at each end of the bent do in fact provide an equivalent spring brace at the top of the bent with a k_{equiv} greater than k_{ideal} as discussed in Section 3.3. This will assure that the bent piles will buckle in a nonsway mode in the transverse direction (about their weak axes) rather that in a sidesway mode in the transverse direction. If $k_{equiv} > k_{ideal}$ then the batter piles will assure a nonsideway buckling mode independent of whether the bent has X-bracing or concrete encased piles. If this is the case then the rather simple screening procedure described in Chapter 6 should be valid for all ALDOT pile bents independent of bent X-bracing and pile encasement.
5. Evaluate flood debris build-up and resulting bent transverse loading and possible failure under this loading
6. Need to work further with ALDOT Maintenance Engineers to determine if bridge bent standards and designs beyond those considered to date are prevalent in ALDOT inventory of bridge bents that may be subjected to an extreme scour event.
7. Model and determine bent vertical failure load (buckling load) using GTSTRUDL Pushover Analysis procedures. This has the potential of providing an easier modeling and more accurate failure load estimates than does FB Pier for cases requiring closer examination.

After performing 1-7 above during the initial part of Phase II, the drafting, testing and refining of a "screening tool" to assess the adequacy of bridge pile bents in extreme scour events will be performed in the remainder of the Phase II work. This will consist of:

1. Draft the screening tool to assess the adequacy of bridge pile bents in the event of an extreme scour event. Include in the narrative description of the step-by-step procedure employed in the screening tool an associated commentary for each step which provides background and the "whys" and "hows" of the working of the screening tool.
2. Draft a user's guide to outline and explain the procedure in using the screening tool.
3. Meet with ALDOT bridge maintenance engineers to discuss the screening tool and user's guide and make refinements as necessary after this meeting.
4. Meet with select ALDOT personnel to test the screening tool and user's guide. ALDOT's bridge maintenance engineer will select the personnel to participate in the "Test Meeting". Further refine the screening tool and/or guide based on feedback from the "Test Meeting".
5. Prepare and conduct a training seminar at ALDOT's office in Montgomery to train ALDOT personnel in how to use the screening tool.
6. Prepare Phase II Final Report.

REFERENCES

1. Granholm, Hjalmer, "On the Elastic Stability of Piles Surrounded by a Supporting Medium, "Ingeniors Vetenskaps Akademien Handlingar Nr89", Stockholm, Sweden, 1929, p 1-56.

2. Ramey, G.E. and Alan P. Hudgins, "Modification of Pile Capacity and Length Prediction Equations Based on Historical Alabama Pile Test Data," Alabama Highway Research HPR Report No. 75, June 1975.

3. Yura, J.A. and Todd A. Helwig, "Bracing for Stability," Notes from Seminar Sponsored by Stability Research Council and AISC, 1997.

4. Chajes, Alexander, Principal of Structural Stability Theory, Prentice-Hall, Inc., Englewood Cliffs, New Jersey, 1974.

5. Timoshenko, S.P. and James M. Gere, Theory of Elastic Stability, 2nd Edit., McGraw-Hill, NY, NY, 1961.

6. Chen, W.F. and E.M. Liu, Structural Stability-Theory and Implementation, Elsevier, NY, NY, 1987.

7. W.C. Young, Roark's Formulas for Stress and Strain, 6th Edition, McGraw-Hill, NY, NY, 1989.

8. Tonias, D.E., Bridge Engineering, McGraw-Hill, NY,NY, 1995.

Appendix A

Bridge, Girder, Barrier Rail, and Pile Section Properties

AASHTO I-Beams

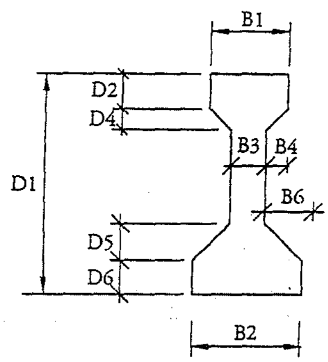

Type I-IV

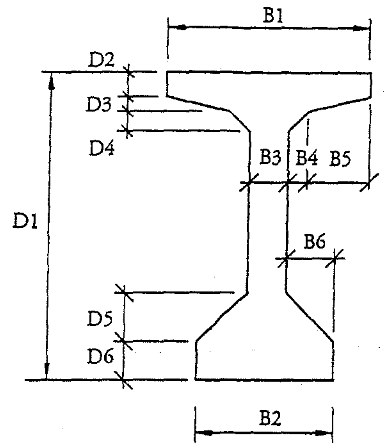

Type V-VI

Dimensions (inches)

Type	D1	D2	D3	D4	D5	D6	B1	B2	B3	B4	B5	B6
I	28.0	4.0	0.0	3.0	5.0	5.0	12.0	16.0	6.0	3.0	0.0	5.0
II	36.0	6.0	0.0	3.0	6.0	6.0	12.0	18.0	6.0	3.0	0.0	6.0
III	45.0	7.0	0.0	4.5	7.5	7.0	16.0	22.0	7.0	4.5	0.0	7.5
IV	54.0	8.0	0.0	6.0	9.0	8.0	20.0	26.0	8.0	6.0	0.0	9.0
V	63.0	5.0	3.0	4.0	10.0	8.0	42.0	28.0	8.0	4.0	13.0	10.0
VI	72.0	5.0	3.0	4.0	10.0	8.0	42.0	28.0	8.0	4.0	13.0	10.0

Properties

Type	Area in.²	y_{bottom} in.	Inertia in.⁴	Weight kip/ft	Maximum Span,* ft
I	276	12.59	22,750	0.287	48
II	369	15.83	50,980	0.384	70
III	560	20.27	125,390	0.583	100
IV	789	24.73	260,730	0.822	120
V	1,013	31.96	521,180	1.055	145
VI	1,085	36.38	733,320	1.130	167

*Based on simple span, HS-25 loading and f'_c = 7,000 psi.

Figure C–6 (a) AASHTO/PCI Standard Bridge Sections (Courtesy PCI, Ref. 12.11)

AASHTO-PCI Bulb-Tees

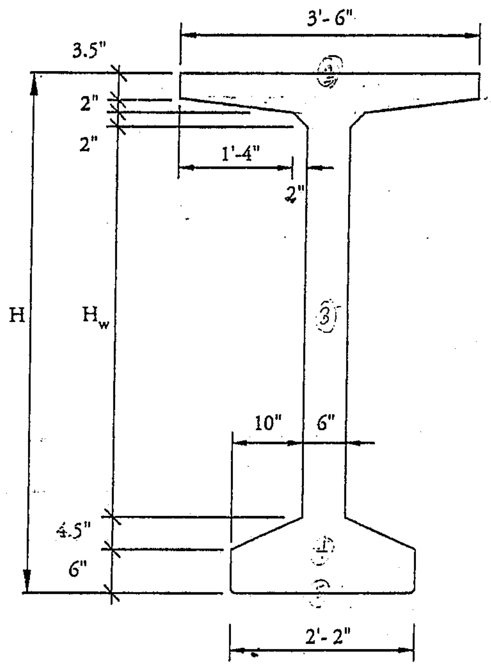

Properties

Type	H in.	H_w in.	Area in.^{2}	Inertia in.^{4}	y_{bottom} in.	Weight kip/ft	Maximum Span,* ft
BT-54	54	36	659	268,077	27.63	0.686	114
BT-63	63	45	713	392,638	32.12	0.743	130
BT-72	72	54	767	545,894	36.60	0.799	146

*Based on simple span, HS-25 loading and f'_c = 7,000 psi.

Figure C–7 (a) AASHTO/PCI Bulb Tees (Courtesy PCI, Ref. 12.11)

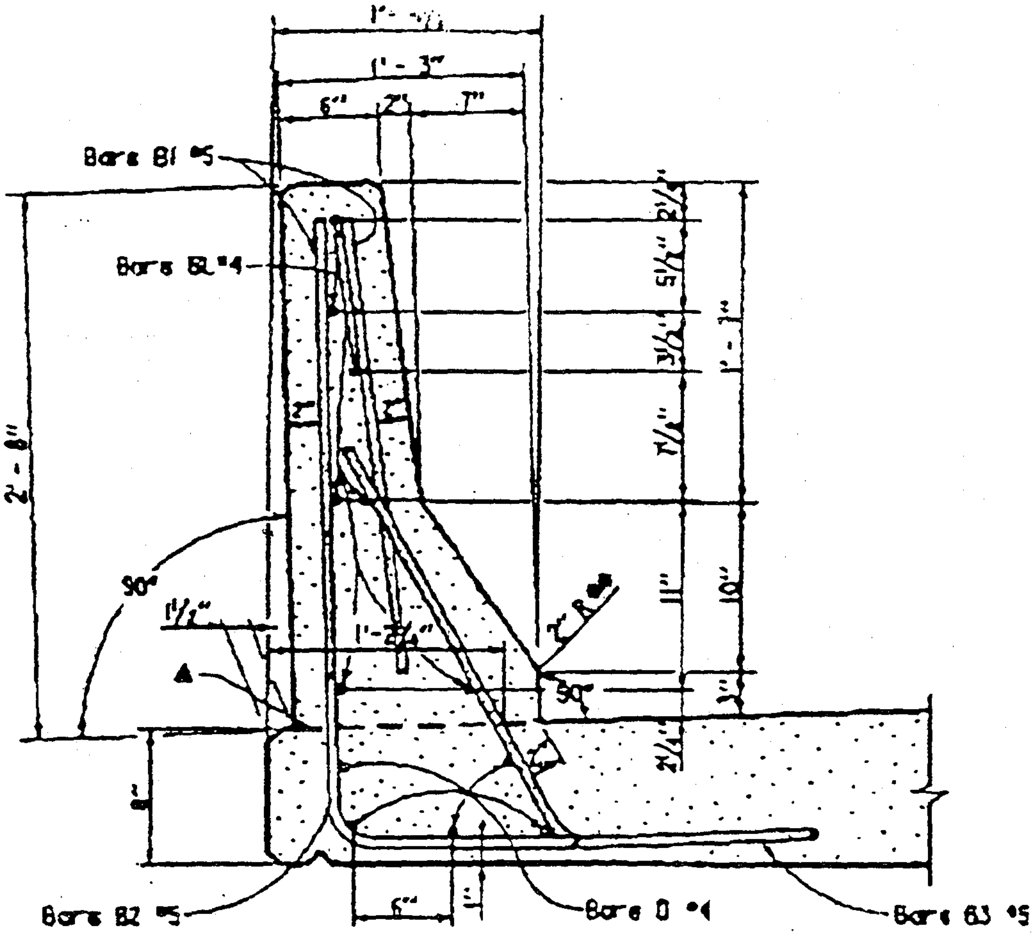

$w = 390$ lb/ft.

TYPICAL BARRIER SECTION-
ALDOT STANDARD

HP PILE SHAPES

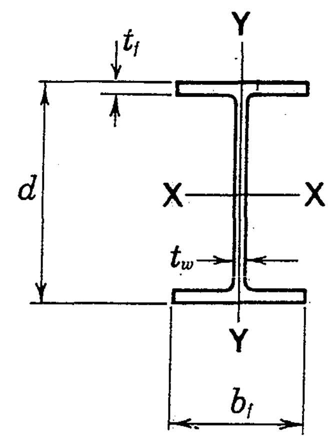

Section Properties

Section	A (in^2)	d (in)	b_f (in)	t_f (in)	t_w (in)	I_x (in^4)	I_y (in^4)	S_x (in^3)	S_y (in^3)	Z_x (in^3)	Z_y (in^3)
HP 12X53	15.5	11.78	12.05	0.435	0.435	393	127	66.8	21.1	74.0	32.2
HP 10X42	12.4	9.70	10.08	0.420	0.415	210	71.7	43.4	14.2	48.3	21.8

1. STEEL HP ALONE:

$E_S = 29{,}000$ ksi

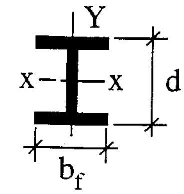

HP 12 x 53
$$\begin{cases} A = 15.5\ in^2 \\ d = 11.78\ in \\ b_f = 12.05\ in. \\ I_x = 393\ in^4 \\ I_y = 127\ in^4 \end{cases}$$

HP 10 x 42
$$\begin{cases} A = 12.4\ in^2 \\ d = 9.70\ in \\ b_f = 10.08\ in \\ I_x = 210\ in^4 \\ I_y = 71.7\ in^4 \end{cases}$$

2. FULL ENCASED SECTION:

Assume $f_c' = 3500$ psi

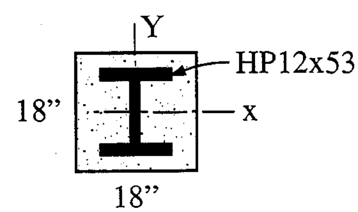

$$E_c = 57{,}000\sqrt{3500} = 3.37 \times 10^6 \text{ psi}$$

$$= 3.37 \times 10^3 \text{ ksi}$$

$$n = \frac{E_s}{E_c} = \frac{29}{3.37} = 8.60$$

Transform to all steel:

$$I_x = I_x^{HP} + \left[\frac{18/n(18)^3}{12} - 2(\frac{18}{n} x\ t_f x\ d_f^{\ 2})\right]$$

$$I_x = 393 + \left[\frac{18/8.6(18)^3}{12} - 2(2.093" x\ 0.435" x\ 5.673^2)\right]$$

$$I_x = 393 + [1017 - 59] = 1351 in^4$$

$$I_y = I_y^{HP} + \left[\frac{(18-2t_f)/n(18)^3}{12}\right]$$

$$I_y = 127 + \left[\frac{(1.992)(18)^3}{12}\right]$$

$I_y = 127 + 968 = 1095\ in^4$

$$A = A^{HP} + \left(\frac{18x18 - A^{HP}}{n}\right)$$

$$A = 15.5 + \left(\frac{324 - 15.5}{8.6}\right)$$

$A = 15.5 + 35.9 = 51.4\ in^2$

Transform to all steel:

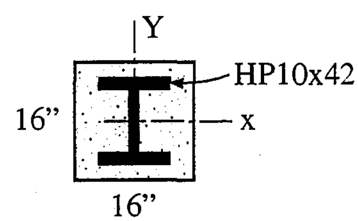

$$I_x = I_x^{HP} + \left[\frac{16/n(16)^3}{12} - 2\left(\frac{16}{n} x\, t_f\, x\, d_f^{\ 2}\right)\right]$$

$$I_x = 210 + \left[\frac{1.86(16)^3}{12} - 2(1.86\,x\,0.42\,x\,4.64^2)\right]$$

$$I_x = 210 + [634.9 - 33.6] = 811\,in^4$$

$$I_y = I_y^{HP} + \left[\frac{(16-2t_f)/n(16)^3}{12}\right]$$

$$I_y = 71.7 + \left[\frac{1.763(16)^3}{12}\right]$$

$$I_y = 71.7 + 601.7 = 673\,\text{in}^4$$

$$A = A^{HP} + \left(\frac{16\text{x}16 - A^{HP}}{n}\right)$$

$$A = 12.4 + \left(\frac{256 - 12.4}{8.6}\right)$$

$$A = 12.4 + 28.3 = 40.7\,\text{in}^2$$

3. <u>PARTIAL ENCASED SECTION (INSIDE OF SPIRAL):</u>

Transform to all steel:

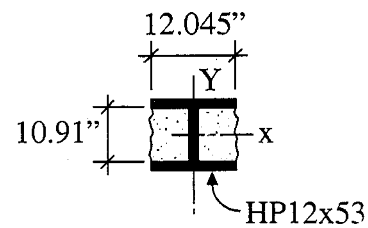

$$I_x = I_x^{HP} + \frac{\frac{(12.045 - t_w)}{n}(10.91)^3}{12}$$

$$I_x = 393 + \frac{(11.60/8.6)(10.91)^3}{12} = 393 + 146 = 539\,\text{in}^4$$

$$I_y = I_y^{HP} + \frac{(10.91/n)(12.045)^3}{12}$$

$$I_y = 127 + \frac{(10.91/8.6)(12.045)^3}{12} = 127 + 184 = 311\,\text{in}^4$$

$$A = A^{HP} + \frac{(12.045 - t_w)10.91}{n}$$

$$A = 15.5 + \frac{(12.045 - 0.445)(10.91)}{8.6}$$

$$A = 15.5 + 14.7 = 30.2\,\text{in}^2$$

Transform to all steel:

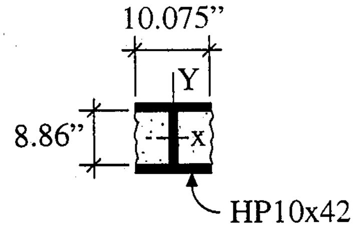

$$I_x = I_x^{HP} + \frac{\frac{(10.075 - t_w)}{n}(8.86)^3}{12}$$

$$I_x = 210 + \frac{(9.66/8.6)(8.86)^3}{12} = 210 + 65 = 275\,in^4$$

$$I_y = I_y^{HP} + \frac{(8.86/n)(10.075)^3}{12}$$

$$I_y = 71.7 + \frac{(8.86/8.6)(10.075)^3}{12} = 71.7 + 87.8 = 159\,in^4$$

$$A = A^{HP} + \frac{(10.075 - t_w)8.86}{n}$$

$$A = 12.4 + \frac{(10.075 - 0.415)8.86}{8.6}$$

$A = 12.4 + 9.9 = 22.3\ in^2$

Bent Pile Limiting Case Equivalent All Steel Section Properties

Section	$I_x(in^4)$	$I_y(in^4)$	$A(in^2)$
Uncased 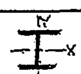			
HP 12 x 53	393	127	15.5
HP 10 x 42	210	71.7	12.4
Full Encased 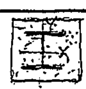			
HP 12x53 (18"x18")	1351	1095	51.4
HP 10x42 (16"x16")	811	673	40.7
Partial Encased 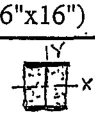			
HP 12x53	539	311	30.2
HP 10x42	275	159	22.3

ALDOT Bridge Superstructure Standards (Subset)

Standard Dwg. No.	Standard Description	Date	Bent Std Used With	Design Loading	Roadway Width	No. Lanes	Span Length	SS or Cont.	Max. No. Cont. Spans	Width of Open Jt. at 70°F	Barrier Rail	Curb Dim.	Support Girders No./Spacing/Type	Diaphragm Dim.	Deck		Interior Span Quantities*		
															Thick-ness	Over-hang	Concrete	Steel	Rebar
S-4034P	34' Prestressed Conc. Bm. Spans with PIP Slab made Cont. for LL	1980	B-4011P	HS 20-44	40'	2	34'	Cont. for LL	8	1 ½"	Jersey	-	6/7'-0"/Type I	11"x2'-4" x 35'	6 1/4"	3'-10 ½"	37.6 yd³	0	12,605 lb.
S-4041P	41' Prestressed Conc. Bm. Spans with PIP Slab made Cont. for LL	1988	B-4011P	HS 20-44	40'	2	41'	Cont. for LL	5	1 ½"	Jersey	-	6/7'-0"/Type I	11"x2'-4" x35'	6 1/4"	3'-10 ½"	45.2 yd³	0	13,425 lb
CSC-40100BR	Contin. Steel Composite Span wiht RC Slab 80'-100'-80' and 80'100'-100'-80'	1977	Not Specified	HS20-44	40'	2	80'-100'-80'	Cont.	3 or 4	1 ½" @ abut.	Jersey	-	6/7'-0"/W36x194 or W96x245 or W36x260	MC 18x42.7 @ 20' or 25' o.c.	6 ½" 8" haunch	3'-10 ½"	294 yd³ (80' span)	375,400 lb	78,850 lb
CS-40100(3) BR	Contin. Welded Girder Span Plate RC Deck 100'-100'-100' span	1977	Not Specified	HS20-44	40'	2 (assumed)	100'-100'-100'	Cont.	3	Not Significant	Jersey	-	6/7'-0"/ 4'-8 1/4" Deep Plate Girders	Structural Steel	6 ½" 9 1/8" haunch	3'-10 ½"	324 yd³	398,228 lb	90,638 lb
SC-4460B	60' composite Steel Beam Span with RC Slab	1970	Not Specified	HS20-44	44'	2 (assumed)	61'-2"	SS	3	1" between each SS.	Open Concrete Rail	11"x11"	6/8'-0"/W36x155 with cover plate on bottom	MC18x427 @ 20' o.c.	6 3/4" 8" haunch	3'-10"	71.6 yd³	67,265 lb	22,970 lb
C-2814-30	RC Deck-Girders 32'-38' Spans 30° Skew	1957	Not Specified	HS20-44	28'	2	32' to 38'	SS	Not Specified	1 1/8"	Open Concrete Rail	17"x11"	4/9'-2 7/8"/RC (16 3/4"x3'-½ " for 34' span)	6"x2'-8"RC	6 ½"	4'-7"	43.61 yd³ (34' Span)	791 lb	14,855 lb
C-2411	RC Deck-Girders 32-38' Spans	1963	Not Specified	H15-44	24'	2	32' to 38'	SS	Not Specified	1"	Open Concrete Rail	1'-6"x11" Safety Curb	4/6'-8"/RC (1'-1"x2'2" for 34' Span)	6"x2'-2"RC	6"	4'-7"	31.75 yd³ (34' Span)	633 lb	10,637 lb

Appendix B

Information Summary from Subset of ALDOT Bridge Superstructure Standards

ALDOT BRIDGE PILE BENT STANDARDS (Subset)

Standard Dwg. No.	Standard Description	Date	Design Loading	Pile	Pile Spacing	Outside Pile Batter	Pile Encasement	Cap	Bearing Pad	Bent Sway Bracing	Girders	Superstructure Connection to Cap
PCB-2434	Precast concrete bent cap for use with steel piling and precast concrete bridge slabs 24' & 34' Spans 24' & 24 ½' Clear Roadway	1990	H15-44 HS20-44	HP 12x53 (5)	5'-9"	1 ½" per ft.	1'-6" sq. or 24"⌀ encasement extending 3' above and 3' below ground or mud line	2' wide 1'-4 3/4"~ 1'-7" deep 27'-6" long	16"x22 ½" x ½" Elastomeric	Single or two story X bracing with ∟ 4 x 3 ½ x 5/16 with 4" leg welded to pile	Bridge Slab SS with 1/4" exp. jt filler	2 grouted #6 bars per span 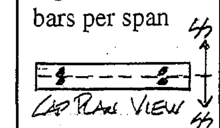
PCB-2832-30	Precast concrete bent cap for use with steel piling and precast concrete bridge slabs, 32' Span, 28' Clear Roadway, 30° Skew	1994	H15-44 HS20-44	HP 12x53 (6)	6'-9"	1 ½" per ft.	1'-6" sq. or 24"⌀ encasement extending 3' above and 3' below ground or mudline	2' wide 1'-9 ½" ~ 2'- 0 ½" deep 36' - 8 ½" long	16"x26"x ½" Elastomeric (skewed)	Single or two story X bracing with ∟ 4 x 3 ½ x 5/16 with 4" leg welded to pile	Bridge Slab SS with 1/4" exp. jt filler	16 grouted #6 bars per span
PCB-2834	Precast concrete bent cap for use with steel piling and precast concrete bridge slabs 24' & 34' Spans 28' Clear Roadway	1990	H15-44 HS20-44	HP 12x53 (5)	6'-10 ½"	1 ½" per ft.	1'6" sq. or 24"⌀ encasement extending 3' above and 3' below ground or mud line	2' wide 1' - 9 1/6 ~ 2'-0 deep 31'-6" long	16"x22 ½" x ½" Elastomeric	Single or two story X bracing with ∟4 x 3 ½ x 5/16 with 4" leg welded to pile	Bridge Slab SS with 1/4" exp. jt filler	2 grouted #6 bars per span
PCB-2834-C	Precast concrete bent cap for use with steel piling and precast concrete bridge slabs for a curved bridge 34' Span 28' Clear Roadway	1993	H15-44 HS20-44	HP12x53 (5)	6'-10 ½"	1 ½" per ft.	1'-6" sq. or 24"⌀ encasement extending 3' above and 3' below ground or mud line	2'-9" wide 1-9 1/16" deep 31'-6" long	16" x 31 ½" x ½" Elastomeric	Single or two story X bracing with ∟ 4 x 3 ½ x 5/16 with 4" leg welded to pile	Bridge Slab SS with 1/4" exp. jt filler	2 grouted #6 bars per span
PCB-2840	Precast concrete bent cap for use with steel piling and precast concrete bridge slabs 40' Span 28' Clear Roadway	2001	HS20-44	HP 12x53 (5)	6'-10 ½"	1 ½" per ft	1'-6" sq. or 24"⌀ encasement extending 3' above and 3' below ground or mud line	2' wide 1'-9 1/16 ~ 2' deep 31'-6" long	16" x 22 ½ x ½" Elastomeric	Single or two story X bracing with ∟ 4 x 3 ½ x 5/16 with 4" leg welded to pile	Bridge Slab SS with 1/4" exp. jt filler	2 grouted #6 bars per span
PCB-2840-CP	Precast concrete bent cap for use with 14" x 14" concrete piling and 24', 34', or 40' precast concrete bridge slabs 28' Clear Roadway	2001	HS20-44	14" x 14" PC (5)	6'-10 ½"	1 ½" per ft	None	2'-3" wide 1'-5 1/16 ~ 1'-8" deep 31'-6" long	16" x 22 ½" x ½" Elastomeric	None	Bridge Slab SS with 1/4" exp. jt filler	7 grouted #6 bars per span
PCB-3540-30	Precast concrete split bent cap for use with steel piling and 32' or 40' prestress concrete bridge slabs 35' Clear Roadway 30° Skew	2001	HS20-44	HP 12x53 (7)	6'-10 ½"	1 ½" per ft.	1'-6" sq. or 24"⌀ encasement extending 3' above and 3' below ground or mud line	2' wide 1'-9 1/16 ~ 2'-1 5/16" deep 45'-6" long	16" x 26" x ½" Elastomeric (skewed)	Single or two story X bracing with ∟ 4 x 3 ½ x 5/16 with 4" leg welded to pile	Bridge Slab SS with 1/4" exp. jt filler	4 grouted #6 bars per span

Appendix C

Information Summary from Subset of ALDOT Bridge Pile Bent Standards

ALDOT BRIDGE PILE BENT STANDARDS (Subset)

Standard Dwg. No.	Standard Description	Date	Design Loading	Pile	Pile Spacing	Outside Pile Batter	Pile Encasement	Cap	Bearing Pad	Bent Sway Bracing	Girders	Superstructure Connection to Cap
PB 2802	Steel Pile Intermediate Bents 24'-34' Spans 28' Roadway	1952	HS20-44	HP 10x42 (4)	8'-0"	1 ½" per ft.	1'-4" sq. encasement extending 3' above and 3' below ground or mud or water line, or to cap if clearance between cap and ground is less than 11'-0"	3' wide @ top 2'-0" deep 27'-2" long	½" Prem. Bit. Filler	Single or two story X bracing with ∟ 4 x 3 ½ x 5/16 with 4" leg welded to pile. Omit sway bracing if pile is encased to cap.	PIP Concrete Girders (prob'ly)	2 - 3/4" ⌀ plain bars embedded in cap per girder (one end only).
PB 2802-45 (45° skew)	Concrete & Steel Pile Intermediate Bent - 4 Pile 24'-34' Spans 28' Roadway (with 1'-6" Safety Curbs)	1957	H20-S16-44	HP 10x42 (4)	11'-4"	1 ½" per ft.	1'-4" sq. encasement extending 3' above and 3' below ground or mud or water line, or to cap if clearance between cap and ground is less than 11'-0".	3' wide @ top 2'-0" deep 40'-8" long	EXP. Packing or ½" Prem. Bit. Filler	Single or two story X bracing with ∟ 4 x 3 ½ x 5/16 with 4" leg welded to pile. Omit sway bracing if pile is encased to cap.	PIP Concrete Girders (prob'ly)	2 - 3/4" ⌀ plain bars embedded in cap per girder (one end only).
PB 2803	Steel Pile Intermediate Bents 32'-38' Spans 28' Roadway (with 1'-6" Safety Curbs)	1952	H20-S16-44	HP 10x42 (5)	6'-6"	1 ½" per ft.	1'-4" sq. encasement extending 3' above and 3' below ground or mud or water line, or to cap if clearance between cap and ground is less than 11'-0".	3' wide @ top 2'-0" deep 29'-0" long	½" Prem. Bit. Filler	Single or two story X bracing with ∟ 4 x 3 ½ x 5/16 with 4" leg welded to pile. Omit sway bracing if pile is encased to cap.	PIP Concrete Girders (prob'ly)	2- 3/4" ⌀ plain bars embedded in cap per girder (one end only).
PB 2834	Steel Pile Intermediate Bents 24'-34' Spans	1968	HS20-44	HP 10x42 (4)	8'-0"	1 ½" per ft.	1'-4" sq. or 22"⌀ encasement extending 3' above and 3' below ground or mud or water line, or to cap if clearance between cap and ground is less than 11'-6".	3' wide @ top 2'-0" ~2'-4" deep 27'-2" long	8" x 14 ½" x 1" Elastomeric with precast Girders	Single or two story X bracing with ∟ 4 x 3 ½ x 5/16 with 4" leg welded to pile. Omit sway bracing if pile is encased to cap.	PIP Concrete or Precast Girders	2 - 3/4" ⌀ plain bars embedded in cap per girder (one end only). (Probably just for PIP girders)
B-3411P	Steel Pile Intermediate Bent (for use with Type I Girders) 34' Roadway	1982	HS20-44	HP 12x53 (5)	7'-6"	1 ½" per ft.	1'-6" sq. or 24" ⌀ encasement extending 3' above and 3' below ground or mud or water line, or to cap if clearance between cap and ground is less than 11'-6".	3' wide @ top 2'-0" ~ 2' - 2 3/4" deep 33'-6" long	6" x 14 ½" x 1" Elastomeric	Single or two story X bracing with ∟ 4 x 3 ½ x 5/16 with 4" leg welded to pile. Omit sway bracing if pile is encased to cap.	AASHTO Type I Girders	2 - 3/4" ⌀ plain bars embedded in cap per girder (one end only) for spans made continuous for LL.
B-4011 P	Steel Pile Intermediate Bent (for use with Type I Girders) 40' Roadway	1979	HS20-44	HP 12x53 (6)	7'-0"	1 ½" per ft.	1'-6" sq. or 24" ⌀ encasement extending 3' above and 3' below ground or mud or water line, or to cap if clearance between cap and ground is less than 11'-6"	3' wide @ top 2'-0" ~ 2' - 2 15/16" deep 38'-6" long	6" x 14 ½" x 1" Elastomeric	Single or two story X bracing with ∟ 4 x 3 ½ x 5/16 with 4" leg welded to pile. Omit sway bracing if pile is encased to cap.	AASHTO Type I Girders	2 - 3/4" ⌀ plain bars embedded in cap per girder (one end only) for spans made continuous for LL.

ALDOT BRIDGE PILE BENT STANDARDS (Subset)

Standard Dwg. No.	Standard Description	Date	Design Loading	Pile	Pile Spacing	Outside Pile Batter	Pile Encasement	Cap	Bearing Pad	Bent Sway Bracing	Girders	Superstructure Connection to Cap
PB-4034 (1)	Steel Pile Intermediate Bent 34' Spans 40' Roadway	1980	HS20-44	HP 12x53 (5)	9'-0"	1 ½" per ft.	1'-6" sq. or 24" ⌀ encasement extending 3' above and 3' below ground or mud or water line, or to cap if clearance between cap and ground is less than 11'-6"	3' wide @ top 2'-0" ~ 2' - 3 1/4" deep 39'-6" long	8" x 10" x ½" Elastomeric	Single or two story X bracing with ⌊ 4 x 3 ½ x 5/16 with 4" leg welded to pile. Omit sway bracing if pile is encased to cap.	Steel or Precast Concrete Girders	4 - 1" ⌀ Anchor bolts for each span with attachment at outside girders.
PCPB-4041	Prestressed Concrete Pile Intermediate Bent 34'-41' Spans 40' Roadway	1975	HS20-44	14" x 14" PC (Std. PSCP-1) (6)	7'-0"	1 ½" per ft.	None	3' wide @ top 2'-0" ~ 2' - 3 1/16" deep 38'-6" long		None		2 - 3/4" ⌀ plain bars embedded in cap per girder (one end only) for fixed bents 4 - 1" ⌀ anchor bolts per girder for expansion bents
B-4411P	Steel Pile Intermediate Bent (for use with Type I Girders) 44' Roadway		HS20-44	HP 12x53 (6)	8'-0"	1 ½" per ft.	1'-6" sq. or 24" ⌀ encasement extending 3' above and 3' below ground or mud or water line, or to cap if clearance between cap and ground is less than 11'-6"	3' wide @ top 2'-0" ~ 2' - 4 11/16" deep 43'-6" long	6' x 14 ½" x 1" Elastomeric	Single or two story X bracing with ⌊ 4 x 3 ½ x 5/16 with 4" leg welded to pile. Omit sway bracing if pile is encased to cap.	AASHTO Type I Girders	2 - 3/4" ⌀ plain bars embedded in cap per girder (one end only) for fixed bents. Guide pedestal at outside girders at expansion bents.
PB-4434 PS	Steel Pile Intermediate Bent 34' Spans with Type I Girders 44' Roadway	1979	HS20-44	HP 12x53 (6)	8'-0"	1 ½" per ft.	1'-6" sq. or 24" ⌀ encasement extending 3' above and 3' below ground or mud or water line, or to cap if clearance between cap and ground is less than 11'-6"	3' wide @ top 2'-0" ~ 2'- 4 11/16" deep 43'-6" long	8" x 14 ½" x 1" Neoprene	Single or two story X bracing with ⌊ 4 x 3 ½ x 5/16 with 4" leg welded to pile. Omit sway bracing if pile is encased to cap.	AASHTO Type I Girders	2 - 3/4" ⌀ plain bars embedded in cap per girder (one end only) for fixed bents. Neoprene pad bonded to cap and girder with epoxy at expansion bent.
PB-3934	Steel Pile Intermediate Bents 24' thru 34' Spans 39'-3" Roadway	1967	HS20-44	HP 10x42 (6)	7'-0"	1 ½" per ft.	1'-4" sq. encasement extending 3' above and 3' below ground or mud or water line, or to cap if clearance between cap and ground is less than 11'-6".	3' wide @ top 2'-0" ~2'-5" deep 38'-6" long	8" x 16" x 1" Neoprene	Single or two story X bracing with ⌊ 4 x 3 ½ x 5/16 with 4" leg welded to pile. Omit sway bracing if pile is encased to cap.	PIP Concrete or Precast Girders	2 - 3/4" ⌀ plain bars embedded in cap per girder (one end only)

ALDOT BRIDGE PILE BENT STANDARDS (Subset)

Standard Dwg. No.	Standard Description	Date	Design Loading	Pile	Pile Spacing	Outside Pile Batter	Pile Encasement	Cap	Bearing Pad	Bent Sway Bracing	Girders	Superstructure Connection to Cap
PB 4034	Steel Pile Intermediate Bents 34' Spans 40' Roadway	1975	HS20-44	HP 10x42 (6)	7'-0"	1 ½" per ft.	1'-4" sq. or 22"⌀ encasement extending 3' above and 3' below ground or mud line, or to cap if clearance between cap and ground is less than 11'-6".	3' wide @ top 2'-0" ~ 2'-4" deep 38'-6" long	8" x 16" x 1" Neoprene Pad	Single or two story X bracing with ∟ 4 x 3 ½ x 5/16 with 4" leg welded to pile. Omit sway bracing if pile is encased to cap.	Precast Concrete	2-3/4" ⌀ plain bars embedded in cap per girder (one end only)
PB-2200	Steel Pile Intermediate Bents 24'-34' Spans 22' Roadway (with 8" curbs)	1951	H15-44	HP 10x42 (3)	8'-6"	1 ½" per ft.	1'-4" sq. encasement extending 3' above and 3' below ground or mud or water line, or to cap if clearance between cap and ground is less than 8'-0".	3' wide @ top 2'-0" deep 20'-0" long	J.M. Packing at expansion end only.	Single or two story X bracing with ∟ 4 x 3 ½ x 5/16 with 4" leg welded to pile. Omit sway bracing if pile is encased to cap.	PIP Concrete Girders (prob'ly)	2-#6 bars embedded in cap per girder (one end only).
PB-2200-45 (45° skew)	Steel Pile Intermediate Bents 24-34' Spans 22' Roadway (with 8" curbs)	1962	H15-44	HP 10x42 (3)	12'-0 1/4"	1 ½" per ft.	1'4" sq. encasement extending 3' above and 3' below ground or mud or water line, or to cap if clearance between cap and ground is less than 11'-0".	3' wide @ top 2'-0" deep 30'-6" long	J.M. Packing or ½" Prem. Bit. Filler	Single or two story X bracing with ∟ 4 x 3 ½ x 5/16 with 4" leg welded to pile. Omit sway bracing if pile is encased to cap.	PIP Concrete Girders (prob'ly)	2-3/4" ⌀ plain bars embedded in cap per girder (one end only).
PB-2202-30 (30° skew)	Steel Pile Intermediate Bents Steel Beams and/or RCDG Spans 22' Roadway (with 8" curbs)	1961	H15-44	HP 10x42 (4)	7'- 1-7/16"	1 ½" per ft.	1'-4" sq. encasement extending 3' above and 3' below ground or mud or water line, or to cap if clearance between cap and ground is less than 8'-0".	3' wide @ top 2'-2" deep 24'-8" long	J.M. Packing or ½" Prem. Bit. Filler.	Single or two story X bracing with ∟ 4 x 3 ½ x 5/16 with 4" leg welded to pile. Omit sway bracing if pile is encased to cap.	Steel I or RCDG Girders	2 - 3/4" ⌀ plain bars embedded in cap per girder (one end only).
PB2202-45 (45° skew)	Steel Pile Intermediate Bents Steel Beams and/or RCDG Spans 22' Roadway (with 8" curbs)		HS15-44	HP 10x42 (4)	8' - 8 11/16"	1 ½" per ft.	1'-4" sq. encasement extending 3' above and 3' below ground or mud or water line, or to cap if clearance between cap and ground is less than 8'-0".	3' wide @ top 2' 0" deep 30'-8" long	J.M. Packing or ½" Prem. Bit. Filler.	Single or two story X bracing with ∟ 4 x 3 ½ x 5/16 with 4" leg welded to pile. Omit sway bracing if pile is encased to cap.	Steel I or RCDG Girders	2 - 3/4" ⌀ plain bars embedded in cap per girder (one end only).

ALDOT BRIDGE PILE BENT STANDARDS (Subset)

Standard Dwg. No.	Standard Description	Date	Design Loading	Pile	Pile Spacing	Outside Pile Batter	Pile Encasement	Cap	Bearing Pad	Bent Sway Bracing	Girders	Superstructure Connection to Cap
PB 2400	Steel Pile Intermediate Bents 24'-42' Spans 24' Roadway (with 1'-6" Safety Curbs)	1952	H15-44 HS20-44	HP 10x42 (4)	6'-8"	1 ½" per ft.	1'-4" sq. encasement extending 3' above and 3' below ground or mud or water line, or to cap if clearance between cap and ground is less than 11'-0".	2' wide @ top 2'-0" deep 23'-0" long	½" Premolded Bit. Filler at Expansion end.	Single or two story X bracing with ∟ 4 x 3 ½ x 5/16 with 4" leg welded to pile. Omit sway bracing if pile is encased to cap.	PIP Concrete Girders (prob'ly)	2 - 3/4" ⌀ plain bars embedded in cap per girder (one end only).
PB-2400-30 (30° skew)	Concrete & Steel Pile Intermediate Bent - 4 Pile 24'-42' Spans 24" Roadway (with 1'-6" Safety Curbs)	1955	H15-44 HS20-44	HP 10x42 (4)	7' - 8 ½"	1 ½" per ft.	1'4" sq. encasement extending 3' above and 3' below ground or mud or water line, or to cap if clearance between cap and ground is less than 11'-0"	3' wide @ top 2'-0" deep 28'-0" long	J.M. Packing or ½" Prem. Bit. Filler	Single or two story X bracing with ∟ 4 x 3 ½ x 5/16 with 4" leg welded to pile. Omit sway bracing if pile is encased to cap.	PIP Concrete Girders (prob'ly)	2 - 3/4" ⌀ plain bars embedded in cap per girder (one end only).
PB-2434	Steel Pile Intermediate Bents 32'-38' Spans 24' Roadway	1973	HS20-44	HP 10x42 (4)	6'-8"	1 ½" per ft.	1'4" sq. encasement extending 3' above and 3' below ground or mud or water line, or to cap if clearance between cap and ground is less than 11'-6".	3' wide @ top 2'-0" ~ 2-2" deep 23'-6" long	½" Prem. Bit. Filler, or 1" x 8" x 16" Elastomeric with AASHTO Type I Girders	Single or two story X bracing with ∟ 4 x 3 ½ x 5/16 with 4" leg welded to pile. Omit sway bracing if pile is encased to cap.	PIP Concrete or AASHTO Type I Girder	2 - 3/4" ⌀ plain bars embedded in cap per girder (one end only). 1" ⌀ Swedged anchor bolts used with Type I girder.
PB-2800	Steel Pile Intermediate Bents 24'-34' Spans 28' Roadway (with 1'-6" Safety Curbs)	1952	HS20-44	HP 10x42 (4)	8'-0"	1 ½" per ft.	1'-4" sq encasement extending 3' above and 3' below ground or mud or water line, or to cap if clearance between cap aqnd ground is less than 11'-0"	3' wide @ top 2'-0" deep 27'-0" long	½" Prem. Bit. Filler	Single or two story X bracing with ∟ 4 x 3 ½ x 5/16 with 4" leg welded to pile. Omit sway bracing if pile is encased to cap.	PIP Concrete Girders (prob'ly)	2 - 3/4" ⌀ plain bars embedded in cap per girder (one end only).
PB-2800-30 (30° skew)	Concrete Steel Pile Intermediate Bent - 4 Pile 24'-34' Spans 28' Roadway (with 1'-6" Safety Curbs)	1952	HS20-44	HP 10x42 (4)	9'-3"	1 ½" per ft.	1'-4" sq. encasement extending 3' above and 3' below ground or mud or water line, or to cap if clearance between cap and ground is less than 11'-0".	3' wide @ top 2' deep 32'-6" long	EXP. Packing or ½" Prem. Bit. Filler	Single or two story X bracing with ∟ 4 x 3 ½ x 5/16 with 4" leg welded to pile. Omit sway bracing if pile is encased to cap.	PIP Concrete Girders (prob'ly)	2 - 3/4" ⌀ plain bars embedded in cap per girder (one end only).

ALDOT BRIDGE PILE BENT STANDARDS (Subset)

Standard Dwg. No.	Standard Description	Date	Design Loading	Pile	Pile Spacing	Outside Pile Batter	Pile Encasement	Cap	Bearing Pad	Bent Sway Bracing	Girders	Superstructure Connection to Cap
PB-4434	Steel Pile Intermediate Bents 32'-38' Spans 44' Roadway	1967	HS20-44	HP 10"x42" (6)	8'-0"	1 ½" per ft.	1'-4" sq. or 22"⌀ encasement extending 3' above and 3' below ground or mud or water line, or to cap if clearance between cap and ground is less than 11'-6".	3' wide @ top 2'-0" ~ 2' - 4 11/16" deep 43'-6" long	8" x 14 ½" x 1" Neoprene	Single or two story X bracing with ∟ 4 x 3 ½ x 5/16 with 4" leg welded to pile. Omit sway bracing if pile is encased to cap.	PIP Concrete or AASHTO Girders	2 - 3/4" ⌀ plain bars embedded in cap per girder (one end only) for final bents. Skid block/guide pedstol at expansion bent 2 - 3/4" ⌀ plain bars per girder for fixed bents and Neoprene pad epoxied to cap and girder for exp. bents for precast girders.
PB-4434-30 (30° skew)	Steel Pile Intermediate Bents 32'-38' Spans 44' Roadway	1967	HS20-44	HP 10x42 (6)	9'-3"	1 ½" per ft.	1'-4" sq. encasement extending 3' above and 3' below ground or mud or water line, or to cap if clearance between cap and ground is less than 11'-6"	3' wide @ top 2'-0" ~ 2'-8" deep 51'-6" long	EXP. Packing or ½" Bit. Filler	Single or two story X bracing with ∟ 4 x 3 ½ x 5/16 with 4" leg welded to pile. Omit sway bracing if pile is encased to cap.	PIP Concrete or AASHTO Girders	Same as above
PB-4434-45 (45° skew)	Steel Pile Intermediate Bents 32'-38' Spans 44' Roadway	1968	HS20-44	HP 10x42 (6)	11'- 3 3/4"	1 ½" per ft.	1-'4" sq. encasement extending 3' above and 3' below ground or mud or water line, or to cap if clearance between cap and ground is less than 11'-6".	3' wide @ top 2'-0" ~ 2'-4" deep 62'-6" long	EXP Packing or ½" Prem. Bit. Filler	Single or two story X bracing with ∟ 4 x 3 ½ x 5/16 with 4" leg welded to pile. Omit sway bracing if pile is encased to cap.	PIP Concrete or AASHTO Girders	Same as above

Appendix D

Pile Capacity Predictions by Soil Mechanics Approach vs. Pile Failure Load for Some Historical Alabama Pile Test Data

**Pile Capacity Predictions by Soil Mechanics Approach vs.
Pile Failure Load for Some Historical Alabama Pile Test Data**

In 1975, Ramey and Hudgins (1) conducted a study for the ALDOT on "Pile Capacity and Length Predictions Based on Historical Alabama Pile Test Data." Some of the results of that study for Steel-H, Precast Concrete and Timber piles are shown in the table and figures below. In these,

P_f = Pile failure load

P_{sm} = Predicted pile failure load by soil mechanics approach

Note in Table D.1 the relatively small values of estimated pile load carried by point bearing (P_{tip}) as compared with that carried by side friction ($P_{friction}$) for the steel H and timber piles; whereas, for the precast concrete piles, a substantial portion of the load is estimated to be carried by point bearing (P_{tip})

Note in Figures D.1 and D.3 the fair but conservative estimate of the pile failure load by P_{sm}. Figure D.2 reflects a good estimate of P_f by the soil mechanics approach for the precast concrete piles.

Figures D.4 and D.6 indicate a slope of the P_f vs. L curves of approximately 1.56 tons per foot. For both of these pile types, Table D.1 reflects almost all of the capacity is coming from side friction ($P_{friction}$). Thus if one backs out the small contribution of P_{tip} to the capacity for these piles, the test data indicate

$$P_{friction} \approx 1.5 \text{ tons per foot}$$

$$\approx 3^k/\text{ft.}$$

However, as indicated in Chapter 3, the top 10-15 feet of soil is normally rather soft and/or loose and does not have the confining overburden pressure as occurs for the deep soil layers. Thus a reasonable estimate for $P_{friction}$ in the top layer(s) that will be scoured away would be

$$P_{friction} \approx 1.5^k/\text{ft.}$$

Thus, for an $S_{50} = 15'$

$$\Delta P_{friction} = -15' \times 1.5^k/\text{ft.} = -22.5^k$$

Or, the pile would lose 22.5^k of its support capacity during the major scour event.

Table D.1. Pile Capacities by Soil Mechanics Approach (1).

Pile Type	Size	Test No.	$P_{FRICTION}$ (tons)	P_{TIP} (tons)	P_{SM} (tons)	P_f (tons)
STEEL H	10X42	2	41	4	45	24
	10X42	10	31	2	33	67
	10X42	11	50	5	55	48
	14X89	15	113	11	124	130
	14X89	16	149	5	154	118
	14X89	17	190	14	204	154
	14X89	18	125	12	137	96
	14X89	19	148	5	153	150
	14X89	20	72	4	76	100
	14X89	21	105	8	113	150
	10X57	23	13	5	18	92
	10X57	24	33	7	40	75
	12X53	25	94	6	100	96
	12X53	26	69	5	74	98
	12X53	27	30	3	33	92
	12X53	28	51	5	56	94
	12X53	29	24	3	27	92
	12X53	30	100	2	102	140
	12X53	31	122	3	125	160
	12X53	32	162	9	171	198
	14X89	42	244	11	255	192
	14X89	43	187	8	195	230
	14X89	44	78	4	82	108
	10X42	50	55	5	60	72
PRECAST CONCRETE	16X16	203	139	49	188	150
	54ϕ	205	392	81	473	390
	20X20	206	85	41	126	164
	20X20	207	35	31	66	196
	12X12	208	138	31	169	142
	12X12	209	26	20	46	54
	12X12	210	19	18	37	55
	16X16	211	35	35	70	98
	16X16	212	23	30	53	68
	24X24	213	230	69	299	280
	36X36	214	360	175	535	532
	24X24	215	179	115	294	315
	36X36	216	436	192	628	610
	54ϕ	217	316	181	497	570
	54ϕ	218	554	124	678	575
	16X16	219	229	77	306	240
	16X16	220	185	58	243	202
	36X36	221	443	233	676	650
	54ϕ	222	550	124	674	670
TIMBER	8-11½	303	21	5	26	46
	7-12	304	71	5	76	57
	7-12	305	70	5	75	56
	7-12	306	70	5	75	64
	7-12	307	63	7	70	71
	7-12	308	70	5	75	88
	7-12	309	68	5	73	57
	7-12	310	70	5	75	72
	7-12	311	47	4	51	72
	7-12	312	60	5	65	80
	9.5-13.8	320	88	8	96	114
	7.8-11	321	47	10	57	48
	8-16	322	99	7	106	96
	7-12	323	60	6	66	128
	7-12	337	45	5	50	87

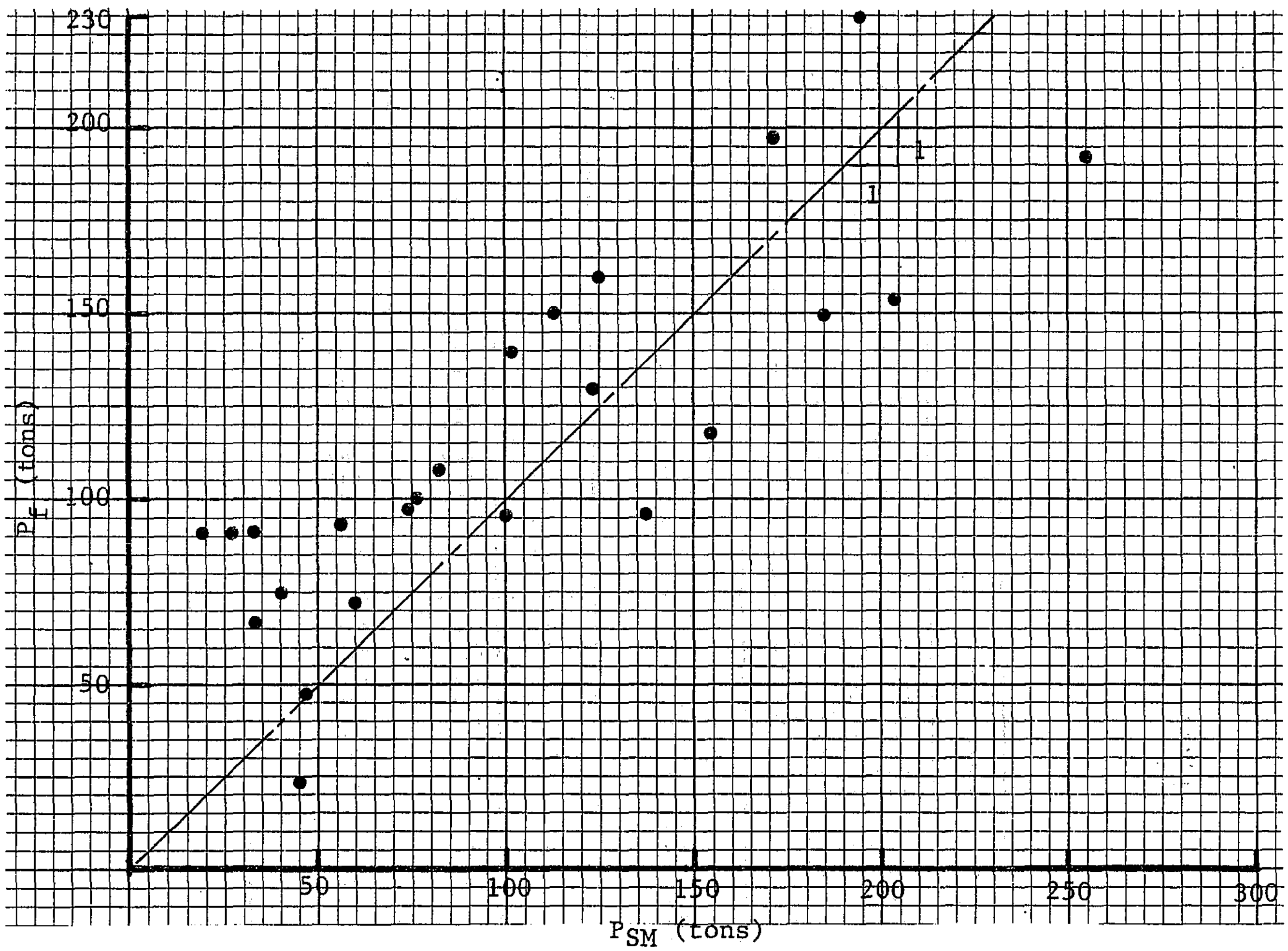

Fig. D.1. P_{SM} vs P_f for Steel-H Piles in Alabama Sandy Soils ($\delta = 0.60\phi$ and $K = 0.8$) (1).

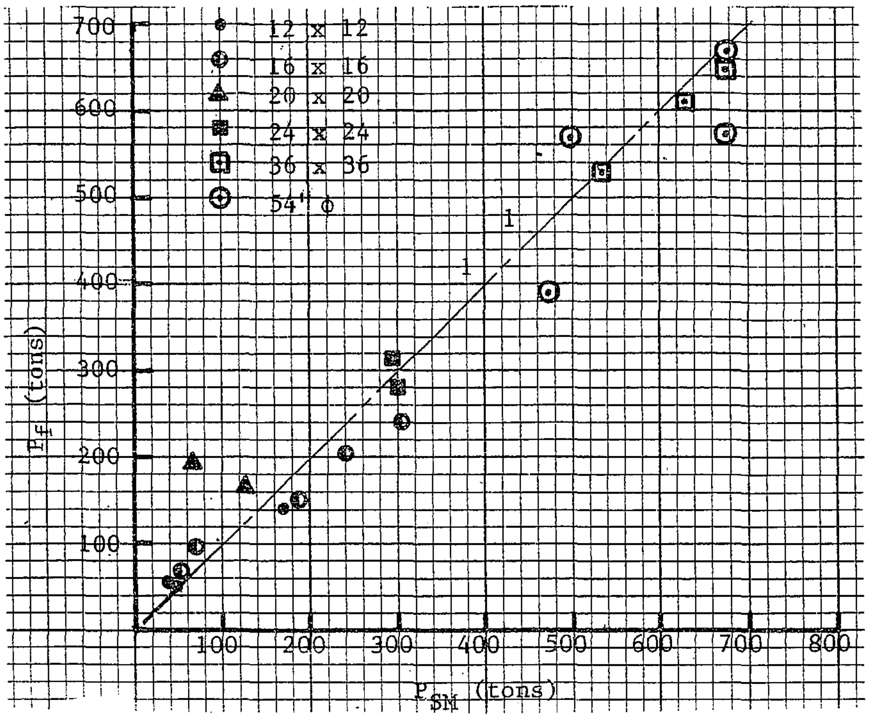

Fig. D.2. P_{SM} vs P_f for Precast Concrete Piles in Alabama Sandy Soils ($\delta = 0.90\phi$ and K = 1.0) (1).

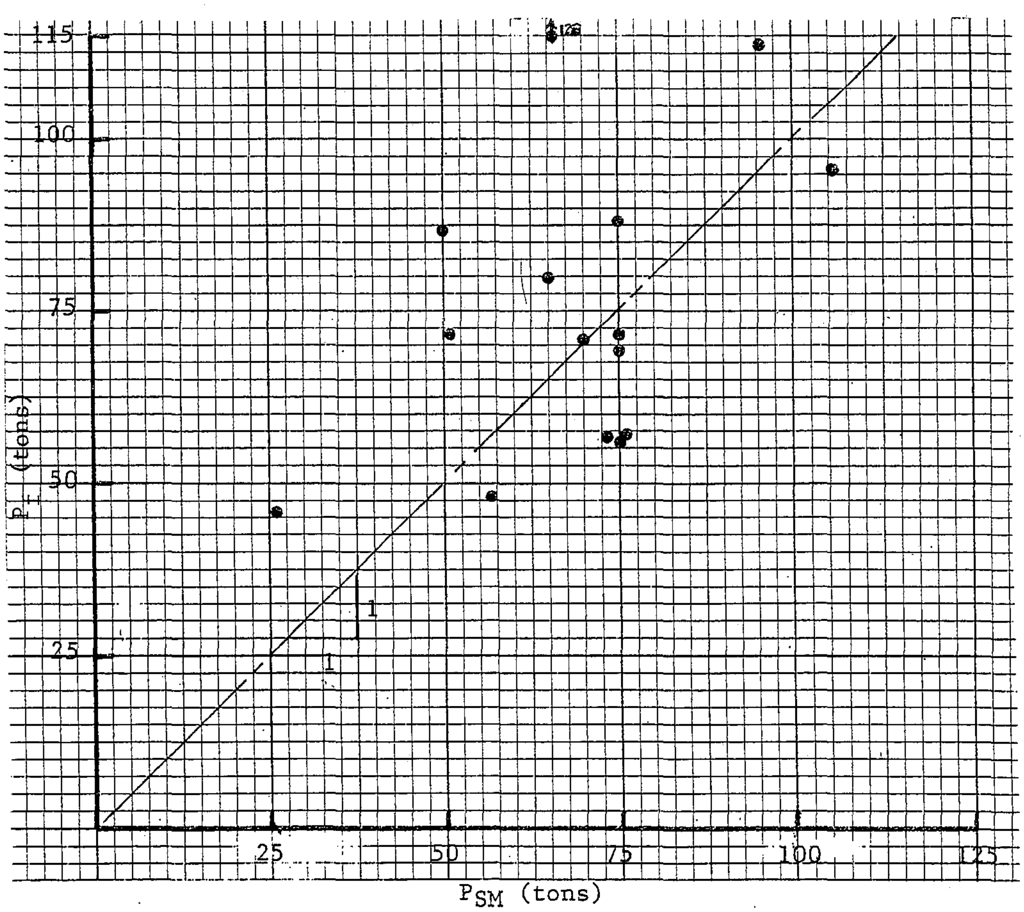

Fig. D.3. P_{SM} vs P_f for Timber Piles in Alabama Sandy Soils ($\delta = 0.75\phi$ and K = 1.5) (1).

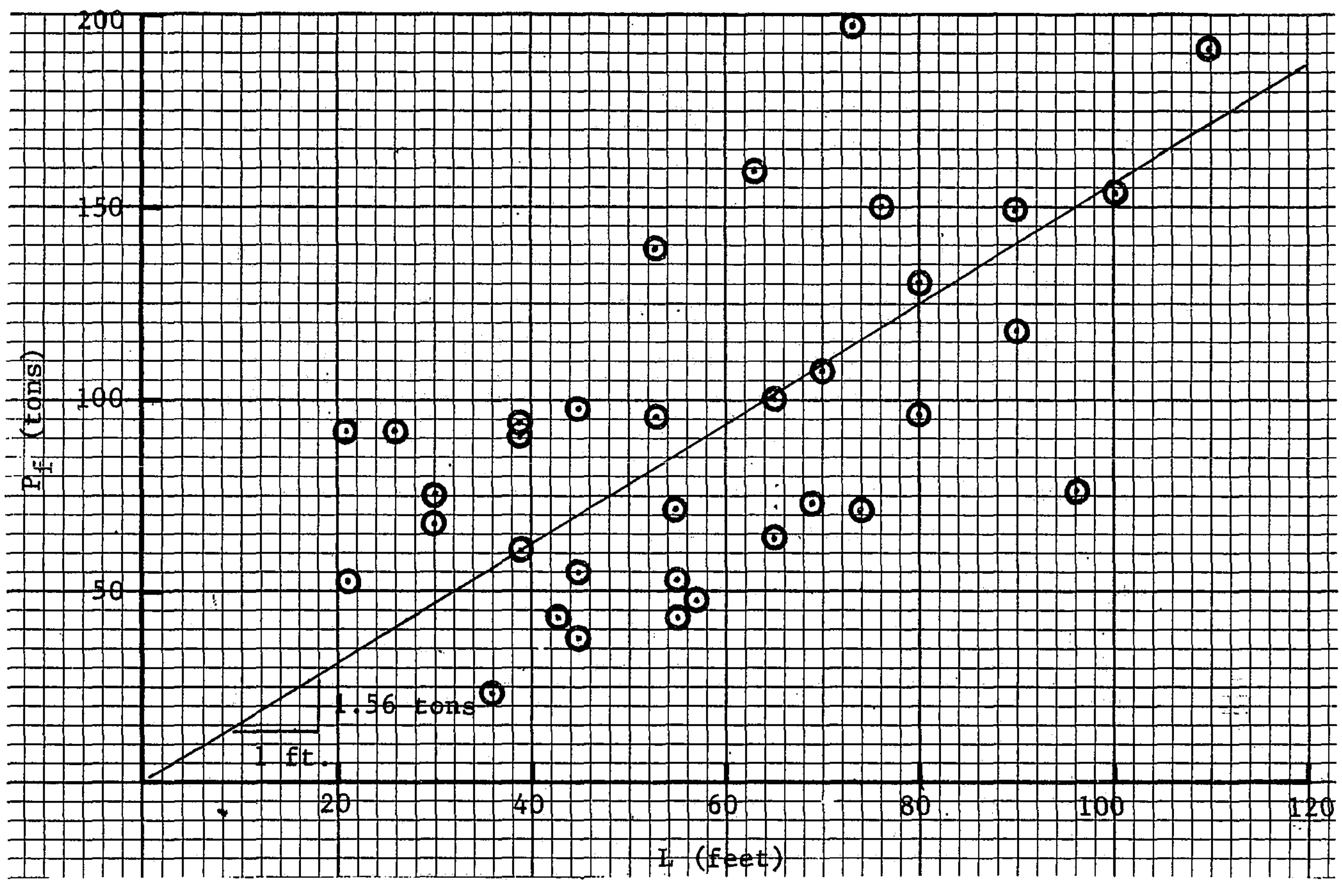

Fig. D.4. L vs. P_f for Steel-H Piles in Alabama Sandy Soils (1).

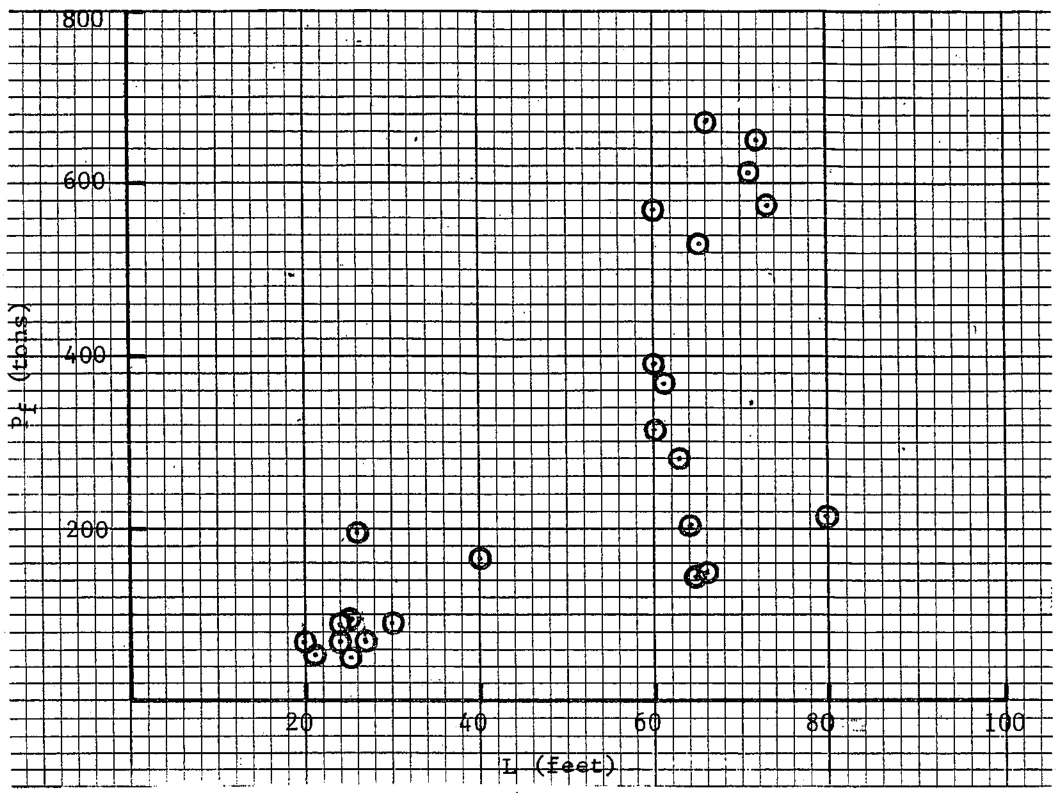

Fig. D.5. L vs. P_f for Precast Concrete Piles in Alabama Sandy Soils (1).

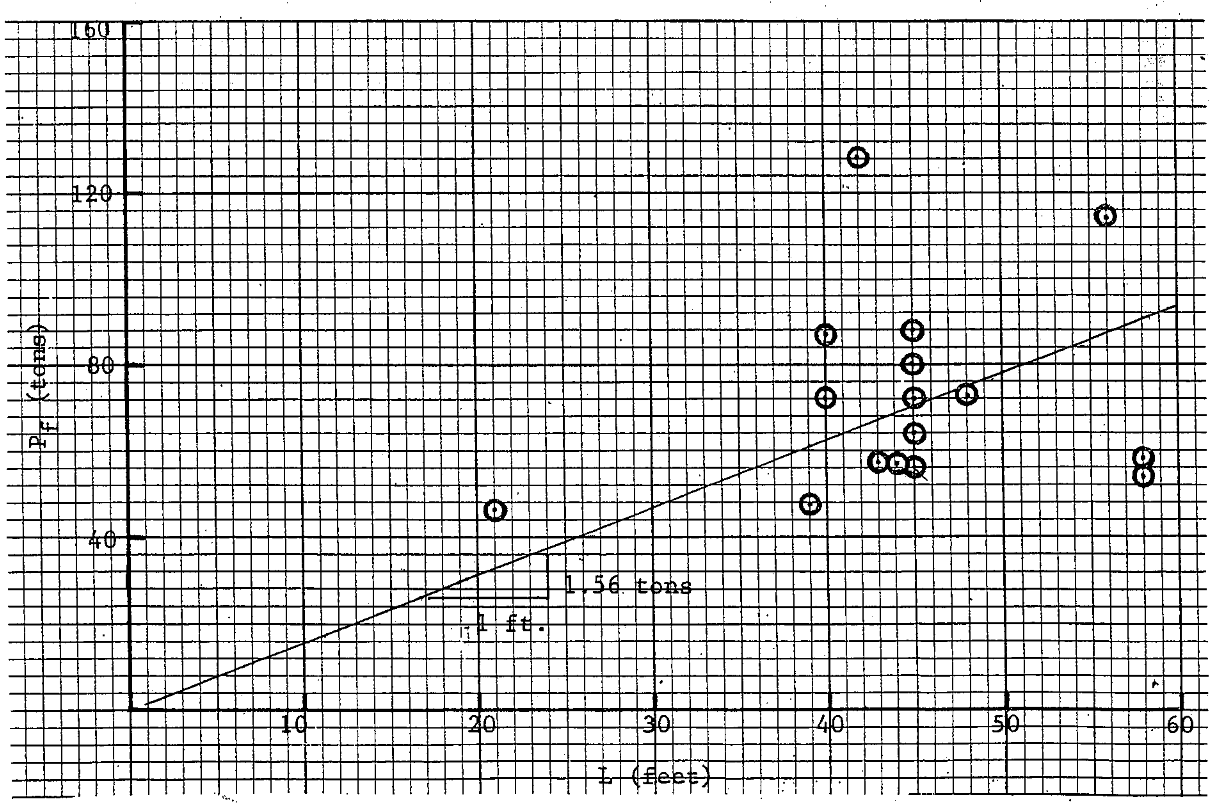

Fig. D.6 L vs. P_f for Timber Piles in Alabama Sandy Soils (1).